

Dissertation  
submitted to the  
Combined Faculties for the Natural Sciences and for Mathematics  
of the Ruperto-Carola University of Heidelberg, Germany  
for the degree of  
Doctor of Natural Sciences

Presented by  
M.Sc. Juliane Kutzner  
born in Dresden, Germany  
Oral-examination: 18.10.2019



**Dissecting SAMHD1's role in the type I  
Interferon induced early Block to HIV-1 Infection  
and its Connection to Cancer**

Referees: Prof. Dr. Martin Müller

Prof. Dr. rer. nat. Dirk Grimm



# 1 Acknowledgement

This thesis was performed under supervision of Torsten Schaller in the Department of Infectious Diseases, Virology, at the University Hospital of Heidelberg from February 2016 until January 2018. As of January 2018 until now supervision was conducted by Prof. Dr. Hans-Georg Kräusslich.

First of all, I thank Thorsten Schaller for giving me the opportunity to work on such a fascinating and multifaceted project in his lab. It was a pleasure working with you side by side in the lab. Thank you for numerous very helpful and fruitful discussions. I highly appreciate your interest in the project after you left the institute.

I also thank Prof. Dr. Hans-Georg Kräusslich for taking me in his group and giving me some helpful advice.

Furthermore, I would like to thank our collaborators Nikolas Herold, Sean Rudd and Nikolaos Tsesmetzis. A special thanks goes to Nikolas Herold for inviting me to Stockholm, for the helpful input throughout my project and for proof reading my thesis.

Thank you to the whole Schaller group (Sarah and Lorenzo) for helping me in the lab.

I would like to thank the whole HGK group for taking me in and of course the Müller and Lozach group as well. A special thank you goes to Robin, Thorsten, David, Frauke, Vojtech, Robin, Daniel, Rene, Lorenzo, Anja, Sarah, Zina and Annica for creating a nice working atmosphere with laughter and fun besides work. Thank you Daniel and Rene for our Magic lunch hour, Robin for our walks in the park and your humor and Annica for our funny shopping trip and wrap lunches and olive jokes.

Very special and warm thanks go to my boyfriend Erik for his unconditional support throughout my studies and my thesis, for giving me the time to write my thesis and for the nice distraction during the weekend. Thank you for your love honey. I also thank Billy for the good distraction on the soccer and baseball field, his silliness, his crazy stories and his love. Now I am almost a doctor and you can call me when you have a medical emergency ☺!

Last but not least, I thank my family: Danke für eure Unterstützung und eure aufmunternden Worte. Ihr habt immer ein offenes Ohr für mich und seid immer für mich da. Ohne euch hätte ich das alles nicht geschafft.

## 2 Abstract

Human immunodeficiency virus-1 (HIV-1) and all other viruses are known to interact with multiple host cellular proteins during their replication in the target cell. While many of these host cellular proteins facilitate viral replication, a number of them are reported to repress viral replication. These host cellular proteins are known as restriction factors and they represent the host's first line of defense against the viral pathogens. Sterile alpha motif and HD domain containing 1 (SAMHD1) has been identified as a HIV-1 restriction factor that blocks early-stage virus replication in dendritic and other myeloid cells.

SAMHD1 is the target of the viral protein x (Vpx) from simian lentiviruses and HIV-2. Vpx mediates the recruitment of the Cullin4-DDB1-DCAF1 ubiquitin ligase machinery to SAMHD1 leading to polyubiquitination and subsequent degradation of SAMHD1. Previous studies on monocyte-derived dendritic cells suggested that the Vpx-induced rescue of HIV-1 infection from early type I IFN-induced blocks was independent of SAMHD1, since Vpx mutant Q76A, which is unable to recruit DCAF1 and to degrade SAMHD1, still increased HIV-1 infection in type I IFN treated cells. The rescue in healthy blood donor cells was not observed when Q76A mutant Vpx virus-like particles were used, suggesting that – in conflict with previous reports – SAMHD1 degradation is required for efficient Vpx-mediated rescue of HIV-1 from the type I IFN-induced early antiviral blocks. To investigate the role of SAMHD1 in the Vpx-mediated rescue of HIV-1 from the type I IFN-induced block in myeloid cells at more detail, we generated CRISPR/Cas9 THP-1 cells, a monocytic acute myeloid leukemia cell line, lacking a functional *SAMHD1* gene. In line with previous studies, the lack of SAMHD1 protein had no impact on the level of the type I IFN-induced early block to HIV-1 infection as compared to control or parental THP-1 cells. However, while Vpx was able to rescue HIV-1 infectivity in parental THP-1 or CRISPR/Cas9 control cells from the type I IFN effects, no rescue was observed when SAMHD1 protein was absent. To investigate whether the enzymatic activity of SAMHD1 was required for the Vpx-mediated rescue of HIV-1 infection from the early type I IFN-induced blocks, we reconstituted expression of wild type or different catalytically-inactive SAMHD1 mutants in *SAMHD1*<sup>-/-</sup> cells and found that Vpx increased HIV-1 infectivity in the presence of wild type, but not H233A mutant SAMHD1, suggesting that the enzymatic activity of SAMHD1 is required for a Vpx-induced rescue of HIV-1 infection from the type I IFN-induced block. We also generated a CRISPR/Cas9 THP-1 cell clone, which had one disrupted SAMHD1 allele and one allele, in which the entire nuclear localization signal (11KRPR14) was deleted in frame, generating an internally NLS-disrupted endogenously expressed SAMHD1 protein. In these cells, SAMHD1 was predominantly localized to the cytoplasm, although a

fraction was also observed in the nucleoplasm, suggesting for an alternative nuclear import pathway, independent of the classical <sup>11</sup>KRPR<sup>14</sup> NLS. In these cells, Vpx still rescued HIV-1 from the type I IFN-induced early block to infection. Of note, SAMHD1 degradation was profoundly delayed, suggesting that Vpx-induced polyubiquitination of SAMHD1 is sufficient to overcome the early IFN-induced block to HIV-1 in myeloid cells. SAMHD1 not only acts as a host restriction factor against lentiviral, endogenous retroviruses, hepatitis B virus, herpesviruses (HSV-1) and poxviruses, mutations in the *SAMHD1* gene have also been linked to the immune disorder Aicardi-Goutières Syndrome (AGS), a genetic disease mimicking congenital virus infection. Recurrent mutations and reduced expression levels of *SAMHD1* have been suggested to play a role for the oncogenesis of several cancers such as colon and Rectum Adenocarcinoma (COAD/READ), lung cancer, cutaneous T-cell lymphoma, acute myeloid leukemia (AML), and chronic lymphocytic leukemia (CLL). Interestingly, SAMHD1's function as a possible tumor suppressor is complexed by its role as a resistance factor in nucleoside analogue-based anti-cancer therapies. Cytarabine (ara-C), a deoxycytidine analog, is the single most important drug in the treatment of AML and other hematological malignancies, exerting its cytotoxic effects through its activated triphosphate (ara-CTP), eventually leading to DNA damage and cell death. We and others demonstrated that SAMHD1 is able to detoxify cells by hydrolytic activity towards ara-CTP. Accordingly, primary AML blasts treated with Vpx to deplete SAMHD1 as well as THP-1 CRISPR/Cas9 SAMHD1 knock-out cells showed increased sensitivity towards ara-C induced cytotoxicity. Using these knock-out cells as a back-bone, we expressed a large panel of SAMHD1 mutants harboring non-synonymous single nucleotide polymorphisms (SNPs) that have been identified in patients with AML, READ, STAD or COAD and performed differential analyses of ara-C sensitivity as well as restriction activity towards HIV-1 infection to unravel possible mechanistic differences in both activities. In this respect neutralization of ara-C induced cytotoxicity was found to be a very good surrogate for the enzymatic dNTPase activity of SAMHD1, and using naturally occurring SAMHD1 variants ensured that these proteins were not artificially defective, hence for the first time a direct comparison of enzymatic activity and anti-HIV-1 activity could be investigated in the same cells. We are currently investigating the effects of these SAMHD1 SNPs on oligomerization and sensitivity for degradation by Vpx. The identification of SAMHD1 SNPs altering the sensitivity to certain anti-cancer chemotherapies could also be a key for future personalized treatment strategies. Furthermore, the ability of our assays to uncouple SAMHD1 enzymatic activity from virus restriction could help to understand the contribution of SAMHD1's dNTPase activity towards HIV-1 restriction and since the Vpx-

induced rescue of HIV-1 infection from the type I IFN induced block was shown to depend on SAMHD1, may help to unravel the IFN-induced early blocks against HIV-1. In Summary, SAMHD1 plays a bigger role in the type I IFN-induced block than currently is appreciated and further investigation of its cellular function may provide insights into the underlying mechanisms and contributing additional factors.



### 3 Zusammenfassung

Das menschlichen Immunschwäche-Virus 1 (HIV-1) und weitere Viren interagieren mit einer Reihe von intrazellulären Proteinen während ihrer Replikation in der Wirtszelle. Während einige von diesen Proteinen die Replikation vorantreiben gibt es aber auch Proteine, die die Replikation behindern. Diese Proteine werden als Restriktionsfaktoren bezeichnet und repräsentieren die erste Abwehr der Wirtszelle gegen Viren. Ein Restriktionsfaktor von HIV-1 ist SAMHD1. SAMHD1's dNTPase Funktion hindert retrovirale Replikation wahrscheinlich durch den Abbau intrazellulärer dNTPs. Vpx von HIV-2 und SIV kann SAMHD1 binden und markiert es für den proteosomalen Abbau mit Hilfe der Cullin-4-DDB1-DCAF1-Ubiquitin-Ligase-Maschinerie. Bisherige Studien in Blutmonozyten differenzierte Makrophagen (MDD)Zellen haben gezeigt, dass die Vpx-induzierte Erhöhung der HIV-1 Infektion von SAMHD1 unabhängig ist, da die Vpx Mutante Q76A, welche nicht in der Lage ist, DCAF1 zu rekrutieren und SAMHD1 zu degradieren, die HIV-1 Infektion erhöht in type 1 IFN  $\alpha$  /LPS vorbehandelten Zellen. Wir zeigen hier, dass in gesunden Blutspendern Vpx Q76A keine Erhöhung der HIV-1-Infektion induziert. Daraus schließen wir, dass SAMHD1-Degradation wahrscheinlich mit ausschlaggebend ist für die Vpx-induzierte Erhöhung der HIV-1 Infektion in IFN-1 vorbehandelten Zellen ist. Um die Vpx-induzierte Erhöhung der HIV-1 Infektion in IFN-1 vorbehandelten Zellen genauer zu charakterisieren, haben wir THP-1-SAMHD1-knock-out-Zellen erstellt. Der Verlust des *SAMHD1*-Gens hatte keinen Einfluss auf den IFN-1 Block, jedoch zeigte sich, dass SAMHD1 fundamental ist für die Vpx-induzierte Erhöhung der HIV-1 Infektion in IFN-1 vorbehandelten Zellen. Desweiteren haben wir untersucht ob SAMHD1 katalytisch aktiv sein muss für die Vpx-induzierte Erhöhung der HIV-1-Infektion. Wir konnten zeigen, dass die katalytisch inaktive SAMHD1-Mutante H233A nicht in der Lage war, die HIV-1-Infektion zu erhöhen in IFN-1 vorbehandelten THP-1-Zellen. Um zu beweisen, dass SAMHD1-Degradation fundamental für die Vpx-induzierte Erhöhung der HIV-1-Infektion in IFN-1-vorbehandelten Zellen ist, haben wir einen CRISPR/Cas9-THP-1-Zellklon erstellt, welcher ein gestörtes *SAMHD1*-Allel hat und dessen anderes Allel keine Zellkernlokalisierungssignal (11KRPR14) mehr beinhaltet. Aufgrund dessen befand sich SAMHD1 in diesem Zellklon im Zytoplasma. Vpx war in der Lage, in dem NLS-Klon die HIV-1 Infektion in IFN-1 behandelten Zellen zu erhöhen. Jedoch war die SAMHD1-Degradation durch Vpx in diesen Zellen deutlich verlangsamt im Vergleich zu parentalen THP-1-Zellen. Darüber hinaus stehen Mutationen in *SAMHD1* mit der Autoimmunerkrankung Aicardi-Goutières-Syndrom (AGS) in Verbindung. Des Weiteren wurde gezeigt, dass Mutationen in *SAMHD1* und reduzierte *SAMHD1*-Expression in Verbindung mit der Entstehung von Krebs

steht wie zum Beispiel bei akuter myeloische Leukämie (AML), chronische lymphatische Leukämie (CLL) und Darmkrebs. SAMHD1 ist auch ein Resistenzfaktor in der Nukleosidanalogs-basierten Krebstherapie. Cytarabin (ara-C) ist ein Deoxycydidinanalogs und ist das wichtigste Krebsmedikament in der Bekämpfung von AML. Die aktive Form von ara-C ist ara-CTP, welche in die DNA eingebaut wird und zum Zelltod führt. Wir und weitere Wissenschaftler haben gezeigt, dass ara-CTP ein Substrat von SAMHD1 ist und SAMHD1 in der Lage ist, ara-CTP zu hydrolysieren. THP-1-Zellen behandelt mit Vpx und *SAMHD1*-knock-out-Zellen haben eine höhere Sensitivität zu ara-C als Kontrollzellen. Wir haben SAMHD1-knock-out-Zellen genutzt, um natürlich vorkommende *SAMHD1*-Einzelnukleotid-Polymorphismen (SNPs), welche in AML, READ, STAD oder COAD identifiziert wurden, zu exprimieren, um deren Effekte auf ara-C-Sensitivität und HIV-1-Restriktion zu untersuchen. *SAMHD1*-SNPs, die die ara-C Sensitivität verändern, können in der personalisierten Bekämpfung von Krebs sehr von Bedeutung sein. Des Weiteren hilft die Analyse von *SAMHD1*-SNPs die Bedeutung der dNTPase Aktivität von SAMHD1 für die HIV-1 Restriktion besser zu charakterisieren.

## 4 Table of content

1	Acknowledgement.....	3
2	Abstract.....	4
3	Zusammenfassung.....	7
4	Table of content.....	9
5	Figure and table legend.....	14
6	Abbreviation.....	17
7	Introduction.....	20
7.1	Human Immunodeficiency Virus Type 1 (HIV-1).....	20
7.2	HIV-Classification, genome organization and virion structure.....	21
7.3	HIV-1 Replication.....	22
7.4	Restriction factors.....	25
7.5	Vpx.....	28
7.6	SAMHD1.....	30
7.6.1	Structure of SAMHD1.....	30
7.6.2	SAMHD1 is an HIV-1 restriction factor.....	31
7.6.3	Deoxynucleotide metabolism overview.....	34
7.6.4	SAMHD1 in cancer.....	35
8	Aims of this thesis.....	36
8.1	SAMHD1's role in the type 1 interferon induced early block to HIV-1 infection.....	36
8.2	Correlation of SAMHD1 dNTPase activity with HIV-1 restriction by using cancer-associated naturally occurring SAMHD1 variants.....	36
9	Material and Methods.....	38
9.1	Material.....	38
9.1.1	Laboratory equipment.....	38
9.1.2	Laboratory materials.....	39
9.1.3	Kits.....	40
9.1.4	Chemicals and reagents.....	40

9.1.5 Buffers and solutions.....	41
9.1.6 Cell culture media.....	42
9.1.7 Enzymes .....	42
9.1.8 Drugs .....	43
9.1.9 Antibodies.....	43
9.1.10 Plasmids and constructs .....	43
9.1.11 Primer .....	45
9.1.12 SAMHD1 SNP constructs .....	45
9.1.13 Software .....	47
9.2 Methods.....	47
9.2.1 Cells.....	47
9.2.2 Virus preparation and infection assay .....	48
9.2.3 Production of VLPs .....	49
9.2.4 Infections .....	49
9.2.5 Generation of CRISPR/Cas9 THP-1 cell clones .....	49
9.2.6 Generation of stable cell lines ectopically expressing proteins.....	50
9.2.7 Growth curves .....	50
9.2.8 Proliferation assays.....	50
9.2.9 Preparation of chemical competent E.coli.....	50
9.2.10 Heat shock transformation and plasmid preparation.....	51
9.2.11 Separation of DNA by agarose gel electrophoresis .....	51
9.2.12 DNA extraction from agarose gels.....	52
9.2.13 Ligation of DNA-fragments .....	52
9.2.14 Analysis of DNA with restriction enzymes.....	52
9.2.15 Polymerase Chain Reaction (PCR) .....	52
9.2.16 PCR-based mutagenesis .....	53
9.2.17 SDS-polyacrylamide-gel electrophoresis (SDS-PAGE) .....	53
9.2.18 Western blotting .....	54

9.2.19	Immunofluorescence and confocal microscopy .....	54
10	Results .....	55
10.1	SAMHD1's role in the type 1 interferon induced early block to HIV-1 infection .....	55
10.1.1	The Vp <sub>xMAC</sub> -induced rescue of HIV-1 from the type I IFN-induced block in MDM depends on SAMHD1.....	55
10.1.2	The Vp <sub>xMAC</sub> -induced rescue of HIV-1 from the type I IFN-induced block in MDM is independent of route of entry.....	57
10.1.3	Vp <sub>xMAC</sub> does not rescue HIV-1 from the type I IFN-induced block in THP-1 SAMHD1 <sup>-/-</sup> cells.....	58
10.1.4	SAMHD1 knockout has no influence on cell proliferation in THP-1 cells .....	61
10.1.5	Characterization of a THP-1 cell line endogenously expressing SAMHD1 with truncated nuclear localization signal (Eg3c6 <sup>+/-</sup> ).....	62
10.1.6	Interferon has no influence on -Vpx- mediated SAMHD1 degradation in cycling THP-1 cells.....	64
10.2	SAMHD1 in cancer.....	65
10.2.1	SAMHD1 SNPs in Rectum Adenocarcinoma (READ).....	71
10.2.2	SAMHD1 SNPs in acute myeloid leukemia (AML).....	73
10.2.3	SAMHD1 SNPs in colon adenocarcinoma (COAD) .....	75
10.2.4	Analysis of the ability of Vpx to degrade human SAMHD1 SNP variants .....	88
10.2.5	SNPs in stomach adenocarcinoma (STAD) .....	89
10.3	SAMHD1 variants that influence post-translational modifications of SAMHD1 and their involvement in HIV-1 restriction and ara-CTP hydrolysis.....	91
10.3.1	The C522 residue of SAMHD1 is crucial for the block to HIV infection but is not involved in conferring resistance to ara-C.....	91
10.3.2	SAMHD1 acetylation has no influence on HIV-1 restriction and only minimally changes the sensitivity of cells to ara-C induced cytotoxicity .....	92
11	Discussion and perspective .....	93
11.1	SAMHD1's role in the type 1 interferon induced early block to HIV-1 infection .....	93

11.1.1	The V <sub>px<sub>MAC</sub></sub> -induced increase of HIV-1 infection in type I IFN treated MDMs is SAMHD1-dependent.....	93
11.1.2	The V <sub>px<sub>MAC</sub></sub> -induced rescue of HIV-1 from the type I IFN-induced block in MDM is independent of the route of entry .....	94
11.1.3	V <sub>px<sub>MAC</sub></sub> does not relieve HIV-1 from the type I IFN-induced block in THP-1 SAMHD1 <sup>-/-</sup> cells.....	94
11.1.4	SAMHD1 knock-out has no influence on cell proliferation in THP-1 cells.....	95
11.1.5	Characterization of a THP-1 cell line endogenously expressing SAMHD1 with truncated nuclear localization signal (THP-1 Eg3c6 <sup>+/-</sup> ).....	96
11.1.6	Type I interferon has no influence on V <sub>px</sub> -mediated SAMHD1 degradation in cycling THP-1 cells .....	98
11.2	Correlation of SAMHD1 dNTPase activity with HIV-1 restriction by using cancer-associated naturally occurring SAMHD1 variants.....	98
11.2.1	SAMHD1 is a mediator of ara-C toxicity in AML cell models.....	98
11.2.2	SAMHD1 SNPs in Cancer .....	100
11.2.2.1	SAMHD1 SNPs in Rectum Adenocarcinoma (READ).....	101
11.2.2.2	SAMHD1 SNPs in acute myeloid leukemia (AML) .....	101
11.2.2.3	SAMHD1 SNPs in colon adenocarcinoma (COAD) .....	102
11.2.2.4	Ability of V <sub>px</sub> to degrade human SAMHD1 SNP variants.....	107
11.2.2.5	SNP in stomach adenocarcinoma (STAD) .....	108
11.3	SAMHD1 variants that influence post-translational modifications of SAMHD1 and their involvement in HIV-1 restriction and ara-CTP hydrolysis.....	108
11.3.1	The C522 residue of SAMHD1 is crucial for the intensive block to HIV infection but presumably not for ara-CTP hydrolysis .....	108
11.3.2	SAMHD1 acetylation has no influence on viral restriction and minimally changes its sensitivity to ara-C induced cytotoxicity .....	109
12	Summary and Outlook .....	110
12.1	SAMHD1's role in the type 1 interferon induced early block to HIV-1 infection ...	110
12.2	Correlation of SAMHD1 dNTPase activity with HIV-1 restriction by using cancer-associated naturally occurring SAMHD1 variants.....	110
13	Publications and contributions .....	112

13.1	Publications.....	112
13.2	Conference Contributions .....	113
13.3	Contributions to this project.....	114
14	References.....	115

## 5 Figure and table legend

Figure 1: HIV-1 genome. ....	22
Figure 2: Schematic representation of the f HIV-1 life cycle. ....	23
Figure 3: Host restrictions factors and viral countermeasures. ....	27
Figure 4: Schematic illustration of Vpx protein from SIV <sub>MAC</sub> and model of Vpx mediated degradation of SAMHD1. ....	29
Figure 5: Schematic representation of SAMHD1 domains. ....	30
Figure 6: Model of SAMHD1 tetramerization. ....	31
Figure 7: Model for SAMHD1 function in HIV-1 restriction. ....	33
Figure 8: Overview of the dNTP metabolism. ....	34
Figure 9: Vpx deficient for SAMHD1 degradation does not relieve HIV-1 from the type I IFN induced block in MDM. ....	56
Figure 10: Vpx mediated increase of HIV-1 infection is independent of entry route. ....	57
Figure 11: Generation of THP1 SAMHD1 CRISPR–Cas9 cells. Vpx mediated rescue of HIV-1 from the type I Interferon-induced block is SAMHD1-dependent. ....	58
Figure 12: Vpx-mediated rescue of HIV-1 from the type I interferon-induced block is SAMHD1-dependent. ....	59
Figure 13: Re-expression of SAMHD1 confirms sensitivity to Vpx. ....	60
Figure 14: SAMHD1 knockout does not significantly alter growth kinetics or cell cycle distribution. ....	61
Figure 15: Generation of THP1 SAMHD1 CRISPR–Cas9 cells with disrupted nuclear localization signal ( <sup>11</sup> KRPR <sup>14</sup> ). ....	62
Figure 16: Vpx-mediated rescue of HIV1 from the type 1 Interferon induced block is independent of SAMHD1 localization and despite reduced SAMHD1 degradation kinetics. ....	63
Figure 17: Vpx mediated SAMHD1 degradation was not influenced by interferon treatment in cycling. ....	64
Figure 18: Ara-C is a substrate of SAMHD1. ....	66
Figure 19: Intracellular conversion of cytarabine (ara-C) to ara-CTP and detoxification mechanism by SAMHD1. ....	67
Figure 20: High SAMHD1 expression levels are crucial for a pronounced block of HIV-1 infection and enhanced cell viability after ara-C treatment. ....	68
Figure 21: SAMHD1's role in tumorigenesis. ....	69



Figure 22: Schematic representation of analyzed SAMHD1 mutations in Rectum Adenocarcinoma (READ).	71
Figure 23: SAMHD1 crystal structure with dCTP bound.	71
Figure 24: Expression of SAMHD1 SNP variants A76T or R305I in THP-1 SAMHD1 <sup>-/-</sup> cells increases HIV-1 restriction and has no impact on ara-C sensitivity.	72
Figure 25: Schematic representation of SAMHD1 Mutations in acute myeloid leukemia (AML).	73
Figure 26: SAMHD1 Dimer-Dimer interface with L178 (yellow) and A338 (blue) (PDB: 4RXR).	73
Figure 27: SAMHD1 catalytic site.	73
Figure 28: Expression of AML SAMHD1 SNP variants L178Q or S214P in THP-1 SAMHD1 <sup>-/-</sup> cells renders these cells more permissive to HIV-1 infection as compared to WT and enhances ara-C sensitivity.	74
Figure 29: Schematic representation of SAMHD1 Mutations in colon adenocarcinoma (COAD) and their appearances in analyzed cases. (adapted from TCGA).	75
Figure 30: Expression of SAMHD1 SNP variant G90R in THP-1 SAMHD1 <sup>-/-</sup> cells impacts HIV-1 restriction and enhances ara-C sensitivity.	77
Figure 31: Expression of SAMHD1 SNP variants A338T and D137N in THP-1 SAMHD1 <sup>-/-</sup> cells and their influence on HIV-1 restriction and sensitivity to ara-C treatment.	78
Figure 32: SAMHD1 allosteric site with D137 residue depicted in orange.	79
Figure 33: SAMHD1 allosteric site.	79
Figure 34: Crystal SAMHD1 tetramer structure.	80
Figure 35: Expression of SAMHD1 SNP variants V133I and A525T in THP-1 SAMHD1 <sup>-/-</sup> cells and their influence on HIV-1 restriction and sensitivity to ara-C treatment.	80
Figure 36: Expression of SAMHD1 SNP variants A525T in THP-1 SAMHD1 <sup>-/-</sup> cells and its influence on phosphorylation and further analyzes of A525S, A525E, A525V and A525Y their influence on HIV-1 restriction and sensitivity to ara-C treatment.	82
Figure 37: SAMHD1 variant A525T is resistant to Vpx-induced degradation and Vpx is unable to rescue HIV-1 from the type I interferon induced block in presence of SAMHD1 A525T.	83
Figure 38: Effects of R348C SAMHD1 variant on the restriction to HIV-1 infection and sensitivity towards ara-C.	83
Figure 39: Allosteric site of SAMHD1 with R451 residue shown in yellow.	84

Figure 40: Effects of R451P and R451C SAMHD1 variant on the restriction to HIV-1 infection and sensitivity towards ara-C. ....	84
Figure 41: Catalytic site of SAMHD1 with dCTP bound. ....	85
Figure 42: SAMHD1 dimer with residue D497 depicted in red. ....	85
Figure 43: Effects of R366H and D467Y SAMHD1 variant on the restriction to HIV-1 infection and sensitivity towards ara-C. ....	86
Figure 44: Effects of K596Rsf*35 SAMHD1 variant on the restriction to HIV-1 infection and sensitivity towards ara-C. ....	86
Figure 46: Allosteric site of SAMHD1. ....	87
Figure 47: Effects of R145Q SAMHD1 variant on the restriction to HIV-1 infection and sensitivity towards ara-C. ....	87
Figure 48: Sensitivity of SAMHD1 variants to Vpx-induced degradation. ....	88
Figure 49: SAMHD1 crystalized tetramer structure with P589 depicted in yellow. ....	89
Figure 50: Expression of SAMHD1 SNP variant P589T in THP-1 SAMHD1 -/- cells has a negative effect on HIV-1 restriction and ara-C sensitivity. ....	89
Figure 51: Effects of cysteine substitutions on the restriction of HIV-1 infection and sensitivity to ara-C. ....	91
Figure 52: Effects of acetylation defective mutant K405R on the restriction to HIV-1 infection and sensitivity to ara-C. ....	92
Table 1 SAMHD1 variants analyzed in this study .....	70
Table 2 Mutation of COAD analyzed and their impact for canonical transcript. ....	76
Table 3 Summary of analyzed SAMHD1 SNPs. ....	90

## 6 Abbreviation

$\mu$	micro
$\mu\text{g}$	micro gram
$\mu\text{l}$	micro liter
$\mu\text{M}$	micro molar
A	adenosine
A1	Allosteric site 1
A2	Allosteric site 2
AML	Acute myeloid leukemia
Amp	ampecilin
APOBEC3G/F	apolipoprotein B mRNA-editing enzyme catalytic polypeptide-like 3G/F
APS	ammonium persulfate
ara-C	cytarabine
Ara-CTP	Arabinofuranosylcytosine triphosphate
BC	benzylcytosine
BSA	bovine serum albumin
CA	capsid protein
CCR	C-C chemokine receptor type
CD4	cluster of Differentiation 4
CD4 <sup>+</sup> T cell	T cell positive for CD4
CLL	Chronic lymphocytic leukemia
COAD	Colon adenocarcinoma
CXCR	C-X-C chemokine receptor
CypA	Cyclophilin A
DCAF1	DDB1 And CUL4 Associated Factor 1
DDB1	DNA damage-binding protein 1
DMEM	Dulbecco's Modified Eagle Medium
DMEM	Dulbecco's Modified Eagle Medium
DMSO	dimethyl sulfoxide
DNA	desoxyribonucleic acid
dNTP	deoxynucleoside triphosphate
dNTP	deoxyribonucleotide triphosphate
dsDNA	double stranded deoxyribonucleic acid

Env	envelope protein
ER	endoplasmic reticulum
ESCRT	endosomal sorting complexes required for transport
EtOH	ethanol
FACS	fluorescence-activated cell sorter
FCS	fetal calf serum
fwd	forward
GFP	Green fluorescent protein
HAART	Highly active antiretroviral therapy
HD domain	histidine–aspartic domains
HIV	human immunodeficiency virus
IFITM	interferon-induced transmembrane
IFN	interferon
kbp	Kilo-base pairs
kDa	kilo Dalton
LTR	Long terminal repeats
MA	matrix protein
MDDC	monocyte-derived dendritic cells
MDM	monocyte-derived macrophages
MeOH	methanol
mM	Millimolar
mRNA	messenger RNA
MX2	Myxovirus-resistance protein 2
NC	nucleocapsid protein
Nef	negative factor
NLS	Nuclear localization signal
nm	nanometer
°C	degree celsius
ORF	open reading frame
PBS	phosphate buffered saline
PCR	polymerase chain reaction
PEI	Polyethyleneimine
PFA	paraformaldehyde
PIC	pre-integration complex

PM	plasma membrane
Pol	polymerase
PR	protease
rev	reverse
RNA	ribonucleic acid
RNR	Ribonucleotide reductase
RPMI	Roswell Park Memorial Institute 1640
RT	reverse transcriptase
RTC	reverse transcription complex
RT-PCR	Real time PCR
SAM	sterile alpha motif
SAMHD1	SAM domain and HD domain-containing protein 1
SD	standard deviation
SDM	Side directed mutagenesis
SDS-PAGE	sodium dodecyl sulfate polyacrylamide gel electrophoresis
SEM	standard error of the mean
shRNA	short hairpin RNA
siRNA	small interfering RNA
SIV	Simian immunodeficiency viruses
SNP	Single Nucleotide Polymorphism
ssRNA	single stranded ribonucleic acid
STAD	Stomach adenocarcinoma
Tat	trans-activator of transcription
TCGA	The Cancer Genome Atlas
TRIM	Tripartite motif-containing protein
U	units
UNAIDS	Joint United Nations Programme on HIV/AIDS
Vif	viral infectivity factor
VLP	virus like particle
Vpr	viral protein R
Vpu	viral protein U
Vpx	Viral protein X
wt	wild type

## 7 Introduction

### 7.1 Human Immunodeficiency Virus Type 1 (HIV-1)

Human immunodeficiency virus 1 (HIV-1) is the primary cause of the acquired immunodeficiency syndrome (AIDS) and was identified in 1983/1984 (Barre-Sinoussi et al., 2004, Gallo et al., 1983). Worldwide, approximately 37 million people are infected with the majority being in developing countries (UNAIDS, 2018), which led to 32.0 million AIDS-related deaths since the start of the epidemic (UNAIDS, 2018). 1.8 million people got newly infected with HIV-1 in 2018 (UNAIDS 2018). Since the first cases of HIV were reported more than 35 years ago, 78 million people have become infected with HIV and 35 million have died from AIDS-related illnesses (UNAIDS 2018). HIV-1 efficiently infects CD4+ T cells, whereas cells of the myeloid lineage are less susceptible for infection with HIV-1 because they exhibit multiple post-entry blocks (Ho et al., 1995). Transmission of HIV occurs by the transfer of blood, semen, pre-ejaculate, vaginal fluid or breast milk.<sup>1</sup> The infection with HIV causes a progressive depletion of CD4+ T cells in the host, ultimately compromising cell-mediated and adaptive immunity. The infected individual becomes more susceptible to life-threatening opportunistic infections, which eventually leads to the patient's death.

Three characteristic stages of HIV-1 infections can be defined (Swanstrom and Coffin, 2012): (1) acute early infection, in which the virus replicates leading to rapid depletion of T cells. (2) Clinical latency, in which HIV viremia is largely controlled, and T cell counts increase again as the virus turns silent and evades the immune system, the latent stage, which can last for several years. (Ozato et al.) (3) AIDS, a stage occurring with decreasing levels of CD4+ T cells and increasing viral load. Among all HIV-infected patients, approximately 17 million are on antiretroviral treatment (UNAIDS, 2016). This treatment consists of highly active antiretroviral therapy (HAART), a multiagent treatment containing at least three drugs, decreasing the patient's viral load by blocking HIV entry. Interferons (IFNs), a set of cytokines, can reduce HIV-1 replication in certain types of natural target cells by inducing the expression of a set of antiviral genes that inhibit HIV-1 replication. This was observed in clinical trials in HIV-1 infected patients (Mildvan et al., 1996, Torriani et al., 2003) as well as in cell culture systems (Bitzegeio et al., 2013, Agy et al., 1995, Ho et al., 1985, Baca-Regen et al., 1994). There are several limiting factors that stand in the way of achieving a complete cure of HIV/AIDS such as the high mutation rates of the virus which leads to the evolution of drug-resistant variants as well as drug toxicity over a long treatment and the latency of the virus in the host genome (Ho

---

<sup>1</sup> <https://www.cdc.gov/hiv/basics/transmission.html>

et al., 2013). To date, there is no vaccine available and current treatments and diagnostics are rather expensive. A new strategy to combat HIV-1 was taken in consideration after a patient known as the “Berlin patient” underwent total remission of HIV-1 after receiving two allogeneic hematopoietic stem-cell transplantations (HSCTs) from a homozygous CCR5 $\Delta$ 32 (CCR5 $\Delta$ 32/ $\Delta$ 32) donor as well as additional total body irradiation (Hutter et al., 2009). CCR5 expression and infection by HIV variants that interact with the CCR5 coreceptor is prevented due to the 32-base-pair deletion leading to HIV-1 resistance in these cells (Simmons et al., 1996). Another patient referred to as “London patient” received HSCT transplantation from homozygous CCR5 $\Delta$ 32 (CCR5 $\Delta$ 32/ $\Delta$ 32) donor in 2012 without chemotherapy and until now no viral load was detected (Gupta et al., 2019). Despite these promising results standard-of-care therapy won't be possible due to the rarity of suitable donors. Therefore, a comprehensive understanding of the HIV-1 life cycle and defining latent reservoirs is crucial for finding an affordable and commercial cure for HIV-1 infection.

## **7.2 HIV-Classification, genome organization and virion structure**

HIV is an enveloped lentivirus belonging to the family *Retroviridae*. It is a single-stranded, positive-sense RNA virus. Once HIV has entered the target cell, the virally encoded reverse transcriptase (RT) reverse transcribes the viral RNA into double-stranded DNA which is a unique feature of Retroviruses. There are multiple strains of HIV-1 which are subdivided in four distinct groups: M (major), following alphabetically N (non-M-non-O), O (outlier) and P (putative) (Hemelaar, 2012). HIV-1 belonging to group M is responsible for approximately 90 % of worldwide HIV infections. On the other hand, HIV-2, an HIV type that shares 50 % sequence homology with HIV-1, shows lower virulence and infectivity (Nyamweya et al., 2013). The other groups are locally confined to sub regions of Africa (Hemelaar, 2012), Portugal and France (Schim van der Loeff and Aaby, 1999, Soriano et al., 1996, Soriano et al., 2000, Damond et al., 2001).

The HIV-1 genome consists of two single stranded RNA molecules 9,7 kb of size that are imbedded in the core of the virus particle. The genome is flanked by short repeats at both ends (U3 and U5) (Wain-Hobson et al., 1985; Ratner et al., 1985). During reverse transcription, those repeats are duplicated, thereby forming the long terminal repeat sequences (LTRs). The 5' LTR region harbors the active promotor which is essential for transcription of the viral genes. The HIV genome consists of three major open reading frames: *gag* which codes for the group specific antigen (GAG) polyprotein; *pol* which codes for integrase, reverse transcriptase and the Pol precursor of viral enzyme protease; and the *envelope (env)* gene coding for Vpu, Vif,

Tat, Rev, Nef, and Vpr. Cellular or viral proteases process these precursors into mature particle-associated proteins. The 55-kDa Gag precursor Pr55<sup>Gag</sup> is cleaved into three independently folded proteins: matrix (MA), capsid (CA), nucleocapsid (NC), p6 domains and spacer peptides during or after the release of progeny virions (Bell and Lever, 2013). The 160 kd Gag-Pol polyprotein consists of the protease (PR), integrase (IN) and reverse transcriptase (RT). Proteolytic digestion by cellular enzymes converts the glycosylated Env precursor into gp120 surface (SU) and gp41 transmembrane (TM). The HIV-Env glycoprotein defines the tropism and mediates the entry into target cells. Cell tropism is mainly determined by CCR5 or CXCR4 expression on target cells (Regoes and Bonhoeffer, 2005). The remaining six open reading frames encode the following proteins: accessory proteins Vif (virion infectivity factor), Vpr (viral protein R), Rev (regulator of virion), Tat (trans activator of transcription), Vpu (viral protein U) and Nef (negative factor) (see Figure 1) (Coffin et al., 1997).

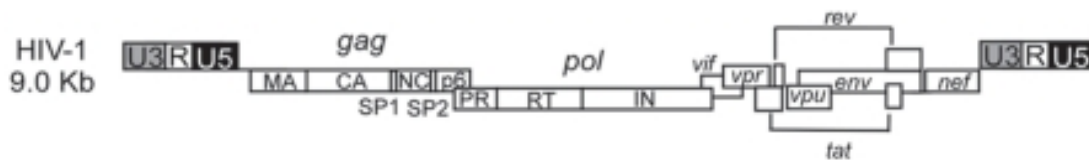


**Figure 1: HIV-1 genome.**

*HIV-1 consists of nine open reading frames. The coding region is flanked by long terminal repeats (LTRs). Gag encodes MA, CA, SP1, NC, SP2 and p6, pol encodes PR, RT and IN domain and the env gene which encodes envelope (Henderson et al.). Additional genes encode a set of accessory proteins vif, vpr, vpu, nef and tat. (Sandmeyer and Clemens, 2010)*

HIV-2 codes for virus protein X (Vpx) instead of Vpu, absence of Vpu is partially responsible for the reduced virulence and infectivity of HIV-2 (Vicenzi and Poli 2013). HIV-1 forms spherical particles measuring ~140 nm in diameter, which are enveloped by a lipid bilayer derived from the host cell plasma membrane (Herold et al.) (Briggs et al., 2003). Particles released from infected cells are initially in an immature state and upon protease activation a major rearrangement takes place. Gag is cleaved at five distinct cleavage sites leading to structural rearrangements resulting in a cone shaped capsid and to the mature, infectious virion containing the viral ribonucleoprotein particle, IN and RT (Campbell and Hope, 2015).

### 7.3 HIV-1 Replication

HIV-1 is a lentivirus and as an intracellular obligate parasite it depends on and exploits the host cell machinery (life cycle depicted in figure 2). The infection cycle starts with the interaction of gp120 which is part of the HIV-1 spike together with gp41 and CD4, the major cell surface receptor for primate lentiviruses (Chan and Kim, 1998, Bour et al., 1995). CD4 binding not



only serves to virion attachment to the target cell but also induces a major rearrangement in the gp41 protein structure, leading to engagement of the co-receptors C-C motif chemokine receptor 5 (CCR5) or C-X-C motif chemokine receptor 4 (CXCR4) (Trkola et al., 1996, Wu et al., 1996). This induces conformational changes taking place in gp41, the hydrophobic region at the N-terminus, the so-called fusion peptide inserts into the host cell membrane (Freed et al., 1990, Weissenhorn et al., 1997, Chan et al., 1997). After the so-called six-helix bundle is formed leading to close proximity of the opposed membranes and the formation of the fusion pore, the viral core is released into the cytoplasm (Herold et al., 2014, Doms and Moore, 2000).

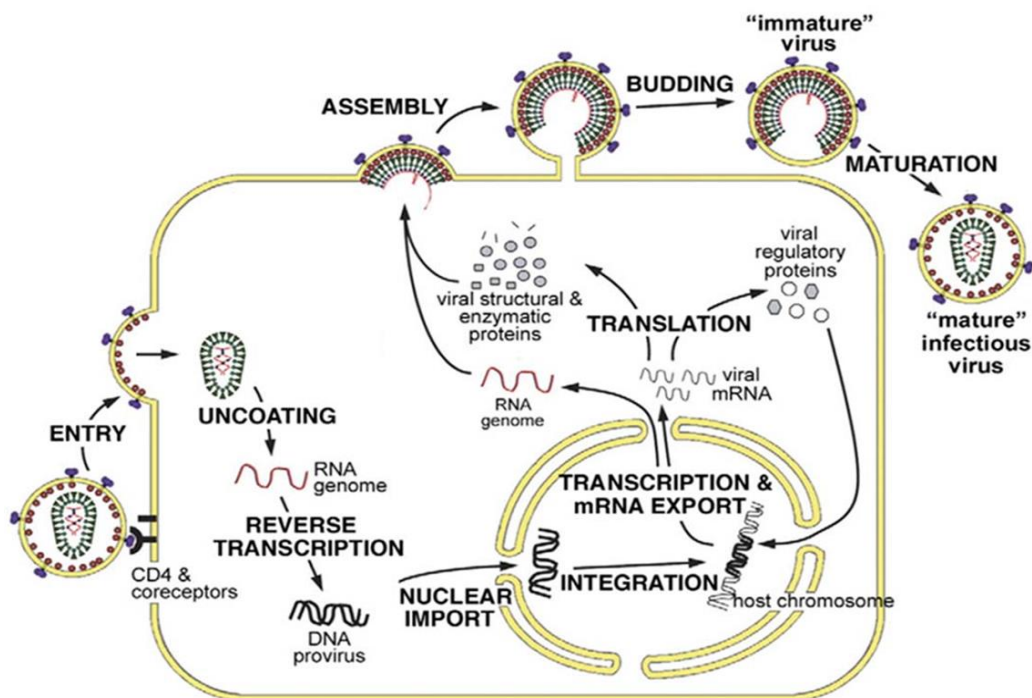


**Figure 2: Schematic representation of the *f* HIV-1 life cycle.**

The first step is the attachment of HIV-1 to a target cell followed by fusion of the virus with the host cell plasma membrane which results in viral core entry. Uncoating and reverse transcription of the viral RNA (vRNA) into viral DNA (vDNA) and the formation of the pre-integration complex takes place in the cytoplasm. The viral genome is transported in the nucleus where integration takes place. Transcription products and mRNA are exported into the cytoplasm where translation of the viral mRNAs into viral proteins occurs. Some viral proteins (e.g. Tat and Rev, both expressed from spliced viral mRNAs) can shuttle back into the nucleus to regulate proviral transcription and expression of viral structural and enzymatic proteins from partially spliced or unspliced mRNAs. These are exported from the nucleus by interaction of Rev with the Rev-response element in a way dependent on the cellular protein Crm1. Gag and GagPol assemble at the plasma membrane and recruit other viral structural proteins to the assembly site. The viral bud is pinched off by the cellular ESCRT machinery. Gag and GagPol are proteolytically cleaved and structural rearrangement takes place to form a mature, infectious viral particle. From (Ganser-Pornillos et al., 2008)

The diverse expression of cellular co-factors or antiviral resistance factors including post- entry restriction factors are often the reason for the differences in HIV-1 infectivity in different cell types. Intriguingly, a majority of restriction factors including tripartite motif-containing protein 5 (TRIM5 $\alpha$ ), apolipoprotein B mRNA editing enzyme, catalytic polypeptide-like 3G (APOBEC3G), sterile-alpha motif and HD domain containing protein 1 (SAMHD1) and myxovirus resistance 2 (MX2) target the early phase of HIV-1 infection at or during reverse

transcription as well as at the step of nuclear import (Malim and Bieniasz, 2012). During the early stages of the infection process the single stranded RNA (ssRNA) is converted into double stranded DNA (dsDNA) by the reverse transcription enzyme which also harbors a ribonuclease H (RNaseH) activity (Baltimore, 1970, Temin and Mizutani, 1992). Reverse transcription presumably takes place in the cytosol where reverse transcription complexes are formed containing ribonucleoproteins, IN and RT and cellular host factors. For DNA synthesis the host cell's dNTP pool is crucial. The synthesized DNA, which is flanked by long terminal repeats (LTRs) and several viral (e.g. RT, IN, CA, Vpr) and cellular (e.g. Lens epithelium-derived growth factor (LEDGF)) proteins form the pre-integration complex (PIC) and are targeted to the nucleus (Maillot et al., 2013). In addition to the linear double stranded viral DNA reverse transcription and nuclear import also yields two types of circular DNA termed 1-LTR and 2-LTR circles, which are a marker for nuclear import (Li et al., 2001). A characteristic feature of retrovirus replication is the integration of the viral genome into the host cell chromosome, preferably in transcriptionally active regions (Schroder et al., 2002). Integration of viral DNA is catalyzed by the viral Integrase (IN) (Farnet et al., 1996). The integrated viral genome (so-called provirus) serves as a template for the synthesis of viral RNA and maintains there for the lifespan of the host cell. It can either remain as a latent provirus or transcriptional activation can take place (Van Lint et al., 2013, Lusic and Siliciano, 2017). Transcription factors are recruited to the promotor in the 5' LTR region, which leads to the expression of viral genes. Tat, Rev and Nef are early transcribed viral accessory proteins which are expressed from fully spliced mRNA that is recognized as 'cellular' mRNA taking the same nuclear export pathway as most cellular mRNAs. The indispensable viral protein Tat increases the efficiency of transcription by binding to transactivation response RNA structure (*Tar*) and recruiting cellular factor such as RNA polymerase II (Kao et al., 1987, Fisher et al., 1986, Dayton et al., 1986). Accumulation of Rev facilitates nuclear export of viral unspliced or partially spliced mRNAs which are not exported by the normal cellular mRNA export pathway and encode Gag and Gag-Pol, Env, Vpr, Vif and Vpu (Jeang et al., 1999, Schwartz et al., 1990). After Gag synthesis, Gag is recruited to the membrane by MA where it anchors to the plasma membrane by using its myristyl residue as an anchor (Ono et al., 2004) and thereby initiates the recruitment of Env, viral GagPol and the accessory proteins Nef, Vpr and Vif and their incorporation into viral particles (Dorfman et al., 1994). Thereby, an immature viral bud is formed which is pinched off and released from the plasma membrane by the recruitment of the cellular ESCRT components (Bieniasz, 2006). In order to initiate infection of a new target cell the virion has to go through a maturation process (Peng et al., 1989, Kohl et al., 1988). The maturation process is initiated

by the activation of the protease which leads to Gag and GagPol cleavage into their components. Furthermore, Env distribution is changed and Gag subunits are rearranged to form the mature virion (Chojnacki et al., 2012).

## **7.4 Restriction factors**

In response to virus infection, cells have evolved antiviral factors, so called restriction factors. The incoming virus is sensed by the host cell proteins and, in response, viral replication and propagation is blocked. Many restriction factors are type I interferon (IFN) induced or type I IFN supports their activity (Schoggins et al., 2011, Jimenez-Guardeno et al., 2019). Type I interferon is a family of innate cytokines, including 13 IFN $\alpha$  subtypes and 2 types of IFN $\beta$  and during acute virus infection, type I interferons are mainly released by plasmacytoid dendritic cells (Fitzgerald-Bocarsly et al., 2008). IFNs can reduce HIV-1 replication in certain types of natural target cells by inducing the expression of a set of antiviral cellular genes that inhibit HIV-1 replication (Li et al., 2014, Chelbi-Alix and Wietzerbin, 2007). Besides being interferon inducible, restriction factors can have the following characteristics: self-sufficient activity, constitutive expression in some cell types, cause a significant decrease in viral infectivity, often act in a species-specific manner and are often antagonized by viral accessory proteins (Blanco-Melo et al., 2012). The following proteins are some of the known restriction factors that target HIV-1 and other primate lentiviruses (Figure 3). Tripartite-motif-containing 5 (TRIM5) proteins (Stremlau et al., 2004), Bone marrow stromal antigen 2 (Tetherin/ BST-2) (Neil et al., 2008, Van Damme et al., 2008), sterile alpha motif and HD domain containing 1 (SAMHD1) (Hrecka et al., 2011, Laguette et al., 2011a) the apolipoprotein B mRNA-editing enzyme catalytic polypeptide-like 3G/F (APOBEC3G/F) proteins (Sheehy et al., 2002), myxovirus resistance 2 (MX2) (Goujon et al., 2013a), serine incorporator 5/3 (Serinc3/5) (Usami et al., 2015, Rosa et al., 2015) and interferon-induced transmembrane proteins (IFITMs) (Lu et al., 2011).

APOBEC3G/F proteins belong to the AID/APOBEC family (apolipoprotein B mRNA editing enzyme, catalytic polypeptide-like) of cytidine deaminase enzymes and they restrict a broad range of viruses including hepatitis B virus as well as endogenous and pathogenic retroviruses (Suspene et al., 2005, Mahieux et al., 2005, Delebecque et al., 2006, Browne and Littman, 2008). In the absence of functional Vif protein and upon HIV-1 infection, APOBEC3G/F are incorporated into budding virions. During reverse transcription of the viral RNA, APOBEC3G/F catalyze cytosine-to-uracil deamination in the newly transcribed viral DNA leading to G-to-A hypermutations. This results in amino acid substitutions and premature STOP

codons which will result in the production of defective proteins as well as non-functional viral particles, achieving a strong inhibition of HIV-1 replication (Zhang et al., 2003, Mangeat et al., 2003, Harris et al., 2003). APOBEC3G binds to viral RNA during reverse transcription and prevents proper elongation by building a ‘road block’ at certain positions (Pollpeter et al., 2018). APOBEC3G/F are normally excluded from virions by the interaction with the viral Vif protein which recruits a ubiquitin ligase complex that leads to proteasomal degradation of APOBEC3G/F and prevents incorporation (Malim, 2006).

Tetherin/BST-2 is a transmembrane protein with an N-terminal transmembrane domain and a C-terminal glycosyl-phosphatidylinositol group. Due to the protein's unique structure, one end of the protein stays attached to the plasma membrane and the other to the viral membrane, hindering HIV-1 release. The trapped virions are eventually internalized and degraded via the endosomal/lysosomal pathway (Neil et al., 2008, Van Damme et al., 2008, Perez-Caballero et al., 2009, Miyakawa et al., 2009).

Tripartite motif (TRIM) proteins are a large family of E3 ubiquitin ligases which are important for cellular processes including cell differentiation, autophagy, carcinogenesis, apoptosis, antiviral immunity, and innate signaling (Ozato et al., 2008, Hatakeyama, 2017, Rajsbaum et al., 2014, Nisole et al., 2005). TRIM proteins consist of an N-terminal RBCC structure, which consists of an N-terminal RING E3 ligase domain (R), one or two B-box domains (B), and a coiled-coil domain (CC). The C-terminal domain(s) divides the TRIM proteins into subgroups. The most frequent domain is the PRYSPRY domain among TRIM family members. The PRYSPRY domain of TRIM5 $\alpha$  is crucial for the binding to the retroviral capsid and determines retroviral restriction (Sawyer et al., 2005, Stremlau et al., 2005, Yap et al., 2005). Certain New World monkey as well as some Old World monkey species have evolved on two independent occasions a fusion protein consisting of the TRIM5 RBCC and cyclophilin A (CypA) ((Song et al., 2005, Newman et al., 2008)). The TRIMCyp fusion protein of the Owl monkeys potently restricts HIV-1 infection, a process that can be antagonized by addition of cyclosporine A, which prevents interaction of the CypA domain with the viral capsid protein, thereby rescuing infection in cells from these monkeys (Keckesova et al., 2006).

The IFITM protein family is encoded by five genes in humans, including the immune-related *IFITM1*, *IFITM2*, and *IFITM3*, as well as *IFITM5* and *IFITM10* which have no characterized roles in immunity (Diamond and Farzan, 2013). Besides some HIV-1 restriction, IFITMs also show strong inhibition activities against dengue virus, influenza A virus, West Nile virus and vesicular stomatitis virus (Lu et al., 2011, Brass et al., 2009, Jiang et al., 2010, Weidner et al.,

2010). Lu et al. demonstrated that IFITMs inhibit the entry step that is mediated by the envelope proteins of certain viruses (Lu et al., 2011), especially IFITM 2 and IFITM3 (Yu et al., 2015). Viruses on the other hand have evolved countermeasures depicted in blue in figure 3. The HIV-1 capsid (CA) protein does not very efficiently interact with human TRIM5alpha although it strongly restricts equine infectious anemia virus (EIAV) and N-tropic murine leukemia virus (N-MLV) (Stremlau et al., 2004, Yap et al., 2004, Hatzioannou et al., 2004, Keckesova et al., 2004). However, a recent report suggested that even this weak interaction can lead to a substantial restrictive effect, in the presence of type I IFNs that activate the immunoproteasome (Jimenez-Guardeno et al., 2019). HIV-1 expresses Vif to counteract APOBEC3G/F and cause its degradation by the proteasome (Goila-Gaur and Strebel, 2008, Sheehy et al., 2002, Yu et al., 2003). HIV-1 Nef binds and prevents antiviral activity of SERINC proteins (Rosa et al., 2015, Usami et al., 2015). HIV-2 and SIVs have evolved the Vpx protein that binds to and induces the degradation of SAMHD1 (Hrecka et al., 2011, Laguette et al., 2011a). The antiretroviral activity of Tetherin is counteracted by the accessory protein Vpu of HIV-1 and by the Env protein of other lentiviruses (Van Damme et al., 2008). To date no apparent antagonistic viral protein against the IFN-induced MX2 protein or against SAMHD1 has been discovered for HIV-1. Restriction factor research, especially identifying novel restriction factors, promises to open up new ways to combat HIV/AIDS.

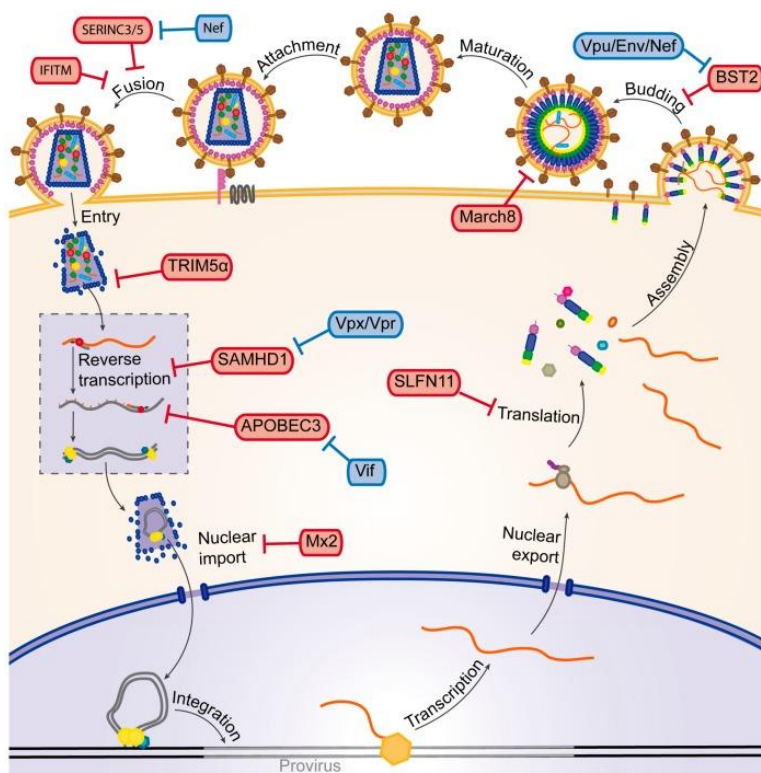


**Figure 3: Host restrictions factors and viral countermeasures.**

Viral host restriction factors are depicted in red and evolved viral countermeasures are shown in blue boxes. From (Seissler et al., 2017)

## 7.5 Vpx

Viral protein x (Vpx) is a 12-16 kDa viral protein encoded by simian immunodeficiency viruses (SIVs) and HIV-2 (Tristem et al., 1990). Vpx is incorporated into viral particles (Henderson et al., 1988, Franchini et al., 1988, Yu et al., 1988, Kappes et al., 1988) via an interaction with the p6 domain of Gag (Wu et al., 1994, Accola et al., 1999, Selig et al., 1999). Vpx harbors a C-terminal non-canonical nuclear localization signal (NLS) (65-SYTKYRYL-72) (Belshan and Ratner, 2003, Rajendra Kumar et al., 2003) as well as a presumed second N-terminal NLS (Singhal et al., 2006a). It is controversial whether Vpx can shuttle between the nucleus and cytoplasm (Belshan and Ratner, 2003, Singhal et al., 2006b). Upon transfection of plasmids encoding Vpx, the majority of the protein localizes to the nucleus (Depienne et al., 2000, Mahalingam et al., 2001, Belshan et al., 2006, Belshan and Ratner, 2003). Mangeot et al. published that the presence of Vpx during the transduction of monocyte-derived dendritic cells (MDDCs) with SIV<sub>MAC</sub> based-lentiviral vectors is crucial for infectivity (Mangeot et al., 2002). Later, it was shown that, when Vpx is delivered *in trans* via virus-like particles (VLPs), HIV-1 transduction of MDMs and MDDCs is increased, which correlates with the accumulation of viral DNA (Goujon et al., 2006). The proteomic studies of Le Rouzic yielded some fundamental insights on Vpx and its function. He as well as the team of Zhao discovered that HIV-1 Vpr recruits the damage-specific DNA binding protein 1 (DDB1)-Cullin 4A (CUL4A) E3 ubiquitin ligase complex through the interaction of VprBP (Zhao et al., 1994, Le Rouzic et al., 2007). In addition, VprBP was shown to be a substrate of DDB1-CUL4A-RBX1/ROC1 complex. VprBP was therefore renamed DDB1-CUL4A-associated factor 1 (DCAF1) (Angers et al., 2006). Le Rouzic *et al.* revealed with the help of the yeast-two hybrid system that Vpx from SIV<sub>MAC</sub> which is homologous to HIV-1 Vpr (Tristem et al., 1990) was able to interact with VprBP/DCAF1 (Le Rouzic et al., 2007). The fact that the interaction was confirmed in mammalian cells (Goujon et al., 2008, Sharova et al., 2008, Srivastava et al., 2008, Bergamaschi et al., 2009) and RNAi-mediated depletion of DDB1 or DCAF1 resulted in reduced infection of HIV-2 as well as SIV<sub>MAC</sub> in macrophages led to the following model: the Vpx protein recruits the DCAF1/DDB1/CUL4A E3 ubiquitin ligase complex initiating proteasomal degradation by poly-ubiquitination of a myeloid cell-specific restriction factor that prevents viral DNA accumulation (Sharova et al., 2008, Srivastava et al., 2008, Bergamaschi et al., 2009). In 2011, two independent studies revealed sterile alpha motif (SAM) and HD-domain containing protein 1 (SAMHD1) as one of the major binding partners of Vpx (Hrecka et al., 2011, Laguette et al., 2011a). Both studies showed that Vpx induces SAMHD1 degradation via proteasomal degradation (Figure 4 B). Lim *et al.* concluded that SAMHD1 antagonism is conserved in all

clades of Vpx proteins in a species-specific way (Lim et al., 2012). HIV-1 infection can be rescued from the type I IFN-induced block in myeloid cells when VLP containing Vpx from SIV<sub>MAC</sub> are added in *trans* prior to infection (Gramberg et al., 2010, Pertel et al., 2011, Goujon et al., 2013b). In contrast, adding Vpx<sub>MAC</sub> prior to infection with SIV<sub>MAC</sub> or HIV-2 does not relieve the type I IFN- induced block from SIV<sub>MAC</sub> nor HIV-2 in monocyte-derived dendritic cells (MDDC) (Pertel et al., 2011). The involvement of SAMHD1 in the Vpx<sub>MAC</sub> mediated rescue from the type I IFN induced block to HIV-1 infection is yet to be determined. Pertel et al. reported that the Vpx mutant Q76A which is unable to bind DCAF1 and to induce SAMHD1 degradation (Srivastava et al., 2008) was still able to rescue HIV-1 infection from the type I IFN response in MDDC (Pertel et al., 2011). Since DCAF1 binding to Vpx is essential for SAMHD1 degradation, SAMHD1's involvement in the Vpx mediated rescue from the type I IFN induced block to HIV-1 infection is questionable.

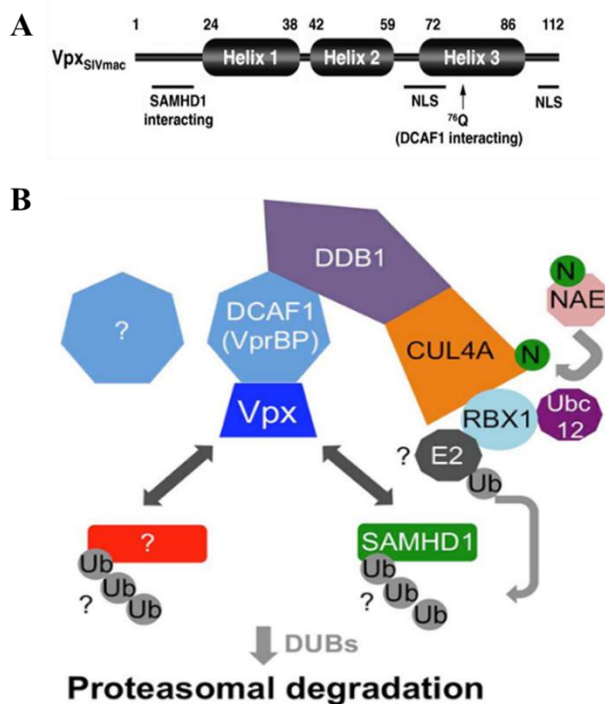


**Figure 4: Schematic illustration of Vpx protein from SIV<sub>MAC</sub> and model of Vpx mediated degradation of SAMHD1.**

**A)** Vpx schematic structure. The three  $\alpha$ -helices of Vpx, the nuclear localization signals (NLS) and the critical residue that determines Vpx interaction with DCAF1 (Q76) as well as the SAMHD1 interaction region are indicated. **B)** Model of Vpx recruitment by DCAF1-DDB1-CUL4A. Vpx binds to DCAF1 and recruits the DDB1-CUL4A-RBX1 E3 ubiquitin ligase complex. Vpx targets like SAMHD1 are ubiquitinated through the interaction of RBX1 with an E2 ligase. Neddylation of CUL4 is important for proper its functionality. RBX1 interacts with the ubiquitin-conjugating enzyme UBC12 which is crucial for the transfer of NEDD8 group from the NEDD8 activating enzyme (NAE). From (A)Zheng et al. 2012, (B)Schaller et al. 2014)

## 7.6 SAMHD1

### 7.6.1 Structure of SAMHD1

SAMHD1 is a 626 amino acid protein harboring an amino-terminal sterile alpha motif (SAM) domain (residues 40-109), a catalytic core domain (HD domain residue 110-599) and a C-terminus (residues 600-626) where the Vpx binding domain resides (Li et al., 2000, Liao et al., 2008) (Figure 5). Due to its nuclear localization signal (NLS) at residue 11-14 (Lys-Arg-Pro-Arg), SAMHD1 is localized in the nucleus (Hofmann et al., 2012, Brandariz-Nunez et al., 2012, Wei et al., 2012, Schaller et al., 2014)

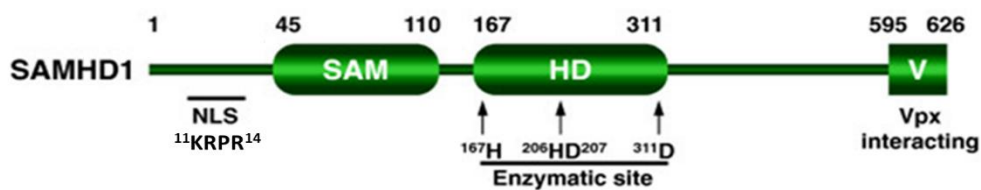


**Figure 5: Schematic representation of SAMHD1 domains.**

*SAMHD1 consists of a SAM and HD domain. The nuclear localization signal (KRPR) resides at the N-terminus of SAMHD1. The Vpx binding domain is located at the -C-terminus. The start and end of each domain is indicated. From (Zheng et al., 2012)*

The SAM domain is also found in other proteins and is commonly involved in protein-protein and protein-DNA/RNA interaction ((Kim and Bowie, 2003). The precise function of the SAMHD1 SAM domain has yet to be determined, but it was observed that it might be dispensable for retroviral restriction even though it might be required for maximal enzymatic activity (Beloglazova et al., 2013, White et al., 2013b). The HD domain of SAMHD1 contains the regulatory sites, the dNTPase active site and is crucial for oligomerization and may be involved in nucleic acid binding (Goldstone et al., 2011, Goncalves et al., 2012b, Koharudin et al., 2014a). The active site within the HD domain consist of a characteristic quartet of metal coordinating histidine and aspartic acid residues (H167, H206, D207 and D311) (Aravind and Koonin, 1998). Expression of the HD domain of SAMHD1 alone is sufficient to restrict HIV-1 infection (White et al., 2013b).

Crosslinking experiments show that SAMHD1 forms oligomers in cells and the enzymatically active form of SAMHD1 is a tetramer (Zhu et al., 2013, Ji et al., 2013). The SAMHD1 monomer consist of two distinct allosteric binding sites A1 and A2 and a substrate-binding site (S). Tetramerization is driven by guanine nucleoside triphosphate (GTP or dGTP) binding to A1 where a network of five specific hydrogen bonds are formed between the base edge of guanine and the surrounding residues of D137, Q142, and R145 (Ji et al., 2013, Yan et al., 2013). A1 has been identified to exclusively bind dGTP or GTP whereas A2 can bind all dNTPs (dATP,



dTTP, dGTP or dCTP (Figure 6). Given the fact that the physiologically GTP concentration is 1,000 fold higher as compared to dGTP (Kennedy et al., 2010) and that tetramer formation is more stable when GTP is bound due to an extra hydrogen bond formation between GTP and V117, it is likely that GTP is the primary allosteric activator (Amie et al., 2013, Koharudin et al., 2014a, Miazzi et al., 2014, Arnold et al., 2015).

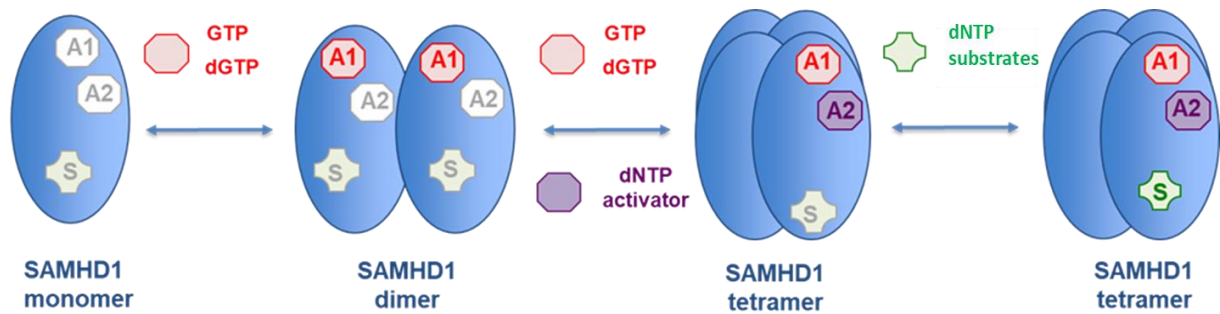


**Figure 6: Model of SAMHD1 tetramerization.**

Each SAMHD1 monomer consists of two allosteric sites A1 and A2 and a Substrate binding site. Under conditions of low level of dNTPs SAMHD1 is found in a monomer dimer equilibrium. Binding of GTP/dGTP to A1 stabilizes the SAMHD1 dimer. Upon elevation of the dNTP level above the activation threshold (1-20 $\mu$ M) GTP/dGTP and dNTP fill the allosteric sites leading to tetramerization of SAMHD1. Activated SAMHD1 can hydrolyze dNTPs to lower the levels of available dNTPs that would otherwise be cytotoxic for the cell and increase the mutation rate. Adapted from Herold et al., 2017b

As mentioned before SAMHD1 is localized in the nucleus. Nevertheless, the antiviral activity of SAMHD1 is not perturbed by disruption of its NLS sequence (Rice et al., 2009a, Brandariz-Nunez et al., 2012, Hofmann et al., 2012, Schaller et al., 2014) but disruption hinders SIV<sub>MAC</sub> Vpx-mediated SAMHD1 degradation (Brandariz-Nunez et al., 2012, Hofmann et al., 2012, Wei et al., 2012, Guo et al., 2013). Hofmann et al. showed that Vpx can bind to cytoplasmic as well as nuclear SAMHD1 (Hofmann et al., 2012). This raises the question why cytoplasmic SAMHD1 is less sensitive to Vpx-mediated degradation.

### 7.6.2 SAMHD1 is an HIV-1 restriction factor

SAMHD1 is a deoxynucleoside-triphosphate (dNTP) triphosphohydrolase (Goldstone et al., 2011, Powell et al., 2011, Yan et al., 2013, Lahouassa et al., 2012) and a restriction factor of HIV-1, likely by reducing the amount of dNTPs necessary for efficient reverse transcription thus reducing reverse transcription and DNA synthesis of the incoming virus (Goldstone et al., 2011, Lahouassa et al., 2012). For that reason HIV-1 infection in myeloid cells and resting CD4<sup>+</sup> T cells is rather inefficient (Lahouassa et al., 2012, St Gelais et al., 2012, Baldauf et al., 2012, Descours et al., 2012) resulting in accumulation of viral DNA reverse transcription intermediates (Korin and Zack, 1999). However, it has to be made clear that SAMHD1 presents only one block of likely several blocks, especially in resting CD4 T cells, since inactivation of

SAMHD1 in these cells does not rescue the large majority of infecting viruses (Descours et al., 2012, Baldauf et al., 2017). It is also still unclear whether the depletion of the intracellular dNTP pool alone is sufficient for HIV-1 restriction. It has been reported more recently that a putative RNase activity of SAMHD1 might be key for antiviral restriction (Beloglazova et al., 2013, Ryoo et al., 2014a). Ryoo et al and Choi et al. reported that SAMHD1 might be able to directly degrade viral RNA based on increased viral RNA levels when SAMHD1 was depleted in MDM, PMA differentiated THP-1 cells and CD4<sup>+</sup> T compared to non-depleted control cells (Ryoo et al., 2014a, Choi et al., 2015). Other groups question the RNase activity and claimed that the observed nuclease activity of immunoprecipitated SAMHD1 is due to an unknown co-purified protein (Seamon et al., 2015, Antonucci et al., 2016). Furthermore SAMHD1-mediated block is reversible in MDM thus it is questionable whether viral RNA degradation is crucial for SAMHD1-mediated lentiviral restriction (Hofmann et al., 2013).

Lentiviral restriction is prohibited by the phosphorylation at the residue T592 of SAMHD1 by the cell cycle regulator cyclin-dependent kinase 1/2 (CDK1/2) in proliferating cells (Cribier et al. 2013, St Gelais et al. 2014). Schott et al. recently reported that SAMHD1 levels did not change with respect to the cell cycle status in HeLa cells (Schott et al., 2018). Furthermore, cell-cycle analysis suggests that SAMHD1 dephosphorylation at T592 is controlled by the cell cycle and occurs during M/G1 transition in proliferating cells. The authors identified PP2A-B55 $\alpha$  holoenzyme as a key regulator of SAMHD1 dephosphorylation and thus switches on antiviral restriction (Schott et al. 2018). The phosphorylation defective mutant of SAMHD1 (T592A) was shown to have antiviral functions in resting as well as dividing U937 cells (Cribier et al. 2013). Furthermore, the SAMHD1 phosphomimetic mutant T592E was unable to restrict HIV-1 infection (Welbourn et al. 2013, White et al. 2013). Despite the discrepancy of SAMHD1's antiviral function in cycling vs. non-cycling cells, the phosphorylation status did not affect SAMHD1's ability to hydrolyze dNTPs, suggesting for an dNTPase-independent restriction mechanism (White et al. 2013).

Recent publication identified that SAMHD1 is not only modified by phosphorylation but can also be modified by acetylation (Lee et al., 2017), SUMOylation (Lamoliatte et al., 2014, Hendriks et al., 2017, Lumpkin et al., 2017) and ubiquitination (Elia et al., 2015). The impact of the mentioned SAMHD1 modification on HIV-1 restriction is yet to be determined. Additionally, redox active cysteines were identified in SAMHD1 and are thought to be required for lentiviral restriction (Wang et al., 2018, Mauney et al., 2017). The C522S amino acid substitution had no detectable detrimental effect on SAMHD1 tetramerization or dNTPase activity *in vitro*. The authors reasoned that nucleotide dependent tetramerization and dNTPase

activity were needed but not sufficient for the block of retroviral infection, suggesting that the redox state of C522 is crucial for the SAMHD1 restriction mechanism of HIV-1 infection. (Wang et al., 2018). The involvement of an SAMHD1 binding partner might modify SAMHD1 and thereby influence HIV-1 restriction. Majer et al. suggested that SAMHD1-mediated restriction involves not only its dNTPase function but rather involves a combination of several modifications and functions of SAMHD1 (Majer et al., 2019). SAMHD1 depletion in dendritic cells or macrophages drastically enhances HIV-1 infection, reflecting that HIV-1 does not encode an obvious SAMHD1 antagonist. Additionally, in the presence of Vpx, HIV-1 experimentally made to infect dendritic cells causes the induction of an antiviral state and cytokine production (Manel et al., 2010). This led to the hypothesis that HIV-1 has evolved to avoid infection of myeloid cells *in vivo* possibly to reduce proinflammatory cytokine production and antigen presentation to minimize adaptive immune responses (Manel et al., 2010). SAMHD1 was shown to be expressed to similar levels in resting CD4+ T cells, MDMs and in activated CD4+ T cells (Baldauf et al., 2012, Descours et al., 2012), hence expression levels alone could not explain differential phenotypes with regards to Vpx-induced rescue of HIV-1 infection.

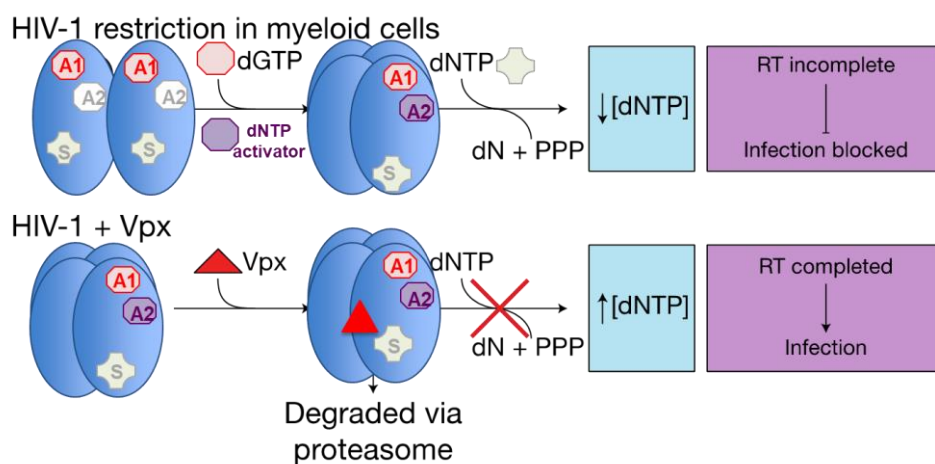


**Figure 7: Model for SAMHD1 function in HIV-1 restriction.**

*In myeloid cells infected with HIV activated SAMHD1 catalyzes the cleavage of dNTPs into the composite deoxynucleoside and inorganic triphosphate. The deoxynucleotide pool is suppressed thus reverse transcription is inhibited leading to a block of HIV-1 infection. In the presence of Vpx, Vpx hijacks the DDB1-CUL4A-RBX1 E3 ubiquitin ligase complex by recruiting DCAF1 thereby initiating proteasomal for degradation of SAMHD1 SAMHD1 can no longer reduce the pool of dNTPs necessary for reverse transcription. modified from (Goldstone et al., 2011)*

### 7.6.3 Deoxynucleotide metabolism overview

Precise regulation of the intracellular dNTP level is crucial to cell survival and genomic integrity (Meuth, 1989, Kumar et al., 2011, Kumar et al., 2010, Buckland et al., 2014). In order to control synthesis and degradation organisms have evolved complex and dynamic mechanisms and checkpoints (Figure 8) (Lane and Fan, 2015, Rampazzo et al., 2010). Enzymes are frequently regulated in a concentration dependent manner with respect to their substrates and products, usually via allosteric activation or inhibition (Hofer et al., 2012, Wallden and Nordlund, 2011, Johansson et al., 2001, Hunsucker et al., 2005, Bianchi and Spychala, 2003). dNTP synthesis consists of two distinct pathways; the *de novo* synthesis and the salvage pathway (Reichard, 1988, Mathews, 2006). The key enzyme in the *de novo* synthesis is the ribonucleotide reductase (RNR) which converts ribonucleoside diphosphate (NDPs) to deoxyribonucleoside diphosphate (dNDPs) which are subsequently phosphorylated to provide dNTPs for DNA synthesis and repair. SAMHD1 and RNR are similar in the way that both have two allosteric sites and one catalytic site. Furthermore the active form of both enzymes is an oligomer (Aye et al., 2015). The salvage pathway is constantly active in the cytosol and in mitochondrial compartments (Figure 8) (Rampazzo et al., 2010).

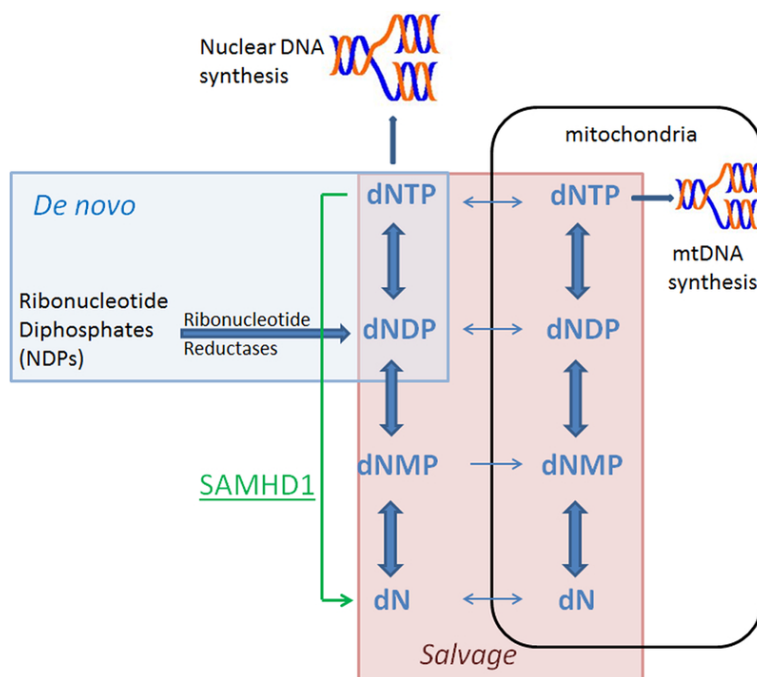


**Figure 8: Overview of the dNTP metabolism.**

The *de novo* pathway of dNTP synthesis is depicted in a blue box and the salvage pathway in red. The salvage pathway consists of complementary pathways in the cytosol and mitochondria. In order to maintain the dNTP level cellular kinases, phosphorylate deoxynucleosides (dN) and deoxynucleotides (dNMP, dNDP), while 5'-deoxynucleotidases and phosphorylases catalyze the opposing reactions. The SAMHD1 triphosphohydrolase reaction is highlighted in green. SAMHD1 is crucial to maintain the dNTP levels. From (Mauney and Hollis, 2018)

#### 7.6.4 *SAMHD1* in cancer

*SAMHD1* not only acts as a host restriction factor for viral infections, mutations in the *SAMHD1* gene have been linked to a genetic immune disorder called Aicardi-Goutières Syndrome (AGS) as well as several types of cancer (Kohnken et al. 2015, Rice et al. 2009). These suggest the involvement of *SAMHD1* in the innate immune response and cancer development through the control of dNTP homeostasis.

Acute myelogenous leukemia (AML) is the most common acute leukemia in adults (Saletta et al., 2014). The backbone treatment against AML is the cytostatic deoxycytidine analog cytarabine (ara-C) (Rowe, 2013). In response to ara-C therapy, AML blasts accumulate the active metabolite ara-C triphosphate (ara-CTP) (Zittoun et al., 1987, Kessel et al., 1969, Heinemann and Jehn, 1990, Estey et al., 1987) which leads to DNA damage due to perturbation of DNA synthesis (Kufe et al., 1984). Antimetabolites such as 2'-deoxyribonucleosides, arabinose nucleoside analogs or other nucleoside derivatives- are an important class of chemotherapeutic agents and are used to treat cancer and viral infection (Balzarini, 2000, Parker, 2009, Hurwitz and Schinazi, 2013, Tsesmetzis et al., 2018). Hollenbaugh et al. studied the effect of stereoselective 2' substitution of nucleoside analogues on *SAMHD1* activity. Modeling of dCTP and ara-CTP into the catalytic pocket of *SAMHD1* and biochemical analysis revealed that dCTP and ara-CTP fit within the catalytic site and are hydrolyzed in the presence of *SAMHD1* (Hollenbaugh et al., 2017).

There is increasing evidence for a tumor suppressor function of *SAMHD1*. Clifford *et al.* found *SAMHD1* mutations in chronic lymphocytic leukemia (CLL) and they propose that mutated *SAMHD1* could contribute to promoting leukemia development (Clifford et al., 2014). Furthermore Rentoft *et al.* analyzed 217 colon adenocarcinomas presented in The Cancer Genome Atlas (TCGA) and identified eight associated *SAMHD1* mutations. These *SAMHD1* mutations were found in hypermutated tumors of which six had mutations in genes encoding mismatch repair components. Furthermore, the calculated mutation rate within the *SAMHD1* gene was higher than random ( $p=0.049$ ) (Rentoft et al., 2016). The *in vitro* dNTPase activity of four chosen amino acid variants (V133I, A338T, R366H, D497Y) were analyzed and all four mutations showed an overall reduced activity in comparison to wildtype with alternating specificity for the canonical dNTPs, which suggested an imbalanced dNTP pool in these cancer-associated mutations. Interestingly, *SAMHD1* R366H had reduced activity toward dTTP, dCTP and dATP, whereas dGTP hydrolysis was almost unaffected (Rentoft et al., 2016).

## **8 Aims of this thesis**

### **8.1 SAMHD1's role in the type 1 interferon induced early block to HIV-1 infection**

SAMHD1 is the target of the Vpx protein from simian lentiviruses and HIV-2 (Hrecka et al., 2011, Laguette et al., 2011b). Vpx mediates the recruitment of the CUL 4-DDB1-DCAF1 ubiquitin ligase machinery to SAMHD1 in order to polyubiquitinate and degrade SAMHD1 (Le Rouzic et al., 2007). Early studies on monocyte-derived dendritic cells suggested that the Vpx-induced rescue of HIV-1 infectivity from early type I IFN-induced blocks was independent of SAMHD1, since the Vpx mutant Q76A, which is unable to recruit DCAF1 and hence unable to degrade SAMHD1, still rescued HIV-1 infection from the type I IFN-induced block (Pertel et al., 2011). To investigate the role of SAMHD1 in the Vpx-mediated rescue of HIV-1 from the type I IFN induced block in myeloid cells, we generated CRISPR/Cas9 THP-1 cells lacking a functional SAMHD1 gene. The aim of the PhD thesis was to investigate SAMHD1's role in the IFN induced block to HIV-1 infection and in the Vpx-mediated rescue of HIV-1 from the type 1 interferon induced block. We also aimed to further characterize known ISGs blocking HIV-1, including IFITMs and MX2 and investigate their involvement in the Vpx mediated increase of infectivity to HIV-1 infection. Despite the fact that HIV-1 does not encode Vpx, Vpx serves as a tool to further characterize the underlying mechanism of ISGs and their involvement in HIV-1 infection.

### **8.2 Correlation of SAMHD1 dNTPase activity with HIV-1 restriction by using cancer-associated naturally occurring SAMHD1 variants**

We and others demonstrated that SAMHD1 is able to detoxify ara-C treated cells by reducing the pool of intracellular ara-CTP (Herold et al. 2017, Schneider et al. 2017). The backbone treatment against AML is the cytostatic deoxycytidine analog cytarabine (ara-C) (Rowe 2013). Several studies reported mutation of SAMHD1 that contribute to the formation of cancer (Rentoft et al., 2016, Clifford et al., 2014).

Cancer associated mutations could lead to imbalanced dNTP levels due to malfunction of the dNTPase, which could also result in differences in ara-CTP hydrolysis. In this way, the ara-C cytotox assay is an ideal tool to directly compare enzymatic activity (ara-C hydrolysis may correlate with dNTPase activity) with HIV-1 restriction in the same cells.

Therefore, I expressed known SAMHD1 single nucleotide polymorphisms (SNPs) that have been correlated with carcinogenesis and analyzed ara-C sensitivity as well as restrictive activity towards HIV-1 infection. The identification of SNPs altering the sensitivity to certain anti-

cancer chemotherapies could be a key for future personalized treatment and understanding the contribution of SAMHD1's dNTPase activity towards HIV-1 restriction and to the type I IFN-induced block in certain cell types may help to develop new strategies to combat HIV/AIDS. Linking both fields and activities will help to untangle the different roles of SAMHD1 in viral restriction, as resistance factor in chemotherapy and as a possible tumor suppressor in certain malignancies.

## 9 Material and Methods

### 9.1 Material

#### 9.1.1 Laboratory equipment

Name	Company
Bacteria Incubator (IN75)	Memmert, Schwabach, Germany
Bacteria Shaker Multitron Pro	Infors, Bottmingen, Switzerland
C1000 Touch Thermal Cycler	BioRad, Hercules, USA
Cell Culture Centrifuge (MegaFuge 40R)	Heraeus, Hanau, Germany
Centrifuge J2HS with rotor JA-10	Beckman Coulter, Brea, USA
CFX 96 Real Time PCR detector (for SG-PERT)	BioRad, Hercules, USA
Electrophoretic Transfer Cell Mini Trans-Blot®	BioRad, Hercules, USA
Flow cytometer FACS Canto II	BD Biosciences, Franklin Lakes, USA
Gel iX Imager (Agarose gel UV-imager)	INTAS Science Imaging, Göttingen, Germany
Ice Maker AF 103	Scotsman, Sprockhövel
Incubator C200	Labotect Labor-Technik-Göttingen, Rosdorf
L8-70M Ultracentrifuge with SW28 and SW32 rotor	Beckman Coulter, Brea, USA
Leica DMIL Led Fluorescent Microscope	Leica Microsystems, Wetzlar
Leica TCS SP8 laser scanning confocal microscope	Leica Microsystems, Wetzlar
Light Microscope ELWD 0.3 T1-SNCP	Nikon Instruments Inc., Melville, USA
Luminoscan Ascent (Luminescence plate reader)	Thermo Scientific, Waltham, USA
Microwave for Agarose gels	Sharp, Cologne
Mini-PROTEAN® Tetra Vertical Electrophoresis Cell	BioRad, Hercules, USA
NanoPhotometer	Implen, Munich
Neubauer Counting Chamber	Marienfeld, Lauda-Königshofen, Germany
PCR FlexCycler2	Analytik Jena, Jena
pH-Meter (FiveEasy)	Mettler-Toledo, Columbus, OH, USA
Plate Reader Inifinite M200 Pro	Tecan, Männedorf, Switzerland
Roller Mixer SRT6	Stuart, Staffordshire, UK
Thermoblock Eppendorf ThermoMixer® comfort	Eppendorf, Hamburg, Germany



### 9.1.2 Laboratory materials

<b>Name</b>	<b>Company</b>
Blotting paper 3MM Chr	Whatman, Dassel, Germany
Cell Culture Dishes (100 x 20 mm) CELLSTAR®	Greiner Bio-One, Kremsmünster, Austria
Cell Culture Flasks (25, 75 and 175 cm <sup>2</sup> ) CELLSTAR®	Greiner Bio-One, Kremsmünster, Austria
Cell Culture Multiwell Plates (6, 12, 24, 48 well) CELLSTAR®	Greiner Bio-One, Kremsmünster, Austria
Counting Chamber Neubauer-improved	Paul Marienfeld GmbH & Co.KG, Lauda-Königshofen, Germany
Cover glasses thickness No. 1 circular	Paul Marienfeld GmbH & Co.KG, Lauda-Königshofen, Germany
Disposable Nitrile Gloves TouchNTuff® 92-600	Ansell, Richmond, Australia
Filtered Tips AvantGuard™ (20 µl)	Midwest Scientific, Valley Park, USA
Filtered Tips OneTouch™ (10 µl, 200 µl, 1000 µl)	Sorenson BioScience, Salt Lake City, USA
Fluid aspiration system BVC professional	VACUUBRAND, Wertheim, Germany
Microscope slides thickness approx. 1 mm	Paul Marienfeld GmbH & Co.KG, Lauda-Königshofen, Germany
Multichannel Pipettes 8- and 12-channel (10 µl, 100 µl, and 300 µl) Eppendorf® Research® plus	Eppendorf, Hamburg, Germany
PCR Tubes (0,2 mL) Eppendorf tubes®	Eppendorf, Hamburg, Germany
PIPETBOY acu 2	INTEGRA Biosciences AG, Zizers, Switzerland
Pipetting Reservoirs (25 mL)	Argos Technologies, Vernon Hills, USA
Plastic paraffin film Parafilm®	Bemis Company, Neenah, USA
Polypropylene Tubes (15 ml, 50 ml) CELLSTAR®	Greiner Bio-One, Kremsmünster, Austria
PVDF membrane, Immobilon-FL 0.45 µm	Merck Millipore, Billerica, USA
Reaction tubes (0.5-2ml)	Sarstedt, Nümbrecht
Serological pipette (5 ml, 10 ml, 25 ml, 50 ml)	Sarstedt, Nümbrecht, Germany
Single Channel Pipettes (P2µl, P10µl, P20µl, P200µl, P1000µl) PIPETMAN Neo®	Gilson Inc., Middleton, USA
Surgical Disposable Scalpels	B. Braun Melsungen, Melsungen, Germany
Syringe filters units (0.22 µm, 0.45 µm) Millex®	Merck Millipore, Billerica, USA
Syringe filters units (0.45 µm) Rotilabo® KH55.1	Carl Roth, Karlsruhe, Germany
Syringes (1ml, 3ml, 5 ml, 10 ml, 60 ml) BD Luer-Lok™	Becton Dickinson, Franklin Lakes, USA
Tubes (0,5 ml, 1.5 ml, 2 ml) SafeSeal	Sarstedt, Nümbrecht, Germany

### 9.1.3 Kits

Name	Company
CD4+ T Cell Enrichment Cocktail RosetteSep™	Stemcell Technologies, Vancouver, Canada
MycoAlert Mycoplasma Detection Kit	Lonza, Basel, Switzerland
NucleoBond PC 500	Macherey-Nagel, Dueren
NucleoBond® Xtra Midi EF	Macherey-Nagel, Dueren, Germany
NucleoSpin® Gel and PCR Clean-up	Macherey-Nagel, Dueren, Germany
QIAamp® DNA Mini Kit	Qiagen, Hilden, Germany
Qiagen Plasmid Plus Midi kit	Qiagen, Hilden
QIAprep® Spin Miniprep Kit	Qiagen, Hilden, Germany
QuikChange Site-Directed Mutagenesis Kit	Agilent Technologies, Santa Clara, USA

### 9.1.4 Chemicals and reagents

Reagent	Company
Agarose	Fisher Bio Reagents, USA
Ammonium persulfate (APS)	Sigma-Aldrich, St. Louis, USA
Blasticidin	Thermo Scientific, Waltham, USA
Bromophenol blue	Chroma, Fürstfeldbruck
BSA 100x	NEB, Ipswich, USA
CellTiter 96® AQueous One Solution	Promega, USA
Clarity Western ECL Substrate	BIO-RAD, USA
DMSO	Merck, Darmstadt, Germany
DNA ladder 1 kb Plus	Thermo Scientific, Waltham, USA
dNTP Set	Thermo Scientific, Waltham, USA
EDTA	Merck, Darmstadt, Germany
Ethanol (99 %) (EtOH)	Zentralbereich INF, Heidelberg
Gel Loading Dye, Purple (6x) for DNA	New England Biolabs, Ipswich, USA
Glycerol	AppliChem GmbH, Darmstadt, Germany
Glycine	Carl Roth, Karlsruhe, Germany
Isopropanol	Sigma-Aldrich, St. Louis, USA
LB Broth (Lennox)	Sigma-Aldrich, St. Louis, USA
Methanol (MeOH)	Sigma-Aldrich, St. Louis, USA
MIDORI <sup>Green</sup> Advance	Nippon Genetics Europe GmbH, Dueren, Germany
Milk powder	Carl Roth, Karlsruhe, Germany
Paraformaldehyde (PFA)	Merck, Darmstadt
PBS Dulbecco Powder	Biochrom GmbH, Berlin, Germany
Phorbol 12-myristate 13-acetate (PMA)	Sigma-Aldrich, St. Louis, USA
Polyethylenimine (PEI)	Sigma-Aldrich, St. Louis, USA
Precision Plus Protein™ WesternC™ Standards	BioRad, Hercules, USA
Protease inhibitor tablets, EDTA-free	Roche, Mannheim

Protein marker (PageRuler Prestained)	Thermo Scientific, Schwerte, Germany
Puromycin	Merck Millipore, Darmstadt
Sodium Acetate	Sigma-Aldrich, St. Louis, USA
Sodium Chloride	Sigma-Aldrich, St. Louis, USA
Sodium dodecyl sulfate (SDS)	Applichem, Karlsruhe
Sucrose	Sigma-Aldrich, St. Louis, USA
Tetramethylethylenediamine (TEMED)	Carl Roth, Karlsruhe, Germany
Trypsin	Biochrom, Berlin, Germany
Tween 20	Carl Roth, Karlsruhe, Germany
$\beta$ -Mercaptoethanol	Sigma-Aldrich, St. Louis, USA

### 9.1.5 Buffers and solutions

Name	Component	Concentration
Buffer TfB1	KAc	30 mM
	RbCl	100 mM
	CaCl	10 mM
	MnCl	50 mM
	glycerol in H <sub>2</sub> O	15 %
Buffer TfB2	PIPES	10 mM
	CaCl <sub>2</sub>	75 mM
	RbCl	10 mM
	glycerol in H <sub>2</sub> O	15%
PBS 1x	H <sub>2</sub> O	
	NaCl	140 mM
	KCl	2.7 mM
	Na <sub>2</sub> HPO <sub>4</sub>	8 mM
	KH <sub>2</sub> PO <sub>4</sub>	1.8 mM
PBS-T	PBS 1x	
	Tween-20	0.1 % (v/v)
SDS blotting buffer	H <sub>2</sub> O	
	Tris	48 mM
	Glycine	39 mM
	SDS	0.04 % (w/v)
	Methanol	20% (v/v)
1x SDS Running Buffer	H <sub>2</sub> O	
	Glycine	190 mM
	SDS	0.1% (w/v)
	Tris HCl	25 mM
SDS sample buffer 3 x (for loading of lysed samples)	ddH <sub>2</sub> O	
	Tris-HCl pH 6.8	150 mM
	SDS	6 % (w/v)

	Glycerol Bromophenol Blue DTT	30 % (w/v) 0.02% (w/v) 150 mM
WB Stripping Buffer	ddH <sub>2</sub> O  NaOH	0.5 M
Mowiol embedding medium	PBS Mowiol 4-88	8mM
WB Blocking Buffer	1 xPBS milk powder	5% (w/v)

### 9.1.6 Cell culture media

Name	Medium	Supplements
DMEM+++	DMEM, high glucose (GIBCO)	10% FCS heat inactivated 100 U/ml penicillin 100 µg/ml streptomycin
RPMI+++	(GIBCO)	10% FCS heat inactivated 100 U/ml penicillin 100 µg/ml streptomycin
Freezing media	FCS	10 % DMSO or glycerol depending on cell type
OptiMEM	OptiMEM (GIBCO)	
Selection media	RPMI (GIBCO)	puromycin or blasticidin

### 9.1.7 Enzymes

Name	Company
GoTaq Hot Start DNA Polymerase	Promega, USA
Pfu Polymerase	Promega, USA
Phusion High Fidelity DNA Polymerase	New England Biolabs, USA
T4 DNA Ligase	New England Biolabs, USA
HindIII	New England Biolabs, USA
DPN1	New England Biolabs, USA
EcoRI	New England Biolabs, USA
Not	New England Biolabs, USA

### 9.1.8 Drugs

Name	Company
IFN $\alpha$ 2 I (Roferon-A, IFN $\alpha$ -2a)	Dr. Kathrin Sutter (Universitätsklinikum Essen)
Cytarabine	Sigma-Aldrich

### 9.1.9 Antibodies

Name	Antigen	Company	Species	Application
3F10	HA	Roche Applied Science, Burgess Hill, UK	mouse, monoclonal, HRP linked	1:5000 in WB
ECL Mouse IgG	mouse IgG	GE Healthcare, Little Chalfont, UK	sheep, polyclonal HRP linked	1: 5000 in WB
ECL Rabbit IgG	rabbit IgG	GE Healthcare, Little Chalfont, UK	donkey, polyclonal HRP linked	1:5000 in WB
SAMHD1	rabbit	Biomol, BETHYL Laboratorie, INC	Polyclonal	1:1000 WB/IF
HSP 90 $\alpha$ / $\beta$	rabbit	SANTA CRUZ Biotechnology	Polyclonal IgG	1:3000 WB
$\beta$ -Actin	mouse	Sigam	monoclonal	1:3000
pSAMHD1	rabbit	Cell Signaling Technology	monoclonal	1:1000 WB

### 9.1.10 Plasmids and constructs

Plasmid name	Description	Source
SIV3+deltaVpx	SIV GagPol encoding plasmid lacking Env, lacking accessory protein Vpx	Caroline Goujon (KCL, London, UK)
pCSXW HASAMHD1	Used to create n-term HA-tagged codon optimized SAMHD1	Torsten Schaller
pCSXW HASAMHD1interm codon optimized	N-terminal HA-tagged N-terminal codon optimized (gRNA escape) human SAMHD1	Template: CSXW HASAMHD1
CSXWdE HAVp <sub>MAC</sub>		Torsten Schaller (UCL London)
CSXWdE HAVp <sub>RCM</sub>		Torsten Schaller (UCL London)

pCSGW	HIV-1 vector encoding GFP	(Bainbridge et al., 2001)
pCSxW	HIV-1 vector	(Schaller et al., 2014)
pCSxW-HA	HIV-1 vector hemagglutinin (HA)- tagged	Torsten Schaller (UCL London UK)
p8.91 (pCMVdR8.91)	HIV GagPol encoding plasmid.	(Zufferey et al., 1997)
plentiCRISPRv2	puromycin resistance marker to express guide RNAs (gRNAs) constructs for CRISPR-mediated genome editing	Addgene, Cambridge, USA
plentiCRISPRv2SAMHD1 gRNA2	gRNA targeting human SAMHD1	Torsten Schaller (Universitätsklinikum Heidelberg)
plentiCRISPRv2SAMHD1 gRNA3	gRNA targeting human SAMHD1	Torsten Schaller (Universitätsklinikum Heidelberg)
pNL4.3	Full-length HIV-1 lab strain NL4.3	Torsten Schaller (UCL London, UK)
pNL4.3-GFP	Full-length NL4.3 encoding GFP in place of Nef followed by an IRES-Nef cassette	Torsten Schaller (UCL London, UK)
pNLENG-IRES-Nef	Full-length NL4.3 encoding GFP in place of Nef followed by an IRES-Nef cassette	(Levy et al., 2004)
pcDNA Vp <sub>xMAC</sub> Q76A flag		Caroline Goujon (KCL London, UK)
SIV3+		Torsten Schaller (UCL London) (Negre et al., 2000, Mangeot et al., 2000)
pMD.G22	VSV-G expression plasmid	Didier Trono lab.

pcDNA WT V <sub>px</sub> <sub>MAC</sub> flag		Caroline Goujon (KCL London, UK)
--	--	-------------------------------------

### 9.1.11 Primer

Sequencing SAMHD1	OTS 230	AAAGAGCTCACAACCCCTCACTCG
	OTS 733	ATTTTGTAATCCAGAGGTTG
	OTS 20	TCATGATCTCGGTCATGGGCC
n-term HA tagged codon optimized SAMHD1 primer	OTS1393	GCATGCGGCCGCTCACATTGGGTCATCTTTAA AAAGC
	OTS1394	ATCGAATTCATGCAGCGAGCCGATTCCGAGCA GCCGTCAAACGACCCAGATGTGACGATTCAC CAAGAACCCCTCAAACAC

The sequencing primer OTS 733/230 bind within the Vector.

### 9.1.12 SAMHD1 SNP constructs

For all SNP constructs n-term HA tagged codon optimized SAMHD1 plasmid was used for mutagenesis.

SNP	Primer name	Sequence
H233A	OTS 293	AGGTGAAATGGACGGCTGAACAAGGCTCAGTTATG
	OTS 294	TAACTGAGCCTTGTTTCAGCCGTCCATTTACCTCC
D311A	OTS79	TGGCATTGATGTGGCCAAATGGGATTATTTTG
	OTS80	ATAATCCCATTTGGCCACATCAATGCCATTTC
T592A	OTS467	AGCCCCACTCATAGCACCTCAAAAAAAGG
	OTS468	TTTTGAGGTGCTATGAGTGGGGCTATAAC
T592E	OTS469	AGCCCCACTCATAGAACCTCAAAAAAAGG
	OTS470	TTTTGAGGTTCTATGAGTGGGGCTATAAC
D137N	OTS884	TCCGAATCATTAAATACACCTCAATTTCAAC
	OTS885	ATTGAGGTGTATTAATGATTCGGACGAGGAG
V133I	OTS1624	ACCCTCTCCTCATCCGAATCATTGATACAC
	OTS1625	ATCAATGATTCGGATGAGGAGAGGGTGGAG
A338T	OTS1626	TTATTAAGTTTACCCGTGTCTGTGAAGTAG

	OTS1627	TTCACAGACACGGGTAAACTTAATAAAGCG
R366H	OTS1628	TGTTCCCACTCACAACCTTTACACCGTAG
	OTS1629	GGTGTAAGAGTTGTGAGTGTGGAACATGTC
D497Y	OTS1630	TGAAGGCTGAATATTTTATAGTGGATGTTATC
	OTS1631	ATCCACTATAAAATATTCAGCCTTCAGTTTC
R145Q	OTS1705	TTCAACGTCTTCAATACATCAAACAGCTG
	OTS1706	GTTTGATGTATTGAAGACGTTGAAATTGAG
G90R	OTS1715	TTGAAAATCTTAGAGTAAGTTCCTTGGGGG
	OTS1717	AGGAACTTACTCTAAGATTTTCAAACGAG
C522A	OTS1854	TGTTAGCTTCTATGCTAAGACTGCCCCAAC
	OTS1855	GGGCAGTCTTAGCATAGAAGCTAACATGATC
C522S	OTS1856	TGTTAGCTTCTATAGTAAGACTGCCCCAAC
	OTS1857	GGGCAGTCTTACTATAGAAGCTAACATGATC
A76T	OTS1861	AAATCACAGGCACATTACTGCCTTGTCTTG
	OTS1862	AGGCAGTAATGTGCCTGTGATTTTCATTTTC
R305I	OTS1873	TATCTAATAAAATAAATGGCATTGATGTGG
	OTS1874	ATCAATGCCATTTATTTTATTAGATACTATC
K596fs	OTS1879	AACACCTCAAAAAAGGAATGGAACGACAG
	OTS1880	TCGTTCCATTCCTTTTTTTGAGGTGTTATG
A525E	OTS1914	TTGTAAGACTGAGCCCAACAGAGCAATCAG
	OTS1915	GCTCTGTTGGGCTCAGTCTTACAATAGAAG
A525S	OTS1916	TTGTAAGACTTCCCCCAACAGAGCAATCAG
	OTS1917	GCTCTGTTGGGGGAAGTCTTACAATAGAAG
A525Y	OTS1918	TTGTAAGACTTACCCCAACAGAGCAATCAG
	OTS1919	GCTCTGTTGGGGTAAGTCTTACAATAGAAG
A525V	OTS1920	TTGTAAGACTGTCCCCAACAGAGCAATCAG
	OTS1921	GCTCTGTTGGGGACAGTCTTACAATAGAAG
P589T	OTS1938	CGATGTTATAGCCCACTCATAACACCTCA
	OTS1939	AGGTGTTATGAGTGTGGCTATAACATCGCC
T608A	OTS1940	AGTCCAAAATCCAGCTCGCCTCCGAGAAGC
	OTS1941	CTTCTCGGAGGCGAGCTGGATTTTGGACTG
R290H	OTS1834	TATAAAGGGCATCCTGAAAACAAAAGCTTC
	OTS1835	TTTTGTTTTTCAGGATGCCCTTTATATGGCC



R348C	OTS1875	AATGAGTTGTGTATTTGTGCTAGAGATAAG
	OTS1876	TCTAGCACAAATACACAACCTCATTGTCTAC
R451P	OTS1711	AAATTGAATACCCTAATCTATTCAAGTATG
	OTS1712	ACTTGAATAGATTAGGGTATTCAATTTGTT
L178Q	OTS1707	TAGCAGGATGTCAAGTTCACGCACTGGGTG
	OTS1708	AGTGCGTGAACCTTGACATCCTGCTAGATAC
A525T	OTS1709	TTGTAAGACTACCCCCAACAGAGCAATCAG
	OTS1710	GCTCTGTTGGGGGTAGTCTTACAATAGAAG
A338V	OTS1713	TTATTAAGTTTGTCCGTGTCTGTGAAGTAG
	OTS1714	TTCACAGACACGGACAACTTAATAAAGCG
K05R	OTS1952	TGCTGGAGGAAGAAAGTATCGCATTTCTAC
	OTS1953	AAATGCGATACTTTCTTCCTCCAGCACCTG
R451C	OTS1656	AAATTGAATACTGTAATCTATTCAAGTATG
	OTS1657	CTTGAATAGATTACAGTATTCAATTTGTTT

### 9.1.13 Software

Name	Source
DNA Dynamo	BlueTractorSoftware Ltd
Excel	Microsoft, Redmond, USA
FACSDiva	BD, Franklin Lakes, USA; RRID:SCR_001456
FlowJo V10	FlowJo LLC, Ashland, USA; RRID:SCR_008520
Graph Pad Prism 5	GraphPad Software, Inc., La Jolla, USA; RRID:SCR_002798
Pymol	Schrödinger

## 9.2 Methods

### 9.2.1 Cells

THP-1 cells as well as their CRISPR–Cas9 derivatives were grown in RPMI-1640 Glutamax (Gibco) supplemented with 10% heat-inactivated fetal calf serum (FCS) and 100 U/ml penicillin and 100 µg/ml streptomycin at 37 °C. Passaging of the cells was performed every 2-3 days. 293T were grown in Dulbecco’ s modified Eagle medium (DMEM Glutamax) (Gibco) with 10% heat-inactivated FCS and 100 U/ml penicillin and 100 µg/ml streptomycin. Passaging of the cells was performed every 2-3 days. For this, cells were washed with PBS and detached from the surface by 0.05% Trypsin/EDTA in PBS. Cells were resuspended in medium and diluted 1:4 (2 days) or 1:6 (3 days). Cell line stocks were maintained by cryo-conservation. For

this purpose, cells were pelleted (1200 rpm, 5 min), resuspended in 1 ml freezing medium (FCS supplemented with 10 % DMSO (adherent cells) or glycerol (suspension cells)) and transferred into a cryo-conservation tube. Tubes were slowly cooled to -80°C in freezing Styrofoam box. For long term storage cells were then transferred to liquid nitrogen. Cells were thawed rapidly and transferred to 75 cm<sup>2</sup> flasks (suspension cells) or 10 cm (adherent cells) dishes containing 10 ml pre-warmed fresh medium. The medium was changed after 24 h.

For preparation of monocyte-derived macrophages (MDM), peripheral blood mononuclear cells (PBMCs) were isolated from 50 ml from buffy coats of healthy blood donors by Ficoll density gradient centrifugation. The buffy coats were diluted 1:2 with PBS, prior to loading 35 ml of the diluted buffy coat on a 15 ml Ficoll cushion. Cells at the interphase of plasma and Ficoll were aspirated and washed twice with PBS. PBMC were seeded in RPMI 1640 medium which was supplemented with 10% heat inactivated FCS and antibiotics for 2 hr at 37°C. Afterwards PBMC were washed so that non-adherent cells were removed, and adherent monocytes were further cultured in RPMI 1640 containing 10% heat inactivated FCS, and 5% human AB serum for 10d until differentiation to macrophages was completed.

### 9.2.2 *Virus preparation and infection assay*

HEK293T cells were transfected with 4 µg polyethylenimine (PEI) per µg DNA in 1 ml of OptiMEM (Gibco) per 10 cm plate 24 h after seeding. For lentiviral vector (LV) production, 4.5 µg of HIV-1 viral plasmid (pCSxW vector, plentiCRISPRv2 or RetroQ vectors encoding respectively the protein, the gRNA or the shRNA of interest) 3 µg of pCMVΔR8.91 GagPol encoding plasmid and 3 µg of VSV-G Env expression plasmid pMD.G2 were mixed into a separate reaction tube with 0,5 ml OptiMem. PEI was premixed with 0,5 ml OptiMEM. Next, both solutions were mixed together and were homogenized by vortexing for short time. The mixture was incubated for at least 15 min at room temperature and added drop-wise onto a ~75 % confluent 10 cm dish of 293T cells prior replaced with new fresh media (8 ml). For VSV-G-pseudotyped full length HIV-1 production, 8 µg HIV-1 GFP reporter viral plasmid pNLENG-IRESNef (Levy et al., 2004) and 2 µg pMD.G2 were transfected per plate. To generate full-length laboratory strains HIV-1NL4.3 4.5 µg pCSGW was cotransfected with 3 µg full-length viral plasmid pNL4.3 and 3 µg pMD.G2. For all virus productions, medium was replaced 24 h post transfection, the viral supernatant was harvested at 48 h and 72 h post transfection. Both collections were pooled and passed through a 0.45 µm cellulose filters to remove all cell debris. Depending on the experiment, viral supernatants were subjected to sucrose purification as described before (Goujon et al., 2013c).

In order to determine infectious titers,  $5 \times 10^4$  HEK293T cells were plated in 96-well plates and infected the next day with 100  $\mu$ l of viral supernatant diluted in a three-fold serial dilution series to obtain six different concentrations. Infected cells were fixed at 48 h post infection and the GFP expression was analyzed by FACS.

### 9.2.3 Production of VLPs

HEK293t cells were grown in 10-cm plates and transfected at a confluence of  $\sim 75\%$  using 4  $\mu$ g polyethylenimine (PEI) per  $\mu$ g DNA in 1 ml of OptiMEM (Gibco) per plate. For SIV<sub>MAC</sub> virus-like particle (VLP) production, plates were transfected with 8  $\mu$ g GagPol encoding plasmid pSIV3+, encoding Vpx (Vpx-VLPs), or with a control plasmid lacking VPX ( $\Delta$ Vpx-VLPs), and 2  $\mu$ g VSV-G encoding plasmid pMD.G22 per plate as described previously (Herold et al. (2017a)). The medium was changed 24 h post-transfection. The supernatant was harvested at 48 h and 72 h and passed through a 0.45- $\mu$ m filter. 30 ml viral supernatant was sucrose-purified and resuspended in 300  $\mu$ l RPMI-1640 containing penicillin/streptomycin. For the transpackaging assay the following plasmid ratio was used 8  $\mu$ g pcDNAwt Vpx flag or Vpx Q76A flag; 8  $\mu$ g control plasmid lacking VPX ( $\Delta$ Vpx-VLPs) and 2  $\mu$ g VSV-G encoding plasmid pMD.G22 per 10 cm plate

### 9.2.4 Infections

$1 \times 10^5$  THP-1 were plated in 100  $\mu$ l media per well in 96-well plates and treated with 500 U IFN $\alpha$  (for Vpx experiments only) and with 25 ng/ml phorbol 12-myristate 13-acetate (Sigma Aldrich) for 24 h. Prior to infection 2  $\mu$ l of Vpx VLP were added. Following Vpx VLP addition 100  $\mu$ l supernatant containing VSV-G pseudotyped GFP-reporter lentiviral vectors or NL4.3GFP-reporter virus were added. Cells were fixed in 4% paraformaldehyde (PFA) 48 h post infection. Infectivity was determined from the percentage of GFP positive cells by flow cytometry using a FACSVerse (BD Biosciences) for THP-1 cells and CELESTA for MDM cells.

Experiments with MDMs were performed in 48-well plates seeding  $5 \times 10^5$  monocytes per well prior to differentiation. For analysis by flow cytometry MDMs were trypsinized for at least 60 min, resuspended and fixed in 4% PFA.

### 9.2.5 Generation of CRISPR/Cas9 THP-1 cell clones

THP-1 cells were transduced with VSV-G pseudotyped HIV-1 LV delivering plentiCRISPRv2SAMHD1g2/g3. Transduced cell populations were selected with 1  $\mu$ g/ml puromycin for at least two weeks. Single-cell clones were generated by limiting dilution and

grown in 96-well plates for at least four weeks in the absence of puromycin. Afterwards cells were expanded and expression of SAMHD1 was analyzed by western blot. Cell clones with no detectable SAMHD1 level were send for sequencing.

Oligonucleotides encoding for SAMHD1 gRNAs were caccgCTCGGGCTGTCATCGCAACG (fwd g2) and aaacCGTTGCGATGACAGCCCGAGc (rev g2), as well as caccgATCGCAACGGGGACGCTTGG (fwd g3) and aaacCCAAGCGTCCCCGTTGCGATc (rev g3).

Clones were genotyped by sequencing of genomic DNA using the following primers:

AGAGCCGCTAGGCTGCCCTG (SAMHD1 fwd 1); AAGGGCTCAACTGTCAGTGAG (SAMHD1 fwd 2); ACTGCCCTCAGTTCTGCTTC (SAMHD1 fwd 3); ATCCTACGAATCGCCTATC (SAMHD1 rev 1); and AGATCCCAATCTACGACTG (SAMHD1 rev 2).

#### 9.2.6 *Generation of stable cell lines ectopically expressing proteins*

Cell lines ectopically expressing proteins of interest were generated by transduction of SAMHD1 knock out cells in 12-well plates with 200 µl concentrated VSV-G-pseudotyped HIV-1 LV encoding gRNA-resistant SAMHD1 wild type, catalytic-dead mutant H233A or SAMHD1 SNPs. 48 h post-transfection, cell lines were expanded in cell flask before analysis.

#### 9.2.7 *Growth curves*

$5 \times 10^3$  THP-1 SAMHD1 CRISPR–Cas9 clones g2-2 and g2-3 were seeded in six-well plates in 2 ml of media. The cell density was determined by counting live cells over a period of 1 week.

#### 9.2.8 *Proliferation assays*

$1 \times 10^5$  THP-1 cells/CRISPR–Cas9 derivatives/ cells overexpressing SAMHD1 derivates were seeded in 96-well tissue culture plates per well and incubated for 72 h at 37 °C with ara-C in triplicate, before incubation with CellTiter 96 AQueous One Solution (Promega) according to the manufacturer's recommendations. Absorbance was measured using the Infinity M200PRO (TECAN), and EC<sub>50</sub> values were calculated using Prism 6 (GraphPad Software).

#### 9.2.9 *Preparation of chemical competent E.coli*

To generate E.coli competent for heat shock transformation the following protocol was used. DH5α or Stb12 E.coli were spread on agar plates without antibiotics and grown overnight at 37 °C. The following day 10 ml LB media were inoculated with a single Stb12/DH5α colony and

bacteria were grown overnight at 350 rpm and 37 °C in a bacterial shaker. The next day 50 ml of LB media was inoculated with 1.25 ml of overnight bacterial culture. Bacteria were grown while shaking at 37 °C until an optical density of  $OD_{550nm}=0.45-0.55$  was reached. The suspension was placed on ice for 10 min. Afterwards bacteria were pelleted by centrifugation at 3000 rpm at 4 °C for 15 min. Pelleted bacteria were resuspended in 20 ml of cooled Tfb1 solution and left on ice for 5 min before they were centrifuged again under the same conditions as stated above. The bacterial pellet was resuspended in 2 ml of cooled Tfb2 solution and left again on ice for 10 min. Tfb1 and Tfb1 solutions were sterile filtered and pre chilled on ice before use. Aliquots of 80  $\mu$ l were pipetted into 0.5 ml Eppendorf tubes, which were immediately thrown into liquid nitrogen. Transformation competent cells were stored at -80 °C.

#### *9.2.10 Heat shock transformation and plasmid preparation*

Chemically competent bacteria were transformed using a heat-shock procedure. 80  $\mu$ l of chemo-competent E. coli DH5 $\alpha$  or Stbl2 bacteria were thawed on ice and subsequently mixed with 1  $\mu$ g plasmid DNA or 5  $\mu$ l ligation product for 40 min on ice. Heat shock was performed for 1,5 min at 42°C followed by incubation on ice for 2 min and afterwards 5 min at RT. Bacteria were directly plated on prewarmed agar plates containing ampicillin.

To amplify plasmid DNA, single colonies were used to inoculate overnight cultures in LB medium containing 100 mg/l ampicillin on a shaker at 37 °C. For small-scale preparations of plasmid DNA 2 ml bacterial culture was grown and purification were performed using the QIAprep Spin Miniprep Kit (Qiagen, Crawley, UK) following the protocols provided with the kits. Medium scale preparation of plasmid DNA was performed using the QIAfilter Plasmid Midi Kit (Qiagen, Crawley, UK) according to the manufacturer's protocol. 100 ml overnight bacterial culture was grown for medium scale preparation. DNA concentration and purity were measured using a nanophotometer. Purity was controlled by verifying that  $OD_{260\text{ nm}}/OD_{280\text{ nm}}$  ratio was between 1.8 and 2.0. DNA solutions were adjusted to 1  $\mu$ g/ $\mu$ l using the respective Elution buffer.

#### *9.2.11 Separation of DNA by agarose gel electrophoresis*

DNA fragments were separated by electrophoresis using 1% agarose in 1x TAE buffer. MIDORI green was used to stain DNA (4  $\mu$ l in 100 ml agarose solution prior to polymerization). The DNA was mixed with DNA loading buffer and loaded into the wells and run at 80 V for 30 min. The size of DNA fragments was compared to a standard ruler (1 kb DNA ladder). Gels were analyzed under UV light.

### 9.2.12 DNA extraction from agarose gels

Extraction and purification of DNA bands from agarose gels was performed using the QIAquick gel extraction Kit (Qiagen, Crawley, UK) according to the manufacturer's protocol. DNA fragments were eluted from the column by adding 30 – 50 µl of water.

### 9.2.13 Ligation of DNA-fragments

For ligation usually 2-4 µg plasmid DNA was digested with appropriate enzymes and were gel purified and eluted into 50 µl of water. Usually 1 µl of digested and purified vector DNA was mixed with 5 µl of insert DNA or PCR product. Vector and insert DNA were mixed with 2 µl 10 × ligase buffer, 1 µl (3 U) T4 DNA-ligase and water to a final volume of 20 µl. After 5-20 min incubation at room temperature 5 to 10 µl of the ligation-mix were added directly to 80 µl competent bacteria for transformation.

### 9.2.14 Analysis of DNA with restriction enzymes

Restriction digests of DNA were performed with enzymes from the manufacturers NEB. Enzymes and buffers were used as stated by the manufacturer and reaction conditions were performed to their protocols.

### 9.2.15 Polymerase Chain Reaction (PCR)

The reaction mixture was prepared on ice. Each reaction contained 250 µM dNTPs (each dNTP), 1 × polymerase buffer, 10 pmol of each primer, 100 ng to 1 µg template DNA and 1 µl (3 U) of PFU polymerase (Promega, Southampton, UK) filled up with H<sub>2</sub>O to a final reaction volume of 50 µl. Annealing temperature as well as elongation time were set depending on the primer composition and the length of the amplified sequence, respectively. Usually 34 cycles were performed. All nucleotide sequences of PCR products were confirmed by sequencing (Eurofins, Ebersberg).

The following thermocycling program was used (Lid 105°C):

Step	Temperature	Duration
1) Initial denaturation	98°C	30 sec
2) Denaturation	98°C	10 sec
3) Annealing	55°C	30 sec
4) Elongation	72°C	15-30 s per kbp
Repeat 2-4		30 cycles
5) Final extension	72°C	7 min
6) store	12°C	

Successful DNA amplification was monitored by running 5 µl product on a 1% agarose gel.

### 9.2.16 PCR-based mutagenesis

To generate plasmids carrying point mutations PCR based mutagenesis was performed according to the Quick-change protocol (Stratagene). To engineer point mutations into a plasmid, PCR was performed as described above using two primers with opposite orientation covering the desired point mutation. Usually, 12 cycles were performed with an elongation time of 40 min for each step, depending on the plasmid length into which the mutation was introduced. Primer annealing temperatures was between 53-55 °C. To avoid errors, *PFU Turbo* DNA Polymerase was used according to the manufacturer protocol. After the amplification, the template plasmid was digested by adding 1 µl of DpnI and 5 µl of NEB cutsmart buffer directly to the PCR reaction mix and incubated at 37 °C for 1-2 h. After digestion, 10 µl of the mix was transformed into competent bacteria. Single cell clones were picked and DNA was send for sequencing.

Step	Temperature	Duration
1) Initial denaturation	95°C	30 sec
2) Denaturation	95°C	10 sec
3) Annealing	55°C	1 min
4) Elongation	68°C	1 min/ kbp of plasmid
Repeat 2-4 12 cycles		
5) Final extension	72°C	10 min
6) store	12°C	

### 9.2.17 SDS-polyacrylamide-gel electrophoresis (SDS-PAGE)

Gels were generated using Acrylamide Solutions TGX™ FastCast™ according to the manufacturer's protocol (Biorad) and an acrylamide concentration of 10 % or 12 % for the separating gel was used. Briefly, for each separating gel 3 ml Resolver A, 3 ml of Resolver B, 3 µl of TEMED were mixed in a 50 ml Falcon Tube before starting gel polymerization by adding 30 µl of 20 % ammonium-persulfate (APS). The separating gel was quickly poured between two glass plates of the Bio-Rad PAGE Gel casting system. To avoid formation of air bubbles, isopropanol was carefully pipetted on top of the separating gel. After polymerization the isopropanol was disposed and washed away with water. The remaining water -was removed by using Whatman paper strips. To prepare the stacking gel, 1 ml of Stacker A, 1 ml of Stacker B, 2 µl TEMED and 10 µl APS were mixed in a 50 ml Falcon tube by briefly vortexing. The solution was carefully added on top of the separating. After polymerization, the glass slides were installed into the Biorad system, filled with SDS-PAGE running buffer and loaded with

20  $\mu$ L sample per lane and 10  $\mu$ L protein size marker. Cells were lysed by addition of denaturing protein sample buffer. The samples were boiled at 98 °C for at least 5 min. Aliquots of cell lysates were loaded onto SDS 10 % or 12 % polyacrylamide gels for electrophoresis. Gel electrophoresis was performed at 150 V for 60 minutes.

#### *9.2.18 Western blotting*

The SDS gel with the separated proteins were transferred to a 0,45  $\mu$ m polyvinylidene fluoride transmembrane (Millipore) using Electrophoretic Transfer Cell Mini Trans-Blot® system (Biorad) at 100 V for 60 min in a styrofoam box with ice water. Membranes were incubated for 1h in PBS containing 0.1 % Tween 20 (pBS-Tween 20) and 5 % (w/v) non fat milk powder to saturate non-specific binding sites. The membrane was washed 3 times for 5 min in PBS-Tween 20. The primary antibody was diluted in PBS-Tween 20 and the membrane was incubated shaking over night at 4 °C. After being washed three times with PBS-Tween 20, the membrane was incubated with the secondary antibody in PBS-Tween 20 shaking at room temperature for 45 min and afterwards washed three times for 5 min with PBS-Tween 20. Membrane-bound secondary antibody was detected by chemiluminescence using ECL western blotting detection reagent. Chemiluminescence was measured by the ECL ChemoCam Imager system (INTAS Science Imaging).

#### *9.2.19 Immunofluorescence and confocal microscopy*

Respected cells were seeded on glass cover slips in 24-well cell culture plates at a concentration of  $2.5 \times 10^4$  cells per well. Prior to seeding the cells in the well pma (25ng/ $\mu$ l) was added to the well. The next day cells were fixed with 4 % paraformaldehyde (w/v) solution for 15 min at room temperature. Afterwards the cells were washed three times with  $1 \times$  PBS. For permeabilization the cells were incubated for 15 min with 500  $\mu$ l 0.5 % Triton-x-100/ PBS (v/v) solution and washed 3 times with  $1 \times$  PBS. In order to block unspecific antibody binding cells were blocked with 5% horse serum in  $1 \times$  PBS for 30 min. The SAMHD1 antibody was diluted 1:200 in  $1 \times$  PBS buffer containing 5 % horse serum (v/v). After 60 min incubation at room temperature the cells were washed 3 times with  $1 \times$  PBS for 5 min and incubated with the secondary antibody conjugated with fluorescent dye Alexa 488, diluted 1:1000 in a  $1 \times$  PBS buffer containing 5 % horse serum (v/v). After 60 min incubation at room temperature in the dark, the cells were washed three times with  $1 \times$  PBS. DRAG 5 (1:2000 dilution) was used for nuclei staining. After DRAG 5 staining the cells were washed again 3 times with  $1 \times$  PBS, rinsed with H<sub>2</sub>O and mounted on glass slides using Mowiol embedding medium (8 mM Mowiol 4-88 in PBS). Immunofluorescence pictures were obtained using a Leica confocal microscope.



## 10 Results

### 10.1 SAMHD1's role in the type 1 interferon induced early block to HIV-1 infection

#### 10.1.1 *The Vpx<sub>MAC</sub>-induced rescue of HIV-1 from the type I IFN-induced block in MDM depends on SAMHD1*

Vpx hijacks the Cullin4- E3 ubiquitin ligase by binding to DCAF1 (Le Rouzic et al., 2007). HIV-2 and SIV<sub>MAC</sub> harboring Vpx mutants unable to bind DCAF are unable to overcome the inhibition of infection in myeloid cells (Srivastava et al., 2008, Bergamaschi et al., 2009). The inhibition of HIV-1 infection in monocyte-derived macrophages (MDM) can be overcome by co-treatment with Vpx-containing SIV<sub>sm</sub> virus-like particles (SIV VLP) (Kaushik et al., 2009, Goujon et al., 2007). Pertel *et al.* and Reinhard *et al.* reported that Vpx Q76A, which is unable to bind DCAF1 and to degrade SAMHD1, was able to rescue HIV-1 infection from the type I IFN-induced block in MDDCs (Pertel et al., 2011, Reinhard et al., 2014). This suggests that the relief from the type I IFN induced block to HIV-1 infection may be independent of SAMHD1. On the other hand Hrecka et al. found out that Vpx mediated degradation of SAMHD1 is necessary to overcome HIV-1 restriction in macrophages (Hrecka et al., 2011). In order to confirm this hypothesis, we tested whether Vpx Q76A would be able to rescue HIV-1 infection in MDM. To do this we used a trans packaging assay, using SIVdelta Vpx and co-transfected SIV Vpx protein encoding plasmids during VLP production, thereby complementing the lack of Vpx by ectopic expression. This transpackaging assay was similarly efficient as using SIV encoding Vpx (Figure 9; Vpx-VLP vs wt Vpx flag trans). MDM were prepared from blood of healthy donors and stimulated with or without IFN overnight. Prior to infection with VSV G-pseudotyped HIV-1 GFP reporter virus Vpx VLP or control VLP were added to the cells. Infection was measured as the percentage of GFP-positive cells 2 days after challenge. Two independent experiments are shown in Figure 9. We found that Q76A was unable to relieve HIV-1 from the type I IFN-induced block in MDM. Wild type Vpx greatly boosted HIV-1 infection with or without IFN. We hypothesized that Vpx recruitment of the DCAF1-Cul4 ubiquitin machinery is required for the efficient increase of HIV-1 infection in type I IFN-induced MDM.

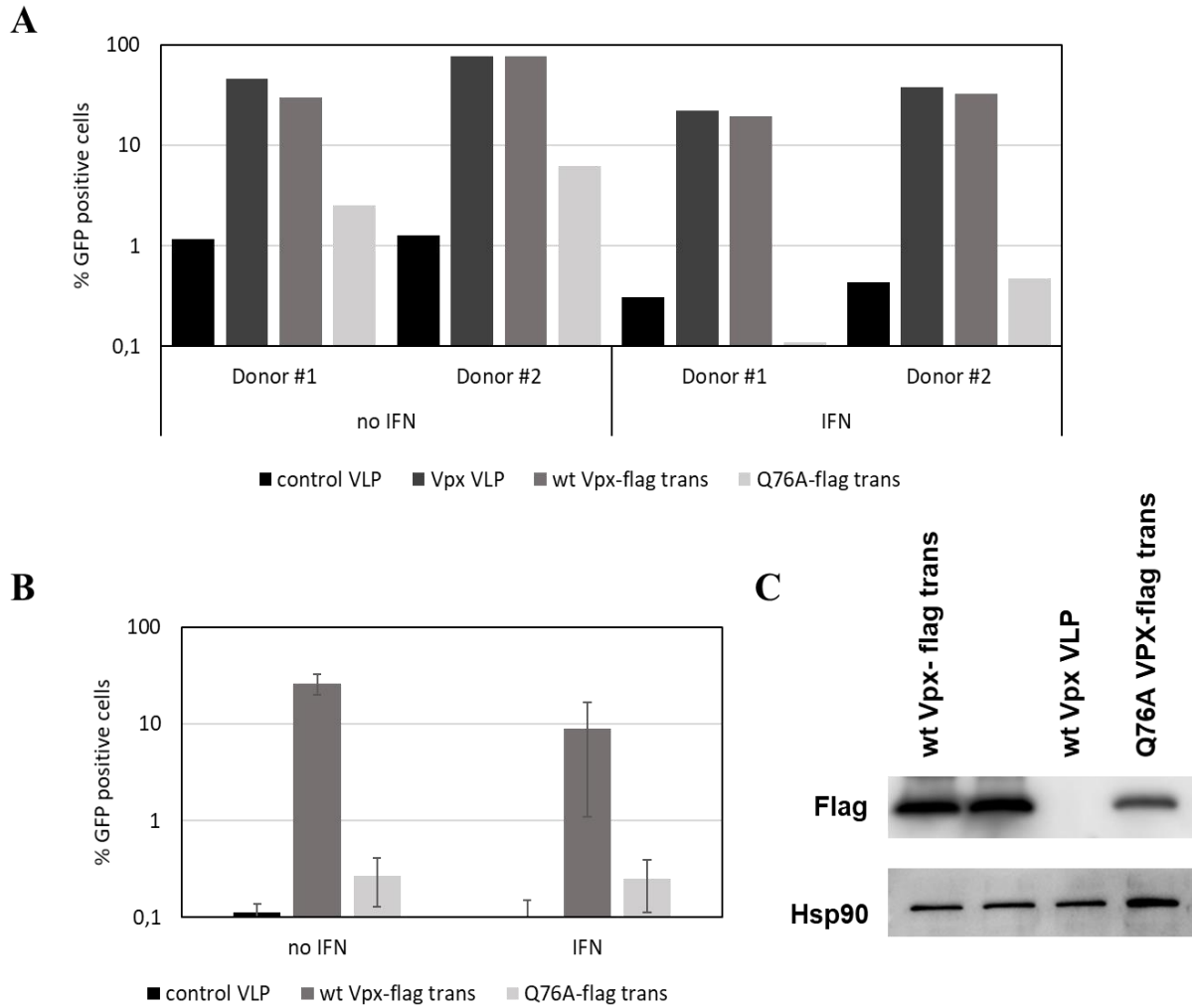


**Figure 9: Vpx deficient for SAMHD1 degradation does not relieve HIV-1 from the type I IFN induced block in MDM.**

**A, B)** MDMs were generated using human AB serum and treated or not with 500 U/ml IFN $\alpha$  2A for 72 h. Prior to infection cells were treated or not with SIV<sub>MAC</sub> Vpx-VLPs, or control (VLPs lacking Vpx). In parallel wild type or mutant Vpx trans packaged into VLPs lacking Vpx were tested. The cells were then infected for 48 h with VSV-G pseudotyped HIV-1NL4.3GFP reporter virus. Thereafter the percentage of GFP-positive cells was determined by flow cytometry. **B)** Mean values GFP positive cells of 3 donors with standard deviations are shown. **C)** Western blot showed similar incorporation of Vpx in trans-packaging assay

10.1.2 *The Vpx<sub>MAC</sub>-induced rescue of HIV-1 from the type I IFN-induced block in MDM is independent of route of entry*

Furthermore, we tested in two donors whether the boost of HIV infection is VSV-G dependent by comparing Bal Env bearing NL4.3GFP with NL4.3GFP pseudotyped with VSV-G. We confirmed that the Vpx mediated increase of HIV-1 infection is not VSV G-pseudotyp dependent in MDM (Figure 10). Although VSV-G pseudo typing enhanced infection up to 2-4-fold.

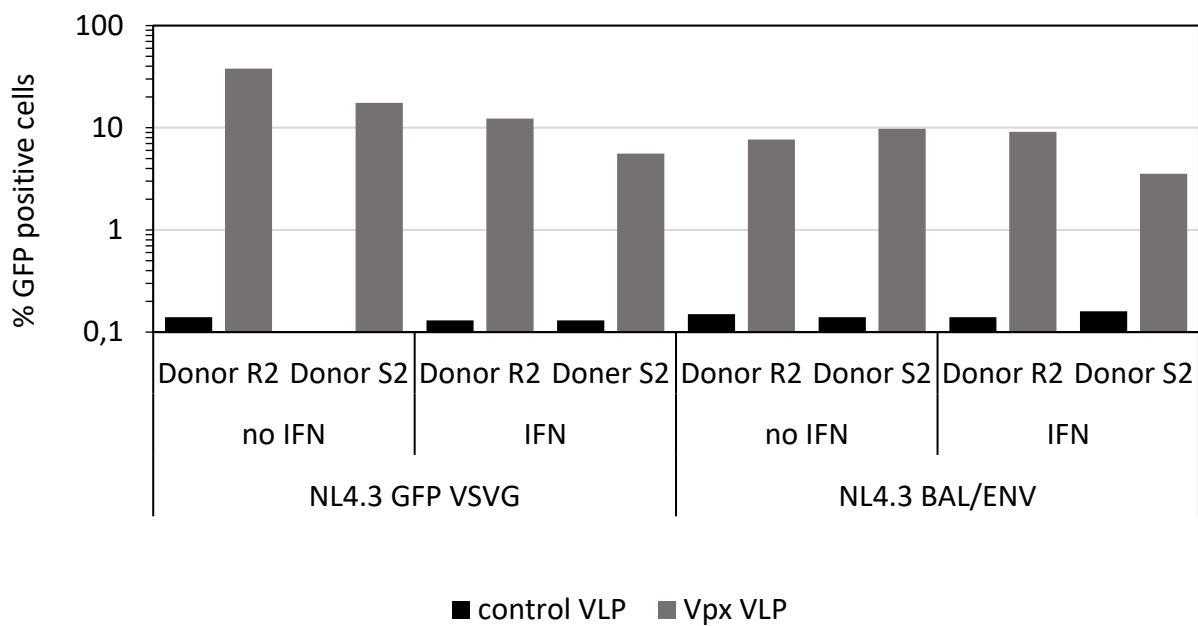


**Figure 10: Vpx mediated increase of HIV-1 infection is independent of entry route.** MDMs were generated using human AB serum and treated or not with 500 U/ml IFN alpha 2A for 24 h. Prior to infection cells were treated or not with SIV<sub>MAC</sub> Vpx-VLPs, or ctrl. VLPs lacking Vpx. The cells were then infected for 72 h with VSV-G pseudotyped HIV-1 NL4.3GFP reporter virus or NL4.3 Bal Env GFP. Thereafter the percentage of GFP-positive cells was determined by flow cytometry

### 10.1.3 *Vpx<sub>MAC</sub>* does not rescue HIV-1 from the type I IFN-induced block in THP-1

#### *SAMHD1*<sup>-/-</sup> cells

We further tested whether the presence of SAMHD1 is required for the Vpx-induced relief of HIV-1 from the type I IFN-induced block by generating and analyzing SAMHD1 CRISPR/Cas9 knock-out cells. We generated single-cell clones of THP-1 cells transduced with CRISPR/Cas9 LVs expressing individual specific guide RNAs (gRNAs). We generated six independent THP-1 single-cell knockout clones. Gene disruption was validated by PCR sequencing across the gRNA target site as well as by immunoblotting (Figure 11).

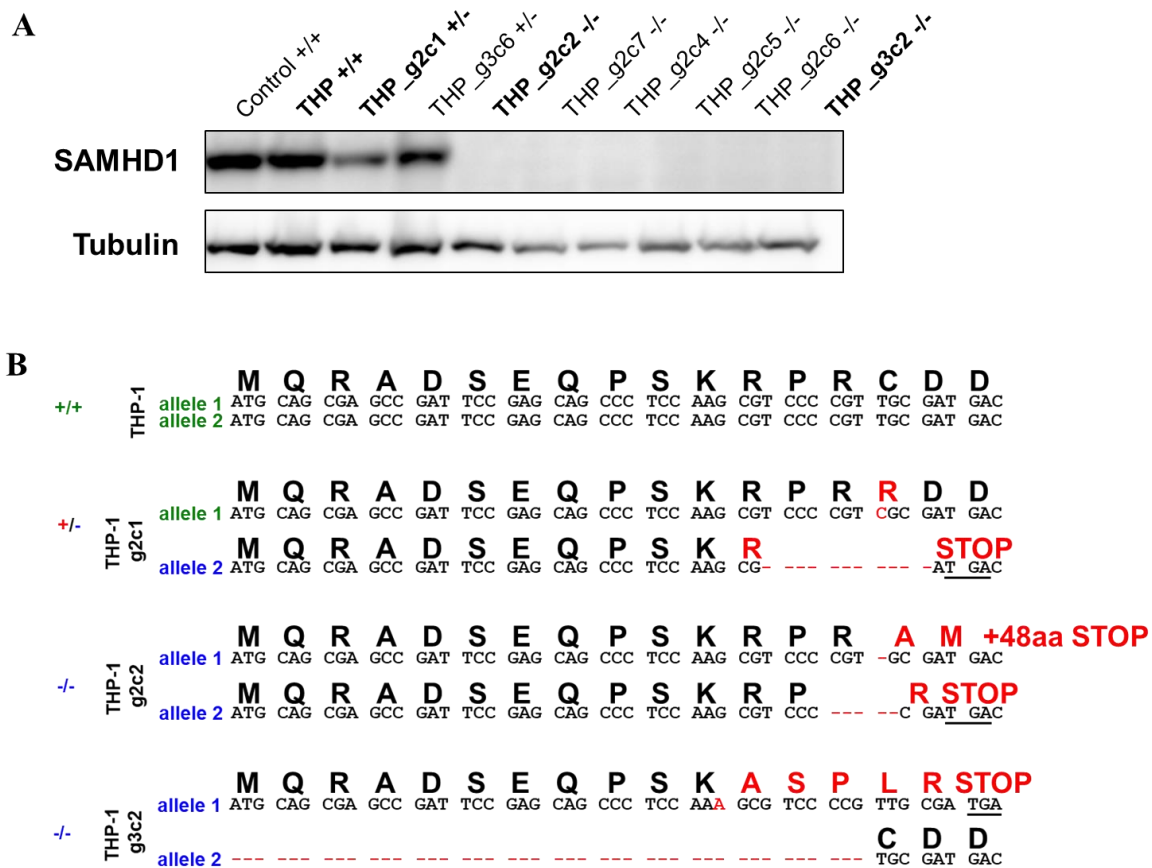


**Figure 11: Generation of THP1 SAMHD1 CRISPR–Cas9 cells. Vpx-mediated rescue of HIV-1 from the type I Interferon-induced block is SAMHD1-dependent.**

A) Individual single-cell clones with disrupted SAMHD1 expression were identified by western blot using mouse monoclonal SAMHD1 antibody 1F9 (Abcam). B) Identified SAMHD1 knock out clones were genotyped by sequencing of PCR products from genomic DNA spanning the gRNA target site.

All generated cell lines were tested for their susceptibility to infection with VSV-G-pseudotyped NL4.3 GFP and their potential to relieve HIV from the IFN induced block when Vpx was supplied. SAMHD1 restricts HIV-1 infection in myeloid cells and dendritic cells but not in most monocytic cell lines such as cycling THP-1 cells (Laguet et al., 2011b, Hrecka et al., 2011). Therefore THP-1 cells were differentiated by use of phorbol 12-myristate 13-acetate (PMA) for 24 h and at the same time 500 U IFN was added. Prior to infection with VSV G pseudotyped NL4.3 GFP reporter virus control Vpx or Vpx VLPs were added. SAMHD1 knock out increased the permissivity of cells to HIV-1 infection by approximately 4-fold in all tested SAMHD1 knockout cell lines (g2c2 and g3c2 shown in Figure 12. Additionally, Vpx was unable to increase HIV-1 infection in type I IFN-treated or untreated cells when SAMHD1 was absent (Figure 12). The Vpx-mediated boost of infection was achieved in THP-1 parental cells as well as in the heterozygous SAMHD1 knock-out cell line g2c1. This indicates that Vpx and SAMHD1 are required for the Vpx-induced boost of HIV-1 infection from the type I IFN-induced block. The Vpx mediated increase of HIV-1 infection, however, is present with or without IFN.

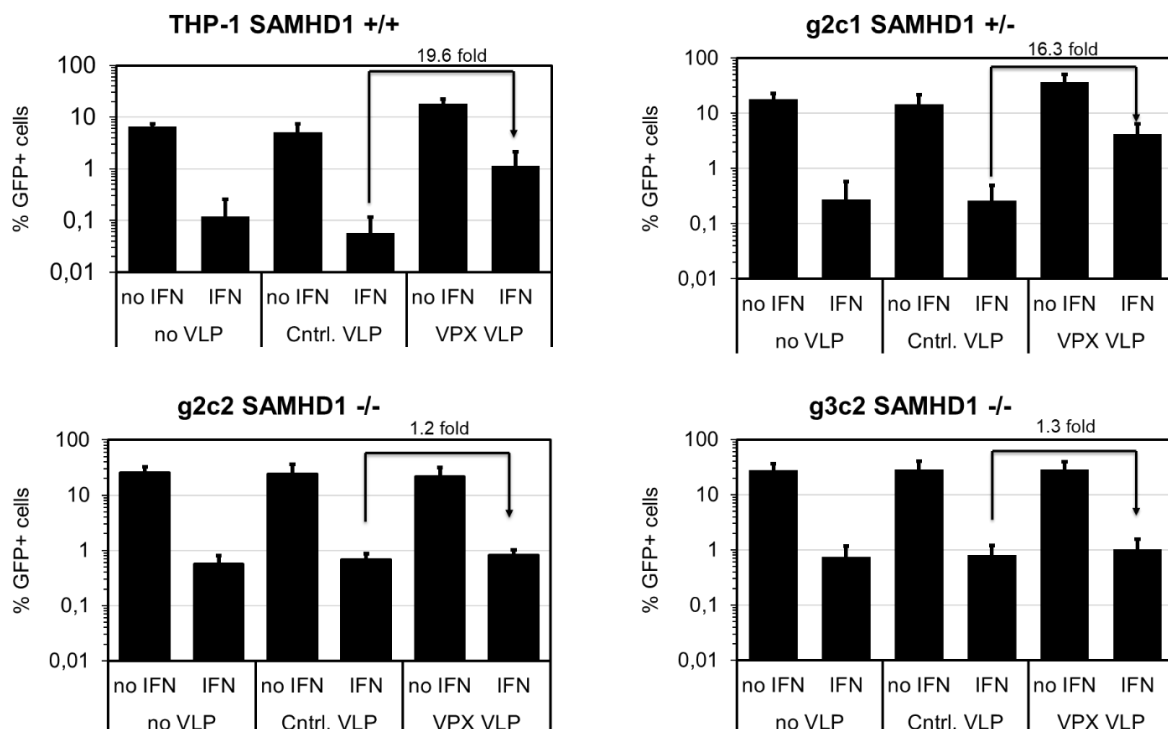


**Figure 12: Vpx-mediated rescue of HIV-1 from the type I interferon-induced block is SAMHD1-dependent.** THP-1 SAMHD1 knock-out clones, g2c2 and g3c2 as well as parental THP-1 and the heterozygous SAMHD1 cell line (g2c1) were pretreated with 25 ng/ml PMA and either with or without 500 U/ml type I interferon for 24 h. Prior to infection with equal amounts of VSV-G-pseudotyped wild-type HIV-1 NL4.3GFP reporter virus cells were treated either with SIV Vpx-VLPs, cntrl. VLPs, or no VLPs. At 48 h after infection the percentage of GFP-positive cells was determined by flow cytometry. Mean values with standard deviation of at least three independent experiments are shown.

In order to further confirm that SAMHD1 is crucial for the Vpx mediated increase of infection we re-expressed amino-terminal HA-tagged codon optimized (CRISPR/Cas9-resistant) SAMHD1 in the SAMHD1 knockout cells. Expression of wild type SAMHD1 reintroduced the block to HIV-1 infection by 6-fold compared to the SAMHD1 knockout clone when cells were differentiated with PMA. The SAMHD1 catalytic-dead mutant H233A showed no block to HIV-infection as reported by (Ryoo et al., 2014a) and Vpx was unable to boost infection (Figure 13).

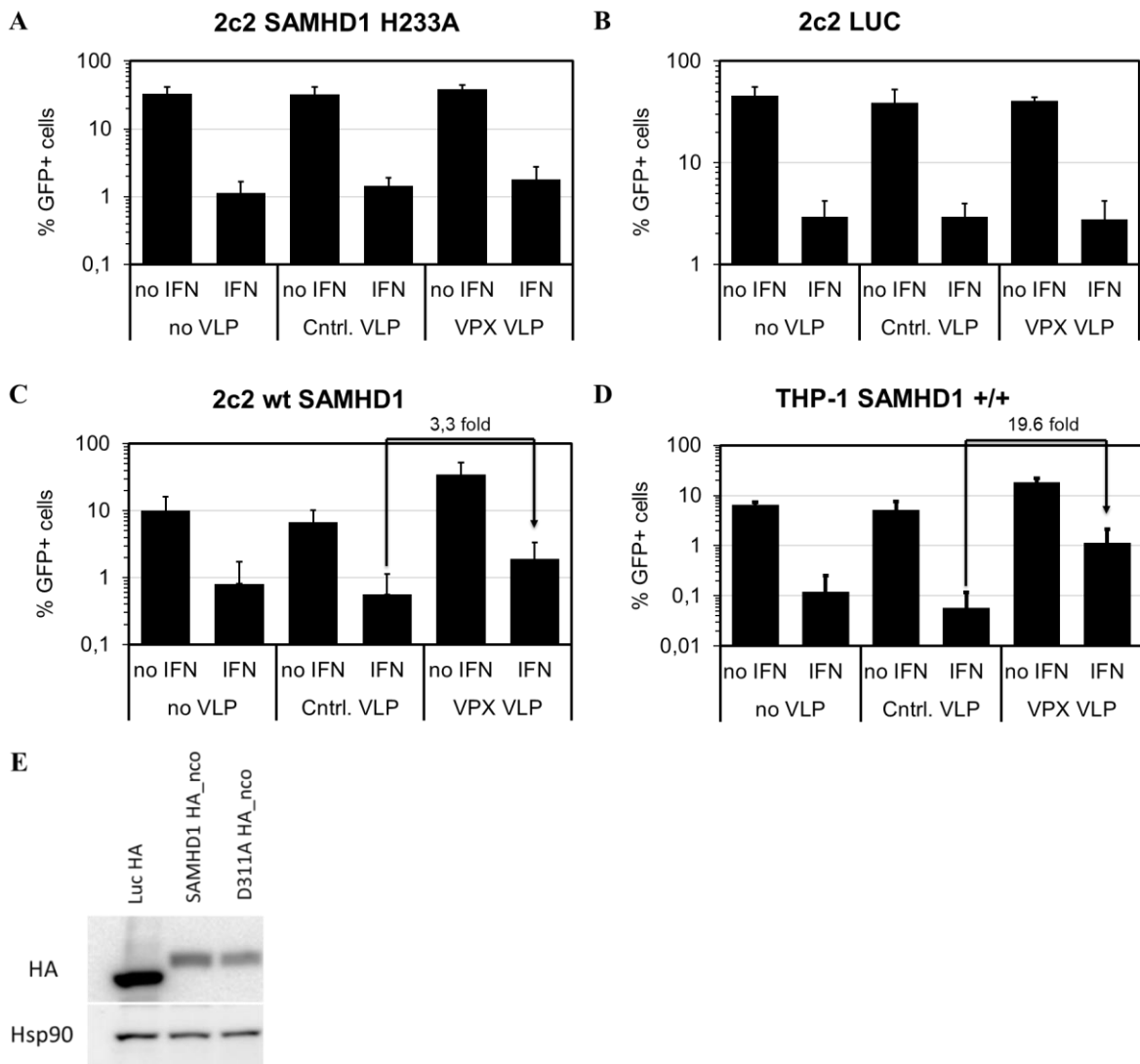


**Figure 13: Re-expression of SAMHD1 confirms sensitivity to Vpx.**

**A,B,C,D)** THP-1 SAMHD1 knockout clone g2c2 was stably transduced with LV encoding either SAMHD1 wildtype, SAMHD1 H233A or Luciferase, were pretreated with 25 ng/ml PMA and either with or without 500 U/ml type 1 alpha interferon for 24 h. Prior to infection with equal amounts of VSV-G-pseudotyped wild-type HIV-1 NL4.3GFP reporter virus cells were treated either with SIV Vpx-VLPs, cntrl. VLPs, or no VLPs. At 48 h after infection the percentage of GFP-positive cells was determined by flow cytometry. Mean values with standard deviation of at least three independent experiments are shown. **E)** Stable expression of SAMHD1 wt and D311A was analyzed by western blot.

#### 10.1.4 SAMHD1 knockout has no influence on cell proliferation in THP-1 cells

The effect of perturbed SAMHD1 expression was studied by many groups and two of them stated that reduced SAMHD1 activity, which increases the amount of dNTPs, results in uncontrolled cell proliferation (Clifford et al., 2014, Rossi, 2014). Bonifati et al. reports that SAMHD1 knockout by CRISPR/Cas9 in myeloid THP-1 cells increased cell proliferation and decreased spontaneous apoptosis (Bonifati et al., 2016). To further characterize the effect of SAMHD1 knockout on cell proliferation we seeded clone g2-2 (SAMHD1(-/-)) and clone g2-3 (SAMHD1(+/+)) in a 6-well plate in 2 ml media and cell density was determined by counting live cells over a period of 1 week. As shown in Figure 14 A no significant increase in cell proliferation was seen. Additionally, our collaborators in Sweden (Nikolas Herold, Sean Rudd and Nikolaos Tsesmetzis) analyzed the cell cycle of g2-3 and g2-2 and observed only a small but significant decrease in sub-G1 cells in the SAMHD1 knockout clone (Figure 14 B).

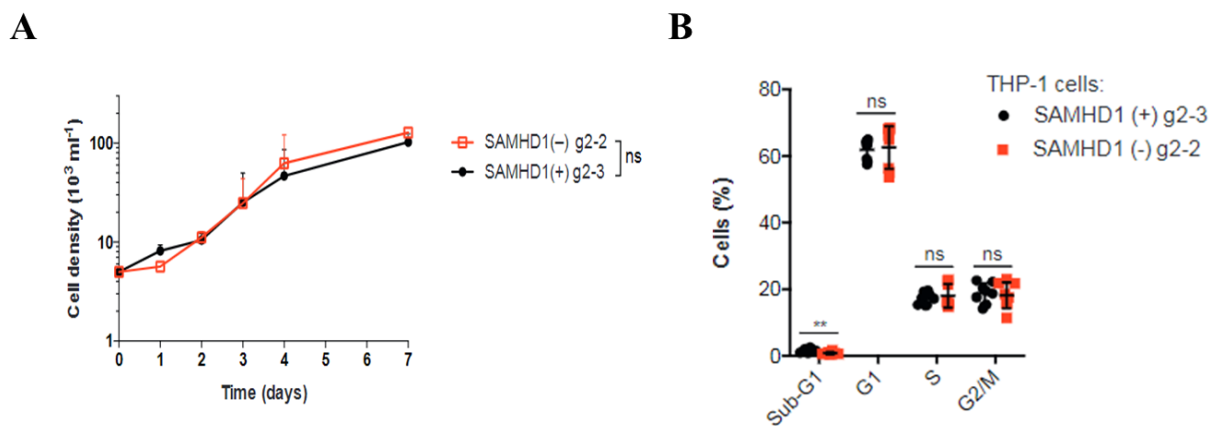


**Figure 14: SAMHD1 knockout does not significantly alter growth kinetics or cell cycle distribution.**

**A)** Growth curve of SAMHD1 knockout THP-1 cells. SAMHD1 CRISPR/Cas9 THP-1 cells, clone g2-2 (SAMHD1(-/-)) and clone g2-3(SAMHD1(+)). Shown are mean values and SEM of 2 independent experiments. Statistical testing was performed using an Extra-sum-of-squares F test of exponential growth curve fitted with Prism 6 (GraphPad Software):  $F=1.919$ ;  $DFn=2$ ;  $DFd=8$ ; ns, not significant( $p=0.2086$ ). **B)** Cell-cycle analysis of SAMHD1 KO (SAMHD1 (-) 2-2) and control cells (SAMHD1 (+)g2-3). The presented cell lines were fixed, and DNA stained with propidium iodide and subjected to flow cytometry analysis. Average of 3 experiments for each cell line performed at least in duplicates are shown alongside representative histograms, error bars indicate SD. Statistically significant differences between SAMHD1 knock out and control cell lines were determined using two-tailed multiple t-tests in Prism 6 (GraphPad Software): THP-1 sub-G1; \*\*,  $p=0.009$ ,  $t=3.04$ ,  $df=14$ ; THP-1 G1, ns, not significant,  $p=0.79$ ,  $t=0.28$ ,  $df=14$ ; \*\*,  $p\leq 0.01$ .; THP-1 S, ns, not significant,  $p=0.56$ ,  $t=0.59$ ,  $df=14$ ; THP-1 G2/M, ns, not significant,  $p=0.72$ ,  $t=0.36$ ,  $df=14$  (Herold et al., 2017a)

10.1.5 Characterization of a THP-1 cell line endogenously expressing SAMHD1 with truncated nuclear localization signal (*Eg3c6*<sup>+/-</sup>)

To answer the question whether Vpx-induced SAMHD1 degradation is required for the rescue from the antiviral state, we generated cells in which SAMHD1 was endogenously truncated in its nuclear localization signal. We and others described that overexpressed SAMHD1 lacking the NLS is completely resistant to Vpx-induced degradation (Brandariz-Nunez et al., 2012, Hofmann et al., 2012, Wei et al., 2012, Guo et al., 2013). Hence, we reasoned that cells endogenously expressing NLS-deleted SAMHD1 would be ideal to test whether the Vpx-induced relief of HIV-1 infection from the type I interferon-induced block would depend on SAMHD1 degradation. The generated cells were designed and selected to contain only one functional SAMHD1 allele, which however harbored an in frame deletion in the NLS region (amino acids <sup>11</sup>KRPR<sup>14</sup>) (Figure 15 A). We found that endogenously expressed SAMHD1 lacking the NLS was excluded from the nucleus using immunofluorescence (Figure 15 B).

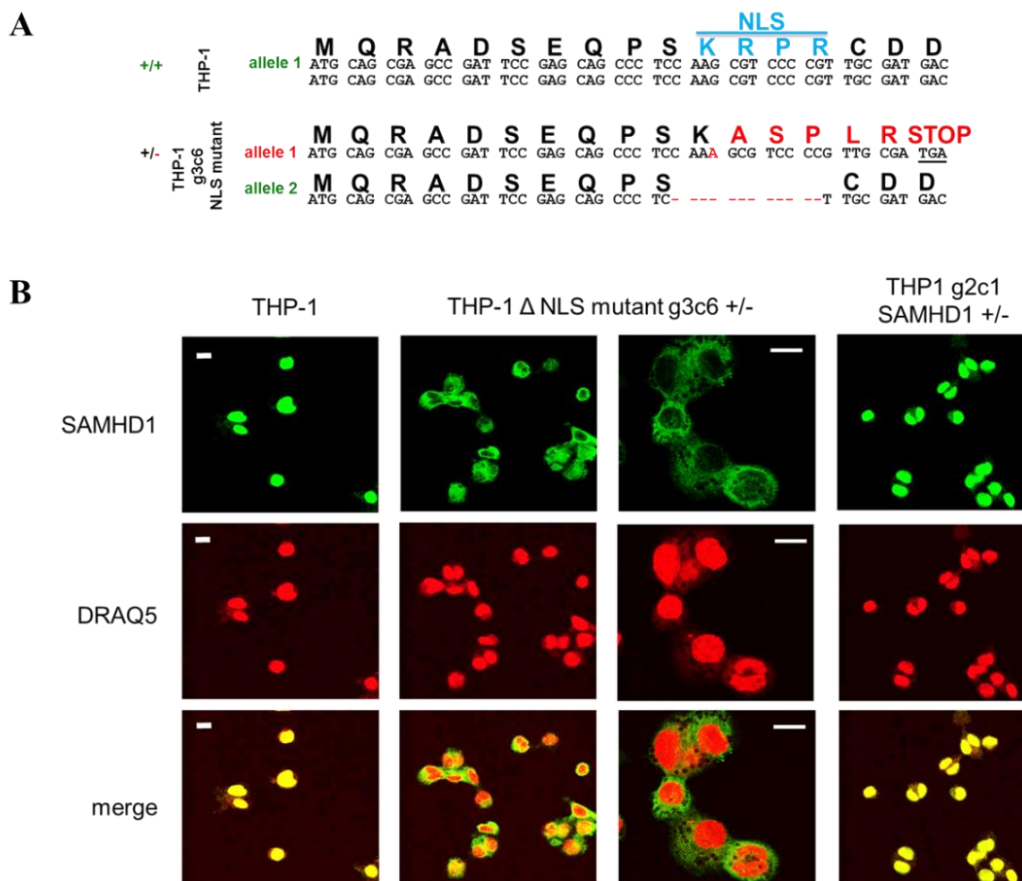


**Figure 15: Generation of THP1 SAMHD1 CRISPR–Cas9 cells with disrupted nuclear localization signal (<sup>11</sup>KRPR<sup>14</sup>).**

**A)** Sequencing analysis of CRISPR/Cas9 THP-1 cell clone, which had one disrupted SAMHD1 allele and one allele, in which the entire nuclear localization signal (11KRPR14) was deleted in frame, generating an internally NLS-disrupted endogenously expressed SAMHD1 protein. **B)** Immunofluorescence-microscopy analysis of SAMHD1 in THP-1, NLS mutant *g3c6* and the heterozygous SAMHD1 mutant clone *g2c1* (+/-). DRAQ5 was used to visualize the nucleus. Scale bar =10 μm.



To our surprise, endogenously SAMHD1 $\Delta$ NLS resisted Vpx-induced degradation, but was not completely refractory to degradation, as suggested for ectopically expressed SAMHD1 $\Delta$ NLS. After 24h Vpx treatment SAMHD1 $\Delta$ NLS levels decreased. SAMHD1 degradation by Vpx was seen after 2 h of Vpx treatment in g2c1 and THP-1 parental cells whereas SAMHD1 levels were unchanged in the NLS mutant g3c6 (Figure 16 C). To test whether the SAMHD1 NLS mutant was able to increase HIV-1 infection when treated with IFN upon Vpx treatment we infected SAMHD1 $\Delta$ NLS treated with IFN with VSV G-pseudotyped NL4.3 GFP in the presence or absence of Vpx-VLPs and found that HIV-1 infection increased 48h after infection in IFN untreated and IFN treated cells (Figure 16). The increase of infection was comparable to THP-1 parental cells. Therefore, the location of SAMHD1 might not be important for the Vpx mediated rescue of HIV-1 from the IFN induced block.

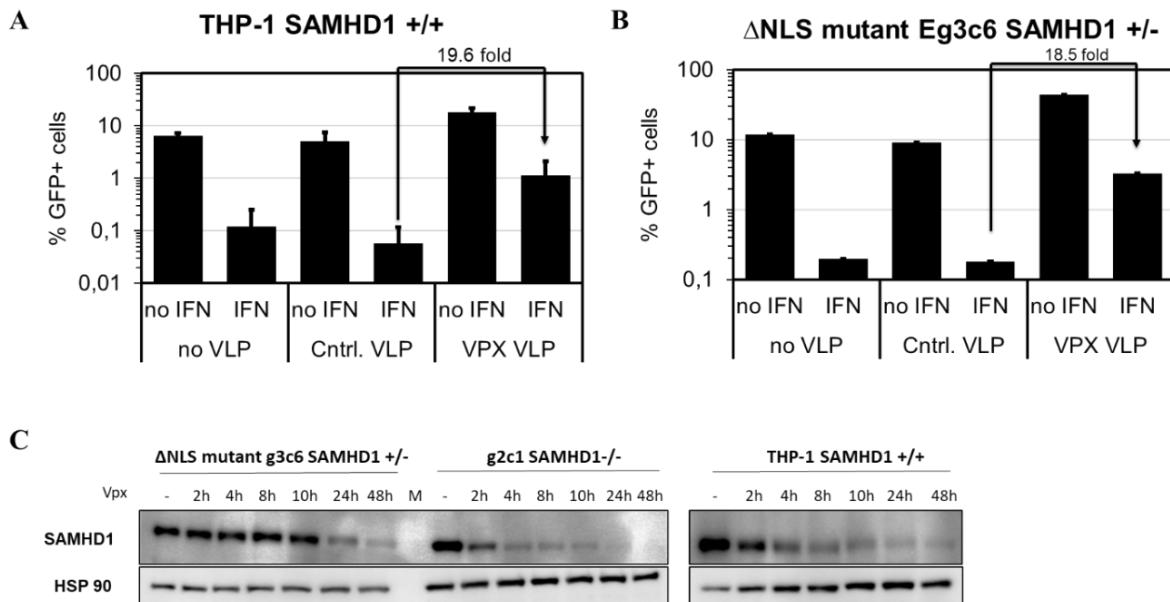


**Figure 16: Vpx-mediated rescue of HIV-1 from the type 1 Interferon induced block is independent of SAMHD1 localization and despite reduced SAMHD1 degradation kinetics.**

**A, B)** THP-1 and NLS mutant g3c6 were pretreated with 25 ng/ml PMA and either with or without 500 U/ml type I interferon for 24 h. Prior to infection with equal amounts of VSV-G-pseudotyped wild-type HIV-1 NL4.3GFP reporter virus cells were treated either with SIV Vpx-VLPs, cntrl. VLP, or no VLPs. At 48 h after infection the percentage of GFP-positive cells was determined by flow cytometry. Mean values with standard deviation of at least three independent experiments are shown. **C)** g2c1, Thp-1 parental and SAMHD1 NLS mutant were seeded in 96 well plates and the same amount of Vpx VLP was added to each well. After 0/2/4/10/24/48 h cells were harvested for western blot analysis.

10.1.6 Interferon has no influence on -Vpx- mediated SAMHD1 degradation in cycling THP-1 cells

Dragin *et al.* (Dragin *et al.*, 2013) and Roesch *et al.* (Roesch *et al.*, 2018) showed that interferon alpha (IFN $\alpha$ ) treatment of THP-1 cells prevents degradation of SAMHD1 following incubation with SIV<sub>MAC</sub> virus-like particles containing Vpx. Since Vpx mediated SAMHD1 degradation might be the reason of the Vpx-mediated increase of HIV-1 infection in interferon alpha treated cells we tested SAMHD1 degradation by Vpx with and without interferon. Further-more, we investigated whether PMA treatment would influence SAMHD1 degradation. THP-1 cells were treated with or without interferon for 24 h and supplemented afterwards with Vpx-VLPs for 16 h or 24 h. In addition, western blot samples were taken of THP-1 cells treated with or without PMA. As published by other groups, complete SAMHD1 degradation was achieved in the presence of Vpx-VLPs. In contrast to Dragin and Roesch *et al.* interferon alpha treatment did not hinder Vpx mediated SAMHD1 degradation (Figure 17).

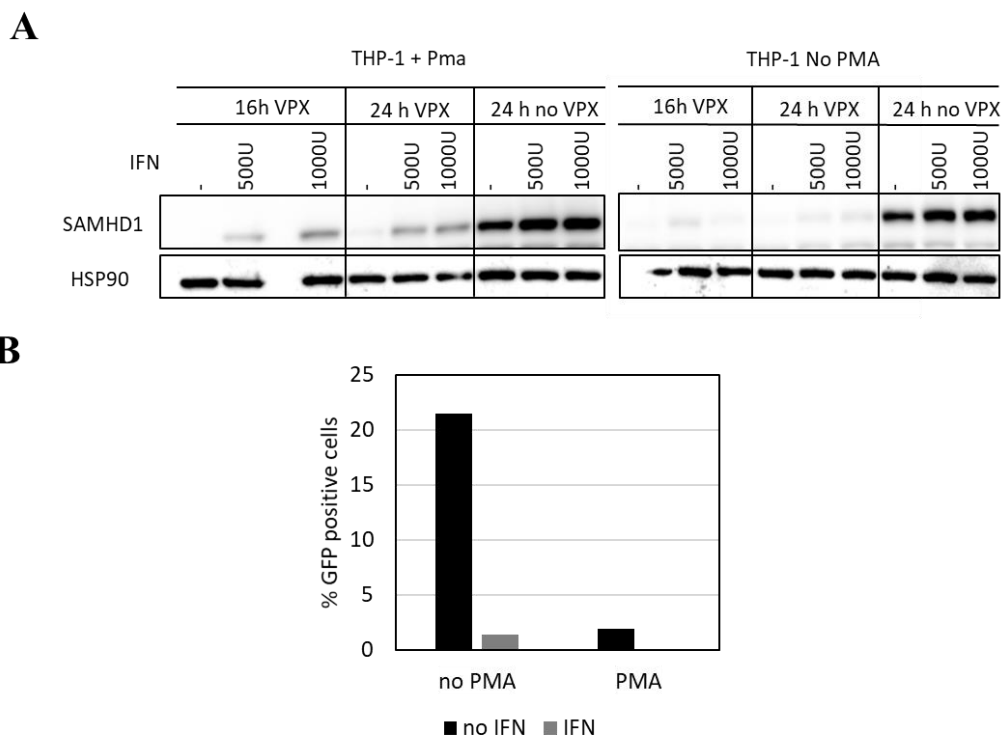


**Figure 17: Vpx mediated SAMHD1 degradation was not influenced by interferon treatment in cycling.**

**A)** THP-1 cells. Western blot samples were taken of THP-1 cells which were treated with or without interferon alpha (500 U and 1000 U) for 24 h and supplemented afterwards with Vpx-VLPs for 16 h or 24 h. This setup was used for THP-1 cells treated with or without PMA for 24 h. **B)** In parallel THP-1 cells were infected with NL4.3 GFP reporter virus and percentage of GFP positive cells were analyzed after 48h of infection by FACS. Cells were either treated with or without PMA and stimulated with or without IFN 24 h prior to infection

PMA and interferon treatment slightly hindered SAMHD1 degradation in the presence of Vpx-VLPs but did not completely block SAMHD1 degradation, a result that is contrasting published data. IFN activity was tested in parallel by blocking HIV-1 infection.

## 10.2 SAMHD1 in cancer

SAMHD1 not only acts as a host restriction factor against viral infections (Hrecka et al., 2011, Laguette et al., 2011a), mutations in the SAMHD1 gene have also been linked to a genetic immune disorder called Aicardi-Goutières Syndrome (AGS) as well as several types of cancer (Kohnken et al., 2015, Rice et al., 2009a). This suggests the involvement of SAMHD1 in the innate immune response and cancer development possibly through the control of dNTP homeostasis. The most active agent against acute myelogenous leukemia (AML) is the deoxycytidine analog cytarabine (ara-C). Outcome in patients with AML ranges from a ~70 % 5-year overall survival rate among children (de Rooij et al., 2015) whereas elderly adult have only a 20 % 2-year overall survival rate (Ossenkoppele and Lowenberg, 2015). The number one reason of ara-C treatment failure and relapse is the patient's response to ara-C treatment. (Styczynski, 2007, Fernandez-Calotti et al., 2005). Ara-C is converted intracellularly into the active metabolite ara-CTP. Ara-CTP can be inserted into DNA which results in DNA damage and stop of DNA synthesis which eventually leads to cell death. Prior to the findings by Herold et al. there was no consistent explanation why patients responded differently to ara-C treatment. One hypothesis was that SAMHD1 might be able to bind and hydrolyze the dCTP-analog ara-CTP and thereby detoxify the active metabolite of ara-C. Our collaborators in Sweden purified recombinant human SAMHD1 and analyzed its *in vitro* activity in an assay where the release of inorganic phosphate produced by the hydrolysis of dCTP or ara-CTP by SAMHD1 was measured. This was done in the presence of nonhydrolyzable dGTP analog or GTP, both functioning as activators. While dGTP can bind to both allosteric sites AS1 and AS2, GTP only binds to AS1. Ara-CTP hydrolysis was achieved with the nonhydrolyzable dGTP analog but not with GTP-activated SAMHD1 (Figure 18 A). Ara-CTP hydrolysis was not as efficient as compared to dCTP hydrolysis in the presence of non-hydrolysable dGTP. The results suggest that ara-CTP exclusively binds to the substrate-binding site and does not serve as an allosteric activator of AS2. To further test the relevance of ara-CTP hydrolysis in cells we used three approaches. Firstly, we treated the AML cell line THP-1 with SIV-Vpx-containing (X) or control (dX) VLPs or no VLPs in the presence or absence of ara-C and measured the efficacy of ara-C induced cytotoxicity. The value of the half-maximal effective concentration (EC<sub>50</sub>) of ara-C was up to 130-fold reduced in cells treated with Vpx VLPs compared to control VLPs, or untreated cells (Figure 18A). Secondly, SAMHD1 knockout in THP-1 cells resulted in similar decreased EC<sub>50</sub> values for ara-C (Figure 18 B). Furthermore, we ectopically expressed CRISPR/Cas9-resistant wild type SAMHD1 or the catalytic dead mutants (H233A) or (D311A) or luciferase as negative control in the SAMHD1 knockout cells and compared the ara-C EC<sub>50</sub>

values. Ectopic expression of WT SAMHD1 sensitized THP-1 SAMHD1 knock-out cells to ara-CTP hydrolysis. In contrast, ectopic expression of the catalytic-dead mutants did not alter the EC<sub>50</sub> value for ara-C as compared to SAMHD1 knock-out cells (Figure 18 D).

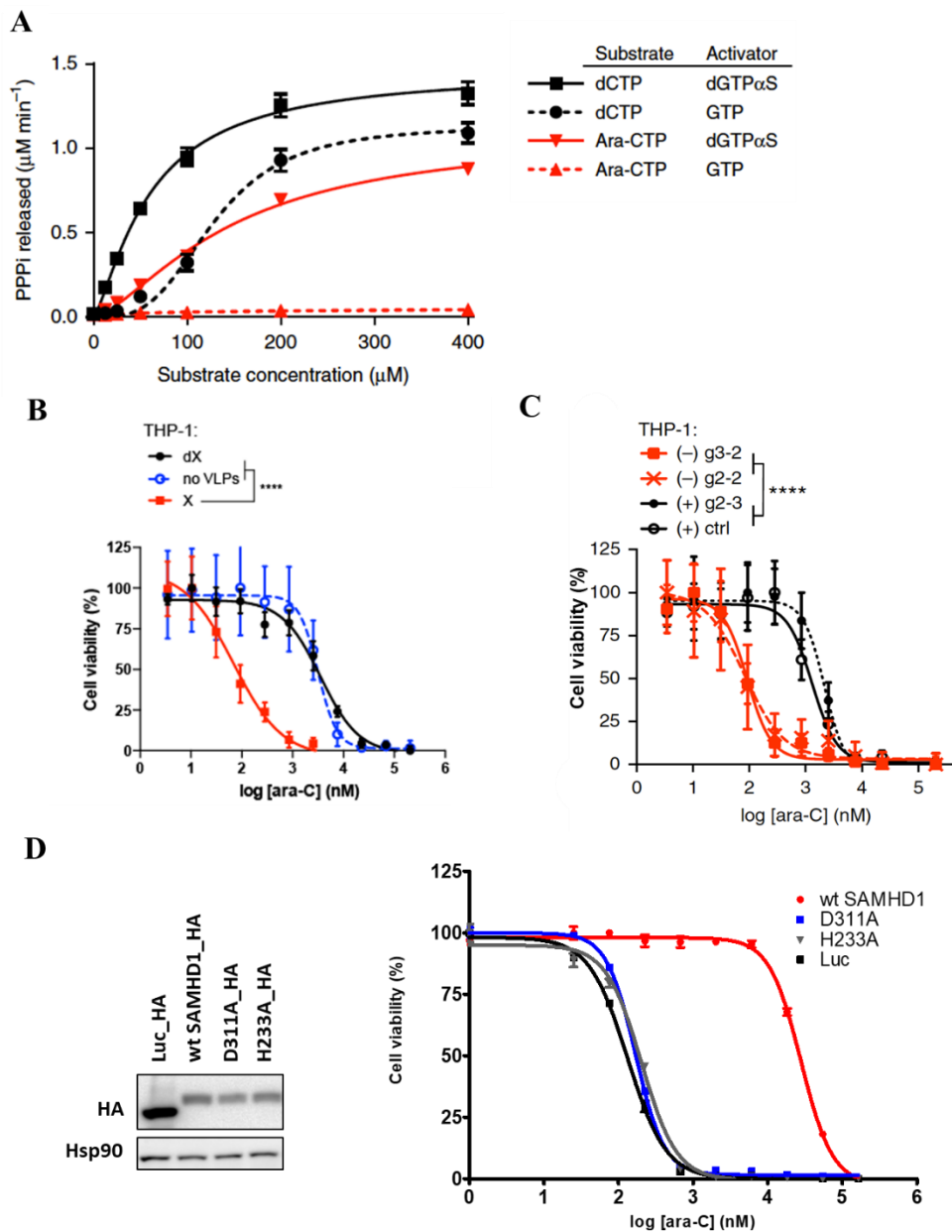


**Figure 18: Ara-C is a substrate of SAMHD1.**

**A)** Substrate-velocity curves measuring the amount of inorganic triphosphate (PPPi) produced from hydrolysis of dCTP or ara-CTP by SAMHD1 in the presence of GTP or a nonhydrolyzable dGTP analog (dGTP $\alpha$ S) in the enzyme-coupled malachite green assay. Error bars indicate s.e.m. of three independent experiments performed at least in triplicate. **B)** Cell viability of THP-1 which were treated with SIV-Vpx-containing (X) or control (dX) VLPs, or PBS (no VLPs) in the presence of ara-C. EC<sub>50</sub> values: THP-1 dX, 3,537 nM, THP-1 X, 69 nM, THP-1 no VLPs, 3,159 nM. Error bars indicate s.d. of a representative of three independent experiments performed in triplicate. **C)** Cell viability of THP-1 clones SAMHD1 knock out clones using CRISPR-Cas9 (g3-2, g2-2) and control clones (ctrl gRNA, g2-3) in the presence of ara-C at the indicated concentrations. EC<sub>50</sub> values: g3-2, 92 nM; g2-2, 82 nM; ctrl gRNA, 1,305 nM, g2-3, 2,170 nM. Error bars indicate s.d. of a representative of three independent experiments performed in triplicates. **D)** THP-1 clones with genetic disruption of SAMHD1 using CRISPR-Cas9 (g2-2) were transduced with the indicated SAMHD1 variant. Cell viability was tested in the presence of ara-C at the indicated concentrations. EC<sub>50</sub> values: HA-Luc, 132 nM; HA-H233A, 168 nM; HA-wt, 27,922 nM; HA-D311A, 168,7 nM. Error bars indicate s.d. of a representative of three independent experiments performed in triplicate. A, B, C from (Herold et al., 2017a)

These results suggested that the increased cytotoxicity of ara-C in SAMHD1 knock-out cells or in THP-1 cells in which SAMHD1 was degraded by Vpx could be the result of increased ara-CTP levels, which would lead to an increased incorporation of ara-CTP into the DNA. The observed data was in line with a model in which SAMHD1 hydrolyses ara-CTP and thereby neutralizes its toxic effects (Hollenbaugh et al., 2017). To analyse this directly, our collaborators measured the intracellular concentration of ara-C metabolites following a 2 h treatment with <sup>3</sup>H-ara-C in THP-1 cell clones that either expressed or lacked SAMHD1. SAMHD1 knockout resulted in 10-fold increased ara-CTP levels, which correlated with a 10-fold increase in DNA incorporated <sup>3</sup>H-ara-C levels in the SAMHD1 knockout THP-1 clone. This indicates that the lethal incorporation of ara-CTP is prevented by SAMHD1's ability to hydrolyze ara-CTP (Figure 19).

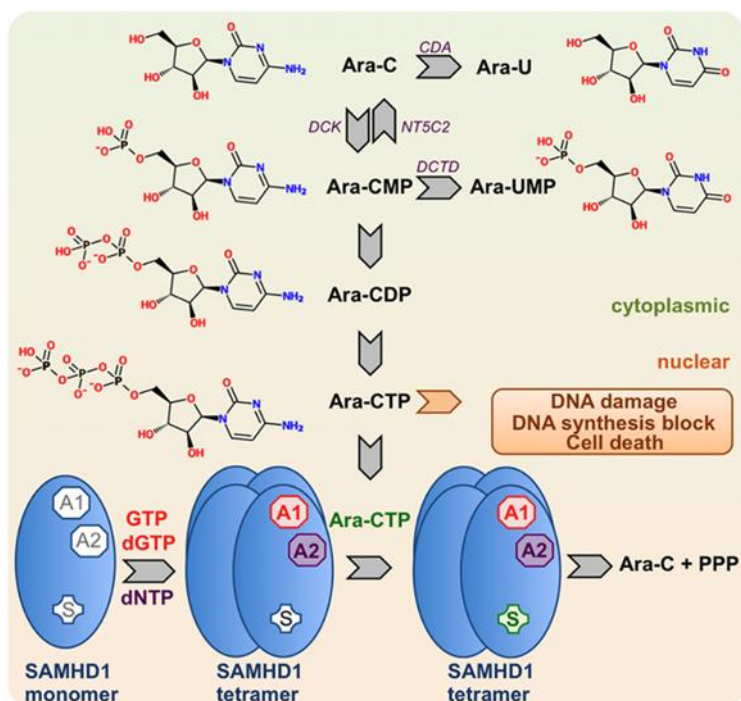


**Figure 19: Intracellular conversion of cytarabine (ara-C) to ara-CTP and detoxification mechanism by SAMHD1.**

The schematic depicts canonical pathways for the intracellular conversion of ara-C to the active metabolite ara-CTP. Ara-CTP can be inserted into DNA which results in DNA damage and stop of DNA synthesis which eventually leads to cell death. Ara-CTP serves as a substrate of SAMHD1. Ara-CTP is a substrate of SAMHD1 and by the hydrolyzation to ara-C + PPP, ara-CTP is inactivated. Abbreviations: CDA, cytidine deaminase; DCK, deoxycytidine kinase; NT5C2, cytosolic nucleotidase-II; DCTD, deoxycytidylate deaminase  
From: (Herold et al., 2017b)

In order to test whether the amount of expressed SAMHD1 influences the block to HIV-1 and cell viability after ara-C treatment we transduced the SAMHD1 <sup>-/-</sup> cell line g2-2 with a serial dilution of lentiviral vector containing HA-tagged WT SAMHD1. After approximately 1 week of transduction cells were differentiated with PMA and infected with a serial dilution of HIV-1 as before and in parallel we measured cytotoxicity to ara-C.

High SAMHD1 expression level is crucial for an extensive block of HIV-1 and increased the EC<sub>50</sub> value of ara-C by 40-fold (WT SAMHD1\_HA compared to wt SAMHD1\_HA 1:16) (Figure 20). The data suggest that a threshold of SAMHD1 protein levels may limit restriction of HIV-1 infection and that this threshold correlates with enhanced resistance to ara-C induced cytotoxicity.

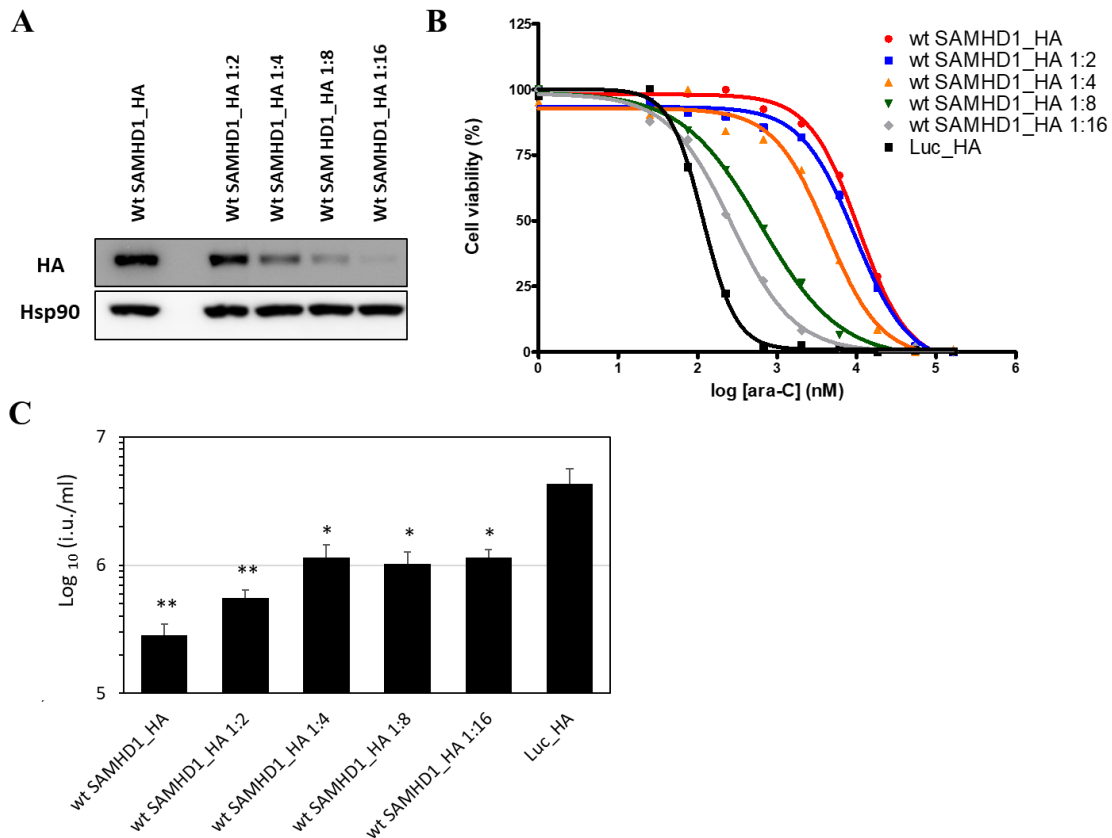


**Figure 20: High SAMHD1 expression levels are crucial for a pronounced block of HIV-1 infection and enhanced cell viability after ara-C treatment.**

**A)** Western blot of SAMHD1 dilution series **B)** Cells were treated with indicated concentrations of cytarabine (ara-C) for 3 days to obtain maximal cytotoxicity and cell viability was determined using a colorimetric proliferation inhibition assay. Error bars indicate s.e.m. of three independent experiments performed at least in triplicate.  $EC_{50}$  values are the following wt SAMHD1\_HA, 10616 nM; wt SAMHD1\_HA 1:2, 9506 nM; wt SAMHD1\_HA 1:4, 4282 nM; wt SAMHD1 1:8, 625,3 nM, wt SAMHD1\_HA 1:16, 264,3 nM; Luc\_HA, 117 nM. **C)** PMA-treated SAMHD1  $-/-$  cells stably expressing the indicated SAMHD1 variants were challenged with serial dilutions of VSV-G-pseudotyped HIV-1 GFP, and the infectious units (i.u.) per ml of inoculum were calculated. Mean titers with standard deviations are depicted and significance to block HIV-1 in cells expressing SAMHD1 compared to no SAMHD1(Luc\_HA) are indicated). Statistical analysis was performed using an unpaired two-tailed *t* test. ns, not statistically significant; \*,  $P < 0.05$ ; \*\*,  $P < 0.01$ .

Herold et al. and Schneider et al. published that malignant leukemic cells can be sensitized to ara-C through degradation of SAMHD1 thereby eliminating the factor which is responsible for ara-CTP hydrolyzes (Herold et al., 2017a, Schneider et al., 2017). SAMHD1 has been suggested as tumor suppressor gene (Johansson et al., 2018, Herold et al., 2017c). Several reports suggest that SAMHD1 inactivation through promoter silencing or mutations within the SAMHD1 reading frame promote tumorigenesis (Landau et al., 2013, Clifford et al., 2014, Rentoft et al., 2016). In addition, miRNAs targeting SAMHD1 expression function as drivers of tumorigenesis (Kohnken et al., 2017). To date there are approximately 197 SAMHD1 mutations known which spread across 26 cancer projects (TCGA) (Figure 21).

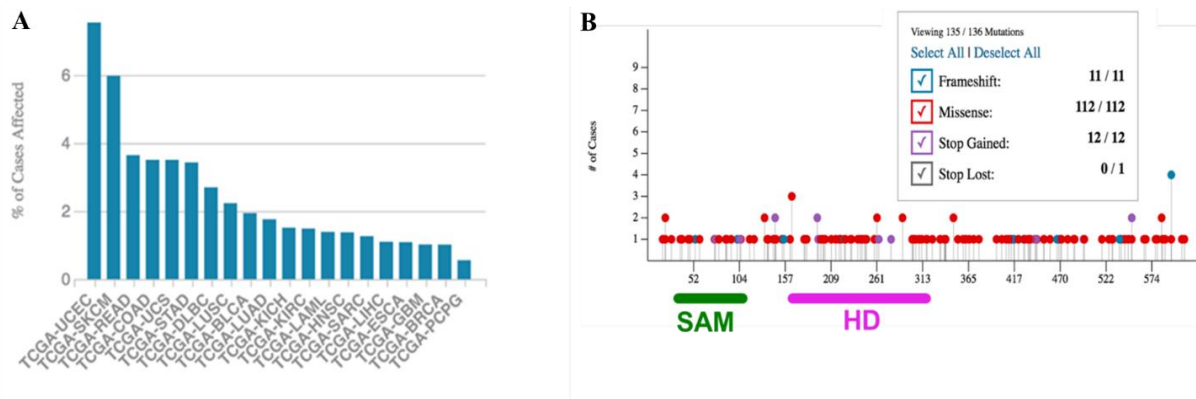


**Figure 21: SAMHD1's role in tumorigenesis.**

**A)** There are 180 cases affected by 197 mutations in SAMHD1 across 26 projects. (according to portal.gdc.cancer.gov) **B)** Distribution of SAMHD1 mutations and occurrence of SAMHD1 mutations in Uterine Corpus Endometrial Carcinoma (UCEC), Rectum Adenocarcinoma (READ), Colon Adenocarcinoma (COAD), Acute Myeloid Leukemia (AML) and Stomach Adenocarcinoma (Manel et al.) (portal.gdc.cancer.gov.)

To further investigate the influence of known SAMHD1 mutation in AML, READ, STAD and COAD (Table 1) on ara-CTP hydrolysis we expressed haemagglutinin (HA)-tagged CRISPR/Cas9-resistant SAMHD1 variants in the THP-1 g2c2 SAMHD1  $-/-$  cell line by using lentiviral vectors. The main goal of this was to use naturally occurring SAMHD1 variants, to avoid artificially generated and possibly deleterious mutants, in order to dissect the role of the enzymatic SAMHD1 activity from its antiviral activity, hence to learn more about the cellular role of SAMHD1 in order to understand its impact on the type I interferon induced block against HIV-1 infection. Prior to performing experiments, we analyzed the expression levels of SAMHD1 variants by western blot. We investigated the sensitivity of the generated cells ectopically expressing SAMHD1 variants to ara-C-induced cytotoxicity. As negative control, we used SAMHD1  $-/-$  cells, which were transduced with HA-tagged Luciferase (HA-Luc). We simultaneously analyzed HIV-1 restriction by these SAMHD1 variants in PMA differentiated cells by infecting them with a serial dilution of VSV-G pseudotyped HIV-1 GFP reporter and FACS analysis 48 h after infection. All experiments were done in triplicates and one representative is shown if not indicated differently.

**Table 1 SAMHD1 variants analyzed in this study**

SNP/ ID	Disease		AA change	PMID/ Ref
	AGS	CANCER		
-	-	-	WT	
Catal.site	-	-	H233A	
Catal.site	-	-	D311A	
		TCGA <sup>2</sup>	D137N	
TCGA-AZ-6598-01A-11D-1771-10	Yes	TCGA <sup>2</sup>	V133I	(Rentoft et al., 2016)
	-	TCGA <sup>2</sup>	A338T	(Rentoft et al., 2016)
TCGA-AD-6889-01A-11D-1924-10	-	TCGA <sup>2</sup>	R366H	(Rentoft et al., 2016)
TCGA-AZ-4315-01A-01D-1408-10	-	TCGA <sup>2</sup>	D497Y	(Rentoft et al., 2016)
rs515726145, TCGA-A6-3808-01A-01W-0995-10	Yes	COSMIC, CLL <sup>1</sup> , TCGA <sup>2</sup>	R145Q	(Rentoft et al., 2016, Clifford et al., 2014) (Rice et al., 2009a)
TCGA-CM-6674-01A-11D-1835-10	-	TCGA <sup>2</sup>	A525T	(Rentoft et al., 2016)
TCGA-AA-A02W-01A-01W-A00E-09	-	TCGA <sup>2</sup>	R451P	(Rentoft et al., 2016)
TCGA-G4-6588-01A-11D-1771-10	-	TCGA <sup>2</sup>	A338V	(Rentoft et al., 2016)
TCGA-CK-4951-01A-01D-1408-10	-	TCGA <sup>2</sup>	G90R	
rs559553527	Yes	CLL <sup>1</sup>	R290H	(Guieze et al., 2015, Goncalves et al., 2012a)
	-	TCGA <sup>2</sup>	K596fs	(Rentoft et al., 2016)
rs761561066, TCGA-AA-A01R-01A-21W-A096-10	-	COSMIC, TCGA <sup>2</sup>	R348C	(Rentoft et al., 2016)
rs141599277	-	COSMIC	A76T	(Rentoft et al., 2016)
TCGA-EI-6917-01A-11D-1924-10	-	COSMIC, TCGA <sup>4</sup>	R305I	(Rentoft et al., 2016)
		TCGA <sup>3</sup>	S214P	
TCGA-AB-2826-03B-01W-0728-08	-	TCGA <sup>3</sup>	L178Q	
		TCGA <sup>5</sup>	P589T	
Acytylation			K405R	(Lee et al., 2017)
Redox			C522S	(Mauney et al., 2017)

<sup>1</sup>: UK clinical trial derived CLL samples (pretreatment and relapsed/refractory trials)

<sup>2</sup>: TCGA-COAD

<sup>3</sup>: TCGA-LAML

<sup>4</sup>: TCGA-READ

<sup>5</sup> TCGA-STAD



### 10.2.1 SAMHD1 SNPs in Rectum Adenocarcinoma (READ)

In Rectum Adenocarcinoma (READ) currently three missense mutation have been described: A76T, R305I and S302Y. According to the TCGA website the variant effect predictor (VEP) impact of all three mutation is moderate and the PolyPhen impact score result is benign for all three mutations.<sup>2</sup> PolyPhen is a tool which predicts the possible impact of an amino acid change on the structure and function of a human protein using physical and comparative considerations.<sup>3</sup> Another prediction tool is VEP which determines the effect of your variants on transcripts, genes and protein sequence, as well as regulatory regions.<sup>4</sup>

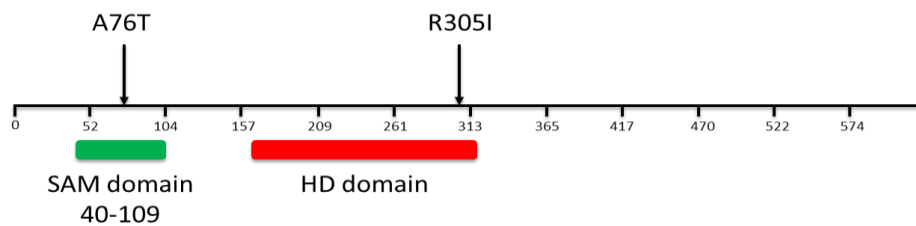


**Figure 22: Schematic representation of analyzed SAMHD1 mutations in Rectum Adenocarcinoma (READ).**

A76 lies within the SAM domain which was not yet crystalized (Figure 22). The R305 mutation residues in close proximity to the active site (Figure 23).

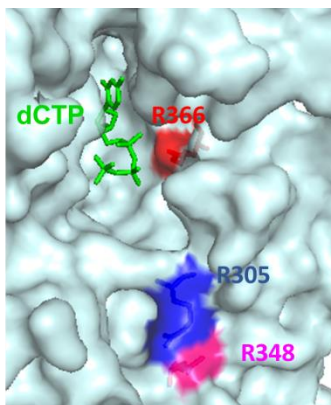


**Figure 23: SAMHD1 crystal structure with dCTP bound.**

R366, R305 and R348 are in close proximity to the active site and might alter ara-CTP and nucleotide binding. (PDB: 4RXX)

SAMHD1 variants A76T and R305I were expressed in the SAMHD1<sup>-/-</sup> cell line g2-2 and comparable expression to WT SAMHD1 was achieved (Figure 24 A). Ectopic expression of WT or A76T as well as R305I increased the EC<sub>50</sub> for ara-C by 94-142-fold. R305I increased the EC<sub>50</sub> for ara-C by 1,5-fold more as compared to WT SAMHD1. Both SAMHD1 variants sufficiently blocked HIV-1 infection and respectively to WT SAMHD1 the block to HIV-1

<sup>2</sup><https://portal.gdc.cancer.gov/>

<sup>3</sup> <http://genetics.bwh.harvard.edu/pph2/>

<sup>4</sup> <https://www.ensembl.org/info/docs/tools/vep/index.html>

infection was slightly increased hence SAMHD1 SNPs mutants A76T or R305I have no negative effect on ara-C sensitivity and increased HIV-1 restriction significantly.

The reasons underlying this enhanced restriction are unclear, but the data suggest that both mutants A76T or R305I may impact permissivity of cells to HIV-1 infection. Whether this is connected to READ needs to be investigated.

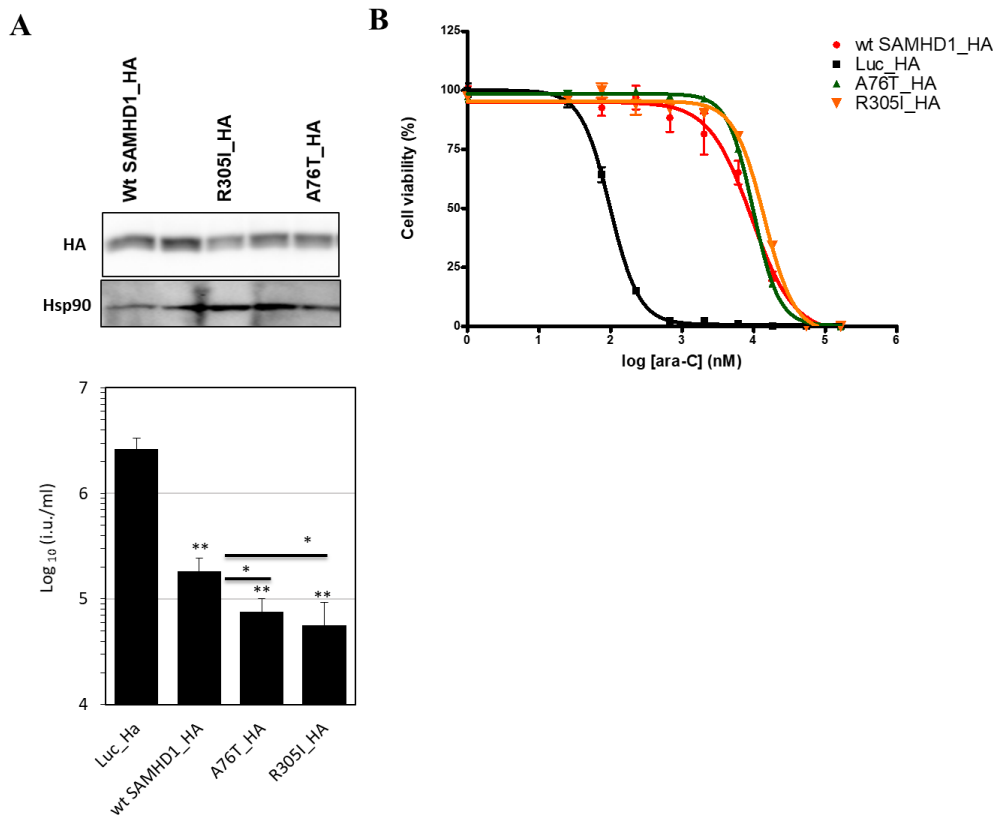


**Figure 24: Expression of SAMHD1 SNP variants A76T or R305I in THP-1 SAMHD1 -/- cells increases HIV-1 restriction and has no impact on ara-C sensitivity.**

**A)** Western blot of SAMHD1 variants **B)** Cells were treated with indicated concentrations of cytarabine (ara-C) for 3 days to obtain maximal cytotoxicity and cell viability was determined using a colorimetric proliferation inhibition assay. Error bars indicate s.d. of a representative of three independent experiments performed in triplicates. EC<sub>50</sub> values are the following wt SAMHD1\_HA, 9333 nM; Luc\_HA, 98,48 nM; A76T, 9850 nM; R305I, 14026 nM **C)** PMA-treated SAMHD1 -/- cells stably expressing the indicated SAMHD1 variants were challenged with serial dilutions of VSV-G-pseudotyped HIV-1 GFP, and the infectious units (i.u.) per ml of inoculum were calculated. Representative of at least 2 independent titrations is shown. Mean titers of at least 3 titration points with standard deviations are depicted and significance to block HIV-1 in cells expressing SAMHD1 compared to no SAMHD1(Luc\_HA) are indicated). Statistical analysis was performed using an unpaired two-tailed *t* test. ns, not statistically significant; \*, *P* < 0.05; \*\*, *P* < 0.01.

### 10.2.2 SAMHD1 SNPs in acute myeloid leukemia (AML)

In 144 analyzed cases of AML there were 2 cases in which SAMHD1 was mutated to either L178Q or S214P. For both substitutions the VEP impact is moderate, SIFT impact is deleterious and the PolyPhen impact predicts that the missense mutations are probably damaging<sup>5</sup>.

S214 is buried in the active site of SAMHD1, while L178 is close to A338, a residue that has functions in COAD (see below).

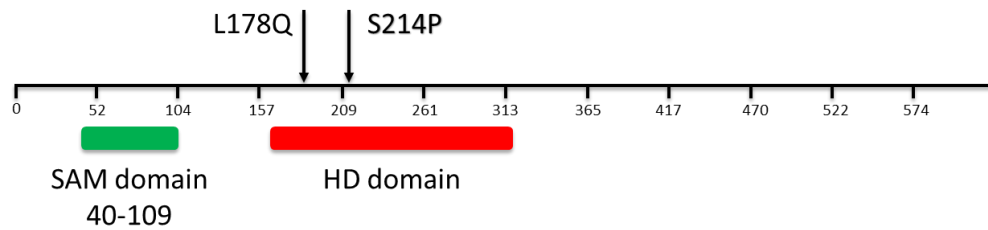


**Figure 25: Schematic representation of SAMHD1 Mutations in acute myeloid leukemia (AML).**

In the crystal structure of Zhu et al. L178 is in close proximity to A338 which might indicate an involvement in the dimer-dimer interface/tetramerization of SAMHD1 (Zhu et al., 2015). The SAMHD1 Residue S214 (Figure 27) lies close to the active site and is directly connected with H215 which interacts with nucleotides (Ahn, 2016).

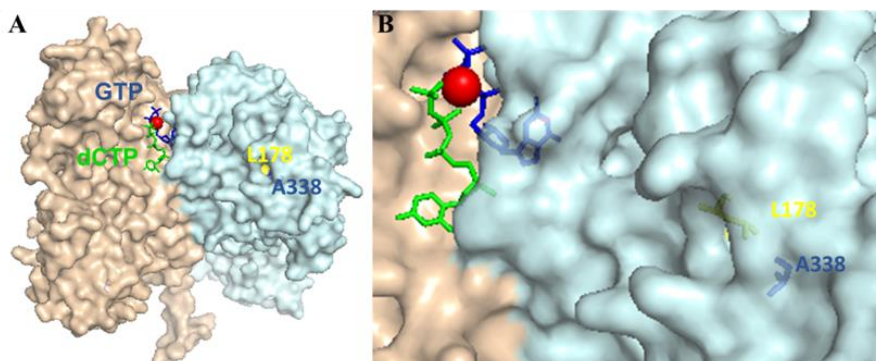


**Figure 26: SAMHD1 Dimer-Dimer interface with L178 (yellow) and A338 (blue) (PDB: 4RXX).**

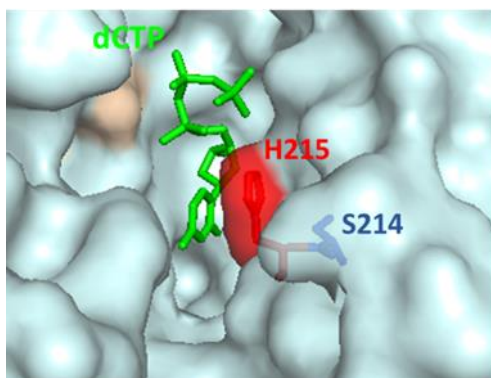


**Figure 27: SAMHD1 catalytic site.**

The residue at the catalytic site H215 is connected to residue S214. (PDB: 4RXX)

<sup>5</sup><https://portal.gdc.cancer.gov/>

We ectopically expressed the two mutants in SAMHD1 knock-out cells as described above. The expression level of the SAMHD1 variant L178Q was significantly lower than wt SAMHD1 expression (referred to as L178Q\_HA\_1 and wt SAMHD1\_HA\_1) (Figure 28 A1). Cell expressing L178Q were similarly permissive to HIV-1 infection as compared to control cells (Figure 28 A3). Expression of L178Q increased the EC<sub>50</sub> value for ara-C by 5.5-fold as compared to control cells. To exclude effects dependent on reduced expression levels of L178Q as compared to WT SAMHD1 we repeated the experiments with cells expressing slightly higher protein levels of L178Q as compared to WT (labeled as 2 in Figure 28 A).

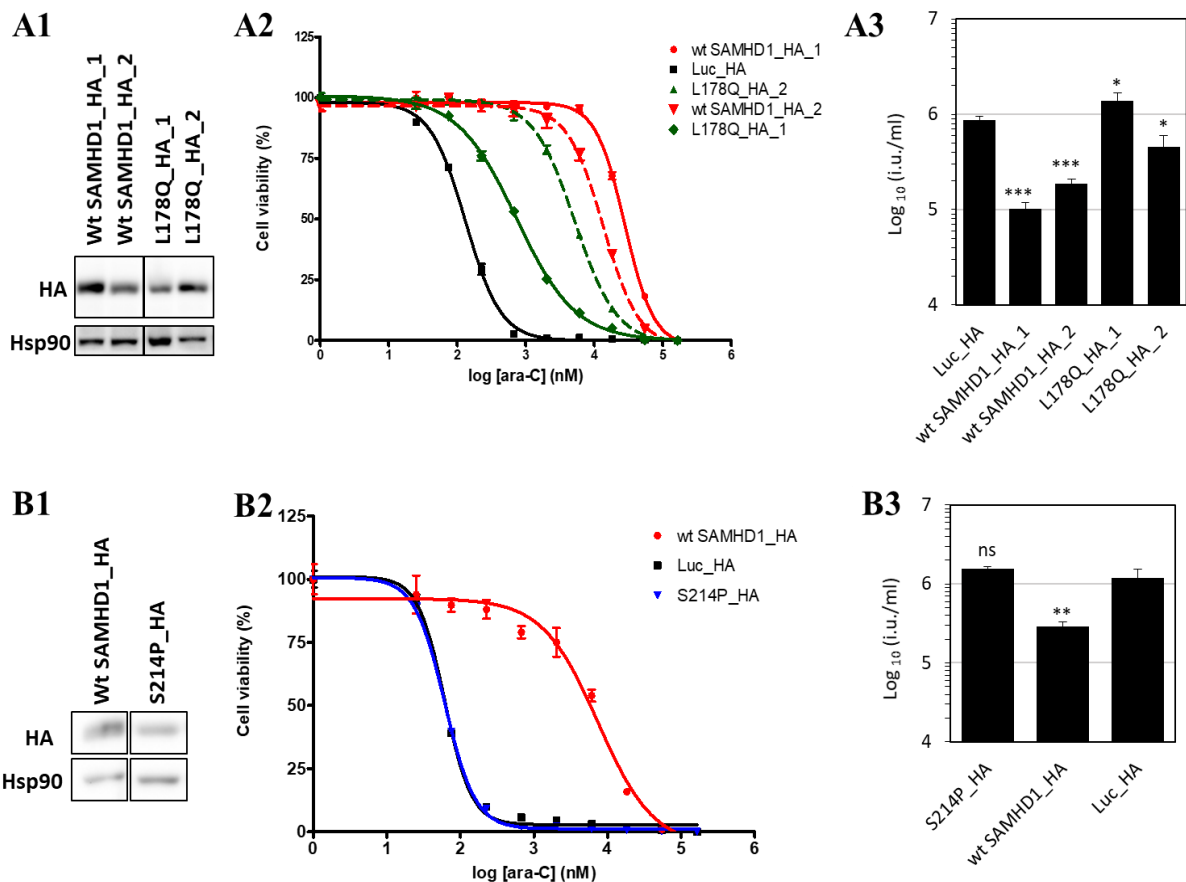


**Figure 28: Expression of AML SAMHD1 SNP variants L178Q or S214P in THP-1 SAMHD1 -/- cells renders these cells more permissive to HIV-1 infection as compared to WT and enhances ara-C sensitivity.**

**A1; B1)** Western blot using an HA-specific Ab to detect HA-tagged SAMHD1 variants and WT **A2; B2)** Cells were treated with indicated concentrations of cytarabine (ara-C) for 3 days to obtain maximal cytotoxicity and cell viability was determined using a colorimetric proliferation inhibition assay. Error bars indicate s.d. of a representative of three independent experiments performed in triplicates. EC<sub>50</sub> values are the following: **A1)** wt SAMHD1\_HA\_1, 27922 nM; wt SAMHD1\_HA\_2, 13585 nM; Luc\_HA, 132,3 nM; L178Q\_HA\_1, 731,3 nM; L178Q\_HA\_2, 5213 nM; **B2)** wt SAMHD1\_HA, 7438 nM; S124P\_HA, 61,51nM; Luc\_HA 61,36 nM **C1;C2)** PMA-treated SAMHD1 -/- cells stably expressing the indicated SAMHD1 variants were challenged with serial dilutions of VSV-G-pseudotyped HIV-1 GFP, and the infectious units (i.u.) per ml of inoculum were calculated. Representative of at least 2 independent titrations is shown. Mean titers of at least 3 titration points with standard deviations are depicted and significance to block HIV-1 in cells expressing SAMHD1 compared to no SAMHD1 (Luc\_HA) are indicated. Statistical analysis was performed using an unpaired two-tailed t test. ns, not statistically significant; \*,  $P < 0.05$ ; \*\*,  $P < 0.01$ ; \*\*\*,  $P < 0.001$

The results showed that SAMHD1 L178Q blocked HIV-1 infection 2.6-fold less as compared to WT SAMHD1, in line with a ca. 5-fold reduced EC<sub>50</sub> for ara-C as compared to WT SAMHD1 (wt SAMHD1\_HA\_2, 13585 nM; L178Q\_HA\_2, 5213 nM). The second SAMHD1 SNP mutant in AML (S214P) did not block HIV-1 infection upon expression and cells expressing this mutant were highly sensitive to ara-C treatment comparable to cells that lack SAMHD1 (Figure 28 B).

The data suggest that the SAMHD1 variant S214P is defective in ara-CTP hydrolysis, as well as inactive in blocking HIV-1 infection. Hence, AML cells expressing the SNP versions L178Q or S214P of SAMHD1 are likely more sensitive to ara-C and detection of these SNPs in AML patients may be predictive for improved chances for an effective ara-C treatment during consolidation therapy (Herold et al., 2017a).

### 10.2.3 SAMHD1 SNPs in colon adenocarcinoma (COAD)

In 59 analyzed cases of COAD 16 mutations of SAMHD1 were identified in the TCGA database. We decided to analyze all 13 missense SNPs and the frameshift mutant K596Rfs\*35. Their distribution within the SAMHD1 protein is depicted in Figure 29. Out of the 13 analyzed mutants 11 were predicted to be damaging by at least one of 3 computational tools (VEP,SIFT,PolyPhen2). Four of the mutated residues (R145, R366, R451 and D137) are located in vicinity of amino acid residues that have been reported to be functionally significant in in vitro studies (Ryoo et al., 2014b, Ji et al., 2013, White et al., 2013b, St Gelais et al., 2018). Among the 36 SAMHD1 mutations in the current Catalogue of Somatic Mutations in Cancer (COSMIC) database only 4 (5,5 %) were silent mutations. The following amino acid substitutions were found in hypermutated tumors (> 12 mutation per 10<sup>6</sup> bases): V133I, A338T, A338V, R366H, D49Y, A525T and K596Rfs\*35 (Rentoft et al., 2016).

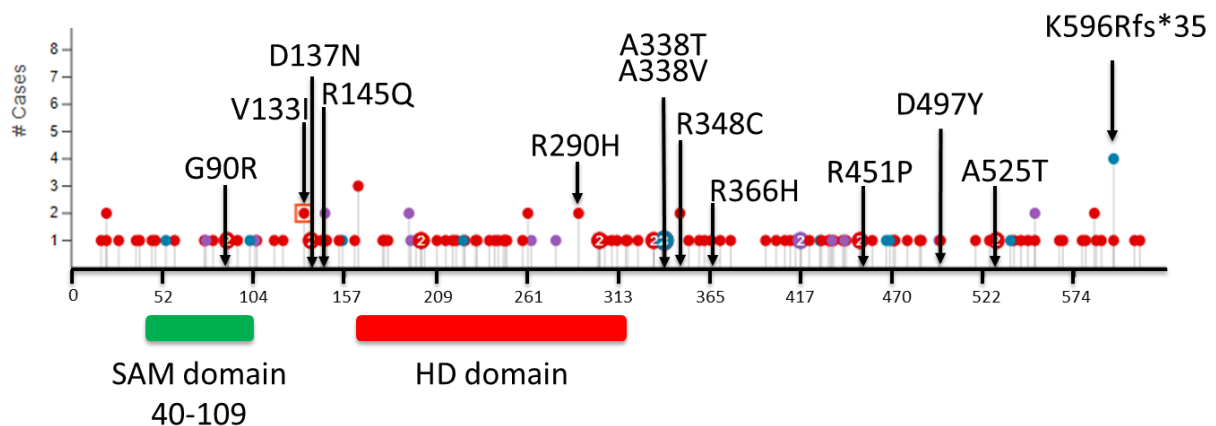


**Figure 29:** Schematic representation of SAMHD1 Mutations in colon adenocarcinoma (COAD) and their appearances in analyzed cases. (adapted from TCGA)

**Table 2 Mutation of COAD analyzed and their impact for canonical transcript.**

Abbreviation: HI: high; MO: moderate; DH: deleterious; TO: tolerated; PR: probably\_damaging; PO: possibly damaging; BE: benign (data from portal.gdc.cancer.gov)

Mutation	Impact		
	VEP	SIFT	PolyPhen
<b>K596Rfs*35</b>	HI	-	-
<b>R451P</b>	MO	DH	PR
<b>R145Q</b>	MO	DH	PR
<b>D137N</b>	MO	DH	PR
<b>R290H</b>	MO	DH	PR
<b>R366H</b>	MO	DH	PO
<b>A525T</b>	MO	DH	BE
<b>R348C</b>	MO	DH	BE
<b>D497Y</b>	MO	DH	BE
<b>G90R</b>	MO	TO	PO
<b>A338T</b>	MO	TO	PO
<b>V133I</b>	MO	TO	BE
<b>A338V</b>	MO	TO	BE

The G90R mutation lies closely to the end of the SAMHD1 SAM domain. Deletion construct studies of SAMHD1 revealed that the SAM domain is dispensable for HIV-1 restriction (White et al., 2013a). When SAMHD1 G90R was ectopically expressed in SAMHD1 knockout cells, protein expression varied in each of the three conducted experiments. Therefore, all three experiments are shown. SAMHD1 G90R mutant has to be expressed at higher protein levels than WT SAMHD1 (G90R\_HA\_2) in order to achieve a significant block to HIV-1 infection (wt SAMHD1\_HA\_2 vs. G90R\_HA\_2). Nevertheless, the block to HIV-1 infection in cells expressing high levels of G90R (G90R\_HA\_1) was 4-fold lower compared to wt SAMHD1 (wt SAMHD1\_HA\_2). Sensitivity to ara-C was 2.4-fold lower compared to wt SAMHD1 with higher expression (G90R\_HA\_1, 5647 nM vs wt SAMHD1\_HA\_2, 13585 nM) (Figure 30 C). The data suggest that COAD tumor cells with SAMHD1 SNP variant G90R may be more sensitive to ara-C and possibly other chemotherapeutic drugs that are converted to substrates for SAMHD1 in cells.

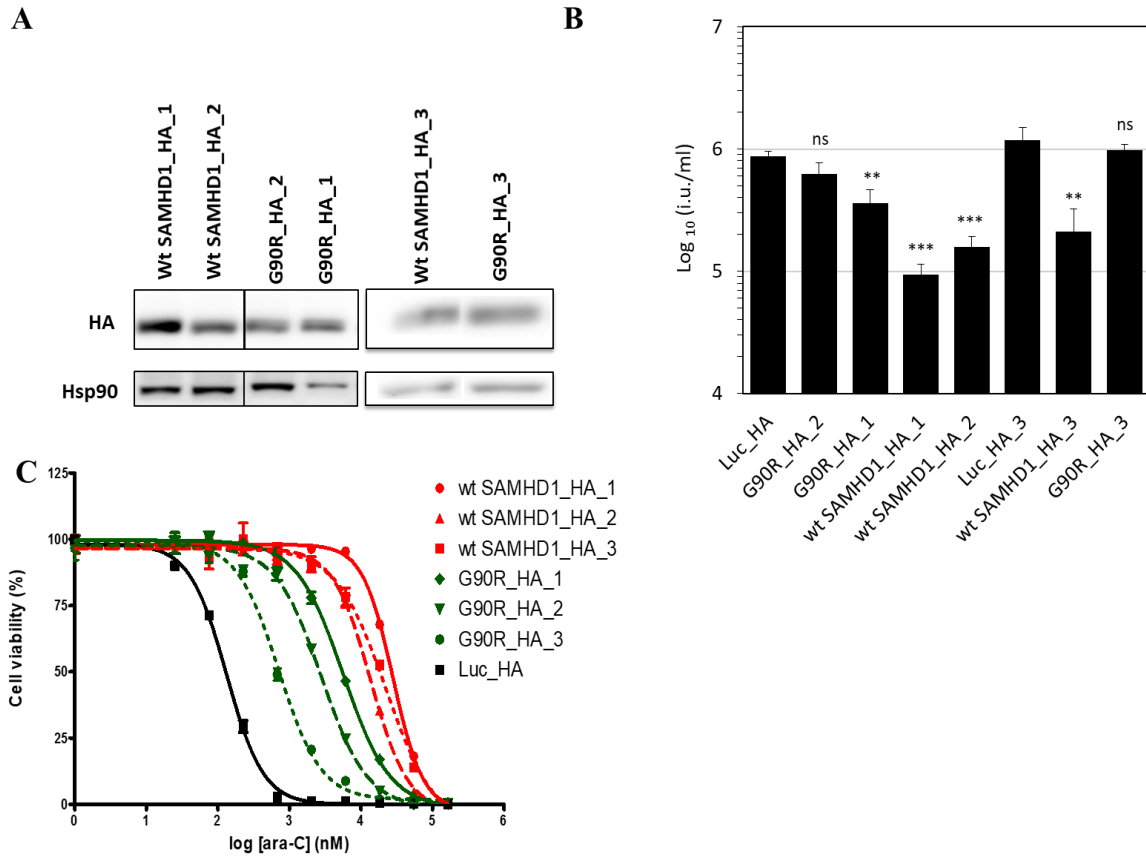


**Figure 30: Expression of SAMHD1 SNP variant G90R in THP-1 SAMHD1<sup>-/-</sup> cells impacts HIV-1 restriction and enhances ara-C sensitivity.**

**A)** Western blot 3 independent G90R and wt SAMHD1 transduction **B)** PMA-treated SAMHD1<sup>-/-</sup> cells stably expressing the indicated SAMHD1 variants were challenged with serial dilutions of VSV-G-pseudotyped HIV-1 GFP, and the infectious units (i.u.) per ml of inoculum were calculated. Mean titers of at least 3 titration points with standard deviations are depicted and significance to block HIV-1 in cells expressing SAMHD1 compared to no SAMHD1 (Luc\_HA) are indicated. Statistical analysis was performed using an unpaired two-tailed t test. ns, not statistically significant; \*, P < 0.05; \*\*, P < 0.01. **C)** Cells were treated with indicated concentrations of cytarabine (ara-C) for 3 days to obtain maximal cytotoxicity and cell viability was determined using a colorimetric proliferation inhibition assay. Error bars indicate s.d. of a representative of three independent experiments performed in triplicates. EC<sub>50</sub> values are the following wt SAMHD1\_HA\_1, 27922 nM; wt SAMHD1\_HA\_2, 13585 nM; wt SAMHD1\_HA\_3, 22287 nM; Luc\_HA, 61,36 nM; G90R\_HA\_1, 5647 nM; G90R\_HA\_2, 2802 nM; G90R\_HA\_3, 713,2 nM

Rentoft et al. analyzed A338T by recombinant protein purification and *in vitro* characterization. *In vitro* the dNTPase activity of A338T was significantly altered (5-6-fold reduction) for all four desoxynucleotide-triphosphates (Rentoft et al., 2016). This would suggest that A338T would not be able to restrict HIV-1 infection and ara-C sensitivity should be comparable to loss of SAMHD1 but only if a loss of dNTPase correlates with a loss of ara-C hydrolysis. In contrast, we found that A338T was still able to restrict HIV-1 infection but to a lesser extent as compared to WT SAMHD1. To our surprise A338T was able to neutralize the ara-C induced cytotoxicity to the same extent as WT SAMHD1 (Figure 31), suggesting that it has no defect in hydrolyzing ara-CTP. The data suggest that SAMHD1 A338T was specifically impaired in HIV-1 restriction

while containing full function in ara-CTP hydrolysis. It is therefore the first naturally occurring SAMHD1 amino acid variant that affects HIV-1 restriction.

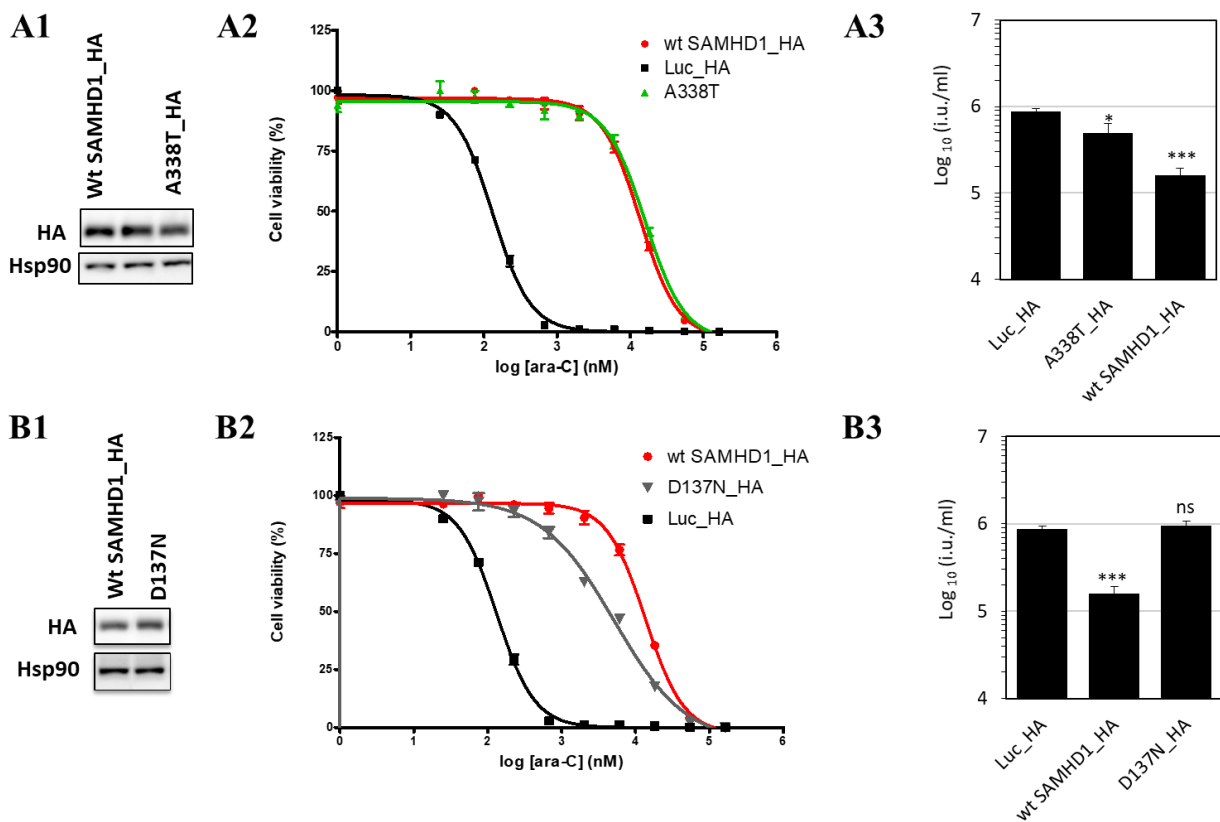


**Figure 31: Expression of SAMHD1 SNP variants A338T and D137N in THP-1 influence on HIV-1 restriction and sensitivity to ara-C treatment.**

**A1; B1)** Western blot of SAMHD1 of SAMHD1 variants and wt SAMHD1 **A2; B2)** Cells were treated with indicated concentrations of cytarabine (ara-C) for 3 days to obtain maximal cytotoxicity and cell viability was determined using a colorimetric proliferation inhibition assay. Error bars indicate s.d. of a representative of three independent experiments performed in triplicates.  $EC_{50}$  values are the following: **A2)** wt SAMHD1\_HA, 13585 nM; Luc\_HA, 132,3 nM; A338T\_HA, 15995 nM; **B2)** wt SAMHD1\_HA, 27922 nM; D137N\_HA, 5143 nM; Luc\_HA 132,3 nM **C1;C2)** PMA-treated SAMHD1  $-/-$  cells stably expressing the indicated SAMHD1 variants were challenged with serial dilutions of VSV-G-pseudotyped HIV-1 GFP, and the infectious units (i.u.) per ml of inoculum were calculated. Representative of at least 2 independent titrations is shown. Mean titers of at least 3 titration points with standard deviations are depicted and significance to block HIV-1 in cells expressing SAMHD1 compared to no SAMHD1(Luc\_HA) are indicated). Statistical analysis was performed using an unpaired two-tailed *t* test. ns, not

The SAMHD1 allosteric site mutant D137N is RNase-positive but dNTPase-negative and is able to restrict HIV-1 infection in PMA treated U937 cells overexpressing D137N (Ryoo et al., 2014a). Herold et al. reported recently that ectopic expression of D137N in SAMHD1 knockout HuT-78 cell line did not increase the  $EC_{50}$  level comparable to wt SAMHD1 expression (Herold et al., 2017a). Residue D137 is part of the allosteric site (Figure 32) and forms hydrogen bonds with GTP (Arnold et al., 2015). In our case D137N expression in THP-1 SAMHD1 knockout cells resulted in a 38-fold decrease in ara-C sensitivity (D137N\_HA, 5143 nM; Luc\_HA 132,3 nM) and HIV-1 was not blocked.



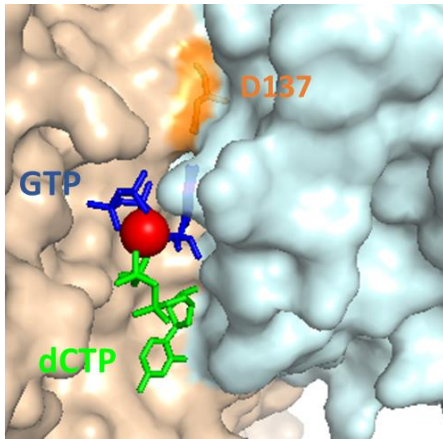


**Figure 32: SAMHD1 allosteric site with D137 residue depicted in orange.**  
*D137N forms hydrogen bonds with the G base. (PDB: 4RXX)*

Rentoft et al. also analyzed V133I by recombinant protein purification and in vitro characterization. In vitro the dNTPase activity of V133I was significantly reduced (1.6-2-fold reduction) but not as strong as observed in vitro for SAMHD1 A338T for all four deoxynucleoside triphosphates (Rentoft et al. 2016). Therefore, we expected a slightly reduced block to HIV-1 infection and ara-C sensitivity should be comparable to wt SAMHD1 with a minor reduction. As seen in Figure 33 V133 resides close to the allosteric site. In our experimental setup V133I expression significantly boosted HIV-1 restriction compared to WT SAMHD1 and ara-C sensitivity was not affected compared to wt SAMHD1. The data suggest that V133I specifically affects HIV-1 restriction but not ara-CTPase activity. SAMHD1 has been involved in intrinsic immunity and it is possible that V133I affects this part of the function of this protein inducing a more potent antiviral state in the cells as compared to WT SAMHD1.

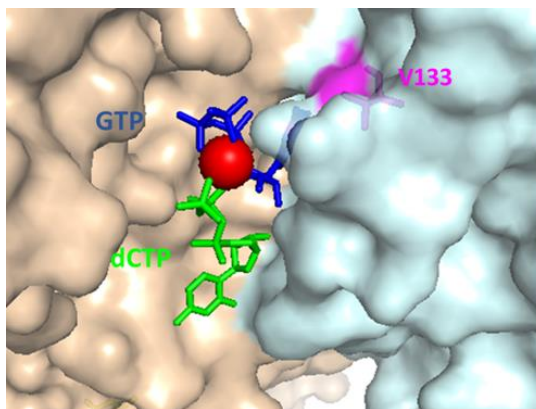


**Figure 33: SAMHD1 allosteric site.**  
*V133 is near the allosteric site pocket. (PDB: 4RXX)*

SAMHD1 A525T was also found associated with COAD (TCGA) and structural analyzed revealed that A525 lies close to the border of the connecting monomers (Figure 34).

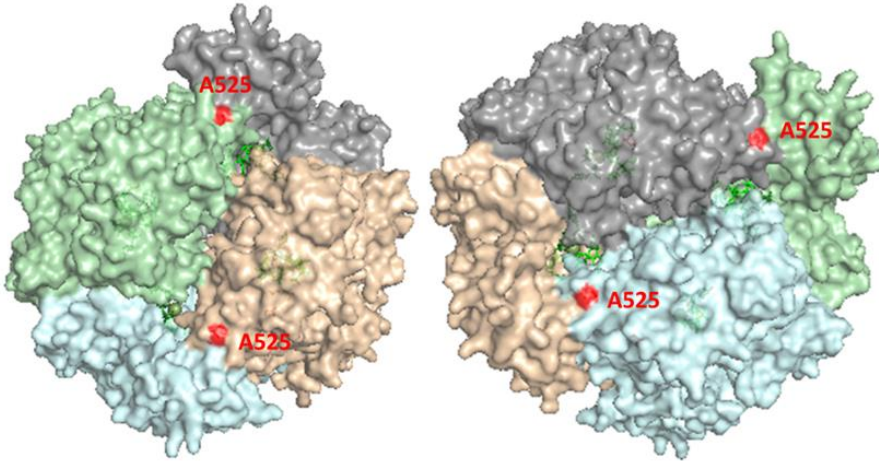


**Figure 34: Crystal SAMHD1 tetramer structure.**  
Residue A525 is depicted in red. (PDB: 4TNP)

We analyzed this mutant in a similar way to the mutants described above. We found that SAMHD1 A525T expression reduced ara-C induced cytotoxicity, hence it is presumably able to detoxify the cell of ara-CTP. In contrast, SAMHD1 A525T was unable to block HIV-1 infection (Figure 35 B2, B3).

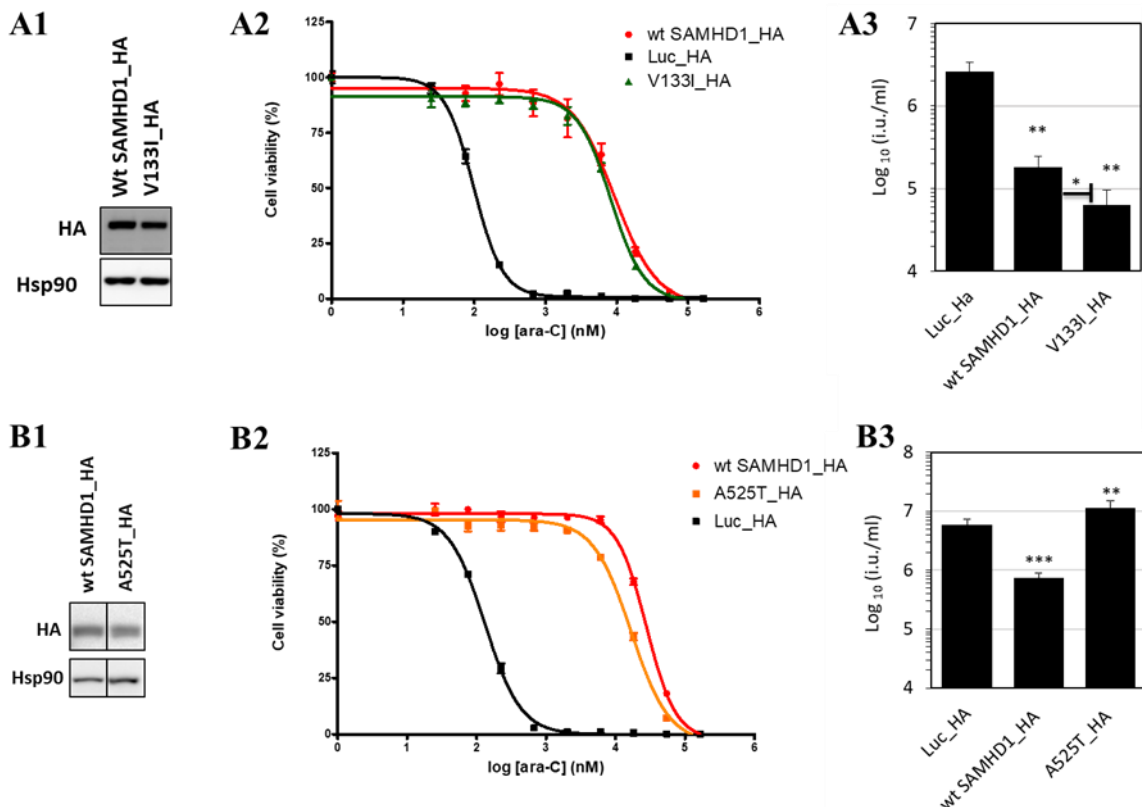


**Figure 35: Expression of SAMHD1 SNP variants V133I and A525T in THP-1 SAMHD1<sup>-/-</sup> cells and their influence on HIV-1 restriction and sensitivity to ara-C treatment.**

**A1; B1)** Western blot of SAMHD1 of SAMHD1 variants and wt SAMHD1 **A2; B2)** Cells were treated with indicated concentrations of cytarabine (ara-C) for 3 days to obtain maximal cytotoxicity and cell viability was determined using a colorimetric proliferation inhibition assay. Error bars indicate s.d. of a representative of three independent experiments performed in triplicates. EC<sub>50</sub> values are the following: **A2)** wt SAMHD1<sub>HA</sub>, 9333 nM; Luc<sub>HA</sub>, 98,48 nM; V133I<sub>HA</sub>, 8222 nM; **B2)** wt SAMHD1<sub>HA</sub>, 27922 nM; A525T<sub>HA</sub>, 16754 nM; Luc<sub>HA</sub>

168,7 nM CI; C2) PMA-treated SAMHD1 <sup>-/-</sup> cells stably expressing the indicated SAMHD1 variants were challenged with serial dilutions of VSV-G-pseudotyped HIV-1 GFP, and the infectious units (i.u.) per ml of inoculum were calculated. Representative of at least 2 independent titrations is shown. Mean titers of at least 3 titration points with standard deviations are depicted and significance to block HIV-1 in cells expressing SAMHD1 compared to no SAMHD1 (Luc\_HA) are indicated). Statistical analysis was performed using an unpaired two-tailed t test. ns, not statistically significant; \*, P < 0.05; \*\*, P < 0.01; \*\*\*, P < 0.001

The phosphorylation prediction screen identified Cdk2 as possible enzyme to phosphorylate the T525 site. A constant phosphorylation could explain the loss of the block to HIV-1 infection, in a similar way as has been described for T592 (White et al., 2013a, Ryoo et al., 2014a, Welbourn et al., 2013, Arnold et al., 2015). We analyzed whether PMA treatment still resulted in T592 dephosphorylation. As seen in figure 36 there are no differences in T592 dephosphorylation between the A525T variant and WT SAMHD1. To further determine the function of this amino acid residue we designed the following SAMHD1 variants: A525S, A525E, A525V and A525Y. All variants neutralized the cytotoxic effects of ara-C but were not able to block HIV-1 infection efficiently (Figure 36).

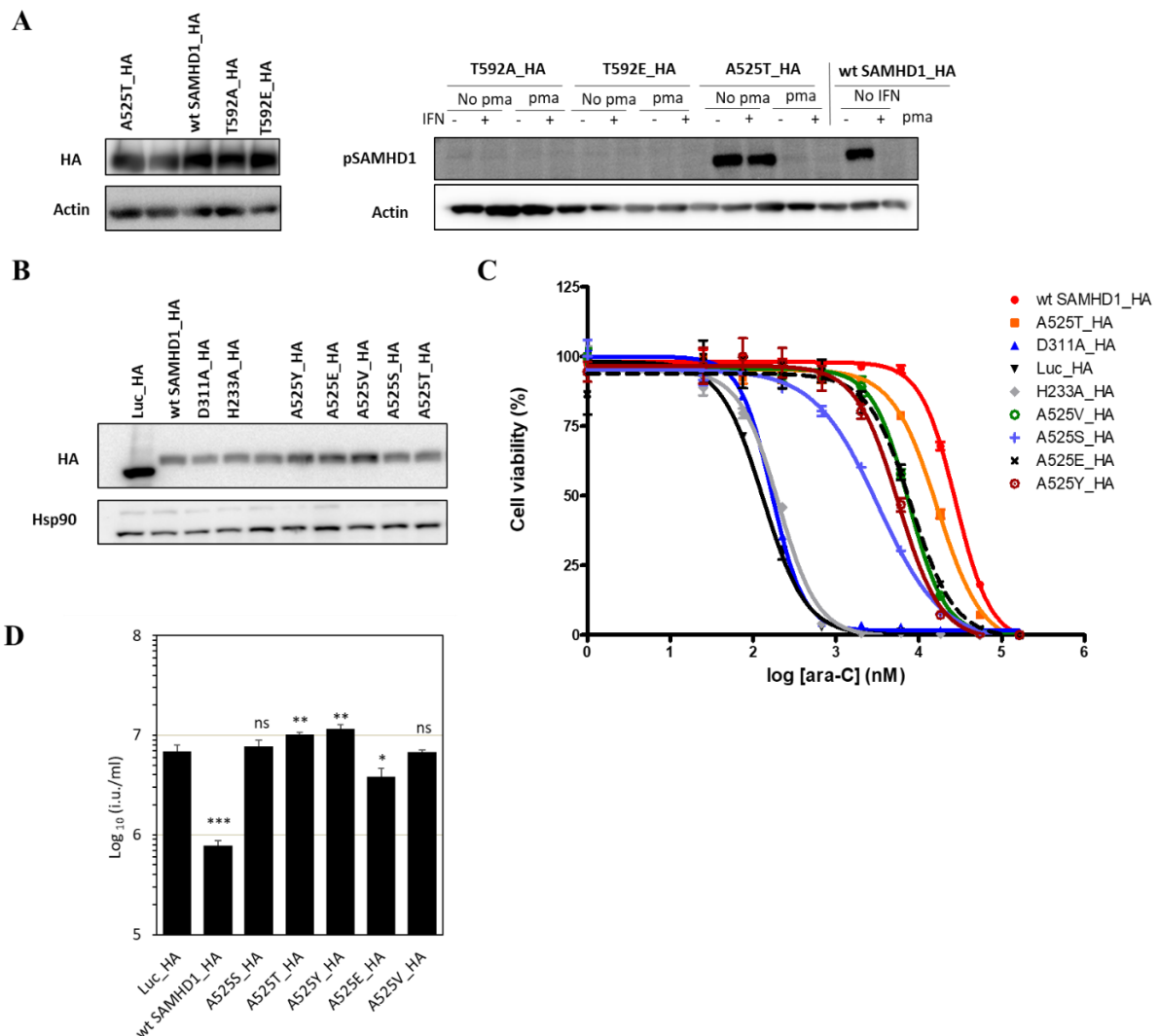
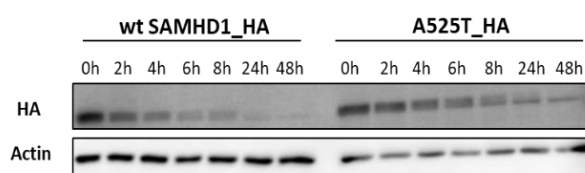


**Figure 36: Expression of SAMHD1 SNP variants A525T in THP-1 SAMHD1 <sup>-/-</sup> cells and its influence on phosphorylation and further analyzes of A525S, A525E, A525V and A525Y their influence on HIV-1 restriction and sensitivity to ara-C treatment.**

**A)** Phosphorylation analyzes by western blot. SAMHD1 variant A525T, wt SAMHD1 and the two phosphomutants T592A or T592E were stably expressed in THP-1 SAMHD1 <sup>-/-</sup> cells. Cells were treated 24 hours with pma +IFN, pma -IFN, no pma +IFN and no pma -IFN. Levels of phosphorylated SAMHD1 were analyzed by western blot. **B)** Variants of SAMHD1 A525 were stably expressed in THP-1 SAMHD1 <sup>-/-</sup> cells and expression was monitored by western blot. **C)** THP-1 SAMHD1 <sup>-/-</sup> cells transduced with SAMHD1 variants of A525 were treated with the indicated concentrations of cytarabine (Ara-C). Cells were treated for 3 days to obtain maximal cytotoxicity and cell viability was determined using a colorimetric proliferation inhibition assay. Error bars indicate s.d. of a representative of three independent experiments performed in triplicates. The EC<sub>50</sub> values are the following: wt SAMHD1\_HA, 27922 nM; Luc\_Ha, 132,3 nM; D311A\_HA, 168,7 nM; H233A\_HA, 203 nM; A525T\_HA, 16754 nM; A525V\_HA, 7576 nM; A525S\_HA, 3239 nM; A525E\_HA, 8157 nM; A525Y\_HA, 5665 nM **c)** PMA-treated SAMHD1 <sup>-/-</sup> cells stably expressing the indicated SAMHD1 variants were challenged with serial dilutions of VSV-G-pseudotyped HIV-1 GFP, and the infectious units (i.u.) per ml of inoculum were calculated. and the infectious units (i.u.) per ml of inoculum were calculated. Representative of at least 2 independent titrations is shown. Mean titers of at least 3 titration points with standard deviations are depicted and significance to block HIV-1 in cells expressing SAMHD1 compared to no SAMHD1(Luc\_HA) are indicated). Statistical analysis was performed using an unpaired two-tailed t test. ns, not statistically significant; \*, P < 0.05; \*\*, P < 0.01; \*\*\*, P < 0.001

This indicates that constant phosphorylation might not be the reason for the lower restriction compared to WT SAMHD1. Only A525E showed a significant but weak block to HIV-1 infection when compared to WT SAMHD1. Furthermore, we tested the ability to rescue HIV-1 from the type I IFN induced block in the A525T variant of SAMHD1 by addition of Vpx. As seen in figure 37 A, when cells expressing the SAMHD1 variant A525T were treated with Vpx VLPs HIV-1 infection was not rescued from the type I IFN induced block (Figure 37 B). However, this could be at least partially explained by reduced degradation kinetics of A525T compared to WT SAMHD1 when challenged with Vpx-VLPs (Figure 37 A). Since Vpx is still able to degrade SAMHD1, binding to DCAF1 is likely not affected in the A525T variant.

**A**



**B**

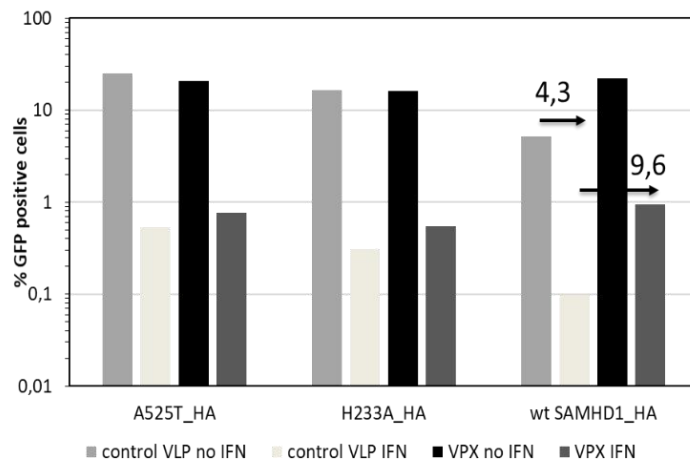


**Figure 37: SAMHD1 variant A525T is resistant to Vpx-induced degradation and Vpx is unable to rescue HIV-1 from the type I interferon induced block in presence of SAMHD1 A525T.**

A) THP-1 SAMHD1 <sup>-/-</sup> cells transduced with wt SAMHD1-HA and the SAMHD1 variant A525T, were plated 1\*10<sup>5</sup> in a 96 well plate and treated with 25 ng/ml PMA for 24 h. Cells were harvested for SAMHD1 western blot analysis after 0h, 2h, 4h, 6h, 8h, 24h, 48h after VPX-VLP treatment. B) THP-1 and THP-1 SAMHD1 <sup>-/-</sup> cells expressing wt SAMHD1-HA, H233A-HA and A525T-HA were pretreated with 25 ng/ml PMA and either with or without 500 U/ml type I interferon for 24 h. Prior to infection with equal amounts of VSV-G-pseudotyped wild-type HIV-1 NL4.3GFP reporter virus cells were treated either with SIV Vpx-VLPs or ctrl. VLP. At 48 h after infection the percentage of GFP-positive cells was determined by flow cytometry. Representative of 2 independent experiments are shown. Numbers indicate fold change.

Next, we assessed mutant R348C which residues close to the active site (Figure 23) was slightly lower expressed as compared to wt SAMHD1. Nevertheless ara- C sensitivity did only marginally increase by 1.4-fold and the block to HIV-1 decreased by 2.4-fold compared to wt SAMHD1 and was significant when statistically analyzed. Since the aim was to identify mutants with different phenotypes with regards to HIV-1 block and ara-C sensitivity this mutant was not studied further.

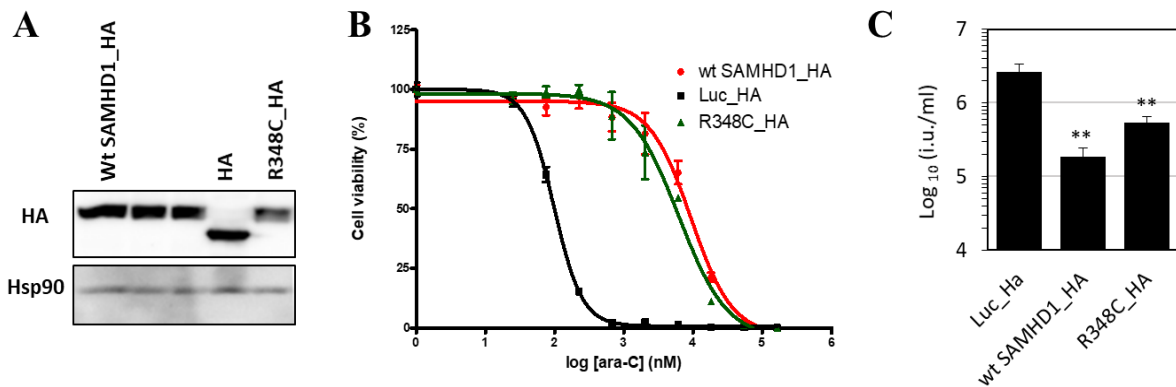


**Figure 38: Effects of R348C SAMHD1 variant on the restriction to HIV-1 infection and sensitivity towards ara-C.**

A) Western blot of SAMHD1 variants and wt SAMHD1 B) Cells were treated with indicated concentrations of cytarabine (ara-C) for 3 days to obtain maximal cytotoxicity and cell viability was determined using a colorimetric proliferation inhibition assay. Experiment was performed in triplicates. Error bars indicate s.d. of a representative of three independent experiments performed in triplicates. EC<sub>50</sub> values are the following wt SAMHD1\_HA, 9333 nM; Luc\_HA, 98,48; R348C\_HA, 6623 nM C) PMA-treated SAMHD1 <sup>-/-</sup> cells stably expressing the indicated SAMHD1 variants were challenged with serial dilutions of VSV-G-pseudotyped HIV-1 GFP, and the infectious units (i.u.) per ml of inoculum were calculated. Representative of at least 2 independent titrations is shown. Mean titers of at least 3 titration points with standard deviations are depicted and significance to block HIV-1 in cells expressing SAMHD1 compared to no SAMHD1(Luc\_HA) are indicated). Statistical analysis was performed using an unpaired two-tailed t test. ns, not statistically significant; \*\*, P < 0.01.

The R451 residue was previously identified as part of the cyclin binding motif (RXL residue 451-453). Structural and functional analyses of R451A mutant revealed that the SAMHD1 tetramer formation is disrupted and that dNTPase activity is lost *in vitro* and in cells (St Gelais et al., 2018). Structural analyzes seen in figure 39 shows that R451 residues between the two monomers which is close to the allosteric site. St. Gelais *et al.* also state that the RXL motif is crucial for HIV-1 restriction and efficient phosphorylation (St Gelais et al., 2018).

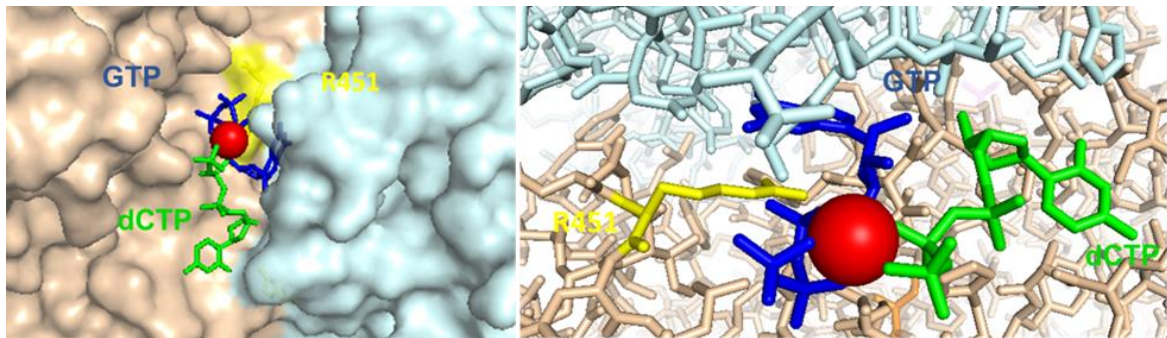


**Figure 39: Allosteric site of SAMHD1 with R451 residue shown in yellow.**  
R451 lies in the interface of the two monomers and close to GTP. (PDB: 4RXR)

Furthermore, R451C and R451L mutation were identified in a CLL patient sample study (Clifford et al., 2014). R451P variant was also identified in COAD. We therefore studied R451P and R451C. Both SAMHD1 variants did not restrict HIV-1 infection and cells expressing these mutants were highly sensitive to ara-C treatment (Figure 40), which is consistent with the observations made by St. Gelais *et al.*s that the RXL motive is crucial for HIV-1 restriction.

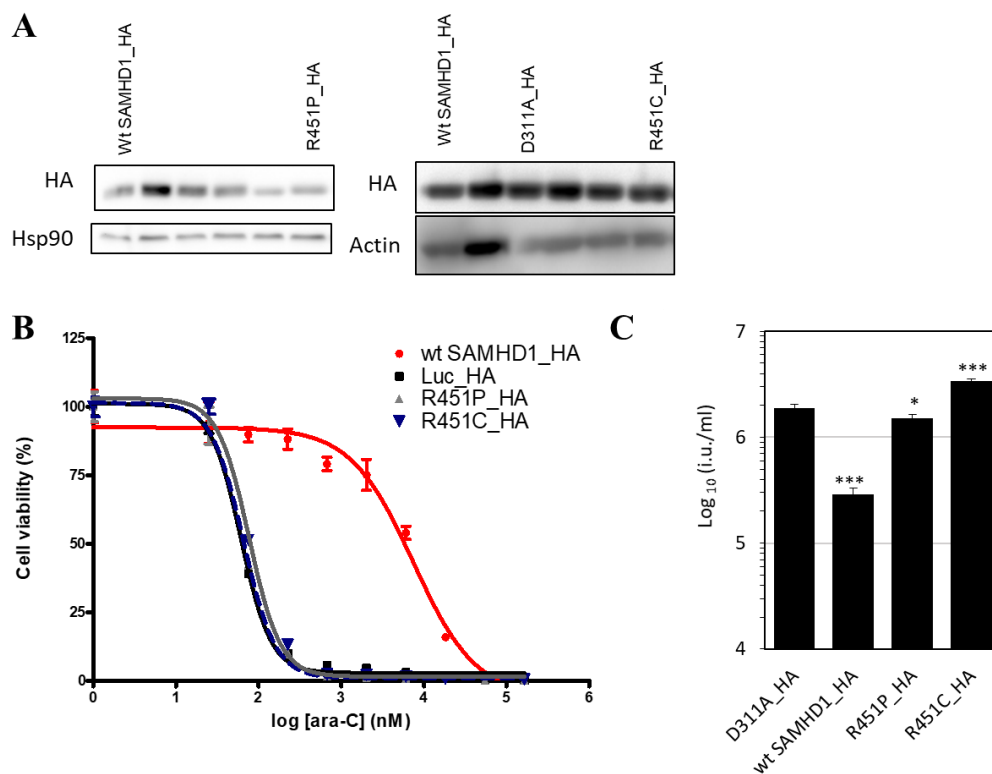


**Figure 40: Effects of R451P and R451C SAMHD1 variant on the restriction to HIV-1 infection and sensitivity towards ara-C.**

A) Western blot of SAMHD1 variants and wt SAMHD1 B) Cells were treated with indicated concentrations of cytarabine (ara-C) for 3 days to obtain maximal cytotoxicity and cell viability was determined using a colorimetric proliferation inhibition assay. Error bars indicate s.d. of a representative of three independent experiments performed in triplicates. EC<sub>50</sub> values are the following wt SAMHD1\_HA, 7438 nM; Luc\_HA, 61,36; R451C\_HA, 76,88 nM; R451P\_HA, 65,82 nM C) PMA-treated SAMHD1 <sup>-/-</sup> cells stably expressing the indicated SAMHD1 variants were challenged with serial dilutions of VSV-G-pseudotyped HIV-1 GFP, and the infectious units (i.u.) per ml of inoculum were calculated. Representative of at least 2 independent titrations is shown. Mean titers of at least 3 titration points with standard deviations are depicted and significance to block HIV-1 in cells expressing SAMHD1 compared to no SAMHD1 (Luc\_HA) are indicated. Statistical analysis was performed using an unpaired two-tailed t test. ns, not statistically significant; \*\*, P < 0.01, \*\*\*, P < 0.001.

Rentoft *et al.* identified colon cancer-associated mutations of *SAMHD1* and studied four mutations in greater detail among those are R366H and D497Y. dNTPase activity assay revealed that D497Y *SAMHD1* variant had nearly abolished dNTPase activity whereas R366H still sustained dNTPase activity but significantly reduced (Rentoft *et al.*, 2016). The R366 resides in the catalytic site of *SAMHD1* (Figure 41) and forms hydrogen bond and stacking interactions with the phosphate, the deoxyribose, and the base of the substrate, respectively. Mutation of this residue to A366 abolished the catalytic activity of *SAMHD1* (Ji *et al.*, 2013).

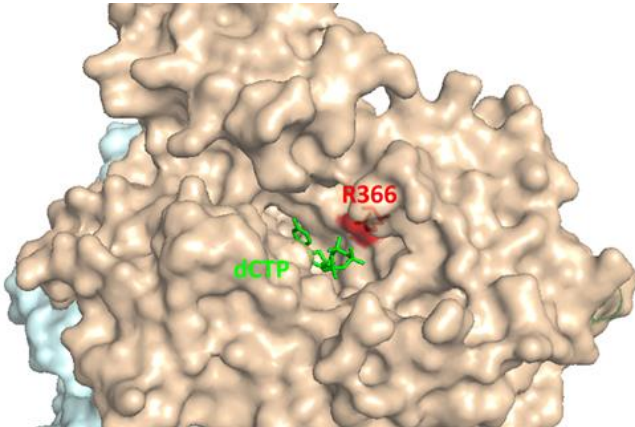


**Figure 41:** Catalytic site of *SAMHD1* with dCTP bound. Residue R366 is depicted in red. (PDB: 4RXX)

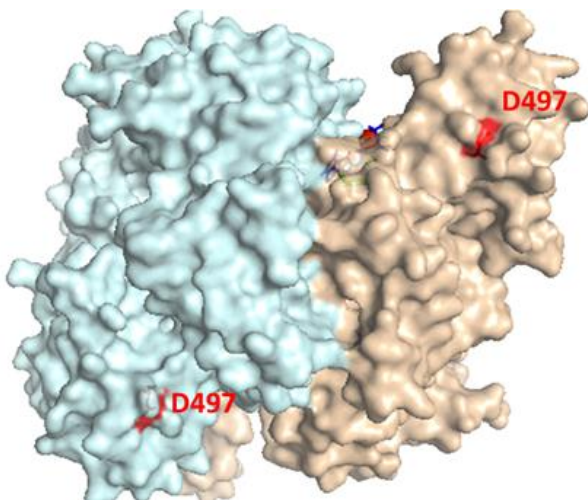


**Figure 42:** *SAMHD1* dimer with residue D497 depicted in red. D497 is not close to the active or allosteric site of *SAMHD1*. (PDB: 4RXX)

Structural analyzes of the D497 residue within the *SAMHD1* tetramer shows that D497 residues not close to the allosteric sites and the catalytic site (Figure 42). Taken both studies in consideration we assumed that both *SAMHD1* variants are unable to block HIV-1 restriction and are sensitive to ara-C treatment. As shown in Figure 43 C both mutants did not restrict HIV-1 and are highly sensitive to ara-C treatment.

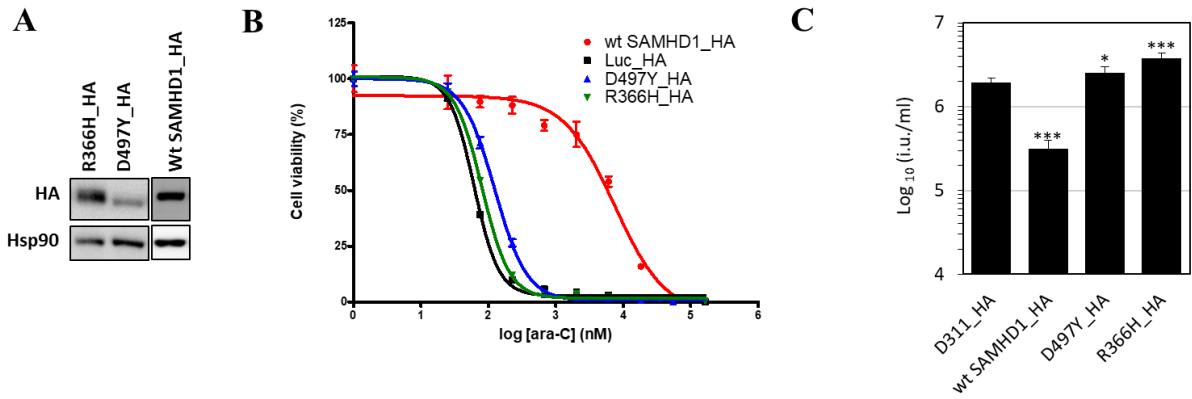


**Figure 43: Effects of R366H and D467Y SAMHD1 variant on the restriction to HIV-1 infection and sensitivity towards ara-C.**

**A)** Western blot of SAMHD1 variants and wt SAMHD1 **B)** Cells were treated with indicated concentrations of cytarabine (ara-C) for 3 days to obtain maximal cytotoxicity and cell viability was determined using a colorimetric proliferation inhibition assay. Error bars indicate s.d. of a representative of three independent experiments performed in triplicates.  $EC_{50}$  values are the following wt SAMHD1\_HA, 7438 nM; Luc\_HA, 61,36; R366H\_HA, 80,53 nM; D497Y\_HA, 124,9 nM **C)** PMA-treated SAMHD1  $-/-$  cells stably expressing the indicated SAMHD1 variants were challenged with serial dilutions of VSV-G-pseudotyped HIV-1 GFP, and the infectious units (i.u.) per ml of inoculum were calculated. Representative of at least 2 independent titrations is shown. Mean titers of at least 3 titration points with standard deviations are depicted and significance to block HIV-1 in cells expressing SAMHD1 compared to no SAMHD1 (Luc\_HA) are indicated). Statistical analysis was performed using an unpaired two-tailed *t* test. ns, not statistically significant; \*\*,  $P < 0.01$ , \*\*\*,  $P < 0.001$ .

The K596Rsf\*35 mutation is reported by TCGA in four cancer types: COAD, Uterine Corpus Endometrial Carcinoma (UCEC), stomach adenocarcinoma (STAD) and Liver Hepatocellular Carcinoma (LIHC). When we tested this SAMHD1 variant we observed that HIV-1 restriction was completely lost but cells expressing this mutant were rendered more resistant to ara-C induced cytotoxicity, even at lower expression levels of the mutant as compared to WT SAMHD1 (Figure 44). This SAMHD1 variant phenocopies the A525T mutant (see above).

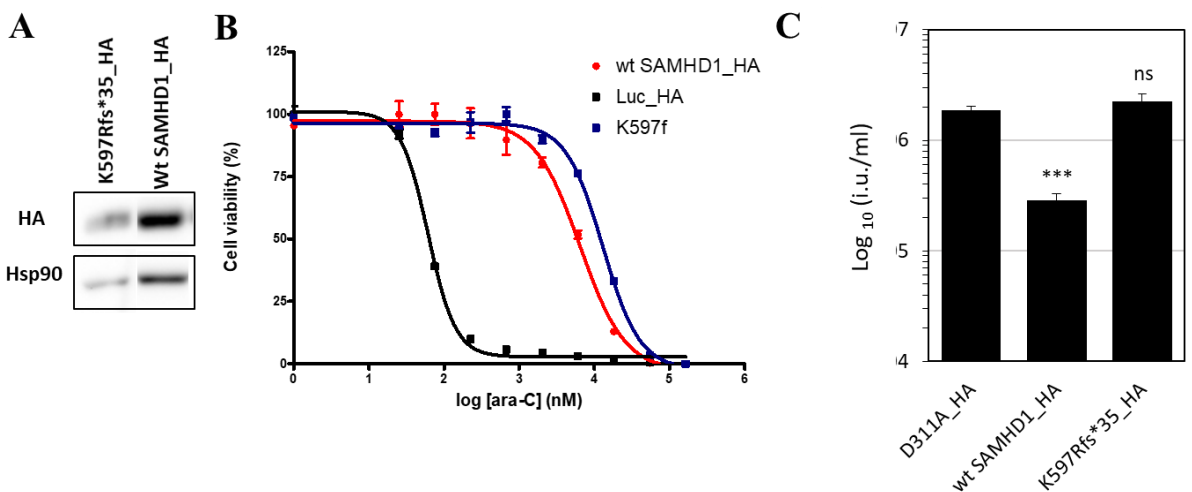


**Figure 44: Effects of K596Rsf\*35 SAMHD1 variant on the restriction to HIV-1 infection and sensitivity towards ara-C.**

**A)** Western blot of SAMHD1 variants and wt SAMHD1 **B)** Cells were treated with indicated concentrations of cytarabine (ara-C) for 3 days to obtain maximal cytotoxicity and cell viability was determined using a colorimetric proliferation inhibition assay. Error bars indicate s.d. of a representative of three independent experiments



performed in triplicates.  $EC_{50}$  values are the following wt SAMHD1\_HA, 6466 nM; Luc\_HA, 61,36; K596Rsf\*35\_HA, 12962 nM C) PMA-treated SAMHD1  $-/-$  cells stably expressing the indicated SAMHD1 variants were challenged with serial dilutions of VSV-G-pseudotyped HIV-1 GFP, and the infectious units (i.u.) per ml of inoculum were calculated. Representative of at least 2 independent titrations is shown. Mean titers of at least 3 titration points with standard deviations are depicted and significance to block HIV-1 in cells expressing SAMHD1 compared to no SAMHD1 (Luc\_HA) are indicated). Statistical analysis was performed using an unpaired two-tailed *t* test. ns, not statistically significant; \*\*,  $P < 0.01$ , \*\*\*,  $P < 0.001$ .

The R145Q was found in COAD, CLL (Clifford et al., 2014) and AGS (Rice et al., 2009a). White *et al.* reported that the R145Q mutant is unable to oligomerize (White et al., 2013b). R145 resides in the primary allosteric site (Figure 45) and is involved in the guanine base recognition ((Zhu et al., 2013, Ji et al., 2014).

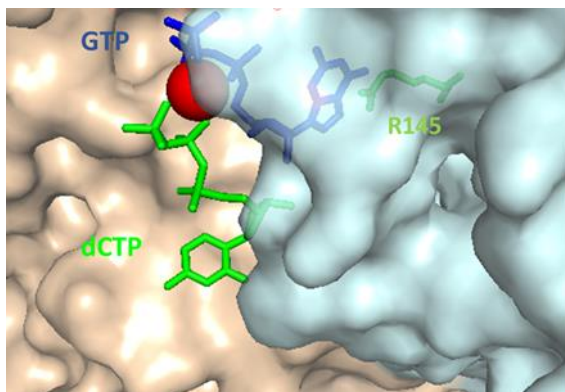


**Figure 45: Allosteric site of SAMHD1.**  
Residue R145 (light green) is in close proximity to GTP.

R145A abolished HIV-1 restriction, which suggests that allosteric activation of SAMHD1 is a requirement for restriction (Koharudin et al., 2014b, Arnold et al., 2015). Our results confirm that R145 is crucial for restriction since R145Q SAMHD1 variant was unable to block HIV-1 infection (Figure 46 C). R145Q expressing cells were sensitive to ara-C treatment comparable to cells lacking SAMHD1 (Figure 46 B).

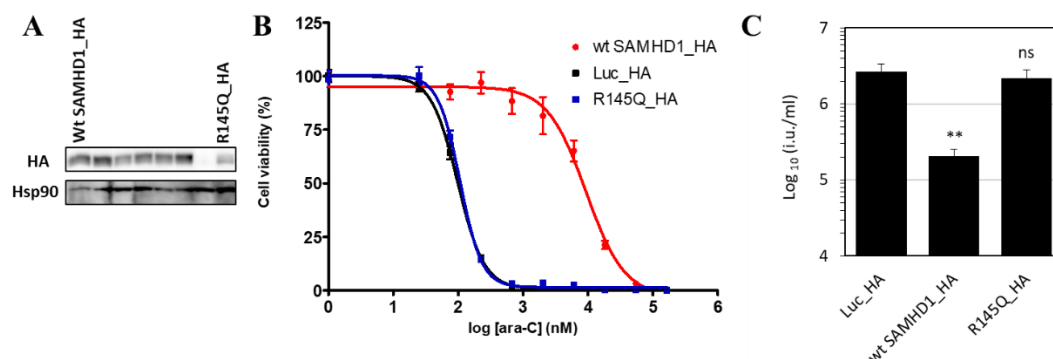


**Figure 46: Effects of R145Q SAMHD1 variant on the restriction to HIV-1 infection and sensitivity towards ara-C.**

A) Western blot of SAMHD1 variants and wt SAMHD1 B) Cells were treated with indicated concentrations of cytarabine (ara-C) for 3 days to obtain maximal cytotoxicity and cell viability was determined using a colorimetric proliferation inhibition assay. Error bars indicate s.d. of a representative of three independent experiments performed in triplicates.  $EC_{50}$  values are the following wt SAMHD1\_HA, 9333 nM; Luc\_HA, 98,48 R145Q\_HA,

107,1 nM C) PMA-treated SAMHD1 <sup>-/-</sup> cells stably expressing the indicated SAMHD1 variants were challenged with serial dilutions of VSV-G-pseudotyped HIV-1 GFP, and the infectious units (i.u.) per ml of inoculum were calculated. Representative of at least 2 independent titrations is shown. Mean titers of at least 3 titration points with standard deviations are depicted and significance to block HIV-1 in cells expressing SAMHD1 compared to no SAMHD1(Luc\_HA) are indicated). Statistical analysis was performed using an unpaired two-tailed t test. ns, not statistically significant; \*\*, P < 0.01.

#### 10.2.4 Analysis of the ability of Vpx to degrade human SAMHD1 SNP variants

Positive selection analysis of SAMHD1 by Laguette et al. revealed that the C-terminal domain of huSAMHD1 is required for Vpx interaction (Laguette et al., 2012). We tested the ability of Vpx from SIV<sub>MAC</sub> to induce degradation of the different SAMHD1 variants. As a control we used SIV<sub>RCM</sub> which is unable to degrade human SAMHD1 (Brandariz-Nunez et al., 2012, White et al., 2013a). As shown in Figure 47 we observed that all SAMHD1 variants were degraded by Vpx<sub>MAC</sub>. The following SAMHD1 variants showed incomplete degradation: A76T, A338T, A525T and L178Q and at least for A338T this was likely not due to increased expression levels (Figure 47).

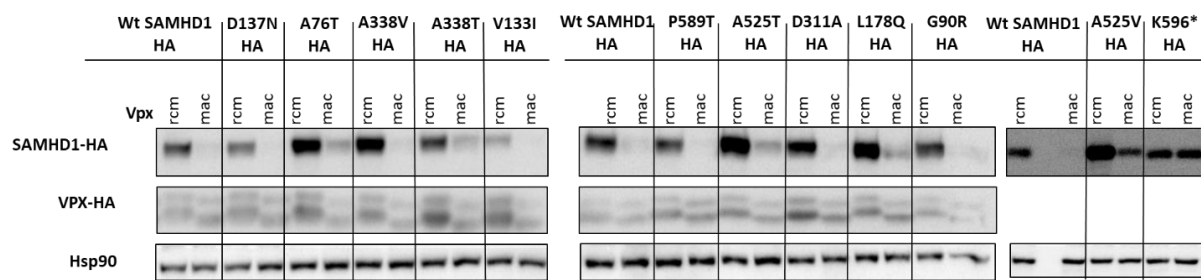


**Figure 47: Sensitivity of SAMHD1 variants to Vpx-induced degradation.**

293T cells were cotransfected with plasmids expressing the indicated SAMHD1 variants and HA-tagged Vpx from SIV<sub>RCM</sub> or SIV<sub>MAC</sub>. 24 hours after transfection the medium was changed and 36 hours after transfection cells were harvested and the expression level of SAMHD1 and Vpx were analyzed by Western blotting using anti-HA antibodies. As loading control an antibody against Hsp90 was used. Similar results were obtained in two independent experiments.

### 10.2.5 SNPs in stomach adenocarcinoma (STAD)

The TCGA database reports that in 42 analyzed STAD patient tumor samples 16 mutations of SAMHD1 were found. A mutation conferring the P589T amino acid substitution was predicted to be damaging by one out of three computational analyses (VEP, SIFT, PolyPhen). P589 lies in close proximity to other monomers (Figure 48).

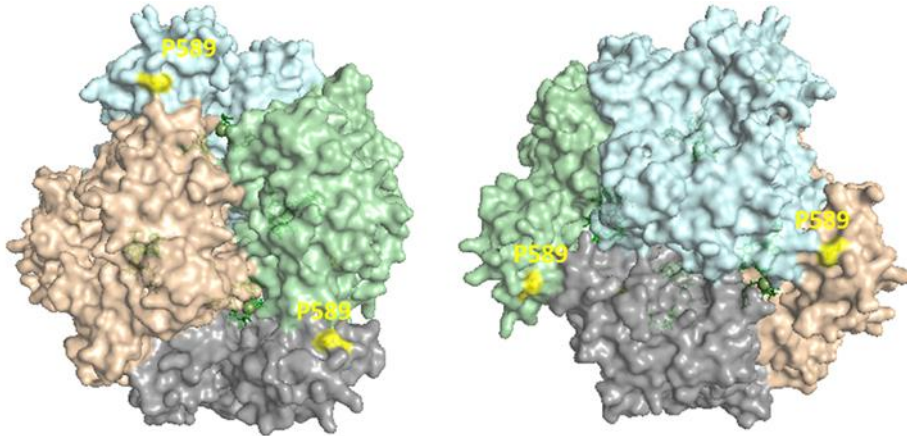


**Figure 48:** SAMHD1 crystalized tetramer structure with P589 depicted in yellow. Residue P589 resides near the Dimer-Dimer interface. (PDB: 4TNP)

When we analyzed this mutant in SAMHD1<sup>-/-</sup> cells HIV-1 restriction was not blocked. Sensitivity of cells expressing SAMHD1 P589T to ara-C induced cytotoxicity increased by 6-fold as compared to WT SAMHD1 however was still 18.8-fold lower than observed in cells lacking SAMHD1 (Figure 49).

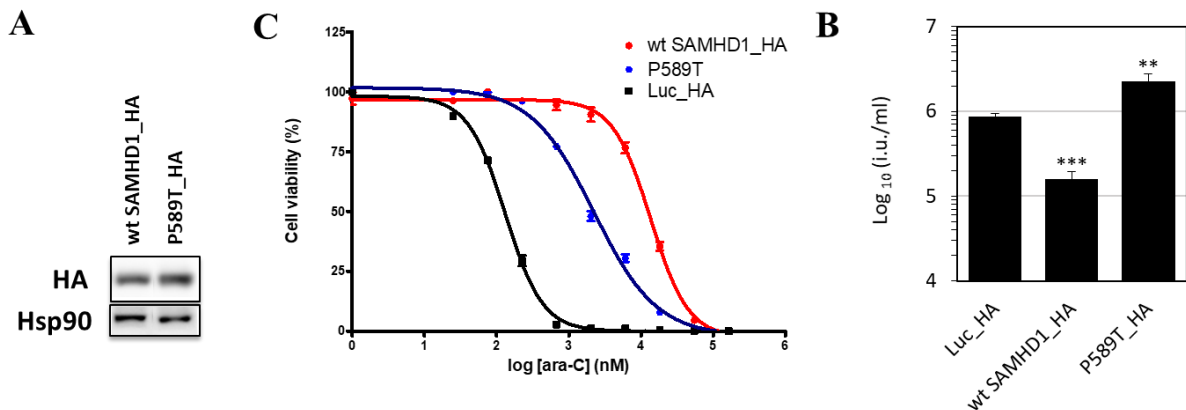


**Figure 49:** Expression of SAMHD1 SNP variant P589T in THP-1 SAMHD1<sup>-/-</sup> cells has a negative effect on HIV-1 restriction and ara-C sensitivity.

**A)** Western blot of SAMHD1 variant and wt SAMHD1 **B)** Cells were treated with indicated concentrations of cytarabine (ara-C) for 3 days to obtain maximal cytotoxicity and cell viability was determined using a colorimetric proliferation inhibition assay. Error bars indicate s.d. of a representative of three independent experiments performed in triplicates. EC<sub>50</sub> values are the following wt SAMHD1\_HA, 13585 nM; Luc\_HA, 132,3 nM; P589T, 2226 nM **C)** PMA-treated SAMHD1<sup>-/-</sup> cells stably expressing the indicated SAMHD1 variants were challenged with serial dilutions of VSV-G-pseudotyped HIV-1 GFP, and the infectious units (i.u.) per ml of inoculum were calculated. Representative of at least 2 independent titrations is shown. Mean titers of at least 3 titration points with standard deviations are depicted and significance to block HIV-1 in cells expressing SAMHD1 compared to no SAMHD1 (Luc\_HA) are indicated). Statistical analysis was performed using an unpaired two-tailed t test. ns, not statistically significant; \*\*, P < 0.01; \*\*\*, P < 0.001.

**Table 3 Summary of analyzed SAMHD1 SNPs.**

Abbreviation and colors: cancer type; Rectum Adenocarcinoma (READ), Acute myeloid leukemia (AML), Colon Adenocarcinoma (COAD), Uterine Corpus Endometrial Carcinoma (UCEC), Stomach Adenocarcinoma (STAD) and Liver Hepatocellular Carcinoma (LIHC), significance of HIV-1 restriction compared to control; ns: not significant; +:  $P < 0.05$ ; ++:  $P < 0.01$ , +++:  $P < 0.001$ , + in red over control cells,  $EC_{50}$  Fold change to wt SAMHD1: in blue reduction compared to wild type and numbers in black increase compared to wt SAMHD1  $EC_{50}$ .

SNP	Cancer type	Significance of HIV-1 restriction compared to control	$EC_{50}$ Fold change to wt SAMHD1	$EC_{50}$ Fold change to LUC
<b>A76T</b>	READ	++	+1,06	100,0
<b>R305I</b>	READ	++	+1,5	142,4
<b>L178Q</b>	AML	+	-2,6	39,4
<b>S214P</b>	AML	ns	-120,9	0
<b>G90R</b>	COAD	++	-2,4	92,0
<b>A338T</b>	COAD	+	+1,2	120,9
<b>D137N</b>	COAD	ns	-5,4	38,9
<b>V133I</b>	COAD	++	-1,1	83,5
<b>A525T</b>	COAD	++	-1,7	99,3
<b>R348C</b>	COAD	++	-1,4	67,2
<b>R451C</b>	COAD	+++	-96,7	1,3
<b>R366H</b>	COAD	+++	-92,4	1,3
<b>D497Y</b>	COAD	+	-59,6	2,0
<b>K597RSf*35</b>	COAD UCEC STAD LIHC	ns	+2,0	211,2
<b>R145</b>	COAD	ns	-87,1	1,08
<b>P589T</b>	STAD	++	-6,1	16,8

### 10.3 SAMHD1 variants that influence post-translational modifications of SAMHD1 and their involvement in HIV-1 restriction and ara-CTP hydrolysis

#### 10.3.1 The C522 residue of SAMHD1 is crucial for the block to HIV infection but is not involved in conferring resistance to ara-C

Wang *et al.* and Mauney *et al.* reported that SAMHD1 is a redox-sensitive enzyme and it poses three redox-active cysteines at the following location: 341, 350 and 522 (Mauney *et al.*, 2017, Wang *et al.*, 2018). Expression of the SAMHD1 variant C522S in PMA-treated U937 cell did not lead to HIV-1 restriction (Wang *et al.*, 2018). They also tested dNTPase activity and capability of tetramerization. The C522S amino acid substitution had no detectable detrimental effect on SAMHD1 tetramerization or dNTPase activity *in vitro*. The authors reasoned that nucleotide dependent tetramerization and dNTPase activity were needed but not sufficient for the block of retroviral infection (Wang *et al.*, 2018), suggesting that the redox state of C522 is crucial for the SAMHD1 restriction mechanism of HIV-1 infection. (Wang *et al.*, 2018). HIV-1 restriction ability of cysteine SAMHD1 mutants was evaluated in PMA-treated THP-1 SAMHD1 *-/-* cells stably expressing either the C522S or C522A SAMHD1 variants using HIV-1 virus expressing GFP, as above (Figure 50 C). Our results revealed that C522S or C522A mutants reduced (C522S by 8-fold; C522A by 6-fold) but not abolished HIV-1 restriction (Figure 50). Despite proper dNTPase function and tetramerization ability (Wang *et al.*, 2018) C522S mutant was 1.4-fold more and C522A mutant was 3-fold more sensitive to ara-C treatment as compared to WT SAMHD1 (Figure 50). The C522S and C522A mutants phenocopied the A338T SAMHD1 mutant (see above).

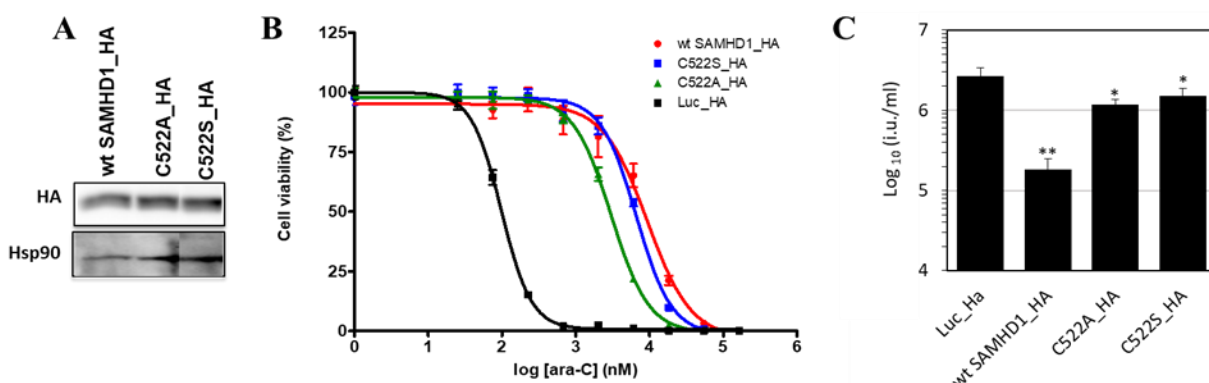


**Figure 50: Effects of cysteine substitutions on the restriction of HIV-1 infection and sensitivity to ara-C.**

A) Western blot of SAMHD1 variants and wt SAMHD1 B) Cells were treated with indicated concentrations of cytarabine (ara-C) for 3 days to obtain maximal cytotoxicity and cell viability was determined using a colorimetric proliferation inhibition assay. Error bars indicate s.d. of a representative of three independent experiments performed in triplicates.  $EC_{50}$  values are the following wt SAMHD1\_HA, 9333 nM; Luc\_HA, 98,48 nM; C522A\_HA, 3015 nM; C522S\_HA, 6622 nM C) PMA-treated SAMHD1 *-/-* cells stably expressing the indicated SAMHD1 variants were challenged with serial dilutions of VSV-G-pseudotyped HIV-1 GFP, and the infectious

units (i.u.) per ml of inoculum were calculated. Representative of at least 2 independent titrations is shown. Mean titers of at least 3 titration points with standard deviations are depicted and significance to block HIV-1 in cells expressing SAMHD1 compared to no SAMHD1(Luc\_HA) are indicated). Statistical analysis was performed using an unpaired two-tailed t test; \*,  $P < 0.05$ ; \*\*,  $P < 0.01$ .

### 10.3.2 SAMHD1 acetylation has no influence on HIV-1 restriction and only minimally changes the sensitivity of cells to ara-C induced cytotoxicity

Lee et al. identified that the lysine residue 405 of SAMHD1 is acetylated by the acetyltransferase arrest defective protein 1 (ARD1) (Lee et al., 2017). Acetylation-defective mutant K405R possess lower dNTPase activity compared to wt acetylated SAMHD1 and acetylation promotes cancer cell proliferation (Lee et al., 2017). The authors imply that SAMHD1 acetylation might be of interest as a target for cancer treatment. They suggested that acetylation may also play a role in non-cycling cells because of its involvement in regulating dNTP levels and its ability to block lentiviral restriction (Lee et al., 2017). Therefore, we analyzed whether SAMHD1 K405R amino acid substitution would influence ara-C sensitivity and HIV-1 restriction in K405R expressing THP-1 SAMHD1  $-/-$  cells. Ara-C sensitivity of cells expressing SAMHD K405R was similar to cells expressing WT SAMHD1 and HIV-1 restriction was comparable to WT SAMHD1 (Figure 51). The data implicates that acetylation may not be critical for SAMHD1's role in lentiviral restriction or ara-CTP hydrolysis.

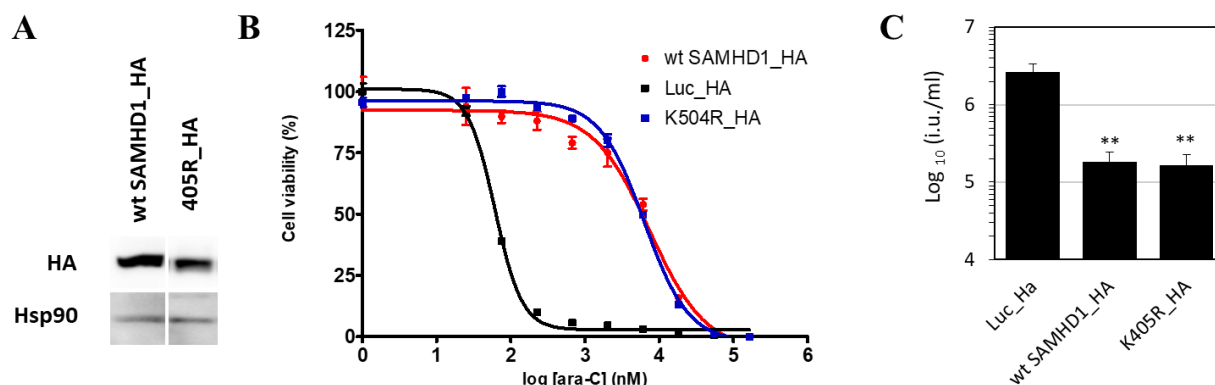


**Figure 51: Effects of acetylation defective mutant K405R on the restriction to HIV-1 infection and sensitivity to ara-C.**

**A)** Western blot of SAMHD1 variant K405R and wt SAMHD1 **B)** Cells were treated with indicated concentrations of cytarabine (ara-C) for 3 days to obtain maximal cytotoxicity and cell viability was determined using a colorimetric proliferation inhibition assay. Error bars indicate s.d. of a representative of three independent experiments performed in triplicates. EC<sub>50</sub> values are the following wt SAMHD1\_HA, 7438 nM; Luc\_HA, 61,36 nM; K405R\_HA, 6274 nM **C)** PMA-treated SAMHD1  $-/-$  cells stably expressing the indicated SAMHD1 variants were challenged with serial dilutions of VSV-G-pseudotyped HIV-1 GFP, and the infectious units (i.u.) per ml of inoculum were calculated. Representative of at least 2 independent titrations is shown. Mean titers of at least 3 titration points with standard deviations are depicted and significance to block HIV-1 in cells expressing SAMHD1 compared to no SAMHD1(Luc\_HA) are indicated). Statistical analysis was performed using an unpaired two-tailed t test. \*\*,  $P < 0.01$ .

# 11 Discussion and perspective

## 11.1 SAMHD1's role in the type 1 interferon induced early block to HIV-1 infection

### *11.1.1 The Vpx<sub>MAC</sub>-induced increase of HIV-1 infection in type I IFN treated MDMs is SAMHD1-dependent*

I have shown that Vpx<sub>MAC</sub> Q76A was unable to relieve HIV-1 from the type I IFN-induced block in MDM. Wild type Vpx on the other hand greatly boosted HIV-1 infection with or without IFN pretreatment. The experiments presented here confirm that SIV<sub>MAC</sub> Vpx rescues HIV-1 infection from the IFN-induced block in MDM (Lahouassa et al., 2012, Hrecka et al., 2011, Srivastava et al., 2008, Reinhard et al., 2014). The magnitude of the rescue was dependent on the donor and reached up to 155-fold, but the increase in type 1 IFN-treated cells was usually more pronounced than in untreated cells, an observation seen before in MDDCs (Pertel et al., 2011). Despite the fact that Vpx is not a HIV-1 accessory protein, it can serve as a tool to identify new HIV-1 restriction factors that are involved in the type 1 IFN-induced block to early infection steps.

We confirmed here that the Vpx mutant (Q76A) which is unable to bind DCAF1 failed to rescue HIV-1 infection in untreated MDMs or THP-1 cells (Lahouassa et al., 2012, Hrecka et al., 2011, Srivastava et al., 2008, Reinhard et al., 2014). Vpx binds to DCAF1 and associates with the DDB1/RBX1/ Cul4A E3 ubiquitin ligase complex (Sharova et al., 2008, Srivastava et al., 2008, Bergamaschi et al., 2009, Hrecka et al., 2007, Belzile et al., 2007, Le Rouzic et al., 2007, Schrofelbauer et al., 2007, Tan et al., 2007). SAMHD1s degradation is initiated by the binding of Vpx to SAMHD1. This induces the degradation of SAMHD1 by Vpx's ability to hijack the DDB1/RBX1/ Cul4A E3 ubiquitin ligase machinery. This indicates that the DCAF1/DDB1/RBX1/ Cul4A E3 ubiquitin ligase complex is crucial for the phenotype reported here. In contrary, Pertel reported that DCAF1/DDB1/RBX1/ Cul4A E3 ubiquitin ligase complex is dispensable and that the Vpx-mediated relieve from the antiviral state was also seen in DCAF1 knockdown in MDDCs (Pertel et al., 2011). Moreover, Pertel et al. showed that Vpx<sub>MAC</sub> Q76A rescued HIV-1 infection under proinflammatory conditions in MDDCs, which stands in contrast to the observations made here. This contrast might be due to cell-type specific effects, e.g. MDDCs may express a different set of DCAF proteins that might still be able to interact with Vpx<sub>MAC</sub> mutant Q76A. Goujon et al. described for example that reduction of DCAF1 had little impact on increasing the HIV-1 infection by Vpx-VLPs (PMID: 18829761). Our results are consistent with a model in which SAMHD1 is an antiviral factor that is crucial for the Vpx mediated relief from the type I antiviral block.

### *11.1.2 The Vpx<sub>MAC</sub>-induced rescue of HIV-1 from the type I IFN-induced block in MDM is independent of the route of entry*

It has been suggested that IFITM proteins can block VSV-G pseudotyped viral infection (Roesch et al., 2018, Yu et al., 2015) and hence we investigated whether the Vpx-induced rescue of the HIV-1 infection from the type I IFN-induced block would rely on VSV-G pseudotyping of HIV-1. We found that also non-pseudotyped R5-tropic BalEnv HIV-1 was efficiently rescued upon Vpx supplement. This suggests that Vpx mediated increase of HIV-1 infection is independent of HIV-1s route of entry.

### *11.1.3 Vpx<sub>MAC</sub> does not relieve HIV-1 from the type I IFN-induced block in THP-1 SAMHD1<sup>-/-</sup> cells*

HIV-1 infection in PMA differentiated THP-1 cells increased by three-fold in response to Vpx without prior treatment of interferon. This magnitude is similar to published data (Goujon et al., 2013c). When THP-1 parental cells were treated prior to infection with type I interferon an up to 19-fold increase in infectivity was seen when infection was performed in the presence of Vpx. In order to test SAMHD1's involvement in the increase of infectivity with or without prior type I IFN treatment we generated *SAMHD1* knock-out THP-1 cell lines by using CRISPR/Cas9 technology. *SAMHD1* knock-out increased the permissivity for HIV-1 infection in PMA-differentiated cells by approximately 4-fold in all tested *SAMHD1* knockout cell clones. This is in line with published data using Vpx-VLPs to degrade SAMHD1 (Goujon et al., 2013c, Pertel et al., 2011). Additionally and surprisingly, Vpx was unable to further increase HIV-1 infection in type I IFN-treated or untreated cells when SAMHD1 was absent. This indicates that in the absence of SAMHD1, no additional increase in infectivity is conferred by Vpx – indicating that SAMHD1 is playing an important role in the IFN block that can be counteracted by Vpx. The Vpx mediated increase of HIV-1 infection is present with or without IFN. However, Vpx mediated increase of HIV-1 infection in IFN treated cells is usually bigger than in IFN untreated cells. This cannot be explained by a simple increase in SAMHD1 protein levels, since SAMHD1 protein levels do not change substantially upon IFN treatment. It is possible however, that the enzymatic activity of SAMHD1 is also regulated by IFN treatment without enhancing the protein levels and that the increased rescue of HIV-1 infectivity is an effect of reduced dNTPase activity of SAMHD1 after IFN treatment. Likewise, IFN-regulated co-factors of SAMHD1 could impact the Vpx-induced rescue (Buffone et al., 2019).

In order to further confirm that SAMHD1 is crucial for the Vpx mediated increase of HIV-1 infection from the type I IFN-induced block we re-expressed CRISPR/Cas9-resistant and



amino-terminal HA-tagged and amino-terminal codon-optimized (refractory to gRNA) SAMHD1 in SAMHD1 knockout cells. Expression of wild type SAMHD1 in SAMHD1 knockout clones reintroduced the block to HIV-1 infection by 6-fold compared to the SAMHD1 knockout clone in the presence or absence of type I IFN treatment. Stable ectopic expression of WT SAMHD1 in the SAMHD1 *-/-* cell line reintroduced the Vpx-mediated increase of HIV-1 infection in those cells in the absence of pretreatment with IFN. The increase was rather small (3.3-fold) as compared to endogenously expressed SAMHD1. One reason underlying this weak Vpx-induced increase in HIV-1 infection may have been the constant high expression of SAMHD1 from the strong SFFV promoter of the integrated lentiviral vector that was used to re-express SAMHD1 in the knockout cells. Vpx, which is delivered by VLPs at a given dose, might not be able to overcome the constant expression of SAMHD1 even with an increase of Vpx. To achieve a greater increase an inducible vector with switch off or knock in mutagenesis could be used to achieve more physiological settings in future studies.

#### *11.1.4 SAMHD1 knock-out has no influence on cell proliferation in THP-1 cells*

The effect of perturbed SAMHD1 expression was studied by many groups and gave controversial results. As an example, reduced SAMHD1 activity results in increased dNTP levels, which could lead to uncontrolled cell proliferation (Clifford et al. 2014, Rossi 2014). Franzolin *et al.* and Kretschmer *et al.* reported that SAMHD1 RNA interference in immortalized fibroblast or HeLa cells, which lead to reduced SAMHD1 levels, results in reduced cell proliferation (Franzolin et al., 2013, Kretschmer et al., 2015). Bonifati et al. reported that SAMHD1 knock-out by CRISPR/Cas9 in myeloid THP-1 cells increased cell proliferation and decreased spontaneous apoptosis (Bonifati et al. 2016). We did not see a significant increase in cell proliferation only a small but significant decrease in sub-G1 cells in the SAMHD1 knockout clones. These results stay in contrast with studies in AGS fibroblasts in which abolished SAMHD1 levels slows down cell proliferation (Franzolin et al., 2013). It is also possible that the reported phenotypes are cell type dependent, e.g. due to off target effects in the different CRISPR/Cas9 clones used by Bonifati and us or that dNTP levels or RNR activity vary between the cells used in different laboratories (Herold et al., 2017c). Therefore, systematic studies have to be conducted in order to verify SAMHD1's involvement in cell cycle progression and proliferation. How IFN $\alpha$  treatment might impact cell proliferation in absence or presence of SAMHD1 and how this could contribute to the Vpx-induced rescue of HIV-1 from the type I IFN-induced block (rescue by Vpx is greater after IFN treatment as compared to untreated cells), is unclear at the moment and warrants further investigations.

### 11.1.5 Characterization of a THP-1 cell line endogenously expressing SAMHD1 with truncated nuclear localization signal (THP-1 Eg3c6+/-)

Previous studies observed that nuclear localization of SAMHD1 is not fundamental for HIV-1 restriction (Rice et al., 2009b, Brandariz-Nunez et al., 2012, Hofmann et al., 2012) but Vpx<sub>MAC</sub> mediated degradation depends on nuclear localization of SAMHD1 (Schaller et al., 2014, Brandariz-Nunez et al., 2012, Hofmann et al., 2012, Wei et al., 2012, Guo et al., 2013).

To answer the question whether Vpx-induced SAMHD1 degradation is required for the rescue from the antiviral state in type I IFN-treated cells, we generated THP-1 cells in which SAMHD1 was endogenously truncated in its nuclear localization signal. These cells contained only one functional SAMHD1 allele, which harbored an in frame deletion of the NLS region. We found that endogenously expressed SAMHD1 lacking the NLS was excluded from the nucleus using immunofluorescence. Comparable to published results using overexpression assays, endogenously expressed SAMHD1 $\Delta$ NLS resisted Vpx-induced degradation (Hofmann et al., 2012, Schaller et al., 2014), however after 24 h Vpx treatment SAMHD1 $\Delta$ NLS levels decreased comparable to WT SAMHD1 treated with Vpx. This indicates that cytoplasmic SAMHD1 can be degraded by Vpx, and that this is likely masked when using overexpression assays. Previous studies on cytoplasmic SAMHD1 used lentiviral vectors overexpressing SAMHD1 NLS mutant K11A in MDM, HeLa or THP-1 cells (Schaller et al., 2014, Brandariz-Nunez et al., 2012, Hofmann et al., 2012, Wei et al., 2012, Guo et al., 2013). Our system is physiologically more relevant since ectopic expression results in high SAMHD1 levels thus SAMHD1 regulation and degradation might not be identical to endogenously expressed SAMHD1. Furthermore, previous studies analyzed the SAMHD1 degradation by Vpx in a rather short time window of 10 hours (Hofmann et al., 2012).

One explanation for the delayed degradation kinetics of SAMHD1 $\Delta$ NLS might be that ubiquitin chains that are appended to cytoplasmic SAMHD1 may differ in the linkage patterns, leading to delayed degradation. Schaller *et al.* tested this hypothesis using overexpression of the SAMHD1 K11A mutant. They observed differences in the polyubiquitination profiles for wild type and K11A SAMHD1, specifically with UbiK11R and UbiK6R, leading to increases in polyubiquitinated SAMHD1 K11A compared to SAMHD1 WT (Schaller et al., 2014). Future studies should investigate whether this holds true for endogenously expressed SAMHD1 lacking the amino-terminal NLS and whether the different linkages may explain reduced degradation kinetics in presence of Vpx. Another limiting factor might be the availability of the DCAF1-DDB1-CUL4A E3 ubiquitin ligase complex factors in the cytoplasm. Hofmann et al tested whether SAMHD1 $\Delta$ NLS binds to Vpx, by examining whether Vpx SAMHD1 complexes

could be pulled-down from cells. It was confirmed that Vpx is able to bind SAMHD1 K11A mutant (Hofmann et al., 2012). This indicates that Vpx binding to SAMHD1 in the cytoplasm is not the limiting factor. Next we tested whether this endogenously expressed SAMHD1 lacking the NLS was able to increase HIV-1 infection in the presence of Vpx. Vpx increased HIV-1 infection by 4-fold, comparable to parental THP-1 cells. Vpx mediated increase in HIV-1 infection in SAMHD1 $\Delta$ NLS cells was comparable to THP-parental cells. This raises the question whether SAMHD1 degradation is necessary for the Vpx mediated increase of HIV-1 infection. The window of infection when SAMHD1 is not degraded by Vpx in the  $\Delta$ NLS cells is around 24 hours. While we have investigated effects on infection in this time window and stopped infection before SAMHD1 $\Delta$ NLS became apparently degraded in immunoblots, we cannot rule out that the observed increase in infection is also due to VSV-G pseudotyped virus trapped in endosomes that infects at later time points when SAMHD1 is degraded. Further HIV-1 infection experiments have to be conducted to investigate the question further, whether degradation of SAMHD1 is required for the Vpx-mediated effects on HIV-1 infection in the presence of a type I IFN-induced antiviral state. For example, proteasomal inhibitors can be used to allow only a brief incubation with Vpx. Comparing the SAMHD1 $\Delta$ NLS mutant cells with parental THP-1 cells treated with Vpx for a short amount of time following infection and addition of proteasomal inhibitors would then allow us to further evaluate whether SAMHD1 degradation is mandatory for the Vpx mediated boost of infection from the antiviral state. Furthermore, a Vpx mutant can be used which is able to bind to DCAF1 but is unable to degrade SAMHD1.

Most of the AGS SAMHD1 variants reside in the nucleus and to varying degrees in the cytoplasm (White et al. 2017, Goncalves et al. 2012b). Studying these mutants might help to understand the need of SAMHD1 to localize to the nucleus. Future investigations of SAMHD1 have to explore the nucleocytoplasmic partitioning of elements of the ubiquitin/proteasome system and their involvement in Vpx mediated SAMHD1 degradation. Recent studies suggest a role for SAMHD1 on DNA replication forks (Coquel et al., 2018), and it will be of interest to understand whether this is the main reason that SAMHD1 is a nuclear protein, suggesting that its antiviral activity may be a byproduct, rather than a specific antiviral feature gained during evolution.

### *11.1.6 Type I interferon has no influence on Vpx-mediated SAMHD1 degradation in cycling THP-1 cells*

Dragin *et al.* and Roesch *et al.* showed that interferon alpha (IFN $\alpha$ ) treatment of THP-1 cells prevented degradation of SAMHD1 following incubation with SIV<sub>MAC</sub> virus-like particles containing Vpx (Dragin *et al.* 2013 Roesch *et al.* 2018). This would suggest that IFN stimulated genes interfere with SAMHD1 degradation by Vpx. Roesch *et al.* reported that IFITM proteins are involved in the IFN $\alpha$  mediated protection of SAMHD1 degradation by blocking VSV-G mediated entry of viral particles delivering Vpx (Roesch *et al.*, 2018). Since Vpx mediated SAMHD1 degradation might be one explanation of the Vpx mediated increase of HIV infection in IFN $\alpha$  treated cells we tested SAMHD1 degradation by Vpx with and without interferon. Furthermore, we investigated whether PMA treatment influences SAMHD1 degradation. As published by other groups complete SAMHD1 degradation was achieved in the presence of Vpx-VLPs. In contrast to Dragin and Roesch *et al.* IFN $\alpha$  treatment did not hinder Vpx mediated SAMHD1 degradation as also seen by Goujon *et al.* (Goujon *et al.*, 2013b). PMA and IFN $\alpha$  treatment together slightly hindered SAMHD1 degradation in the presence of Vpx-VLPs but did not completely block SAMHD1 degradation. In order to verify that IFITMs are not involved in the Vpx mediated degradation of SAMHD1 we created IFITM knockout cell lines in which we will further test SAMHD1 degradation by Vpx and use these tools to study the involvement of IFITM proteins in the Vpx-mediated increase of HIV-1 infectivity.

## **11.2 Correlation of SAMHD1 dNTPase activity with HIV-1 restriction by using cancer-associated naturally occurring SAMHD1 variants**

### *11.2.1 SAMHD1 is a mediator of ara-C toxicity in AML cell models*

The most active agent against myelogenous leukemia (AML) is the cytostatic deoxycytidine analog cytarabine (ara-C) which is usually given in combination with an anthracycline (Ossenkoppele and Lowenberg, 2015). The American Cancer Society's estimates for about 61,780 new leukemia cases and 21,450 of them account for acute myeloid leukemia (AML). They further predict that 10,920 people mostly adults will die in 2019 of AML. The global annual incidence of leukemia in 2018 were 437,033 cases.<sup>6</sup>

The active metabolite of ara-C is ara-CTP which is incorporated into the DNA and causes DNA damage and eventually leads to cell death. One reason for AML therapy to fail is the decrease

---

<sup>6</sup> <https://www.wcrf.org/dietandcancer/cancer-trends/worldwide-cancer-data>

in the active metabolite ara-CTP (Zittoun et al., 1987, Early et al., 1982, Estey et al., 1987, Heinemann and Jehn, 1990, Hiddemann et al., 1996, Kessel et al., 1969, Rustum et al., 1987, Smyth et al., 1976, Yamauchi et al., 2001). Thus, there is a need to identify new strategies to treat AML patients.

We and other have shown that ara-CTP is a substrate of SAMHD1 and thereby we determined SAMHD1 as key factor in dictating sensitivity of AML blast to ara-C (Schneider et al., 2017, Herold et al., 2017a, Hollenbaugh et al., 2017). Ara-C-induced cytotoxicity was substantially increased in THP-1 SAMHD1 knock-out cells and in THP-1 cells where SAMHD1 was degraded by Vpx-containing-virus-like particles (VLPs). We further assessed the importance of catalytic active SAMHD1 for ara-C hydrolysis by ectopic expression of CRISPR/Cas9-resistant WT SAMHD1 or catalytic site mutants in THP-1 SAMHD1 knockout cells. Only WT SAMHD1 was able to decrease ara-C cytotoxicity, indicating that the enzymatic function is critical for the detoxification. We concluded that the dNTPase activity of SAMHD1 is crucial for reducing the toxic effect of ara-C treatment. This opened for us and for the first time the possibility to investigate directly in the same cells in parallel the antiviral activity against HIV-1 and the enzymatic dNTPase activity of SAMHD1 with this ara-C cytotox assay. This investigation is important to understand the impact of the SAMHD1 enzymatic activity in the IFN-induced block to HIV-1. To further address SAMHD1s involvement in ara-C sensitivity of cells *in vivo* our collaborators in Schweden tested the effect of differential SAMHD1 expression in AML tumor cells in a heterotopic and orthotopic AML mouse model. Lack of SAMHD1 increased the sensitivity to ara-C treatment as seen *in vitro*. *In vivo* analysis of catalytic dead SAMHD1 revealed that mice transplanted with cells expressing wt SAMHD1 were more resistant to ara-C treatment than mice transplanted with cells expressing the catalytic dead mutants of SAMHD1. This confirmed that catalytic active SAMHD1 is required for ara-C detoxification (Herold et al., 2017a).

For further research SAMHD1 levels in AML blast have to be monitored during AML therapy. But not only protein levels are important since some cancer associated natural SAMHD1 polymorphisms showed differential activities in neutralizing ara-C induced cytotoxicity. The goal would be to use SAMHD1 as biomarker to treat patients according to their SAMHD1 levels or to their SAMHD1 sequence. Another strategy would be to include SAMHD1 inhibitors in AML therapy. Our collaborators tested this by delivering Vpx to AML cells by using VSV-G pseudotyped VLPs. To date only *ex vivo* application of lentiviral vectors has been tested in clinical trials to alter hematopoietic stem cells which are administered after changes are applied (Booth et al., 2016, Mamcarz et al., 2019, Mansilla-Soto et al., 2016). In order to treat AML

SAMHD1 levels have to be changed *in vivo* but *in vivo* trials have not yet been conducted and are only in preparation (Alton et al., 2017). Alternative ways to deliver Vpx besides VLPs would be the use of small DNA viruses (Kienle et al., 2012), coupling of Vpx to antibodies targeting AML cells (Gamis et al., 2014), mRNA-based therapeutics (Sahin et al., 2014) or liposomal packaging of Vpx (Morrell et al., 2008, Chen et al., 2014). As previously reported SAMHD1 possesses tumor suppressor function in lung cancer (Wang et al., 2014), CLL (Clifford et al., 2014), COAD (Rentoft et al., 2016) and cutaneous T-cell lymphoma (Merati et al., 2015, Kodigepalli et al., 2017). Our collaborators at the Karolinska Institute in Stockholm proposed that SAMHD1 has tumor suppressor function as well in AML. Since there is a negative trend of low SAMHD1 expression on overall survival and event free survival it is possible that the missing dNTP regulation fuels tumor growth (Herold et al., 2017a). Furthermore, germ line mutations of SAMHD1 are one cause of AGS which leads to inflammatory reactions (Rice et al., 2009b). Hence it is understandable that constant down regulation of SAMHD1 is not favorable for the AML patient. Therefore, SAMHD1 levels should only be downregulated while ara-C therapy is ongoing, and the innate immune response should be monitored closely. Another more cost efficient, controllable and with presumed fewer off targets effect as lentiviral therapy approach would be small molecule inhibitors of SAMHD1. This warrants further investigations. SAMHD1 is a promising biomarker and further studies have to focus on SAMHD1s role in genome stability and cell homeostasis

### 11.2.2 SAMHD1 SNPs in Cancer

We showed that SAMHD1 is able to detoxify cells treated with ara-C by hydrolyzing the active metabolite ara-CTP (Herold et al., 2017a). To date there are approximately 197 SAMHD1 mutations known, which spread across 26 cancer projects (TGGA) and some of them may be associated with tumorigenesis.

We wanted to investigate the influence of known SAMHD1 mutation of AML, READ and COAD on ara-CTP hydrolysis and susceptibility to HIV-1 infection therefore we expressed these CRISPR/Cas9-resistant SAMHD1 variants in the THP-1 g2c2 SAMHD1 -/- cell line by using lentiviral vectors. In order to get a better impression how much SAMHD1 is needed to block HIV-1 infection and detoxify the cells after ara-C treatment performed a titration of SAMHD1 lentiviral vector. High SAMHD1 expression levels are crucial for an extensive block of HIV-1 infection and increased the EC<sub>50</sub> value of ara-C by 40-fold (wt SAMHD1\_HA compared to wt SAMHD1\_HA diluted 1:16). Even weak SAMHD1 expression caused some HIV-1 restriction and ara-CTP hydrolysis. The data showed that there was no detectable

threshold that was required for HIV-1 restriction or ara-C neutralization, however, and as predicted, both were strongest when SAMHD1 expression levels were highest. This was also confirmed by dose-dependent Vpx-mediated SAMHD1 reduction which is associated with dose-dependent sensitization to ara-C in THP-1 cells (Herold et al., 2017a).

#### 11.2.2.1 SAMHD1 SNPs in Rectum Adenocarcinoma (READ)

In Rectum Adenocarcinoma (READ) currently three missense mutation are known: A76T, R305I and S302Y. SAMHD1 variants A76T or R305I were expressed in the SAMHD1<sup>-/-</sup> cell line g2-2. Ectopic expression of wt or A76T as well as R305I increased the EC<sub>50</sub> for ara-C by 94 to 142-fold compared Luc-HA transduced cells. R305I increased the EC<sub>50</sub> for ara-C by 1.5-fold compared to wt SAMHD1. Both SAMHD1 variants efficiently blocked HIV-1 infection and surprisingly even significantly stronger as compared to WT SAMHD1. R305 resides closely to the active site and the modification might have positively influenced ara-CTP binding and dCTP respectively. Beloglazova *et al.* reported that alanine replacement of R305 had a negative effect on nuclease function (which is controversial) and dGTP hydrolysis (Beloglazova et al., 2013). Since HIV-1 restriction was not perturbed it would be surprising but not unlikely that R305I would show decreased dNTPase activity. Further analyses of the dNTPase activity and nuclease activity (although this is highly controversial) of R305I have to be conducted. A76 is part of the SAM domain. White *et al.* reported that the SAM domain is dispensable for HIV-1 restriction, oligomerization and RNA binding (White et al., 2013a) in contrary Beloglazova *et al.* published that the SAM domain is required for maximal activity and nucleic acid binding (Beloglazova et al., 2013). Here we report that change in the SAM domain can indeed lead to a presumably more active form of SAMHD1. READ is commonly treated with 5- Fluorouracil and capecitabine.<sup>7</sup> Both antimetabolites have to be tested for their hydrolyzes by SAMHD1. Our collaborators have preliminary results that both antimetabolites can be hydrolyzed by SAMHD1. Therefore, further experiments have to investigate whether both READ SNPs respond differently to these drugs.

#### 11.2.2.2 SAMHD1 SNPs in acute myeloid leukemia (AML)

In 144 analyzed cases of AML there were 2 cases in which SAMHD1 was mutated at positions L178Q as well as S214P, respectively. Comparable expression of L178Q to wt SAMHD1 resulted in a minor but significant HIV-1 block and 2.6-fold reduction of ara-C EC<sub>50</sub> compared to wt SAMHD1. Cells expressing lower amount of L178Q as compared to WT SAMHD1 did

---

<sup>7</sup> [www.cancer.org/cancer/colon-rectal-cancer/treating/by-stage-rectum.html](http://www.cancer.org/cancer/colon-rectal-cancer/treating/by-stage-rectum.html)

not block HIV-1 infection and showed increased EC<sub>50</sub> value by 5.5-fold compared to control cells. AML patients with the L178Q mutation would presumably respond better to ara-C treatment depending on their SAMHD1 expression levels. L178Q mutation might influence dNTPase function of SAMHD1 leading to elevated dNTP levels which may increase HIV-1 infection.

The second SNP in AML S214P did not block HIV-1 infection and was highly sensitive to ara-C treatment comparable to loss of SAMHD1 activity. S214 is buried in the catalytic site of SAMHD1 and changes at this site likely greatly influence dNTPase activity of SAMHD1 and hydrolysis of ara-CTP. Future studies will have to investigate this using primary AML cells with these SAMHD1 SNP variants. Herold et al. previous evaluation of SAMHD1 levels in malignant cells can be used to help determine the dose of ara-C needed to achieve sufficient antineoplastic activity while avoiding excessive ara-C toxicity (Herold et al., 2017a). Our findings suggest that protein levels as well as SAMHD1 mutations can alter the sensitivity towards ara-C treatment.

#### 11.2.2.3 SAMHD1 SNPs in colon adenocarcinoma (COAD)

In 59 analyzed cases of COAD database there were 16 mutations of SAMHD1 found in the TCGA database. We decided to further analyze all 13 missense SNPs and the frameshift mutant K596Rfs\*35. Trifluridine is one of the drugs used to treat colon cancer (Sueda et al., 2016, Scagliotti et al., 2016, Bando et al., 2016). In our previous study we tested whether trifluridine besides ara-C is a substrate of SAMHD1. SAMHD1 <sup>-/-</sup> cells displayed increased sensitivity toward trifluridine suggesting that triphosphate variants of trifluridine could be possible SAMHD1 substrates (Herold et al., 2017b). Further analysis including *in vitro* activity assay, *in vivo* experiments and cohort studies have to be conducted to further verify trifluridine as a substrate of SAMHD1. If SAMHD1 is as well able to hydrolyze triphosphate variants of trifluridine it would be of great interest to study COAD SAMHD1 variants which commonly occur and their response to trifluridine. This would be the next step to personalized medicine. Analyzing the expression level of SAMHD1 in tumors of COAD patients could help to administer the exact dose to get the greatest response of the drug. This would also presumably minimize side effects since COAD SAMHD1 variants can influence hydrolyzes of the drug. Hence a lower dose of the drug is needed to achieve aimed results.

#### 1. G90R variant

The G90R mutation lies closely to the end of the SAMHD1 SAM domain. Deletion construct studies of SAMHD1 revealed that the SAM domain is dispensable for HIV-1 restriction (Powell



et al., 2011, White et al., 2013b, Goldstone et al., 2011, Yan et al., 2013, Brandariz-Nunez et al., 2012). Our expression studies of G90R showed that the G90R variant has to be higher expressed than wt SAMHD1 in order to achieve at least a 2.4-fold lower EC<sub>50</sub> compared to wt SAMHD1. The block to HIV-1 was significant but 4-fold lower compared to wt SAMHD1. Lower expression of G90R compared to wt SAMHD1 did not block HIV-1 infection. Taken in consideration that according to White *et al.* the SAM domain is dismissible, SAMHD1 variants with changes located in the SAM domain should have no defect in HIV-1 restriction but yet G90R SAMHD1 variant showed significantly decreased HIV-1 restriction efficiency and cells expressing this variant were more sensitive to ara-C treatment than compared to cells expressing wt SAMHD1. The SAM domain might have been underestimated in the involvement of HIV-1 restriction. The SAM domains can potentially interact in a homodimeric fashion, as well as with other protein domains or even with RNA (Qiao and Bowie, 2005; Rice et al., 2009). White *et al.* tested whether the SAM domain of SAMHD1 would form homodimeric complexes by an oligomerization assays which revealed that full-length SAMHD1 does not interact with the SAMHD1 variant (1–150) that contains the SAM domain, suggesting that the SAM domain of SAMHD1 might not be interacting with itself in the context of a dimeric SAMHD1. The drawback of this experiment is that the SAMHD1 variant 1–150 that contains the SAM domain might be a misfolded protein (White et al., 2017). Recent work by Buzovetsky *et al.* showed that the SAM domain of mouse SAMHD1 is critical for its activation and regulation. They were also able to achieve the crystal structure of full-length mSAMHD1 protein (Buzovetsky et al., 2018). The structure of full-length human SAMHD1 has not yet been discovered. All published structures of human SAMHD1 only contain the catalytic HD domain (Goldstone et al., 2011, Ji et al., 2013, Zhu et al., 2013). A structural understanding of the full-length SAMHD1 is important as the SAM domain is required for mSAMHD1 catalysis and is likely important for regulating hSAMHD1 activity. The prior mentioned A76T SAMHD1 variant which also resides in the SAM domain showed the opposite phenotype to G90R, i.e. it enhanced the block to HIV-1 infection. This strengthens our hypothesis that the SAM domain might be involved in the HIV-1 restriction mechanism of SAMHD1.

## **2. A338T, V133I, R366H or D497Y SAMHD1 variants**

Rentoft et al. analyzed all four colon associated SAMHD1 amino acid changes by recombinant protein purification and in vitro characterization. In vitro dNTPase activity of A338T was significantly altered for all four nucleoside triphosphates tested (Rentoft et al. 2016). This would suggest that A338T would show at least a reduced block to HIV-1 infection and ara-C sensitivity should be altered as well. In our case A338T was still able to restrict HIV-1 infection

but to a minor extent as compared to wt SAMHD1 (3-fold reduction). To our surprise A338T was able to neutralize the ara-C induced cytotoxicity, suggesting that this mutant was able to hydrolyze ara-CTP to the same extent as wt SAMHD1. This might uncouple the ability of SAMHD1s dNTPase activity and its ara-CTP hydrolysis function and will need further investigation by e.g. measuring intracellular dNTP levels in cells expressing this mutant. In vitro dNTPase activity of V133I was significantly altered but not as strong as A338T SAMHD1 variant mentioned above (1.6-2 fold reduction) for all four nucleoside triphosphates (Rentoft et al. 2016). In our experimental setup V133I expression significantly boosted the block to HIV-1 infection compared to wt SAMHD1 and ara-C sensitivity was comparable to wt SAMHD1. V133 lies close to the allosteric site. Alteration of V133 might increase the affinity of dNTPs thereby decreasing dNTP levels. The in vitro dNTPase activity assay by Rentoft et al. revealed that D497Y SAMHD1 variant had nearly abolished dNTPase activity whereas R366H still sustained dNTPase activity but significantly reduced (Rentoft et al. 2016). The R366 resides in the catalytic site of SAMHD1 and forms hydrogen bond and stacking interactions with the phosphate, the deoxyribose, and the base of the substrate, respectively. Mutation of this residue to A366 abolished the catalytic activity of SAMHD1. Ji *et al.* suggested that this might be due to miss binding and orientation of the dGTP substrate for catalysis (Ji et al. 2013). Taken both studies in consideration we assumed that both SAMHD1 variants are unable to block HIV-1 restriction and are sensitive to ara-C treatment. Indeed, both mutants did not restrict HIV-1 and are highly sensitive to ara-C treatment.

### **3. A525T variant**

The SAMHD1 variant A525T did not show any defect when compared to WT SAMHD1 with respect to neutralize the cytotoxic effect of ara-C, hence presumably was able to detoxify the cell of ara-CTP but had lost its ability to block HIV-1 infection completely. The phosphorylation prediction screen identified Cdk 2 as possible enzyme to phosphorylate the T525 site. A constant phosphorylation could explain the loss of the block to HIV-1 infection. We therefore analyzed whether PMA treatment still resulted in T592 dephosphorylation. T592 dephosphorylation was seen in the A525T mutant. To further determine the function of this amino acid residue we designed the following SAMHD1 variants: A525S, A525E (phosphomimetic), A525V or A525Y. All variants rescued ara-C-induced cytotoxicity hence presumably hydrolyzed ara-CTP but were not able to block HIV-1 infection efficiently. This indicates that constant phosphorylation might not be the reason for the higher infectivity compared to wild type expressed SAMHD1. Only A525E showed a significant but weak block to HIV-1 infection when compared to wt SAMHD1. This suggests that the A525 residue is

critical for the block to HIV-1 infection and uncouples ara-CTP hydrolysis (and dNTPase function) from HIV-1 restriction. Furthermore, we tested the ability of Vpx to rescue HIV-1 from the type I IFN induced block in the cells expressing the A525T variant of SAMHD1. The expressed SAMHD1 variant was not able to rescue HIV-1 from the type I IFN induced block upon Vpx addition. The reason for this was likely that A525T displayed decreased degradation kinetics compared to wild type expressed SAMHD1 when challenged with VPX-VLPs. Since Vpx was still able to degrade SAMHD1, binding to DCAF1 was likely not affected for the A525T variant. There might be other factors involved in the increase of HIV-1 upon Vpx treatment.

#### **4. D137N variant**

In the experiments shown here cells expressing SAMHD1 D137N showed a comparable sensitivity to ara-C induced cytotoxicity as compared to WT SAMHD1, however HIV-1 restriction was completely lost. Ryoo et al. published that the D137N mutant had completely lost dNTPase activity in vitro using dATP, dGTP, dCTP and dTTP. In contrast, Antonucci et al (Nature medicine 2016) showed that D137N could hydrolyze effectively dNTPs, however with slightly reduced efficiency as compared to the WT protein, which is in line with our observation that D137N was capable almost to WT levels to neutralize ara-C induced cytotoxicity. Choi et al (Retrovirology, 2015) published that D137N restricts HIV-1 as wt SAMHD1 using U937 cells and Antonucci also saw that HIV-1 infection was reduced by SAMHD1 D137N, similar to WT. While we cannot explain why we did not observe restriction by SAMHD1 D137N, one possible explanation could be a cell-type-dependent activity of D137N since we used THP-1 SAMHD1 knockout cells overexpressing D137N while the previous experiments by Antonucci et al. or Choi et al. were conducted in PMA differentiated U937 cells. Recently Riess et al. showed that U937 express low levels of SAMHD1, which can be induced by IFN treatment (Riess et al., 2017). Further investigation of a cell-type dependent activity of D137N needs to clarify the underlying reasons for the observed differences.

#### **5. R451A variant**

The R451 residue was previously identified as part of the cyclin binding motif (RXL residue 451-453). Structural and functional analyses of R451A revealed that tetramer formation was disrupted in this SAMHD1 variant and dNTPase activity was lost in in vitro and in cells. St. Gelais et al. also stated that the RXL motif was crucial for HIV-1 restriction and efficient phosphorylation (St Gelais et al. 2018). Furthermore R451C and R451L mutation were identified in a CLL patient sample study (Clifford et al. 2014). R451P variant was also

identified in COAD. We further studied R451P and R451C. Both SAMHD1 variants were unable to restrict HIV-1 infection and cells expressing these mutants were highly sensitive to ara-C treatment which confirms St. Gelais *et al.*'s observations that the RXL motif is crucial for HIV-1 restriction and it is also fundamental for ara-CTP hydrolysis.

## 6. K596Rsf\*35 variant

The K596Rsf\*35 mutation is reported by TCGA in four cancer types: COAD, Uterine Corpus Endometrial Carcinoma (UCEC), Stomach adenocarcinoma (STAD) and Liver Hepatocellular Carcinoma (LIHC). This SAMHD1 variant lost HIV-1 restriction but was still able to presumably hydrolyze ara-CTP comparable to wt SAMHD1. The C-terminus of SAMHD1 (residues 600–626), contains a conserved di-hydrophobic amino acid motif (Leu620-Phe621) which can be recognized by cell cycle regulatory proteins (Yan *et al.*, 2015).

The antiviral activity of SAMHD1 can be post-translationally modulated by phosphorylation at Thr592 by cyclinA2-CDK complex in cycling cells. Cyclin A2 binds the conserved di-hydrophobic residues (Leu620-Phe621) at the C-terminus of SAMHD1 and CDK mediates phosphorylation at Thr592 (Cribier *et al.*, 2013). Overexpression of Mutation phosphomimetic mutants T592D or T592E did not restrict HIV-1 replication while no-phosphorylatable Mutants T592A and T592V were able to restrict HIV-1 infection (White *et al.*, 2013a, Ryoo *et al.*, 2014b, Welbourn *et al.*, 2013, Arnold *et al.*, 2015). In contrast, all four T592 mutants were efficiently able to deplete ara-CTP. This suggest that dNTPase activity is not alone sufficient for lentiviral restriction (White *et al.*, 2013b, Welbourn *et al.*, 2013, Welbourn and Strebel, 2016). C terminal deletion studies (584-626) by *Arnold et al.* in U937 cells abolished the block to HIV-1 restriction. They report that the C- terminal region is indispensable for stable tetramer formation *in vitro*. However transient tetramers were crystalized. Additionally, they were able to show that by mutating R372 tetramerization was completely lost and the dNTPase activity was severely impaired which completely abolished restriction activity of SAMHD1. This would indicate that stable tetramer formation is required for restriction. However, even so dNTPase activity was 10-fold reduced in SAMHD1 C-terminal deletion mutants it was not completely abolished and the Km for substrates was not severely affected (Arnold *et al.*, 2015). This is an indication that catalysis might not depend on stable tetramer formation. As Ji *et al.* reported SAMHD1's affinity in the catalytic site for dNTPs is the following: dCTP > dGTP/dTTP > dATP (Ji *et al.*, 2014). Structural analyzes have to verify whether ara-CTP is chosen over the other dNTPs. However, this would be one explanation why K596f is still able to presumably hydrolyze ara-CTP giving the fact that part of the C-terminal domain is missing leading to no phosphorylation and unstable tetramer formation.

## 7. R145Q variant

The R145Q was found in COAD (TCGA), CLL (Clifford et al. 2014) and AGS (Rice et al. 2009a). White *et al.* reported that the R145Q mutation is unable to oligomerize (White et al. 2013b). R145 resides in the primary allosteric site and is involved in the guanine base recognition. A145 abolished restriction which suggest that allosteric activation of SAMHD1 is a further requirement for restriction (Koharudin et al. 2014b, Arnold et al. 2015a). Our results confirmed that R145 is crucial for restriction since R145Q SAMHD1 variant was unable to block HIV-1. R145Q expressing cells were sensitive to ara-C treatment comparable to cells lacking SAMHD1.

Overall, three SAMHD1 variants (A338T; A525T and K596Rsf\*35) showed EC<sub>50</sub> comparable to wt SAMHD1 but HIV-1 restriction was completely lost (A525T, K596Rsf\*35) or significantly reduced compared to wt SAMHD1 (A338T). This indicates that ara-C hydrolysis cannot be used as an indicator for HIV-1 restriction. All three SAMHD1 variants should still be able to tetramerize otherwise the ara-C detoxification ability of SAMHD1 would also be lost as seen in R451A SAMHD1 variant which is unable to form tetramers.

### 11.2.2.4 Ability of Vpx to degrade human SAMHD1 SNP variants

We proposed that Vpx VLPs can be used to alter SAMHD1 levels. Therefore, we wanted to analyze whether cancer-associated SAMHD1 amino acid variations would alter Vpx-mediated SAMHD1 degradation. This could also reveal which domains in SAMHD1 may affect the Vpx-induced rescue of HIV-1 infection in type I IFN-treated cells, e.g. by revealing interfaces important for interaction with co-factors involved in the IFN-induced block (Buffone et al., 2019). Laguette et al mapped the Vpx interaction with SAMHD1 to the C terminal domain of SAMHD1 and identified residues 595-626 to be involved in the binding to SAMHD1 (Laguette et al., 2012). Therefore, only K596Rsf\*35 should be insensitive to Vpx-induced degradation. Lim *et al.* reported that the SAM domain and N-terminal harbor positive selection residues sensitive to Vpx besides the C-terminus (Lim et al., 2012). Another report proposed a model whereby Vpx interacts with the oligomeric interface of SAMHD1, implementing that oligomeric SAMHD1 is required for Vpx mediated SAMHD1 degradation (Fregoso et al., 2013). Some of the analyzed AGS SAMHD1 by White *et al.* which reside not in the C-terminus of SAMHD1 were defective in oligomerization and their ability to be degraded by Vpx was also defective? (White et al., 2017). We analyzed wt SAMHD1, D137N, A76T, A338T, A338V, V133I, P589T, A525T, D311A, L178Q, G90R and K596Rsf\*35 for their sensitivity to

Vpx-induced degradation. All SAMHD1 variants analyzed besides K596Rsf\*35 were degraded efficiently by Vpx, mostly comparable to WT SAMHD1. White et al. analyzed R145Q which was unable to be degraded by Vpx but contrary to Fregoso *et al.* was not able to oligomerize (White et al., 2017). Further SAMHD1 variants have to be analyzed for their oligomerization status and their ability to be degraded by Vpx to verify Fregoso *et al.*'s hypothesis.

#### 11.2.2.5 SNP in stomach adenocarcinoma (STAD)

The TCGA database reports that in 42 analyzed patient tumor samples of stomach adenocarcinoma 16 mutations of SAMHD1 were found. P589T mutation was predicted to be damaging by one out of three computational analyses (VEP, SIFT, PolyPhen). HIV-1 restriction was not blocked in SAMHD1<sup>-/-</sup> cells expressing the P589T variant and sensitivity towards ara-C decreased by 18.8-fold compared to loss of SAMHD1. This is another example of a complete loss of HIV-1 restriction but SAMHD1 variant P589T is still able to presumably hydrolyze ara-CTP.

### 11.3 SAMHD1 variants that influence post-translational modifications of SAMHD1 and their involvement in HIV-1 restriction and ara-CTP hydrolysis

#### 11.3.1 The C522 residue of SAMHD1 is crucial for the intensive block to HIV infection but presumably not for ara-CTP hydrolysis

Retroviral restriction ability of cysteine SAMHD1 mutants was evaluated in PMA-treated THP-1 SAMHD1<sup>-/-</sup> cells stably expressing the C522S and C522A SAMHD1 variants were challenged with increasing amounts of HIV-1 virus expressing GFP as a reporter of infection. This study revealed that C522S and C522A mutations reduced (C522S 8-fold reduction; C522A 6-fold reduction) but not completely abolished HIV-1 restriction. Both mutations decreased the ara-C detoxifying ability of SAMHD1 slightly (C522S 1.4-fold decrease of EC<sub>50</sub>; C522A mutant 3-fold decrease of EC<sub>50</sub> compared to wt SAMHD1).

Wang *et al.* and Mauney *et al.* reported that SAMHD1 is a redox-sensitive enzyme and it poses three redox-active cysteines at the following location: 341, 350 and 522 (Mauney et al. 2017, Wang et al. 2018). Expression of the SAMHD1 variant C522S in PMA-treated U937 cell did not lead to HIV-1 restriction. They also tested dNTPase activity and capability of tetramerization. C522S mutation has no detectable negative effect on SAMHD1 tetramerization and dNTPase activity *in vitro*. They reasoned that nucleotide-dependent tetramerization and dNTPase activity is needed but not sufficient for the block of retroviral replication. Suggesting that the redox activity of C522 is crucial for the block to HIV-1 infection. (Wang et al. 2018).

This is another example of a SAMHD1 variant which appears to be functioning properly in ara-C hydrolysis (if dNTPase and ara-CTPase function are correlated) but fails to restrict HIV-1, like the phosphomimetic mutants T592E and T592D or D137N (see above). Wang *et al.* suggest that one likely possibility might be that tetramerization is only one of several ways' dNTP hydrolysis can be activated and it might involve phosphorylation and redox activity of C522 together. This however is in conflict with C522S and C522A's ability to hydrolyze ara-CTP. Ara-C detoxification by SAMHD1 is therefore not as dependent on the redox state as HIV-1 restriction.

### *11.3.2 SAMHD1 acetylation has no influence on viral restriction and minimally changes its sensitivity to ara-C induced cytotoxicity*

Lee *et al.* identified that the lysine residue 405 of SAMHD1 is acetylated by the acetyltransferase arrest defective protein 1 (ARD1). Acetylation defective mutant K405R possess lower dNTPase activity compared to wt acetylated SAMHD1 and acetylation promotes cancer cell proliferation (Lee et al., 2017). They imply that SAMHD1 acetylation might be of interest as a target for cancer treatment. Therefore, we analyzed K405R influence on ara-C sensitivity and its restriction capability towards HIV-1 in PMA treated K405R expressing THP-1 SAMHD1 *-/-* cells. A minor increase in ara-C sensitivity of 1.18-fold was seen which can be explained by lower expression of K405R compared to wt SAMHD1. HIV-1 restriction was comparable to wt. This stays in conflict with K405R decreased hydrolyzation ability (Lee et al., 2017). Which implicates that acetylation might not be critical for SAMHD1's role in lentiviral restriction in pma treated THP-1 cells and ara-C hydrolysis in THP-1 cells. Lee *et al.* used HEK293T and HeLa cells for their analyzes (Lee et al., 2017). Furthermore acetylation of SAMHD1 peaked during the G1 phase of the cell cycle and resulted in the increased dNTPase activity of the enzyme in vitro (Lee et al., 2017). Our HIV-1 infection study was conducted with pma treated noncycling THP-1 cells. Hence the acetylation effect might not be pronounced in noncycling cells. THP-1 cells and other cell lines have to be evaluated in respect to their ARD1 levels as well as acetylation of SAMHD1 at residue K405 to rule out a cell type dependent acetylation. Furthermore K405R's dNTPase function has to be evaluated further.

## **12 Summary and Outlook**

### **12.1 SAMHD1's role in the type 1 interferon induced early block to HIV-1 infection**

We could show that Vpx mutant Q76A which is unable to bind DCAF1 is unable to increase HIV-1 infection in macrophages treated with interferon, suggesting that SAMHD1 degradation is required for efficient Vpx-mediated rescue of HIV-1 from the type I IFN-induced early antiviral blocks in macrophages. CRISPR/Cas9 THP-1 cells lacking a functional *SAMHD1* gene did not impact the level of the type I IFN-induced early block to HIV-1 infection as well as cell proliferation as compared to control or parental THP-1 cells. However, while Vpx was able to rescue HIV-1 infectivity in parental THP-1 or CRISPR/Cas9 control cells, no rescue was observed when SAMHD1 protein was absent.

To investigate whether the enzymatic activity of SAMHD1 was required for the Vpx-mediated rescue of HIV-1 infection from the early type I IFN-induced blocks, we reconstituted expression of wild type or different catalytically-inactive SAMHD1 mutants in *SAMHD1*<sup>-/-</sup> cells and found that Vpx increased HIV-1 infectivity in the presence of wild type, but not H233A mutant SAMHD1, suggesting that the enzymatic activity of SAMHD1 is required for a Vpx-induced rescue of HIV-1 infection from the type I IFN-induced block. We were able to generate a CRISPR/Cas9 THP-1 cell clone, which had one disrupted SAMHD1 allele and one allele, in which the entire nuclear localization signal (<sup>11</sup>KRPR<sup>14</sup>) was deleted in frame, generating an internally NLS-disrupted endogenously expressed SAMHD1 protein. In these cells, SAMHD1 was localized to the cytoplasm. In these cells, Vpx still rescued HIV-1 from the type I IFN-induced early blocks to infection. Of note, SAMHD1 degradation was profoundly delayed, suggesting that Vpx-induced polyubiquitination of SAMHD1 is sufficient to overcome early IFN-induced blocks to HIV-1. This hypothesis has to be further tested, however. To further characterize SAMHD1's role in the Vpx mediated increase of HIV-1 infectivity other cell lines have to be tested as well to get a better understanding of SAMHD1's broad function.

### **12.2 Correlation of SAMHD1 dNTPase activity with HIV-1 restriction by using cancer-associated naturally occurring SAMHD1 variants**

We used the finding by our collaborators at the Karolinska Institute in Stockholm that SAMHD1 expressed in cell lines reduces their sensitivity to ara-C-induced cytotoxicity as a surrogate model for measuring dNTPase activity of SAMHD1 and to correlate it in the same cells with HIV-1 infection. This not only opened to us the possibility to investigate the correlation of SAMHD1's dNTPase activity with HIV-1 restriction, it also provided an assay to



investigate which parts of SAMHD1 are important for the Vpx-induced HIV-1 infection rescue in type I IFN-treated cells by using a set of naturally occurring SAMHD1 variants present in certain types of cancers.

Overall, three SAMHD1 variants (A338T; A525T and K596Rsf\*35) showed EC<sub>50</sub> in ara-C cytotoxicity experiments comparable to wt SAMHD1 but HIV-1 restriction was completely lost (A525T, K596Rsf\*35) or significantly reduced compared to wt SAMHD1 (A338T). Another mutant P589T lost HIV-1 restriction completely but was still able to presumably hydrolyze ara-CTP. We also identified three SAMHD1 mutants, which were able to restrict HIV-1 significantly better than wt SAMHD1 (V133I, A76T and R305I). Furthermore, we could show that 6 SAMHD1 SNP lost their ability to restrict HIV-1 and were highly sensitive to ara-C treatment. Further analyses have to focus on characterization of dNTPase activity, ara-CTP hydrolysis and tetramer formation. We are currently working on purifying the human SAMHD1 variants and afterwards we will analyze the activity of these variants in vitro as previously shown (Herold et al., 2017a). In addition to biochemical characterization of their catalytic activity, we will also look at protein stability using in vitro thermal shift assays. This assay will inform us about the stability of the SAMHD1 variants.

If we find a naturally occurring SAMHD1 SNP with its dNTPase activity still intact this might indicate that the dNTPase activity of SAMHD1 is not exclusively responsible for the block to HIV-1 infection. There is the possibility that cofactor binding might influence dNTPase activity. Identification of those SAMHD1 SNPs which are unable to block HIV-1 infection in newly infected HIV-1 patients could give hints to a possibly fast proceeding of HIV infection. An early onset of aggressive treatment might be necessary to keep the virus load under control. Hence it is of great interest to further study SAMHD1 SNPs and screen HIV-1 patients as well as cancer patients for SAMHD1 SNPs. In summary it is very likely that SAMHD1 does not restrict HIV-1 by one single function, but through a combination of several pathways.

Analyzes of two SAMHD1 variants with mutated residues in the SAM domain altered HIV-1 restriction and ara-CTP hydrolysis. Up until now it was thought that the is dismissible for HIV-1 restriction (White et al., 2013a). The structure of full-length human SAMHD1 has not yet been discovered therefore scientist should aim to crystalize the full length SAMHD1 protein so that the function of the SAM domain can be evaluated.

## 13 Publications and contributions

### 13.1 Publications

Schaller T, Bulli L, Pollpeter D, Betancor G, Kutzner J, Apolonia L, Herold N, Burk R, Malim MH

**Effects of Inner Nuclear Membrane Proteins SUN1/UNC-84A and SUN2/UNC-84B on the Early Steps of HIV-1 Infection.**

J Virol. 2017 Sep 12;91(19). pii: e00463-17. doi: 10.1128/JVI.00463-17. Print 2017 Oct 1.

Herold N, Rudd SG, Sanjiv K, Kutzner J, Myrberg IH, Paulin CBJ, Olsen TK, Helleday T, Henter JI, Schaller T

**With me or against me: Tumor suppressor and drug resistance activities of SAMHD1.**

Exp Hematol. 2017 Aug;52:32-39. doi: 10.1016/j.exphem.2017.05.001. Epub 2017 May 11.

Herold N, Rudd SG, Sanjiv K, Kutzner J, Bladh J, Paulin CBJ, Helleday T, Henter JI, Schaller T.

**SAMHD1 protects cancer cells from various nucleoside-based antimetabolites.**

Cell Cycle. 2017 Jun 3;16(11):1029-1038. doi: 10.1080/15384101.2017.1314407. Epub 2017 Apr 24.

Herold N, Rudd SG, Ljungblad L, Sanjiv K, Myrberg IH, Paulin CB, Heshmati Y, Hagenkort A, Kutzner J, Page BD, Calderón-Montaña JM, Loseva O, Jemth AS, Bulli L, Axelsson H, Tesi B, Valerie NC, Höglund A, Bladh J, Wiita E, Sundin M, Uhlin M, Rassidakis G, Heyman M, Tamm KP, Warpman-Berglund U, Walfridsson J, Lehmann S, Grandér D, Lundbäck T, Kogner P, Henter JI, Helleday T, Schaller T.

**Targeting SAMHD1 with the Vpx protein to improve cytarabine therapy for hematological malignancies.**

Nat Med. 2017 Feb;23(2):256-263. doi: 10.1038/nm.4265. Epub 2017 Jan 9.

Bulli L, Apolonia L, Kutzner J, Pollpeter D, Goujon C, Herold N, Schwarz SM, Giernat Y, Keppler OT, Malim MH, Schaller T.

**Complex Interplay between HIV-1 Capsid and MX2-Independent Alpha Interferon-Induced Antiviral Factors.**

J Virol. 2016 Jul 27;90(16):7469-7480. doi: 10.1128/JVI.00458-16. Print 2016 Aug 15.

Cindy Buffone, Juliane Kutzner, Silvana Opp, Alicia Martinez-Lopez, Anastasia Selyutina, Si Ana Coggings, Lydia R. Studdard, Lingmei Ding, Baek Kim, Paul Spearman, Torsten Schaller, Felipe Diaz-Griffero

**The ability of SAMHD1 to block HIV-1 but not SIV requires expression of MxB**

Virology. 2019 May; 531: 260–268. Published online 2019 Mar 30.

Al-Shehabi H, Fiebig U, Kutzner J, Denner J, Schaller T, Bannert N, Hofmann H.

**Human SAMHD1 restricts the xenotransplantation relevant porcine endogenous retrovirus (PERV) in non-dividing cells.**

Conference contributions J Gen Virol. 2019 Apr;100(4):656-661. doi: 10.1099/jgv.0.001232. Epub 2019 Feb 15.

### **13.2 Conference Contributions**

Juliane Kutzner, Nikolas Herold, Sean G. Rudd and Torsten Schaller

Poster presentation: **Insights into the SAMHD1 viral restriction mechanism and cancer resistance to nucleoside analogue-based therapies by the analysis of naturally occurring cancer-associated single nucleotide polymorphisms**

Retroviruses, Cold Spring Harbor Laboratory, NY, USA, 2018

Juliane Kutzner and Torsten Schaller

Poster presentation: **SAMHD1 is required for the Vpx-mediated rescue of HIV-1 infection from the type I IFN-induced antiviral block in myeloid cells** Retroviruses, Cold Spring Harbor Laboratory, NY, USA, 2018

### **13.3 Contributions to this project**

All data shown in this thesis was acquired and analyzed by me, if not stated otherwise. Contributions to this thesis are described as follows:

Nikolas Herold, Sean Rudd and Nikolaos Tsesmetzis conducted the following experiments: cell viability assay of Vpx treated THP-1 cells and SAMHD1 knock-out cells and graph distribution, SAMHD1 growth kinetics graph and cell cycle distribution experiments and graph design.

## 14 References

- ACCOLA, M. A., BUKOVSKY, A. A., JONES, M. S. & GOTTLINGER, H. G. 1999. A conserved dileucine-containing motif in p6(gag) governs the particle association of Vpx and Vpr of simian immunodeficiency viruses SIV(mac) and SIV(agm). *J Virol*, 73, 9992-9.
- AGY, M. B., ACKER, R. L., SHERBERT, C. H. & KATZE, M. G. 1995. Interferon treatment inhibits virus replication in HIV-1- and SIV-infected CD4+ T-cell lines by distinct mechanisms: evidence for decreased stability and aberrant processing of HIV-1 proteins. *Virology*, 214, 379-86.
- AHN, J. 2016. Functional organization of human SAMHD1 and mechanisms of HIV-1 restriction. *Biol Chem*, 397, 373-9.
- ALTON, E. W., BEEKMAN, J. M., BOYD, A. C., BRAND, J., CARLON, M. S., CONNOLLY, M. M., CHAN, M., CONLON, S., DAVIDSON, H. E., DAVIES, J. C., DAVIES, L. A., DEKKERS, J. F., DOHERTY, A., GEA-SORLI, S., GILL, D. R., GRIESENBACH, U., HASEGAWA, M., HIGGINS, T. E., HIRONAKA, T., HYNDMAN, L., MCLACHLAN, G., INOUE, M., HYDE, S. C., INNES, J. A., MAHER, T. M., MORAN, C., MENG, C., PAUL-SMITH, M. C., PRINGLE, I. A., PYTEL, K. M., RODRIGUEZ-MARTINEZ, A., SCHMIDT, A. C., STEVENSON, B. J., SUMNER-JONES, S. G., TOSHNER, R., TSUGUMINE, S., WASOWICZ, M. W. & ZHU, J. 2017. Preparation for a first-in-man lentivirus trial in patients with cystic fibrosis. *Thorax*, 72, 137-147.
- AMIE, S. M., BAMBARA, R. A. & KIM, B. 2013. GTP is the primary activator of the anti-HIV restriction factor SAMHD1. *J Biol Chem*, 288, 25001-6.
- ANGERS, S., LI, T., YI, X., MACCOSS, M. J., MOON, R. T. & ZHENG, N. 2006. Molecular architecture and assembly of the DDB1-CUL4A ubiquitin ligase machinery. *Nature*, 443, 590-3.
- ANTONUCCI, J. M., ST GELAIS, C., DE SILVA, S., YOUNT, J. S., TANG, C., JI, X., SHEPARD, C., XIONG, Y., KIM, B. & WU, L. 2016. SAMHD1-mediated HIV-1 restriction in cells does not involve ribonuclease activity. *Nat Med*, 22, 1072-1074.
- ARAVIND, L. & KOONIN, E. V. 1998. The HD domain defines a new superfamily of metal-dependent phosphohydrolases. *Trends Biochem Sci*, 23, 469-72.
- ARNOLD, L. H., GROOM, H. C., KUNZELMANN, S., SCHWEFEL, D., CASWELL, S. J., ORDONEZ, P., MANN, M. C., RUESCHENBAUM, S., GOLDSTONE, D. C., PENNELL, S., HOWELL, S. A., STOYE, J. P., WEBB, M., TAYLOR, I. A. & BISHOP, K. N. 2015. Phospho-dependent Regulation of SAMHD1 Oligomerisation Couples Catalysis and Restriction. *PLoS Pathog*, 11, e1005194.
- AYE, Y., LI, M., LONG, M. J. & WEISS, R. S. 2015. Ribonucleotide reductase and cancer: biological mechanisms and targeted therapies. *Oncogene*, 34, 2011-21.
- BACA-REGEN, L., HEINZINGER, N., STEVENSON, M. & GENDELMAN, H. E. 1994. Alpha interferon-induced antiretroviral activities: restriction of viral nucleic acid synthesis and progeny virion production in human immunodeficiency virus type 1-infected monocytes. *J Virol*, 68, 7559-65.
- BAINBRIDGE, J. W., STEPHENS, C., PARSLEY, K., DEMAISON, C., HALFYARD, A., THRASHER, A. J. & ALI, R. R. 2001. In vivo gene transfer to the mouse eye using an HIV-based lentiviral vector; efficient long-term transduction of corneal endothelium and retinal pigment epithelium. *Gene Ther*, 8, 1665-8.
- BALDAUF, H. M., PAN, X., ERIKSON, E., SCHMIDT, S., DADDACHA, W., BURGGRAF, M., SCHENKOVA, K., AMBIEL, I., WABNITZ, G., GRAMBERG, T., PANITZ, S., FLORY, E., LANDAU, N. R., SERTEL, S., RUTSCH, F., LASITSCHKA, F., KIM,

- B., KÖNIG, R., FACKLER, O. T. & KEPPLER, O. T. 2012. SAMHD1 restricts HIV-1 infection in resting CD4(+) T cells. *Nat Med*, 18.
- BALDAUF, H. M., STEGMANN, L., SCHWARZ, S. M., AMBIEL, I., TROTARD, M., MARTIN, M., BURGGRAF, M., LENZI, G. M., LEJK, H., PAN, X., FREGOSO, O. I., LIM, E. S., ABRAHAM, L., NGUYEN, L. A., RUTSCH, F., KONIG, R., KIM, B., EMERMAN, M., FACKLER, O. T. & KEPPLER, O. T. 2017. Vpx overcomes a SAMHD1-independent block to HIV reverse transcription that is specific to resting CD4 T cells. *Proc Natl Acad Sci U S A*, 114, 2729-2734.
- BALTIMORE, D. 1970. RNA-dependent DNA polymerase in virions of RNA tumour viruses. *Nature*, 226, 1209-11.
- BALZARINI, J. 2000. Effect of antimetabolite drugs of nucleotide metabolism on the anti-human immunodeficiency virus activity of nucleoside reverse transcriptase inhibitors. *Pharmacol Ther*, 87, 175-87.
- BANDO, H., DOI, T., MURO, K., YASUI, H., NISHINA, T., YAMAGUCHI, K., TAKAHASHI, S., NOMURA, S., KUNO, H., SHITARA, K., SATO, A. & OHTSU, A. 2016. A multicenter phase II study of TAS-102 monotherapy in patients with pre-treated advanced gastric cancer (EPOC1201). *Eur J Cancer*, 62, 46-53.
- BARRE-SINOUSI, F., CHERMANN, J. C., REY, F., NUGEYRE, M. T., CHAMARET, S., GRUEST, J., DAUGUET, C., AXLER-BLIN, C., VEZINET-BRUN, F., ROUZIOUX, C., ROZENBAUM, W. & MONTAGNIER, L. 2004. Isolation of a T-lymphotropic retrovirus from a patient at risk for acquired immune deficiency syndrome (AIDS). 1983. *Rev Invest Clin*, 56, 126-9.
- BELL, N. M. & LEVER, A. M. 2013. HIV Gag polyprotein: processing and early viral particle assembly. *Trends Microbiol*, 21, 136-44.
- BEOGLAZOVA, N., FLICK, R., TCHIGVINTSEV, A., BROWN, G., POPOVIC, A., NOCEK, B. & YAKUNIN, A. F. 2013. Nuclease activity of the human SAMHD1 protein implicated in the Aicardi-Goutieres syndrome and HIV-1 restriction. *J Biol Chem*, 288, 8101-10.
- BELSHAN, M., MAHNKE, L. A. & RATNER, L. 2006. Conserved amino acids of the human immunodeficiency virus type 2 Vpx nuclear localization signal are critical for nuclear targeting of the viral pre-integration complex in non-dividing cells. *Virology*, 346, 118-26.
- BELSHAN, M. & RATNER, L. 2003. Identification of the nuclear localization signal of human immunodeficiency virus type 2 Vpx. *Virology*, 311, 7-15.
- BELZILE, J. P., DUISIT, G., ROUGEAU, N., MERCIER, J., FINZI, A. & COHEN, E. A. 2007. HIV-1 Vpr-mediated G2 arrest involves the DDB1-CUL4AVPRBP E3 ubiquitin ligase. *PLoS Pathog*, 3, e85.
- BERGAMASCHI, A., AYINDE, D., DAVID, A., LE ROUZIC, E., MOREL, M., COLLIN, G., DESCAMPS, D., DAMOND, F., BRUN-VEZINET, F., NISOLE, S., MARGOTTIN-GOGUET, F., PANCINO, G. & TRANSY, C. 2009. The human immunodeficiency virus type 2 Vpx protein usurps the CUL4A-DDB1 DCAF1 ubiquitin ligase to overcome a postentry block in macrophage infection. *J Virol*, 83, 4854-60.
- BIANCHI, V. & SPYCHALA, J. 2003. Mammalian 5'-nucleotidases. *J Biol Chem*, 278, 46195-8.
- BIENIASZ, P. D. 2006. Late budding domains and host proteins in enveloped virus release. *Virology*, 344, 55-63.
- BITZEIGEIO, J., SAMPIAS, M., BIENIASZ, P. D. & HATZIOANNOU, T. 2013. Adaptation to the interferon-induced antiviral state by human and simian immunodeficiency viruses. *J Virol*, 87, 3549-60.

- BLANCO-MELO, D., VENKATESH, S. & BIENIASZ, P. D. 2012. Intrinsic cellular defenses against human immunodeficiency viruses. *Immunity*, 37, 399-411.
- BONIFATI, S., DALY, M. B., ST GELAIS, C., KIM, S. H., HOLLENBAUGH, J. A., SHEPARD, C., KENNEDY, E. M., KIM, D. H., SCHINAZI, R. F., KIM, B. & WU, L. 2016. SAMHD1 controls cell cycle status, apoptosis and HIV-1 infection in monocytic THP-1 cells. *Virology*, 495, 92-100.
- BOOTH, C., GASPAR, H. B. & THRASHER, A. J. 2016. Treating Immunodeficiency through HSC Gene Therapy. *Trends Mol Med*, 22, 317-327.
- BOUR, S., GELEZIUNAS, R. & WAINBERG, M. A. 1995. The human immunodeficiency virus type 1 (HIV-1) CD4 receptor and its central role in promotion of HIV-1 infection. *Microbiol Rev*, 59, 63-93.
- BRANDARIZ-NUNEZ, A., VALLE-CASUSO, J. C., WHITE, T. E., LAGUETTE, N., BENKIRANE, M., BROJATSCH, J. & DIAZ-GRIFFERO, F. 2012. Role of SAMHD1 nuclear localization in restriction of HIV-1 and SIVmac. *Retrovirology*, 9, 49.
- BRASS, A. L., HUANG, I. C., BENITA, Y., JOHN, S. P., KRISHNAN, M. N., FEELEY, E. M., RYAN, B. J., WEYER, J. L., VAN DER WEYDEN, L., FIKRIG, E., ADAMS, D. J., XAVIER, R. J., FARZAN, M. & ELLEDGE, S. J. 2009. The IFITM proteins mediate cellular resistance to influenza A H1N1 virus, West Nile virus, and dengue virus. *Cell*, 139, 1243-54.
- BRIGGS, J. A. G., WILK, T., WELKER, R., KRÄUSSLICH, H.-G. & FULLER, S. D. 2003. Structural organization of authentic, mature HIV-1 virions and cores. *The EMBO journal*, 22, 1707-1715.
- BROWNE, E. P. & LITTMAN, D. R. 2008. Species-specific restriction of apobec3-mediated hypermutation. *J Virol*, 82, 1305-13.
- BUCKLAND, R. J., WATT, D. L., CHITTOOR, B., NILSSON, A. K., KUNKEL, T. A. & CHABES, A. 2014. Increased and imbalanced dNTP pools symmetrically promote both leading and lagging strand replication infidelity. *PLoS Genet*, 10, e1004846.
- BUFFONE, C., KUTZNER, J., OPP, S., MARTINEZ-LOPEZ, A., SELYUTINA, A., COGGINGS, S. A., STUDDARD, L. R., DING, L., KIM, B., SPEARMAN, P., SCHALLER, T. & DIAZ-GRIFFERO, F. 2019. The ability of SAMHD1 to block HIV-1 but not SIV requires expression of MxB. *Virology*, 531, 260-268.
- BUZOVETSKY, O., TANG, C., KNECHT, K. M., ANTONUCCI, J. M., WU, L., JI, X. & XIONG, Y. 2018. The SAM domain of mouse SAMHD1 is critical for its activation and regulation. *Nat Commun*, 9, 411.
- CAMPBELL, E. M. & HOPE, T. J. 2015. HIV-1 capsid: the multifaceted key player in HIV-1 infection. *Nat Rev Microbiol*, 13, 471-83.
- CHAN, D. C., FASS, D., BERGER, J. M. & KIM, P. S. 1997. Core structure of gp41 from the HIV envelope glycoprotein. *Cell*, 89, 263-73.
- CHAN, D. C. & KIM, P. S. 1998. HIV entry and its inhibition. *Cell*, 93, 681-4.
- CHELBI-ALIX, M. K. & WIETZERBIN, J. 2007. Interferon, a growing cytokine family: 50 years of interferon research. *Biochimie*, 89, 713-8.
- CHEN, J. J., JIN, M. X., ZHU, S. L., LI, F. & XING, Y. 2014. The Synthesis and characteristic study of transferrin-conjugated liposomes carrying brain-derived neurotrophic factor. *Biomed Mater Eng*, 24, 2089-99.
- CHOI, J., RYOO, J., OH, C., HWANG, S. & AHN, K. 2015. SAMHD1 specifically restricts retroviruses through its RNase activity. *Retrovirology*, 12, 46.
- CHOJNACKI, J., STAUDT, T., GLASS, B., BINGEN, P., ENGELHARDT, J., ANDERS, M., SCHNEIDER, J., MULLER, B., HELL, S. W. & KRAUSSLICH, H. G. 2012. Maturation-dependent HIV-1 surface protein redistribution revealed by fluorescence nanoscopy. *Science*, 338, 524-8.

- CLIFFORD, R., LOUIS, T., ROBBE, P., ACKROYD, S., BURNS, A., TIMBS, A. T., WRIGHT COLOPY, G., DREAU, H., SIGAUX, F., JUDDE, J. G., ROTGER, M., TELENTI, A., LIN, Y. L., PASERO, P., MAELFAIT, J., TITSIAS, M., COHEN, D. R., HENDERSON, S. J., ROSS, M. T., BENTLEY, D., HILLMEN, P., PETTITT, A., REHWINKEL, J., KNIGHT, S. J., TAYLOR, J. C., CROW, Y. J., BENKIRANE, M. & SCHUH, A. 2014. SAMHD1 is mutated recurrently in chronic lymphocytic leukemia and is involved in response to DNA damage. *Blood*, 123, 1021-31.
- COQUEL, F., SILVA, M. J., TECHER, H., ZADOROZHNY, K., SHARMA, S., NIEMINUSZCZY, J., METTLING, C., DARDILLAC, E., BARTHE, A., SCHMITZ, A. L., PROMONET, A., CRIBIER, A., SARRAZIN, A., NIEDZWIEDZ, W., LOPEZ, B., COSTANZO, V., KREJCI, L., CHABES, A., BENKIRANE, M., LIN, Y. L. & PASERO, P. 2018. SAMHD1 acts at stalled replication forks to prevent interferon induction. *Nature*, 557, 57-61.
- CRIBIER, A., DESCOURS, B., VALADÃO, ANA LUIZA C., LAGUETTE, N. & BENKIRANE, M. 2013. Phosphorylation of SAMHD1 by Cyclin A2/CDK1 Regulates Its Restriction Activity toward HIV-1. *Cell Reports*, 3, 1036-1043.
- DAMOND, F., APETREI, C., ROBERTSON, D. L., SOUQUIERE, S., LEPRETRE, A., MATHERON, S., PLANTIER, J. C., BRUN-VEZINET, F. & SIMON, F. 2001. Variability of human immunodeficiency virus type 2 (hiv-2) infecting patients living in france. *Virology*, 280, 19-30.
- DAYTON, A. I., SODROSKI, J. G., ROSEN, C. A., GOH, W. C. & HASELTINE, W. A. 1986. The trans-activator gene of the human T cell lymphotropic virus type III is required for replication. *Cell*, 44, 941-7.
- DE ROOIJ, J. D., ZWAAN, C. M. & VAN DEN HEUVEL-EIBRINK, M. 2015. Pediatric AML: From Biology to Clinical Management. *J Clin Med*, 4, 127-49.
- DELEBECQUE, F., SUSPENE, R., CALATTINI, S., CASARTELLI, N., SAIB, A., FROMENT, A., WAIN-HOBSON, S., GESSAIN, A., VARTANIAN, J. P. & SCHWARTZ, O. 2006. Restriction of foamy viruses by APOBEC cytidine deaminases. *J Virol*, 80, 605-14.
- DEPIENNE, C., ROQUES, P., CREMINON, C., FRITSCH, L., CASSERON, R., DORMONT, D., DARGEMONT, C. & BENICHOU, S. 2000. Cellular distribution and karyophilic properties of matrix, integrase, and Vpr proteins from the human and simian immunodeficiency viruses. *Exp Cell Res*, 260, 387-95.
- DESCOURS, B., CRIBIER, A., CHABLE-BESSIA, C., AYINDE, D., RICE, G., CROW, Y., YATIM, A., SCHWARTZ, O., LAGUETTE, N. & BENKIRANE, M. 2012. SAMHD1 restricts HIV-1 reverse transcription in quiescent CD4(+) T-cells. *Retrovirology*, 9, 87.
- DIAMOND, M. S. & FARZAN, M. 2013. The broad-spectrum antiviral functions of IFIT and IFITM proteins. *Nat Rev Immunol*, 13, 46-57.
- DOMS, R. W. & MOORE, J. P. 2000. HIV-1 membrane fusion: targets of opportunity. *J Cell Biol*, 151, F9-14.
- DORFMAN, T., MAMMANO, F., HASELTINE, W. A. & GOTTLINGER, H. G. 1994. Role of the matrix protein in the virion association of the human immunodeficiency virus type 1 envelope glycoprotein. *J Virol*, 68, 1689-96.
- DRAGIN, L., NGUYEN, L., LAHOUESSA, H., SOURISCE, A., KIM, B., RAMIREZ, C. & MARGOTTIN-GOGUET, F. 2013. Interferon- $\alpha$  blocks HIV-1 infection in non-dividing myeloid cells despite SAMHD1 degradation and high deoxynucleoside triphosphates supply. *Retrovirology*, 10, P69-P69.
- EARLY, A. P., PREISLER, H. D., SLOCUM, H. & RUSTUM, Y. M. 1982. A pilot study of high-dose 1-beta-D-arabinofuranosylcytosine for acute leukemia and refractory lymphoma: clinical response and pharmacology. *Cancer Res*, 42, 1587-94.



- ELIA, A. E., BOARDMAN, A. P., WANG, D. C., HUTTLIN, E. L., EVERLEY, R. A., DEPHOURE, N., ZHOU, C., KOREN, I., GYGI, S. P. & ELLEDGE, S. J. 2015. Quantitative Proteomic Atlas of Ubiquitination and Acetylation in the DNA Damage Response. *Mol Cell*, 59, 867-81.
- ESTEY, E., PLUNKETT, W., DIXON, D., KEATING, M., MCCREDIE, K. & FREIREICH, E. J. 1987. Variables predicting response to high dose cytosine arabinoside therapy in patients with refractory acute leukemia. *Leukemia*, 1, 580-3.
- FARNET, C. M., WANG, B., LIPFORD, J. R. & BUSHMAN, F. D. 1996. Differential inhibition of HIV-1 pre-integration complexes and purified integrase protein by small molecules. *Proc Natl Acad Sci U S A*, 93, 9742-7.
- FERNANDEZ-CALOTTI, P., JORDHEIM, L. P., GIORDANO, M., DUMONTET, C. & GALMARINI, C. M. 2005. Substrate cycles and drug resistance to 1-beta-D-arabinofuranosylcytosine (araC). *Leuk Lymphoma*, 46, 335-46.
- FISHER, A. G., FEINBERG, M. B., JOSEPHS, S. F., HARPER, M. E., MARSELLE, L. M., REYES, G., GONDA, M. A., ALDOVINI, A., DEBOUK, C., GALLO, R. C. & ET AL. 1986. The trans-activator gene of HTLV-III is essential for virus replication. *Nature*, 320, 367-71.
- FITZGERALD-BOCARSLY, P., DAI, J. & SINGH, S. 2008. Plasmacytoid dendritic cells and type I IFN: 50 years of convergent history. *Cytokine Growth Factor Rev*, 19, 3-19.
- FRANCHINI, G., RUSCHE, J. R., O'KEEFFE, T. J. & WONG-STAAAL, F. 1988. The human immunodeficiency virus type 2 (HIV-2) contains a novel gene encoding a 16 kD protein associated with mature virions. *AIDS Res Hum Retroviruses*, 4, 243-50.
- FRANZOLIN, E., PONTARIN, G., RAMPAZZO, C., MIAZZI, C., FERRARO, P., PALUMBO, E., REICHARD, P. & BIANCHI, V. 2013. The deoxynucleotide triphosphohydrolase SAMHD1 is a major regulator of DNA precursor pools in mammalian cells. *Proc Natl Acad Sci U S A*, 110, 14272-7.
- FREED, E. O., MYERS, D. J. & RISSER, R. 1990. Characterization of the fusion domain of the human immunodeficiency virus type 1 envelope glycoprotein gp41. *Proc Natl Acad Sci U S A*, 87, 4650-4.
- FREGOSO, O. I., AHN, J., WANG, C., MEHRENS, J., SKOWRONSKI, J. & EMERMAN, M. 2013. Evolutionary toggling of Vpx/Vpr specificity results in divergent recognition of the restriction factor SAMHD1. *PLoS Pathog*, 9, e1003496.
- GALLO, R. C., SARIN, P. S., GELMANN, E. P., ROBERT-GUROFF, M., RICHARDSON, E., KALYANARAMAN, V. S., MANN, D., SIDHU, G. D., STAHL, R. E., ZOLLA-PAZNER, S., LEIBOWITZ, J. & POPOVIC, M. 1983. Isolation of human T-cell leukemia virus in acquired immune deficiency syndrome (AIDS). *Science*, 220, 865-7.
- GAMIS, A. S., ALONZO, T. A., MESHINCHI, S., SUNG, L., GERBING, R. B., RAIMONDI, S. C., HIRSCH, B. A., KAHWASH, S. B., HEEREMA-MCKENNEY, A., WINTER, L., GLICK, K., DAVIES, S. M., BYRON, P., SMITH, F. O. & APLENC, R. 2014. Gemtuzumab ozogamicin in children and adolescents with de novo acute myeloid leukemia improves event-free survival by reducing relapse risk: results from the randomized phase III Children's Oncology Group trial AAML0531. *J Clin Oncol*, 32, 3021-32.
- GANSER-PORNILLOS, B. K., YEAGER, M. & SUNDQUIST, W. I. 2008. The structural biology of HIV assembly. *Curr Opin Struct Biol*, 18, 203-17.
- GOILA-GAUR, R. & STREBEL, K. 2008. HIV-1 Vif, APOBEC, and intrinsic immunity. *Retrovirology*, 5, 51.
- GOLDSTONE, D. C., ENNIS-ADENIRAN, V., HEDDEN, J. J., GROOM, H. C. T., RICE, G. I., CHRISTODOULOU, E., WALKER, P. A., KELLY, G., HAIRE, L. F., YAP, M. W., DE CARVALHO, L. P. S., STOYE, J. P., CROW, Y. J., TAYLOR, I. A. & WEBB, M.

2011. HIV-1 restriction factor SAMHD1 is a deoxynucleoside triphosphate triphosphohydrolase. *Nature*, 480, 379-382.
- GONCALVES, A., KARAYEL, E., RICE, G. I., BENNETT, K. L., CROW, Y. J., SUPERTIFURGA, G. & BURCKSTUMMER, T. 2012a. SAMHD1 is a nucleic-acid binding protein that is mislocalized due to aicardi-goutieres syndrome-associated mutations. *Human mutation*.
- GONCALVES, A., KARAYEL, E., RICE, G. I., BENNETT, K. L., CROW, Y. J., SUPERTIFURGA, G. & BURCKSTUMMER, T. 2012b. SAMHD1 is a nucleic-acid binding protein that is mislocalized due to aicardi-goutieres syndrome-associated mutations. *Hum Mutat*, 33, 1116-22.
- GOUJON, C., ARFI, V., PERTEL, T., LUBAN, J., LIENARD, J., RIGAL, D., DARLIX, J. L. & CIMARELLI, A. 2008. Characterization of simian immunodeficiency virus SIVSM/human immunodeficiency virus type 2 Vpx function in human myeloid cells. *J Virol*, 82, 12335-45.
- GOUJON, C., JARROSSON-WUILLEME, L., BERNAUD, J., RIGAL, D., DARLIX, J. L. & CIMARELLI, A. 2006. With a little help from a friend: increasing HIV transduction of monocyte-derived dendritic cells with virion-like particles of SIV(MAC). *Gene Ther*, 13, 991-4.
- GOUJON, C., MONCORGE, O., BAUBY, H., DOYLE, T., WARD, C. C., SCHALLER, T., HUE, S., BARCLAY, W. S., SCHULZ, R. & MALIM, M. H. 2013a. Human MX2 is an interferon-induced post-entry inhibitor of HIV-1 infection. *Nature*, 502, 559-62.
- GOUJON, C., RIVIERE, L., JARROSSON-WUILLEME, L., BERNAUD, J., RIGAL, D., DARLIX, J. L. & CIMARELLI, A. 2007. SIVSM/HIV-2 Vpx proteins promote retroviral escape from a proteasome-dependent restriction pathway present in human dendritic cells. *Retrovirology*, 4, 2.
- GOUJON, C., SCHALLER, T., GALAO, R. P., AMIE, S. M., KIM, B., OLIVIERI, K., NEIL, S. J. & MALIM, M. H. 2013b. Evidence for IFN $\alpha$ -induced, SAMHD1-independent inhibitors of early HIV-1 infection. *Retrovirology*, 10, 23.
- GOUJON, C., SCHALLER, T., GALÃO, R. P., AMIE, S. M., KIM, B., OLIVIERI, K., NEIL, S. J. D. & MALIM, M. H. 2013c. Evidence for IFN $\alpha$ -induced, SAMHD1-independent inhibitors of early HIV-1 infection. *Retrovirology*, 10, 23.
- GRAMBERG, T., SUNSERI, N. & LANDAU, N. R. 2010. Evidence for an activation domain at the amino terminus of simian immunodeficiency virus Vpx. *J Virol*, 84, 1387-96.
- GUIEZE, R., ROBBE, P., CLIFFORD, R., DE GUIBERT, S., PEREIRA, B., TIMBS, A., DILHUYDY, M. S., CABES, M., YSEBAERT, L., BURNS, A., NGUYEN-KHAC, F., DAVI, F., VERONESE, L., COMBES, P., LE GARFF-TAVERNIER, M., LEBLOND, V., MERLE-BERAL, H., ALSOLAMI, R., HAMBLIN, A., MASON, J., PETTITT, A., HILLMEN, P., TAYLOR, J., KNIGHT, S. J., TOURNILHAC, O. & SCHUH, A. 2015. Presence of multiple recurrent mutations confers poor trial outcome of relapsed/refractory CLL. *Blood*, 126, 2110-7.
- GUO, H., WEI, W., WEI, Z., LIU, X., EVANS, S. L., YANG, W., WANG, H., GUO, Y., ZHAO, K., ZHOU, J. Y. & YU, X. F. 2013. Identification of critical regions in human SAMHD1 required for nuclear localization and Vpx-mediated degradation. *PLoS One*, 8, e66201.
- GUPTA, R. K., ABDUL-JAWAD, S., MCCOY, L. E., MOK, H. P., PEPPA, D., SALGADO, M., MARTINEZ-PICADO, J., NIJHUIS, M., WENSING, A. M. J., LEE, H., GRANT, P., NASTOULI, E., LAMBERT, J., PACE, M., SALASC, F., MONIT, C., INNES, A. J., MUIR, L., WATERS, L., FRATER, J., LEVER, A. M. L., EDWARDS, S. G., GABRIEL, I. H. & OLAVARRIA, E. 2019. HIV-1 remission following CCR5 $\Delta$ 32/ $\Delta$ 32 haematopoietic stem-cell transplantation. *Nature*, 568, 244-248.

- HARRIS, R. S., BISHOP, K. N., SHEEHY, A. M., CRAIG, H. M., PETERSEN-MAHRT, S. K., WATT, I. N., NEUBERGER, M. S. & MALIM, M. H. 2003. DNA deamination mediates innate immunity to retroviral infection. *Cell*, 113, 803-9.
- HATAKEYAMA, S. 2017. TRIM Family Proteins: Roles in Autophagy, Immunity, and Carcinogenesis. *Trends Biochem Sci*, 42, 297-311.
- HATZIOANNOU, T., PEREZ-CABALLERO, D., YANG, A., COWAN, S. & BIENIASZ, P. D. 2004. Retrovirus resistance factors Ref1 and Lv1 are species-specific variants of TRIM5alpha. *Proc Natl Acad Sci U S A*, 101, 10774-9.
- HEINEMANN, V. & JEHN, U. 1990. Rationales for a pharmacologically optimized treatment of acute nonlymphocytic leukemia with cytosine arabinoside. *Leukemia*, 4, 790-6.
- HEMELAAR, J. 2012. The origin and diversity of the HIV-1 pandemic. *Trends Mol Med*, 18, 182-92.
- HENDERSON, L. E., SOWDER, R. C., COPELAND, T. D., BENVENISTE, R. E. & OROSZLAN, S. 1988. Isolation and characterization of a novel protein (X-ORF product) from SIV and HIV-2. *Science*, 241, 199-201.
- HENDRIKS, I. A., LYON, D., YOUNG, C., JENSEN, L. J., VERTEGAAL, A. C. & NIELSEN, M. L. 2017. Site-specific mapping of the human SUMO proteome reveals co-modification with phosphorylation. *Nat Struct Mol Biol*, 24, 325-336.
- HEROLD, N., ANDERS-OSSWEIN, M., GLASS, B., ECKHARDT, M., MULLER, B. & KRAUSSLICH, H. G. 2014. HIV-1 entry in SupT1-R5, CEM-ss, and primary CD4+ T cells occurs at the plasma membrane and does not require endocytosis. *J Virol*, 88, 13956-70.
- HEROLD, N., RUDD, S. G., LJUNGBLAD, L., SANJIV, K., MYRBERG, I. H., PAULIN, C. B., HESHMATI, Y., HAGENKORT, A., KUTZNER, J., PAGE, B. D., CALDERON-MONTANO, J. M., LOSEVA, O., JEMTH, A. S., BULLI, L., AXELSSON, H., TESI, B., VALERIE, N. C., HOGLUND, A., BLADH, J., WIITA, E., SUNDIN, M., UHLIN, M., RASSIDAKIS, G., HEYMAN, M., TAMM, K. P., WARPMAN-BERGLUND, U., WALFRIDSSON, J., LEHMANN, S., GRANDER, D., LUNDBACK, T., KOGNER, P., HENTER, J. I., HELLEDAY, T. & SCHALLER, T. 2017a. Targeting SAMHD1 with the Vpx protein to improve cytarabine therapy for hematological malignancies. *Nat Med*, 23, 256-263.
- HEROLD, N., RUDD, S. G., SANJIV, K., KUTZNER, J., BLADH, J., PAULIN, C. B. J., HELLEDAY, T., HENTER, J. I. & SCHALLER, T. 2017b. SAMHD1 protects cancer cells from various nucleoside-based antimetabolites. *Cell Cycle*, 16, 1029-38.
- HEROLD, N., RUDD, S. G., SANJIV, K., KUTZNER, J., MYRBERG, I. H., PAULIN, C. B. J., OLSEN, T. K., HELLEDAY, T., HENTER, J. I. & SCHALLER, T. 2017c. With me or against me: Tumor suppressor and drug resistance activities of SAMHD1. *Exp Hematol*, 52, 32-39.
- HIDDEMANN, W., SCHLEYER, E., UNTERHALT, M., KERN, W. & BUCHNER, T. 1996. Optimizing therapy for acute myeloid leukemia based on differences in intracellular metabolism of cytosine arabinoside between leukemic blasts and normal mononuclear blood cells. *Ther Drug Monit*, 18, 341-9.
- HO, D. D., HARTSHORN, K. L., ROTA, T. R., ANDREWS, C. A., KAPLAN, J. C., SCHOOLEY, R. T. & HIRSCH, M. S. 1985. Recombinant human interferon alfa-A suppresses HTLV-III replication in vitro. *Lancet*, 1, 602-4.
- HO, D. D., NEUMANN, A. U., PERELSON, A. S., CHEN, W., LEONARD, J. M. & MARKOWITZ, M. 1995. Rapid turnover of plasma virions and CD4 lymphocytes in HIV-1 infection. *Nature*, 373, 123-126.
- HO, Y. C., SHAN, L., HOSMANE, N. N., WANG, J., LASKEY, S. B., ROSENBLOOM, D. I., LAI, J., BLANKSON, J. N., SILICIANO, J. D. & SILICIANO, R. F. 2013.

- Replication-competent noninduced proviruses in the latent reservoir increase barrier to HIV-1 cure. *Cell*, 155, 540-51.
- HOFER, A., CRONA, M., LOGAN, D. T. & SJOBERG, B. M. 2012. DNA building blocks: keeping control of manufacture. *Crit Rev Biochem Mol Biol*, 47, 50-63.
- HOFMANN, H., LOGUE, E. C., BLOCH, N., DADDACHA, W., POLSKY, S. B., SCHULTZ, M. L., KIM, B. & LANDAU, N. R. 2012. The Vpx lentiviral accessory protein targets SAMHD1 for degradation in the nucleus. *J Virol*, 86, 12552-60.
- HOFMANN, H., NORTON, T. D., SCHULTZ, M. L., POLSKY, S. B., SUNSERI, N. & LANDAU, N. R. 2013. Inhibition of CUL4A Neddylation causes a reversible block to SAMHD1-mediated restriction of HIV-1. *J Virol*, 87, 11741-50.
- HOLLENBAUGH, J. A., SHELTON, J., TAO, S., AMIRALAEI, S., LIU, P., LU, X., GOETZE, R. W., ZHOU, L., NETTLES, J. H., SCHINAZI, R. F. & KIM, B. 2017. Substrates and Inhibitors of SAMHD1. *PLoS One*, 12, e0169052.
- HRECKA, K., GIERSZEWSKA, M., SRIVASTAVA, S., KOZACZKIEWICZ, L., SWANSON, S. K., FLORENS, L., WASHBURN, M. P. & SKOWRONSKI, J. 2007. Lentiviral Vpr usurps Cul4-DDB1[VprBP] E3 ubiquitin ligase to modulate cell cycle. *Proc Natl Acad Sci U S A*, 104, 11778-83.
- HRECKA, K., HAO, C., GIERSZEWSKA, M., SWANSON, S. K., KESIK-BRODACKA, M., SRIVASTAVA, S., FLORENS, L., WASHBURN, M. P. & SKOWRONSKI, J. 2011. Vpx relieves inhibition of HIV-1 infection of macrophages mediated by the SAMHD1 protein. *Nature*, 474, 658-661.
- HUNSUCKER, S. A., MITCHELL, B. S. & SPYCHALA, J. 2005. The 5'-nucleotidases as regulators of nucleotide and drug metabolism. *Pharmacol Ther*, 107, 1-30.
- HURWITZ, S. J. & SCHINAZI, R. F. 2013. Prodrug strategies for improved efficacy of nucleoside antiviral inhibitors. *Curr Opin HIV AIDS*, 8, 556-64.
- HUTTER, G., NOWAK, D., MOSSNER, M., GANEPOLA, S., MUSSIG, A., ALLERS, K., SCHNEIDER, T., HOFMANN, J., KUCHERER, C., BLAU, O., BLAU, I. W., HOFMANN, W. K. & THIEL, E. 2009. Long-term control of HIV by CCR5 Delta32/Delta32 stem-cell transplantation. *N Engl J Med*, 360, 692-8.
- JEANG, K. T., XIAO, H. & RICH, E. A. 1999. Multifaceted activities of the HIV-1 transactivator of transcription, Tat. *J Biol Chem*, 274, 28837-40.
- JI, X., TANG, C., ZHAO, Q., WANG, W. & XIONG, Y. 2014. Structural basis of cellular dNTP regulation by SAMHD1. *Proc Natl Acad Sci U S A*, 111, E4305-14.
- JI, X., WU, Y., YAN, J., MEHRENS, J., YANG, H., DELUCIA, M., HAO, C., GRONENBORN, A. M., SKOWRONSKI, J., AHN, J. & XIONG, Y. 2013. Mechanism of allosteric activation of SAMHD1 by dGTP. *Nat Struct Mol Biol*, 20, 1304-9.
- JIANG, D., WEIDNER, J. M., QING, M., PAN, X. B., GUO, H., XU, C., ZHANG, X., BIRK, A., CHANG, J., SHI, P. Y., BLOCK, T. M. & GUO, J. T. 2010. Identification of five interferon-induced cellular proteins that inhibit west nile virus and dengue virus infections. *J Virol*, 84, 8332-41.
- JIMENEZ-GUARDENO, J. M., APOLONIA, L., BETANCOR, G. & MALIM, M. H. 2019. Immunoproteasome activation enables human TRIM5alpha restriction of HIV-1. *Nat Microbiol*, 4, 933-940.
- JOHANSSON, K., RAMASWAMY, S., LJUNGCRANTZ, C., KNECHT, W., PISKUR, J., MUNCH-PETERSEN, B., ERIKSSON, S. & EKLUND, H. 2001. Structural basis for substrate specificities of cellular deoxyribonucleoside kinases. *Nat Struct Biol*, 8, 616-20.
- JOHANSSON, P., KLEIN-HITPASS, L., CHOIDAS, A., HABENBERGER, P., MAHBOUBI, B., KIM, B., BERGMANN, A., SCHOLTYSIK, R., BRAUSER, M., LOLLIES, A., SIEBERT, R., ZENZ, T., DÜHRSEN, U., KÜPPERS, R. & DÜRIG, J. 2018. SAMHD1 is recurrently mutated in T-cell prolymphocytic leukemia. *Blood Cancer J*, 8, 11.

- KAO, S. Y., CALMAN, A. F., LUCIW, P. A. & PETERLIN, B. M. 1987. Anti-termination of transcription within the long terminal repeat of HIV-1 by tat gene product. *Nature*, 330, 489-93.
- KAPPEL, J. C., MORROW, C. D., LEE, S. W., JAMESON, B. A., KENT, S. B., HOOD, L. E., SHAW, G. M. & HAHN, B. H. 1988. Identification of a novel retroviral gene unique to human immunodeficiency virus type 2 and simian immunodeficiency virus SIVMAC. *J Virol*, 62, 3501-5.
- KAUSHIK, R., ZHU, X., STRANSKA, R., WU, Y. & STEVENSON, M. 2009. A cellular restriction dictates the permissivity of nondividing monocytes/macrophages to lentivirus and gammaretrovirus infection. *Cell Host Microbe*, 6, 68-80.
- KECKESOVA, Z., YLINEN, L. M. & TOWERS, G. J. 2004. The human and African green monkey TRIM5 $\alpha$  genes encode Ref1 and Lv1 retroviral restriction factor activities. *Proc Natl Acad Sci U S A*, 101, 10780-5.
- KECKESOVA, Z., YLINEN, L. M. & TOWERS, G. J. 2006. Cyclophilin A renders human immunodeficiency virus type 1 sensitive to Old World monkey but not human TRIM5 $\alpha$  antiviral activity. *J Virol*, 80, 4683-90.
- KENNEDY, E. M., GAVEGNANO, C., NGUYEN, L., SLATER, R., LUCAS, A., FROMENTIN, E., SCHINAZI, R. F. & KIM, B. 2010. Ribonucleoside triphosphates as substrate of human immunodeficiency virus type 1 reverse transcriptase in human macrophages. *J Biol Chem*, 285, 39380-91.
- KESSEL, D., HALL, T. C. & ROSENTHAL, D. 1969. Uptake and phosphorylation of cytosine arabinoside by normal and leukemic human blood cells in vitro. *Cancer Res*, 29, 459-63.
- KIENLE, E., SENIS, E., BORNER, K., NIOPEK, D., WIEDTKE, E., GROSSE, S. & GRIMM, D. 2012. Engineering and evolution of synthetic adeno-associated virus (AAV) gene therapy vectors via DNA family shuffling. *J Vis Exp*.
- KIM, C. A. & BOWIE, J. U. 2003. SAM domains: uniform structure, diversity of function. *Trends Biochem Sci*, 28, 625-8.
- KODIGEPALLI, K. M., LI, M., LIU, S. L. & WU, L. 2017. Exogenous expression of SAMHD1 inhibits proliferation and induces apoptosis in cutaneous T-cell lymphoma-derived HuT78 cells. *Cell Cycle*, 16, 179-188.
- KOHARUDIN, L. M., WU, Y., DELUCIA, M., MEHRENS, J., GRONENBORN, A. M. & AHN, J. 2014a. Structural basis of allosteric activation of sterile  $\alpha$  motif and histidine-aspartate domain-containing protein 1 (SAMHD1) by nucleoside triphosphates. *J Biol Chem*, 289, 32617-27.
- KOHARUDIN, L. M., WU, Y., DELUCIA, M., MEHRENS, J., GRONENBORN, A. M. & AHN, J. 2014b. Structural basis of allosteric activation of sterile  $\alpha$  motif and histidine-aspartate domain-containing protein 1 (SAMHD1) by nucleoside triphosphates. *J Biol Chem*, 289, 32617-27.
- KOHL, N. E., EMINI, E. A., SCHLEIF, W. A., DAVIS, L. J., HEIMBACH, J. C., DIXON, R. A., SCOLNICK, E. M. & SIGAL, I. S. 1988. Active human immunodeficiency virus protease is required for viral infectivity. *Proc Natl Acad Sci U S A*, 85, 4686-90.
- KOHNKEN, R., KODIGEPALLI, K. M., MISHRA, A., PORCU, P. & WU, L. 2017. MicroRNA-181 contributes to downregulation of SAMHD1 expression in CD4 $^{+}$  T-cells derived from Sezary syndrome patients. *Leuk Res*, 52, 58-66.
- KOHNKEN, R., KODIGEPALLI, K. M. & WU, L. 2015. Regulation of deoxynucleotide metabolism in cancer: novel mechanisms and therapeutic implications. *Mol Cancer*, 14, 176.
- KORIN, Y. D. & ZACK, J. A. 1999. Nonproductive human immunodeficiency virus type 1 infection in nucleoside-treated G0 lymphocytes. *J Virol*, 73, 6526-32.

- KRETSCHMER, S., WOLF, C., KONIG, N., STAROSKE, W., GUCK, J., HAUSLER, M., LUKSCH, H., NGUYEN, L. A., KIM, B., ALEXOPOULOU, D., DAHL, A., RAPP, A., CARDOSO, M. C., SHEVCHENKO, A. & LEE-KIRSCH, M. A. 2015. SAMHD1 prevents autoimmunity by maintaining genome stability. *Ann Rheum Dis*, 74, e17.
- KUFE, D., SPRIGGS, D., EGAN, E. M. & MUNROE, D. 1984. Relationships among Ara-CTP pools, formation of (Ara-C)DNA, and cytotoxicity of human leukemic cells. *Blood*, 64, 54-8.
- KUMAR, D., ABDULOVIC, A. L., VIBERG, J., NILSSON, A. K., KUNKEL, T. A. & CHABES, A. 2011. Mechanisms of mutagenesis in vivo due to imbalanced dNTP pools. *Nucleic Acids Res*, 39, 1360-71.
- KUMAR, D., VIBERG, J., NILSSON, A. K. & CHABES, A. 2010. Highly mutagenic and severely imbalanced dNTP pools can escape detection by the S-phase checkpoint. *Nucleic Acids Res*, 38, 3975-83.
- LAGUETTE, N., RAHM, N., SOBHIAN, B., CHABLE-BESSIA, C., MÜNCH, J., SNOECK, J., SAUTER, D., SWITZER, W. M., HENEINE, W., KIRCHHOFF, F., DELSUC, F., TELENTI, A. & BENKIRANE, M. 2012. Evolutionary and functional analyses of the interaction between the myeloid restriction factor SAMHD1 and the lentiviral Vpx protein. *Cell Host Microbe*, 11, 205-17.
- LAGUETTE, N., SOBHIAN, B., CASARTELLI, N., RINGEARD, M., CHABLE-BESSIA, C., SEGERAL, E., YATIM, A., EMILIANI, S., SCHWARTZ, O. & BENKIRANE, M. 2011a. SAMHD1 is the dendritic- and myeloid-cell-specific HIV-1 restriction factor counteracted by Vpx. *Nature*, 474, 654-657.
- LAGUETTE, N., SOBHIAN, B., CASARTELLI, N., RINGEARD, M., CHABLE-BESSIA, C., SEGERAL, E., YATIM, A., EMILIANI, S., SCHWARTZ, O. & BENKIRANE, M. 2011b. SAMHD1 is the dendritic- and myeloid-cell-specific HIV-1 restriction factor counteracted by Vpx. *Nature*, 474, 654-7.
- LAHOUESSA, H., DADDACHA, W., HOFMANN, H., AYINDE, D., LOGUE, E. C., DRAGIN, L., BLOCH, N., MAUDET, C., BERTRAND, M., GRAMBERG, T., PANCINO, G., PRIET, S., CANARD, B., LAGUETTE, N., BENKIRANE, M., TRANSY, C., LANDAU, N. R., KIM, B. & MARGOTTIN-GOGUET, F. 2012. SAMHD1 restricts the replication of human immunodeficiency virus type 1 by depleting the intracellular pool of deoxynucleoside triphosphates. *Nature Immunology*, 13, 223.
- LAMOLIATTE, F., CARON, D., DURETTE, C., MAHROUCHE, L., MAROUI, M. A., CARON-LIZOTTE, O., BONNEIL, E., CHELBI-ALIX, M. K. & THIBAUT, P. 2014. Large-scale analysis of lysine SUMOylation by SUMO remnant immunoaffinity profiling. *Nat Commun*, 5, 5409.
- LANDAU, D. A., CARTER, S. L., STOJANOV, P., MCKENNA, A., STEVENSON, K., LAWRENCE, M. S., SOUGNEZ, C., STEWART, C., SIVACHENKO, A., WANG, L., WAN, Y., ZHANG, W., SHUKLA, S. A., VARTANOV, A., FERNANDES, S. M., SAKSENA, G., CIBULSKIS, K., TESAR, B., GABRIEL, S., HACOEN, N., MEYERSON, M., LANDER, E. S., NEUBERG, D., BROWN, J. R., GETZ, G. & WU, C. J. 2013. Evolution and impact of subclonal mutations in chronic lymphocytic leukemia. *Cell*, 152, 714-26.
- LANE, A. N. & FAN, T. W. 2015. Regulation of mammalian nucleotide metabolism and biosynthesis. *Nucleic Acids Res*, 43, 2466-85.
- LE ROUZIC, E., BELAIDOUNI, N., ESTRABAUD, E., MOREL, M., RAIN, J. C., TRANSY, C. & MARGOTTIN-GOGUET, F. 2007. HIV1 Vpr arrests the cell cycle by recruiting DCAF1/VprBP, a receptor of the Cul4-DDB1 ubiquitin ligase. *Cell Cycle*, 6, 182-8.
- LEE, E. J., SEO, J. H., PARK, J. H., VO, T. T. L., AN, S., BAE, S. J., LE, H., LEE, H. S., WEE, H. J., LEE, D., CHUNG, Y. H., KIM, J. A., JANG, M. K., RYU, S. H., YU, E.,

- JANG, S. H., PARK, Z. Y. & KIM, K. W. 2017. SAMHD1 acetylation enhances its deoxynucleotide triphosphohydrolase activity and promotes cancer cell proliferation. *Oncotarget*, 8, 68517-68529.
- LEVY, D. N., ALDROVANDI, G. M., KUTSCH, O. & SHAW, G. M. 2004. Dynamics of HIV-1 recombination in its natural target cells. *Proc Natl Acad Sci U S A*, 101, 4204-9.
- LI, G., CHENG, M., NUNOYA, J., CHENG, L., GUO, H., YU, H., LIU, Y. J., SU, L. & ZHANG, L. 2014. Plasmacytoid dendritic cells suppress HIV-1 replication but contribute to HIV-1 induced immunopathogenesis in humanized mice. *PLoS Pathog*, 10, e1004291.
- LI, L., OLVERA, J. M., YODER, K. E., MITCHELL, R. S., BUTLER, S. L., LIEBER, M., MARTIN, S. L. & BUSHMAN, F. D. 2001. Role of the non-homologous DNA end joining pathway in the early steps of retroviral infection. *Embo j*, 20, 3272-81.
- LI, N., ZHANG, W. & CAO, X. 2000. Identification of human homologue of mouse IFN-gamma induced protein from human dendritic cells. *Immunol Lett*, 74, 221-4.
- LIAO, W., BAO, Z., CHENG, C., MOK, Y. K. & WONG, W. S. 2008. Dendritic cell-derived interferon-gamma-induced protein mediates tumor necrosis factor-alpha stimulation of human lung fibroblasts. *Proteomics*, 8, 2640-50.
- LIM, E. S., FREGOSO, O. I., MCCOY, C. O., MATSEN, F. A., MALIK, H. S. & EMERMAN, M. 2012. The ability of primate lentiviruses to degrade the monocyte restriction factor SAMHD1 preceded the birth of the viral accessory protein Vpx. *Cell Host Microbe*, 11, 194-204.
- LU, J., PAN, Q., RONG, L., HE, W., LIU, S. L. & LIANG, C. 2011. The IFITM proteins inhibit HIV-1 infection. *J Virol*, 85, 2126-37.
- LUMPKIN, R. J., GU, H., ZHU, Y., LEONARD, M., AHMAD, A. S., CLAUSER, K. R., MEYER, J. G., BENNETT, E. J. & KOMIVES, E. A. 2017. Site-specific identification and quantitation of endogenous SUMO modifications under native conditions. *Nat Commun*, 8, 1171.
- LUSIC, M. & SILICIANO, R. F. 2017. Nuclear landscape of HIV-1 infection and integration. *Nat Rev Microbiol*, 15, 69-82.
- MAHALINGAM, S., VAN TINE, B., SANTIAGO, M. L., GAO, F., SHAW, G. M. & HAHN, B. H. 2001. Functional analysis of the simian immunodeficiency virus Vpx protein: identification of packaging determinants and a novel nuclear targeting domain. *J Virol*, 75, 362-74.
- MAHIEUX, R., SUSPENE, R., DELEBECQUE, F., HENRY, M., SCHWARTZ, O., WAIN-HOBSON, S. & VARTANIAN, J. P. 2005. Extensive editing of a small fraction of human T-cell leukemia virus type 1 genomes by four APOBEC3 cytidine deaminases. *J Gen Virol*, 86, 2489-94.
- MAILLOT, B., LEVY, N., EILER, S., CRUCIFIX, C., GRANGER, F., RICHERT, L., DIDIER, P., GODET, J., PRADEAU-AUBRETON, K., EMILIANI, S., NAZABAL, A., LESBATS, P., PARISSI, V., MELY, Y., MORAS, D., SCHULTZ, P. & RUFF, M. 2013. Structural and functional role of INI1 and LEDGF in the HIV-1 pre-integration complex. *PLoS One*, 8, e60734.
- MAJER, C., SCHUSSLER, J. M. & KONIG, R. 2019. Intertwined: SAMHD1 cellular functions, restriction, and viral evasion strategies. *Med Microbiol Immunol*.
- MALIM, M. H. 2006. Natural resistance to HIV infection: The Vif-APOBEC interaction. *C R Biol*, 329, 871-5.
- MALIM, M. H. & BIENIASZ, P. D. 2012. HIV Restriction Factors and Mechanisms of Evasion. *Cold Spring Harb Perspect Med*, 2.
- MAMCARZ, E., ZHOU, S., LOCKEY, T., ABDELSAMED, H., CROSS, S. J., KANG, G., MA, Z., CONDORI, J., DOWDY, J., TRIPLETT, B., LI, C., MARON, G., ALDAVE BECERRA, J. C., CHURCH, J. A., DOKMECI, E., LOVE, J. T., DA MATTA AIN, A.

- C., VAN DER WATT, H., TANG, X., JANSSEN, W., RYU, B. Y., DE RAVIN, S. S., WEISS, M. J., YOUNGBLOOD, B., LONG-BOYLE, J. R., GOTTSCHALK, S., MEAGHER, M. M., MALECH, H. L., PUCK, J. M., COWAN, M. J. & SORRENTINO, B. P. 2019. Lentiviral Gene Therapy Combined with Low-Dose Busulfan in Infants with SCID-X1. *N Engl J Med*, 380, 1525-1534.
- MANEL, N., HOGSTAD, B., WANG, Y., LEVY, D. E., UNUTMAZ, D. & LITTMAN, D. R. 2010. A cryptic sensor for HIV-1 activates antiviral innate immunity in dendritic cells. *Nature*, 467, 214-7.
- MANGEAT, B., TURELLI, P., CARON, G., FRIEDLI, M., PERRIN, L. & TRONO, D. 2003. Broad antiretroviral defence by human APOBEC3G through lethal editing of nascent reverse transcripts. *Nature*, 424, 99-103.
- MANGEOT, P. E., DUPERRIER, K., NEGRE, D., BOSON, B., RIGAL, D., COSSET, F. L. & DARLIX, J. L. 2002. High levels of transduction of human dendritic cells with optimized SIV vectors. *Mol Ther*, 5, 283-90.
- MANGEOT, P. E., NEGRE, D., DUBOIS, B., WINTER, A. J., LEISSNER, P., MEHTALI, M., KAISERLIAN, D., COSSET, F. L. & DARLIX, J. L. 2000. Development of minimal lentivirus vectors derived from simian immunodeficiency virus (SIVmac251) and their use for gene transfer into human dendritic cells. *J Virol*, 74, 8307-15.
- MANSILLA-SOTO, J., RIVIERE, I., BOULAD, F. & SADELAIN, M. 2016. Cell and Gene Therapy for the Beta-Thalassemias: Advances and Prospects. *Hum Gene Ther*, 27, 295-304.
- MATHEWS, C. K. 2006. DNA precursor metabolism and genomic stability. *Faseb j*, 20, 1300-14.
- MAUNEY, C. H. & HOLLIS, T. 2018. SAMHD1: Recurring roles in cell cycle, viral restriction, cancer, and innate immunity. *Autoimmunity*, 51, 96-110.
- MAUNEY, C. H., ROGERS, L. C., HARRIS, R. S., DANIEL, L. W., DEVARIE-BAEZ, N. O., WU, H., FURDUI, C. M., POOLE, L. B., PERRINO, F. W. & HOLLIS, T. 2017. The SAMHD1 dNTP Triphosphohydrolase Is Controlled by a Redox Switch. *Antioxid Redox Signal*.
- MERATI, M., BUETHE, D. J., COOPER, K. D., HONDA, K. S., WANG, H. & GERSTENBLITH, M. R. 2015. Aggressive CD8(+) epidermotropic cutaneous T-cell lymphoma associated with homozygous mutation in SAMHD1. *JAAD Case Rep*, 1, 227-9.
- MEUTH, M. 1989. The molecular basis of mutations induced by deoxyribonucleoside triphosphate pool imbalances in mammalian cells. *Exp Cell Res*, 181, 305-16.
- MIAZZI, C., FERRARO, P., PONTARIN, G., RAMPAZZO, C., REICHARD, P. & BIANCHI, V. 2014. Allosteric regulation of the human and mouse deoxyribonucleotide triphosphohydrolase sterile alpha-motif/histidine-aspartate domain-containing protein 1 (SAMHD1). *J Biol Chem*, 289, 18339-46.
- MILDVAN, D., BASSIAKOS, Y., ZUCKER, M. L., HYSLOP, N., JR., KROWN, S. E., SACKS, H. S., ZACHARY, J., PAREDES, J., FESSEL, W. J., RHAME, F., KRAMER, F., FISCHL, M. A., POIESZ, B., WOOD, K., RUPRECHT, R. M., KIM, J., GROSSBERG, S. E., KASDAN, P., BERGE, P., MARSHAK, A. & PETTINELLI, C. 1996. Synergy, activity and tolerability of zidovudine and interferon-alpha in patients with symptomatic HIV-1 infection: AIDS Clinical Trial Group 068. *Antivir Ther*, 1, 77-88.
- MIYAKAWA, K., RYO, A., MURAKAMI, T., OHBA, K., YAMAOKA, S., FUKUDA, M., GUATELLI, J. & YAMAMOTO, N. 2009. BCA2/Rabring7 promotes tetherin-dependent HIV-1 restriction. *PLoS Pathog*, 5, e1000700.
- MORRELL, N. T., LEUCHT, P., ZHAO, L., KIM, J. B., TEN BERGE, D., PONNUSAMY, K., CARRE, A. L., DUDEK, H., ZACHLEDEROVA, M., MCELHANEY, M.,



- BRUNTON, S., GUNZNER, J., CALLOW, M., POLAKIS, P., COSTA, M., ZHANG, X. M., HELMS, J. A. & NUSSE, R. 2008. Liposomal packaging generates Wnt protein with in vivo biological activity. *PLoS One*, 3, e2930.
- NEGRE, D., MANGEOT, P. E., DUISIT, G., BLANCHARD, S., VIDALAIN, P. O., LEISSNER, P., WINTER, A. J., RABOURDIN-COMBE, C., MEHTALI, M., MOULLIER, P., DARLIX, J. L. & COSSET, F. L. 2000. Characterization of novel safe lentiviral vectors derived from simian immunodeficiency virus (SIVmac251) that efficiently transduce mature human dendritic cells. *Gene Ther*, 7, 1613-23.
- NEIL, S. J., ZANG, T. & BIENIASZ, P. D. 2008. Tetherin inhibits retrovirus release and is antagonized by HIV-1 Vpu. *Nature*, 451, 425-30.
- NEWMAN, R. M., HALL, L., KIRMAIER, A., POZZI, L. A., PERY, E., FARZAN, M., O'NEIL, S. P. & JOHNSON, W. 2008. Evolution of a TRIM5-CypA splice isoform in old world monkeys. *PLoS Pathog*, 4, e1000003.
- NISOLE, S., STOYE, J. P. & SAIB, A. 2005. TRIM family proteins: retroviral restriction and antiviral defence. *Nat Rev Microbiol*, 3, 799-808.
- NYAMWEYA, S., HEGEDUS, A., JAYE, A., ROWLAND-JONES, S., FLANAGAN, K. L. & MACALLAN, D. C. 2013. Comparing HIV-1 and HIV-2 infection: Lessons for viral immunopathogenesis. *Rev Med Virol*, 23, 221-40.
- ONO, A., ABLAN, S. D., LOCKETT, S. J., NAGASHIMA, K. & FREED, E. O. 2004. Phosphatidylinositol (4,5) biphosphate regulates HIV-1 Gag targeting to the plasma membrane. *Proc Natl Acad Sci U S A*, 101, 14889-94.
- OSSENKOPPELE, G. & LOWENBERG, B. 2015. How I treat the older patient with acute myeloid leukemia. *Blood*, 125, 767-74.
- OZATO, K., SHIN, D. M., CHANG, T. H. & MORSE, H. C., 3RD 2008. TRIM family proteins and their emerging roles in innate immunity. *Nat Rev Immunol*, 8, 849-60.
- PARKER, W. B. 2009. Enzymology of purine and pyrimidine antimetabolites used in the treatment of cancer. *Chem Rev*, 109, 2880-93.
- PENG, C., HO, B. K., CHANG, T. W. & CHANG, N. T. 1989. Role of human immunodeficiency virus type 1-specific protease in core protein maturation and viral infectivity. *J Virol*, 63, 2550-6.
- PEREZ-CABALLERO, D., ZANG, T., EBRAHIMI, A., MCNATT, M. W., GREGORY, D. A., JOHNSON, M. C. & BIENIASZ, P. D. 2009. Tetherin inhibits HIV-1 release by directly tethering virions to cells. *Cell*, 139, 499-511.
- PERTEL, T., REINHARD, C. & LUBAN, J. 2011. Vpx rescues HIV-1 transduction of dendritic cells from the antiviral state established by type 1 interferon. *Retrovirology*, 8, 49.
- POLLPETER, D., PARSONS, M., SOBALA, A. E., COXHEAD, S., LANG, R. D., BRUNS, A. M., PAPAIOANNOU, S., MCDONNELL, J. M., APOLONIA, L., CHOWDHURY, J. A., HORVATH, C. M. & MALIM, M. H. 2018. Deep sequencing of HIV-1 reverse transcripts reveals the multifaceted antiviral functions of APOBEC3G. *Nat Microbiol*, 3, 220-233.
- POWELL, R. D., HOLLAND, P. J., HOLLIS, T. & PERRINO, F. W. 2011. Aicardi-Goutieres syndrome gene and HIV-1 restriction factor SAMHD1 is a dGTP-regulated deoxynucleotide triphosphohydrolase. *J Biol Chem*, 286, 43596-600.
- RAJENDRA KUMAR, P., SINGHAL, P. K., VINOD, S. S. & MAHALINGAM, S. 2003. A non-canonical transferable signal mediates nuclear import of simian immunodeficiency virus Vpx protein. *J Mol Biol*, 331, 1141-56.
- RAJSBAUM, R., GARCIA-SASTRE, A. & VERSTEEG, G. A. 2014. TRIMmunity: the roles of the TRIM E3-ubiquitin ligase family in innate antiviral immunity. *J Mol Biol*, 426, 1265-84.

- RAMPAZZO, C., MIAZZI, C., FRANZOLIN, E., PONTARIN, G., FERRARO, P., FRANGINI, M., REICHARD, P. & BIANCHI, V. 2010. Regulation by degradation, a cellular defense against deoxyribonucleotide pool imbalances. *Mutat Res*, 703, 2-10.
- REGOES, R. R. & BONHOEFFER, S. 2005. The HIV coreceptor switch: a population dynamical perspective. *Trends Microbiol*, 13, 269-77.
- REICHARD, P. 1988. Interactions between deoxyribonucleotide and DNA synthesis. *Annu Rev Biochem*, 57, 349-74.
- REINHARD, C., BOTTINELLI, D., KIM, B. & LUBAN, J. 2014. Vpx rescue of HIV-1 from the antiviral state in mature dendritic cells is independent of the intracellular deoxynucleotide concentration. *Retrovirology*, 11, 12.
- RENTOFT, M., LINDELL, K., TRAN, P., CHABES, A. L., BUCKLAND, R. J., WATT, D. L., MARJAVAARA, L., NILSSON, A. K., MELIN, B., TRYGG, J., JOHANSSON, E. & CHABES, A. 2016. Heterozygous colon cancer-associated mutations of SAMHD1 have functional significance. *Proc Natl Acad Sci U S A*, 113, 4723-8.
- RICE, G. I., BOND, J., ASIPU, A., BRUNETTE, R. L., MANFIELD, I. W., CARR, I. M., FULLER, J. C., JACKSON, R. M., LAMB, T., BRIGGS, T. A., ALI, M., GORNALL, H., COUTHARD, L. R., AEBY, A., ATTARD-MONTALTO, S. P., BERTINI, E., BODEMER, C., BROCKMANN, K., BRUETON, L. A., CORRY, P. C., DESGUERRE, I., FAZZI, E., CAZORLA, A. G., GENER, B., HAMEL, B. C., HEIBERG, A., HUNTER, M., VAN DER KNAAP, M. S., KUMAR, R., LAGAE, L., LANDRIEU, P. G., LOURENCO, C. M., MAROM, D., MCDERMOTT, M. F., VAN DER MERWE, W., ORCESI, S., PRENDIVILLE, J. S., RASMUSSEN, M., SHALEV, S. A., SOLER, D. M., SHINAWI, M., SPIEGEL, R., TAN, T. Y., VANDERVER, A., WAKELING, E. L., WASSMER, E., WHITTAKER, E., LEBON, P., STETSON, D. B., BONTHRON, D. T. & CROW, Y. J. 2009a. Mutations involved in Aicardi-Goutieres syndrome implicate SAMHD1 as regulator of the innate immune response. *Nat Genet*, 41, 829-32.
- RICE, G. I., BOND, J., ASIPU, A., BRUNETTE, R. L., MANFIELD, I. W., CARR, I. M., FULLER, J. C., JACKSON, R. M., LAMB, T., BRIGGS, T. A., ALI, M., GORNALL, H., COUTHARD, L. R., AEBY, A., ATTARD-MONTALTO, S. P., BERTINI, E., BODEMER, C., BROCKMANN, K., BRUETON, L. A., CORRY, P. C., DESGUERRE, I., FAZZI, E., CAZORLA, A. G., GENER, B., HAMEL, B. C., HEIBERG, A., HUNTER, M., VAN DER KNAAP, M. S., KUMAR, R., LAGAE, L., LANDRIEU, P. G., LOURENCO, C. M., MAROM, D., MCDERMOTT, M. F., VAN DER MERWE, W., ORCESI, S., PRENDIVILLE, J. S., RASMUSSEN, M., SHALEV, S. A., SOLER, D. M., SHINAWI, M., SPIEGEL, R., TAN, T. Y., VANDERVER, A., WAKELING, E. L., WASSMER, E., WHITTAKER, E., LEBON, P., STETSON, D. B., BONTHRON, D. T. & CROW, Y. J. 2009b. Mutations involved in Aicardi-Goutières syndrome implicate SAMHD1 as regulator of the innate immune response. *Nat Genet*, 41, 829-32.
- RIESS, M., FUCHS, N. V., IDICA, A., HAMDORF, M., FLORY, E., PEDERSEN, I. M. & KONIG, R. 2017. Interferons Induce Expression of SAMHD1 in Monocytes through Down-regulation of miR-181a and miR-30a. *J Biol Chem*, 292, 264-277.
- ROESCH, F., OHAINLE, M. & EMERMAN, M. 2018. A CRISPR screen for factors regulating SAMHD1 degradation identifies IFITMs as potent inhibitors of lentiviral particle delivery. *Retrovirology*, 15, 26.
- ROSA, A., CHANDE, A., ZIGLIO, S., DE SANCTIS, V., BERTORELLI, R., GOH, S. L., MCCAULEY, S. M., NOWOSIELSKA, A., ANTONARAKIS, S. E., LUBAN, J., SANTONI, F. A. & PIZZATO, M. 2015. HIV-1 Nef promotes infection by excluding SERINC5 from virion incorporation. *Nature*, 526, 212-7.
- ROSSI, D. 2014. SAMHD1: a new gene for CLL. *Blood*, 123, 951-2.

- ROWE, J. M. 2013. Important milestones in acute leukemia in 2013. *Best Pract Res Clin Haematol*, 26, 241-4.
- RUSTUM, Y. M., RIVA, C. & PREISLER, H. D. 1987. Pharmacokinetic parameters of 1-beta-D-arabinofuranosylcytosine (ara-C) and their relationship to intracellular metabolism of ara-C, toxicity, and response of patients with acute nonlymphocytic leukemia treated with conventional and high-dose ara-C. *Semin Oncol*, 14, 141-8.
- RYOO, J., CHOI, J., OH, C., KIM, S., SEO, M., KIM, S.-Y., SEO, D., KIM, J., WHITE, T. E., BRANDARIZ-NUÑEZ, A., DIAZ-GRIFFERO, F., YUN, C.-H., HOLLENBAUGH, J. A., KIM, B., BAEK, D. & AHN, K. 2014a. The ribonuclease activity of SAMHD1 is required for HIV-1 restriction. *Nature Medicine*, 20, 936.
- RYOO, J., CHOI, J., OH, C., KIM, S., SEO, M., KIM, S. Y., SEO, D., KIM, J., WHITE, T. E., BRANDARIZ-NUNEZ, A., DIAZ-GRIFFERO, F., YUN, C. H., HOLLENBAUGH, J. A., KIM, B., BAEK, D. & AHN, K. 2014b. The ribonuclease activity of SAMHD1 is required for HIV-1 restriction. *Nat Med*, 20, 936-41.
- SAHIN, U., KARIKO, K. & TURECI, O. 2014. mRNA-based therapeutics--developing a new class of drugs. *Nat Rev Drug Discov*, 13, 759-80.
- SALETTA, F., SENG, M. S. & LAU, L. M. S. 2014. Advances in paediatric cancer treatment. *Translational Pediatrics*, 3, 156-182.
- SANDMEYER, S. B. & CLEMENS, K. A. 2010. Function of a retrotransposon nucleocapsid protein. *RNA Biol*, 7, 642-54.
- SAWYER, S. L., WU, L. I., EMERMAN, M. & MALIK, H. S. 2005. Positive selection of primate TRIM5alpha identifies a critical species-specific retroviral restriction domain. *Proc Natl Acad Sci U S A*, 102, 2832-7.
- SCAGLIOTTI, G., NISHIO, M., SATOUCHI, M., VALMADRE, G., NIHO, S., GALETTA, D., CORTINOVIS, D., BENEDETTI, F., YOSHIHARA, E., MAKRIS, L., INOUE, A. & KUBOTA, K. 2016. A phase 2 randomized study of TAS-102 versus topotecan or amrubicin in patients requiring second-line chemotherapy for small cell lung cancer refractory or sensitive to frontline platinum-based chemotherapy. *Lung Cancer*, 100, 20-23.
- SCHALLER, T., POLLPETER, D., APOLONIA, L., GOUJON, C. & MALIM, M. H. 2014. Nuclear import of SAMHD1 is mediated by a classical karyopherin  $\alpha/\beta$ 1 dependent pathway and confers sensitivity to VpxMAC induced ubiquitination and proteasomal degradation. *Retrovirology*, 11, 29.
- SCHIM VAN DER LOEFF, M. F. & AABY, P. 1999. Towards a better understanding of the epidemiology of HIV-2. *Aids*, 13 Suppl A, S69-84.
- SCHNEIDER, C., OELLERICH, T., BALDAUF, H. M., SCHWARZ, S. M., THOMAS, D., FLICK, R., BOHNENBERGER, H., KADERALI, L., STEGMANN, L., CREMER, A., MARTIN, M., LOHMEYER, J., MICHAELIS, M., HORNUNG, V., SCHLIEMANN, C., BERDEL, W. E., HARTMANN, W., WARDELMANN, E., COMOGLIO, F., HANSMANN, M. L., YAKUNIN, A. F., GEISSLINGER, G., STROBEL, P., FERREIROS, N., SERVE, H., KEPPLER, O. T. & CINATL, J., JR. 2017. SAMHD1 is a biomarker for cytarabine response and a therapeutic target in acute myeloid leukemia. *Nat Med*, 23, 250-255.
- SCHOGGINS, J. W., WILSON, S. J., PANIS, M., MURPHY, M. Y., JONES, C. T., BIENIASZ, P. & RICE, C. M. 2011. A diverse range of gene products are effectors of the type I interferon antiviral response. *Nature*, 472, 481-5.
- SCHOTT, K., FUCHS, N. V., DERUA, R., MAHBOUBI, B., SCHNELLBÄCHER, E., SEIFRIED, J., TONDERA, C., SCHMITZ, H., SHEPARD, C., BRANDARIZ-NUÑEZ, A., DIAZ-GRIFFERO, F., REUTER, A., KIM, B., JANSSENS, V. & KÖNIG, R. 2018. Dephosphorylation of the HIV-1 restriction factor SAMHD1 is mediated by PP2A-B55 $\alpha$  holoenzymes during mitotic exit. *Nat Commun*, 9, 2227.

- SCHRODER, A. R., SHINN, P., CHEN, H., BERRY, C., ECKER, J. R. & BUSHMAN, F. 2002. HIV-1 integration in the human genome favors active genes and local hotspots. *Cell*, 110, 521-9.
- SCHROFELBAUER, B., HAKATA, Y. & LANDAU, N. R. 2007. HIV-1 Vpr function is mediated by interaction with the damage-specific DNA-binding protein DDB1. *Proc Natl Acad Sci U S A*, 104, 4130-5.
- SCHWARTZ, S., FELBER, B. K., FENYO, E. M. & PAVLAKIS, G. N. 1990. Env and Vpu proteins of human immunodeficiency virus type 1 are produced from multiple bicistronic mRNAs. *J Virol*, 64, 5448-56.
- SEAMON, K. J., SUN, Z., SHLYAKHTENKO, L. S., LYUBCHENKO, Y. L. & STIVERS, J. T. 2015. SAMHD1 is a single-stranded nucleic acid binding protein with no active site-associated nuclease activity. *Nucleic Acids Res*, 43, 6486-99.
- SEISSLER, T., MARQUET, R. & PAILLART, J. C. 2017. Hijacking of the Ubiquitin/Proteasome Pathway by the HIV Auxiliary Proteins. *Viruses*, 9.
- SELIG, L., PAGES, J. C., TANCHOU, V., PREVERAL, S., BERLIOZ-TORRENT, C., LIU, L. X., ERDTMANN, L., DARLIX, J., BENAROUS, R. & BENICHOUS, S. 1999. Interaction with the p6 domain of the gag precursor mediates incorporation into virions of Vpr and Vpx proteins from primate lentiviruses. *J Virol*, 73, 592-600.
- SHAROVA, N., WU, Y., ZHU, X., STRANSKA, R., KAUSHIK, R., SHARKEY, M. & STEVENSON, M. 2008. Primate Lentiviral Vpx Commandeers DDB1 to Counteract a Macrophage Restriction. *PLoS Pathog*, 4.
- SHEEHY, A. M., GADDIS, N. C., CHOI, J. D. & MALIM, M. H. 2002. Isolation of a human gene that inhibits HIV-1 infection and is suppressed by the viral Vif protein. *Nature*, 418, 646-50.
- SIMMONS, G., WILKINSON, D., REEVES, J. D., DITTMAR, M. T., BEDDOWS, S., WEBER, J., CARNEGIE, G., DESSELBERGER, U., GRAY, P. W., WEISS, R. A. & CLAPHAM, P. R. 1996. Primary, syncytium-inducing human immunodeficiency virus type 1 isolates are dual-tropic and most can use either Lestr or CCR5 as coreceptors for virus entry. *J Virol*, 70, 8355-60.
- SINGHAL, P. K., KUMAR, P. R., RAO, M. R., KYASANI, M. & MAHALINGAM, S. 2006a. Simian immunodeficiency virus Vpx is imported into the nucleus via importin alpha-dependent and -independent pathways. *J Virol*, 80, 526-36.
- SINGHAL, P. K., RAJENDRA KUMAR, P., SUBBA RAO, M. R. & MAHALINGAM, S. 2006b. Nuclear export of simian immunodeficiency virus Vpx protein. *J Virol*, 80, 12271-82.
- SMYTH, J. F., ROBINS, A. B. & LEESE, C. L. 1976. The metabolism of cytosine arabinoside as a predictive test for clinical response to the drug in acute myeloid leukaemia. *Eur J Cancer*, 12, 567-73.
- SONG, B., JAVANBAKHT, H., PERRON, M., PARK, D. H., STREMLAU, M. & SODROSKI, J. 2005. Retrovirus restriction by TRIM5alpha variants from Old World and New World primates. *J Virol*, 79, 3930-7.
- SORIANO, V., GOMES, P., HENEINE, W., HOLGUIN, A., DORUANA, M., ANTUNES, R., MANSINHO, K., SWITZER, W. M., ARAUJO, C., SHANMUGAM, V., LOURENCO, H., GONZALEZ-LAHOZ, J. & ANTUNES, F. 2000. Human immunodeficiency virus type 2 (HIV-2) in Portugal: clinical spectrum, circulating subtypes, virus isolation, and plasma viral load. *J Med Virol*, 61, 111-6.
- SORIANO, V., GUTIERREZ, M., CABALLERO, E., CILLA, G., FERNANDEZ, J. L., AGUILERA, A., TUSET, C., DRONDA, F., MARTIN, A. M., CARBALLO, E., LOPEZ, I. & GONZALEZ-LAHOZ, J. 1996. Epidemiology of HIV-2 infection in Spain. The HIV-2 Spanish Study Group. *Eur J Clin Microbiol Infect Dis*, 15, 383-8.

- SRIVASTAVA, S., SWANSON, S. K., MANEL, N., FLORENS, L., WASHBURN, M. P. & SKOWRONSKI, J. 2008. Lentiviral Vpx accessory factor targets VprBP/DCAF1 substrate adaptor for cullin 4 E3 ubiquitin ligase to enable macrophage infection. *PLoS Pathog*, 4, e1000059.
- ST GELAIS, C., DE SILVA, S., AMIE, S. M., COLEMAN, C. M., HOY, H., HOLLENBAUGH, J. A., KIM, B. & WU, L. 2012. SAMHD1 restricts HIV-1 infection in dendritic cells (DCs) by dNTP depletion, but its expression in DCs and primary CD4+ T-lymphocytes cannot be upregulated by interferons. *Retrovirology*, 9, 105.
- ST GELAIS, C., KIM, S. H., MAKSIMOVA, V. V., BUZOVETSKY, O., KNECHT, K. M., SHEPARD, C., KIM, B., XIONG, Y. & WU, L. 2018. A Cyclin-Binding Motif in Human SAMHD1 Is Required for Its HIV-1 Restriction, dNTPase Activity, Tetramer Formation, and Efficient Phosphorylation. *J Virol*, 92.
- STREMLAU, M., OWENS, C. M., PERRON, M. J., KIESSLING, M., AUTISSIER, P. & SODROSKI, J. 2004. The cytoplasmic body component TRIM5alpha restricts HIV-1 infection in Old World monkeys. *Nature*, 427, 848-53.
- STREMLAU, M., PERRON, M., WELIKALA, S. & SODROSKI, J. 2005. Species-specific variation in the B30.2(SPRY) domain of TRIM5alpha determines the potency of human immunodeficiency virus restriction. *J Virol*, 79, 3139-45.
- STYCZYNSKI, J. 2007. Drug resistance in childhood acute myeloid leukemia. *Curr Pharm Biotechnol*, 8, 59-75.
- SUEDA, T., SAKAI, D., KUDO, T., SUGIURA, T., TAKAHASHI, H., HARAGUCHI, N., NISHIMURA, J., HATA, T., HAYASHI, T., MIZUSHIMA, T., DOKI, Y., MORI, M. & SATOH, T. 2016. Efficacy and Safety of Regorafenib or TAS-102 in Patients with Metastatic Colorectal Cancer Refractory to Standard Therapies. *Anticancer Res*, 36, 4299-306.
- SUSPENE, R., GUETARD, D., HENRY, M., SOMMER, P., WAIN-HOBSON, S. & VARTANIAN, J. P. 2005. Extensive editing of both hepatitis B virus DNA strands by APOBEC3 cytidine deaminases in vitro and in vivo. *Proc Natl Acad Sci U S A*, 102, 8321-6.
- SWANSTROM, R. & COFFIN, J. 2012. HIV-1 pathogenesis: the virus. *Cold Spring Harb Perspect Med*, 2, a007443.
- TAN, L., EHRLICH, E. & YU, X. F. 2007. DDB1 and Cul4A are required for human immunodeficiency virus type 1 Vpr-induced G2 arrest. *J Virol*, 81, 10822-30.
- TEMIN, H. M. & MIZUTANI, S. 1992. RNA-dependent DNA polymerase in virions of Rous sarcoma virus. 1970. *Biotechnology*, 24, 51-6.
- TORRIANI, F. J., RIBEIRO, R. M., GILBERT, T. L., SCHRENK, U. M., CLAUSON, M., PACHECO, D. M. & PERELSON, A. S. 2003. Hepatitis C virus (HCV) and human immunodeficiency virus (HIV) dynamics during HCV treatment in HCV/HIV coinfection. *J Infect Dis*, 188, 1498-507.
- TRISTEM, M., MARSHALL, C., KARPAS, A., PETRIK, J. & HILL, F. 1990. Origin of vpx in lentiviruses. *Nature*, 347, 341-2.
- TRKOLA, A., DRAGIC, T., ARTHOS, J., BINLEY, J. M., OLSON, W. C., ALLAWAY, G. P., CHENG-MAYER, C., ROBINSON, J., MADDON, P. J. & MOORE, J. P. 1996. CD4-dependent, antibody-sensitive interactions between HIV-1 and its co-receptor CCR-5. *Nature*, 384, 184-7.
- TSESMETZIS, N., PAULIN, C. B. J., RUDD, S. G. & HEROLD, N. 2018. Nucleobase and Nucleoside Analogues: Resistance and Re-Sensitisation at the Level of Pharmacokinetics, Pharmacodynamics and Metabolism. *Cancers (Basel)*, 10.
- USAMI, Y., WU, Y. & GOTTLINGER, H. G. 2015. SERINC3 and SERINC5 restrict HIV-1 infectivity and are counteracted by Nef. *Nature*, 526, 218-23.

- VAN DAMME, N., GOFF, D., KATSURA, C., JORGENSON, R. L., MITCHELL, R., JOHNSON, M. C., STEPHENS, E. B. & GUATELLI, J. 2008. The interferon-induced protein BST-2 restricts HIV-1 release and is downregulated from the cell surface by the viral Vpu protein. *Cell Host Microbe*, 3, 245-52.
- VAN LINT, C., BOUCHAT, S. & MARCELLO, A. 2013. HIV-1 transcription and latency: an update. *Retrovirology*, 10, 67.
- WALLDEN, K. & NORDLUND, P. 2011. Structural basis for the allosteric regulation and substrate recognition of human cytosolic 5'-nucleotidase II. *J Mol Biol*, 408, 684-96.
- WANG, J. L., LU, F. Z., SHEN, X. Y., WU, Y. & ZHAO, L. T. 2014. SAMHD1 is down regulated in lung cancer by methylation and inhibits tumor cell proliferation. *Biochem Biophys Res Commun*, 455, 229-33.
- WANG, Z., BHATTACHARYA, A., WHITE, T., BUFFONE, C., MCCABE, A., NGUYEN, L. A., SHEPARD, C. N., PARDO, S., KIM, B., WEINTRAUB, S. T., DEMELER, B., DIAZ-GRIFFERO, F. & IVANOV, D. N. 2018. Functionality of Redox-Active Cysteines Is Required for Restriction of Retroviral Replication by SAMHD1. *Cell Rep*, 24, 815-823.
- WEI, W., GUO, H., HAN, X., LIU, X., ZHOU, X., ZHANG, W. & YU, X. F. 2012. A novel DCAF1-binding motif required for Vpx-mediated degradation of nuclear SAMHD1 and Vpr-induced G2 arrest. *Cell Microbiol*, 14, 1745-56.
- WEIDNER, J. M., JIANG, D., PAN, X. B., CHANG, J., BLOCK, T. M. & GUO, J. T. 2010. Interferon-induced cell membrane proteins, IFITM3 and tetherin, inhibit vesicular stomatitis virus infection via distinct mechanisms. *J Virol*, 84, 12646-57.
- WEISSENHORN, W., DESSEN, A., HARRISON, S. C., SKEHEL, J. J. & WILEY, D. C. 1997. Atomic structure of the ectodomain from HIV-1 gp41. *Nature*, 387, 426-30.
- WELBOURN, S., DUTTA, S. M., SEMMES, O. J. & STREBEL, K. 2013. Restriction of virus infection but not catalytic dNTPase activity is regulated by phosphorylation of SAMHD1. *J Virol*, 87, 11516-24.
- WELBOURN, S. & STREBEL, K. 2016. Low dNTP levels are necessary but may not be sufficient for lentiviral restriction by SAMHD1. *Virology*, 488, 271-7.
- WHITE, T. E., BRANDARIZ-NUÑEZ, A., MARTINEZ-LOPEZ, A., KNOWLTON, C., LENZI, G., KIM, B., IVANOV, D. & DIAZ-GRIFFERO, F. 2017. A SAMHD1 mutation associated with Aicardi-Goutières syndrome uncouples the ability of SAMHD1 to restrict HIV-1 from its ability to downmodulate type I interferon in humans. *Hum Mutat*, 38, 658-668.
- WHITE, T. E., BRANDARIZ-NUÑEZ, A., VALLE-CASUSO, J. C., AMIE, S., NGUYEN, L., KIM, B., BROJATSCH, J. & DIAZ-GRIFFERO, F. 2013a. Contribution of SAM and HD domains to retroviral restriction mediated by human SAMHD1. *Virology*, 436, 81-90.
- WHITE, T. E., BRANDARIZ-NUNEZ, A., VALLE-CASUSO, J. C., AMIE, S., NGUYEN, L. A., KIM, B., TUZOVA, M. & DIAZ-GRIFFERO, F. 2013b. The retroviral restriction ability of SAMHD1, but not its deoxynucleotide triphosphohydrolase activity, is regulated by phosphorylation. *Cell Host Microbe*, 13, 441-51.
- WU, L., GERARD, N. P., WYATT, R., CHOE, H., PAROLIN, C., RUFFING, N., BORSETTI, A., CARDOSO, A. A., DESJARDIN, E., NEWMAN, W., GERARD, C. & SODROSKI, J. 1996. CD4-induced interaction of primary HIV-1 gp120 glycoproteins with the chemokine receptor CCR-5. *Nature*, 384, 179-83.
- WU, X., CONWAY, J. A., KIM, J. & KAPPES, J. C. 1994. Localization of the Vpx packaging signal within the C terminus of the human immunodeficiency virus type 2 Gag precursor protein. *J Virol*, 68, 6161-9.
- YAMAUCHI, T., KAWAI, Y., GOTO, N., KISHI, S., IMAMURA, S., YOSHIDA, A., URASAKI, Y., FUKUSHIMA, T., IWASAKI, H., TSUTANI, H., MASADA, M. &

- UEDA, T. 2001. Close correlation of 1-beta-D-arabinofuranosylcytosine 5'-triphosphate, an intracellular active metabolite, to the therapeutic efficacy of N(4)-behenoyl-1-beta-D-arabinofuranosylcytosine therapy for acute myelogenous leukemia. *Jpn J Cancer Res*, 92, 975-82.
- YAN, J., HAO, C., DELUCIA, M., SWANSON, S., FLORENS, L., WASHBURN, M. P., AHN, J. & SKOWRONSKI, J. 2015. CyclinA2-Cyclin-dependent Kinase Regulates SAMHD1 Protein Phosphohydrolase Domain. *J Biol Chem*, 290, 13279-92.
- YAN, J., KAUR, S., DELUCIA, M., HAO, C., MEHRENS, J., WANG, C., GOLCZAK, M., PALCZEWSKI, K., GRONENBORN, A. M., AHN, J. & SKOWRONSKI, J. 2013. Tetramerization of SAMHD1 is required for biological activity and inhibition of HIV infection. *J Biol Chem*, 288, 10406-17.
- YAP, M. W., NISOLE, S., LYNCH, C. & STOYE, J. P. 2004. Trim5alpha protein restricts both HIV-1 and murine leukemia virus. *Proc Natl Acad Sci U S A*, 101, 10786-91.
- YAP, M. W., NISOLE, S. & STOYE, J. P. 2005. A single amino acid change in the SPRY domain of human Trim5alpha leads to HIV-1 restriction. *Curr Biol*, 15, 73-8.
- YU, J., LI, M., WILKINS, J., DING, S., SWARTZ, T. H., ESPOSITO, A. M., ZHENG, Y. M., FREED, E. O., LIANG, C., CHEN, B. K. & LIU, S. L. 2015. IFITM Proteins Restrict HIV-1 Infection by Antagonizing the Envelope Glycoprotein. *Cell Rep*, 13, 145-156.
- YU, X., YU, Y., LIU, B., LUO, K., KONG, W., MAO, P. & YU, X. F. 2003. Induction of APOBEC3G ubiquitination and degradation by an HIV-1 Vif-Cul5-SCF complex. *Science*, 302, 1056-60.
- YU, X. F., ITO, S., ESSEX, M. & LEE, T. H. 1988. A naturally immunogenic virion-associated protein specific for HIV-2 and SIV. *Nature*, 335, 262-5.
- ZHANG, H., YANG, B., POMERANTZ, R. J., ZHANG, C., ARUNACHALAM, S. C. & GAO, L. 2003. The cytidine deaminase CEM15 induces hypermutation in newly synthesized HIV-1 DNA. *Nature*, 424, 94-8.
- ZHAO, L. J., MUKHERJEE, S. & NARAYAN, O. 1994. Biochemical mechanism of HIV-1 Vpr function. Specific interaction with a cellular protein. *J Biol Chem*, 269, 15577-82.
- ZHENG, Y.-H., JEANG, K.-T. & TOKUNAGA, K. 2012. Host restriction factors in retroviral infection: promises in virus-host interaction. *Retrovirology*, 9, 112.
- ZHU, C.-F., WEI, W., PENG, X., DONG, Y.-H., GONG, Y. & YU, X.-F. 2015. The mechanism of substrate-controlled allosteric regulation of SAMHD1 activated by GTP. *Acta Crystallographica Section D*, 71, 516-524.
- ZHU, C., GAO, W., ZHAO, K., QIN, X., ZHANG, Y., PENG, X., ZHANG, L., DONG, Y., ZHANG, W., LI, P., WEI, W., GONG, Y. & YU, X. F. 2013. Structural insight into dGTP-dependent activation of tetrameric SAMHD1 deoxynucleoside triphosphate triphosphohydrolase. *Nat Commun*, 4, 2722.
- ZITTOUN, R., MARIE, J. P., DELANIAN, S., SUBERVILLE, A. M. & THEVENIN, D. 1987. Prognostic value of in vitro uptake and retention of cytosine arabinoside in acute myelogenous leukemia. *Semin Oncol*, 14, 269-75.
- ZUFFEREY, R., NAGY, D., MANDEL, R. J., NALDINI, L. & TRONO, D. 1997. Multiply attenuated lentiviral vector achieves efficient gene delivery in vivo. *Nat Biotechnol*, 15, 871-5.